Physical Volcanology, Sedimentology, Stratigraphy and Petrochemistry of the Berry Creek Metavolcanics: An Archean calc-alkaline complex, Lake of the Woods, Ontario

by

James Gregory Davison

A Thesis submitted in partial fulfillment of the requirements for Master of Science degree in Geology at Brock University, St. Catharines, Ontario.

April, 1984

Graduated Fall 1984

TABLE OF CONTENTS

LIST OF FIGURES

LIST OF PLATES

LIST OF TABLES

ABSTRACT

The steeply dipping, isoclinally folded early Precambrian (Archean) Berry Creek Metavolcanic Complex comprises primary to resedimented pyroclastic, epiclastic and autoclastic deposits. Tephra erupted from central volcanic edifices was dumped by mass flow mechanisms into peripheral volcanosedimentary depressions. Sedimentation has been essentially contemporaneous with eruption and transport of tephra.

The monolithic to heterolithic tuffaceous horizons are interpreted as subaerial to subaqueous pumice and ash flows, secondary debris flows, lahars, slump deposits and turbidites. Monolithic debris flows, derived from crumble breccia and dome talus, formed during downslope collapse and subsequent gravity flowage. Heterolithic tuff, lahars and lava flow morphologies suggest at least temporary emergence of the edifice. Local collapse may have accompanied pyroclastic volcanism.

The tephra, produced by hydromagmatic to magmatic eruptions, were rapidly transported, by primary and secondary mechanisms, to a shallow littoral to deep water subaqueous fan developed upon the subjacent mafic metavolcanic platform. Deposition resulted from traction, traction carpet, and suspension sedimentation from laminar to turbulent flows. Facies mapping revealed proximal (channel to overbank) to distal facies epiclastics (greywackes, argillite) intercalated with proximal vent to medial fan facies crystal rich ash flows, debris flows,

bedded tuff and shallow water to deep water lava flows. Framework and matrix support debris flows exhibit a variety of subaqueous sedimentary structures, e.g., coarse tail grading, double grading, inverse to normal grading, graded stratified pebbly horizons, erosional channels. Pelitic to psammitic AE turbidites also contain primary structures, e.g., flames, load casts, dewatering pipes.

Despite low to intermediate pressure greenschist to amphibolite grade metamorphism and variably penetrative deformation, relicts of pumice fragments and shards were recognized as recrystallized quartzofeldspathic pseudomorphs. The mafic to felsic metavolcanics and metasediments contain blasts of hornblende, actinolite, garnet, pistacitic epidote, staurolite, albitic plagioclase, and rarely andalusite and cordierite.

The mafic metavolcanics (Adams River Bay, Black River, Kenu Lake, Lobstick Bay, Snake Bay) display tholeiitic trends with komatiitic affinities. Chemical variations are consistent with high level fractionation of olivine, plagioclase, amphibole, and later magnetite from a parental komatiite. The intermediate to felsic (64-74% SiO2) metavolcanics generally exhibit calc-alkaline trends. The compositional discontinuity, defined by major and trace element diversity, can be explained by a mechanism involving two different magma sources. Application of fractionation series models are inconsistent with the observed data. The tholeiitic

basalts and basaltic andesites are probably derived by low pressure fractionation of a depleted (high degree of partial melting) mantle source. The depleted (low Y, Zr) calc-alkaline metavolcanics may be produced by partial melting of a geochemically evolved source, e.g., tonalite-trondhjemite, garnet amphibolite or hydrous basalt.

INTRODUCTION

Depositional interaction between tephra, reworked secondary epiclastics and primary to locally reworked juvenile pyroclastic debris has often been overlooked by geologists in favour of regional studies of Archean volcanism (e.g., Wilson et al. 1977; Goodwin 1977; Jolly 1977, 1980). Prior to 1970, the majority of scientific papers dealt with descriptive accounts of greenstone belt stratigraphy, geochemistry and magmatotectonic implications with only cursory emphasis towards the physical volcanological problems.

A better understanding of Archean physical volcanology has spawned from the recognition of the significance of the detailed physical parameters. Firstly, Sangster (1972) outlined the association of volcanogenic and sulfide deposits to particular physicochemical environments in the greenstone belt. Secondly, recent deep sea drilling, coring and detailed morphogenetic (textural or component) mapping of Recent to Tertiary volcanogenic deposits, commonly associated with volcanic islands (Sparks et al. 1980; Sigurdsson et al. 1980), has improved our comprehension of the mechanisms involved during these paroxysmal eruptions.

The importance of facies studies within Archean metavolcanic belts has been described by Ayres and his co-workers for the past decade in northwestern Ontario and Manitoba (e.g., Ayres 1976, 1980, 1981; Buck 1978; Gordanier 1976; Peloquin et al. 1981). Similar metavolcanic and metasedimentary belts in other areas of

the Precambrian Shield have been described by Ayres (1969, 1977); Tasse et al. (1978); Walker and Pettijohn (1971); and Ricketts et al. (1982). Dimroth and Demarcke (1978), Tasse et al. (1978), and reviews of Lajoie (1979) made important contributions to the physical, chemical, and sedimentological parameters of greenstone belt explosive volcanism. Preserved primary textures and structures within the deformed and metamorphosed Archean belts can be utilized as criteria to generate models of physical volcanological evolution and schematic paleogeographic reconstructions (e.g., Henderson 1972; Turner and Walker 1973; Gordanier 1976; Hallberg et al. 1976; Ayres 1977; Thurston 1980; Wood 1980; Eriksson 1981; Dunlop and Buick 1981; Dimroth et al. 1982; Goodwin 1982; Morton and Nebel 1983).

ONGOING RESEARCH AND PURPOSE OF PRESENT STUDY

Detailed studies of Archean volcanism are extremely important in the followup and descriptive efforts towards a thorough understanding and simplification of the patchwork Archean stratigraphy. Despite metamorphism, geochemical alteration, and deformation, well preserved sections of metavolcanics and metasediments are locally evident (e.g., Anhaeusser 1969; Viljoen and Viljoen 1969; Henderson 1972; Tasse et al. 1972; Ayres 1977; Dimroth and Demarcke 1978; Edwards 1979, 1982; Van Wagoner and Van Wagoner 1981; Ricketts et al. 1982).

Most Archean volcanic sequences were described as subaqueous assemblages, while more recent discussions of volcanogenic sedimentation outline evidence of subaqueous to subaerial transition zones (Ayres 1969, 1977, 1981; Car 1975, 1976; Van Wagoner and Van Wagoner 1981; Ferreira 1980) and subaerial volcanism (Thurston 1980) and sedimentation (Car 1975, 1976; Buck 1978; Gordanier 1978; Ferreira 1980; Wood 1980). The recognition of surf or beach zones has markedly changed the earlier views of Archean sedimentaion, with the presence of subaerial to subaqueous platforms (Ayres 1980, 1981; Barley 1981; Eriksson 1981).

Recent studies outline the importance of the subaerial to subaqueous interface in the development of pyroclastic flows (subaqueous gravity or debris flows) (Sigurdsson et al. 1980; Sparks et al. 1980). Depositional mechanics described from these sequences can be readily applied to Archean analogs of pyroclastic and lava flow deposits (Tasse et al. 1978; Dimroth and Demarcke 1978; Peloquin et al. 1981; Dimroth et al. 1982; Morton and Nebel 1983).

The purpose of this study of the Berry Creek Complex is: 1) to discuss the stratigraphic relationships, on regional and detailed scales; 2) to map lithofacies types to provide an insight into spatial and temporal evolution of the physical volcanology and sedimentation mechanisms; 3) to provide petrographic descriptions of the relict primary textures, mineralogy and metamorphic assemblages of the Berry Creek Complex and the regional geology and 4) to

discuss the geochemical character of the Berry Creek Complex and the associated mafic metavolcanic groups.

SCOPE OF RESEARCH

Detailed study of the Berry Creek Complex has taken the form of regional mapping, as part of an Ontario Geological Survey project (Johns and Davison 1982) with detailed followup work in key areas of well exposed statigraphy (see Figure 1). The field work was supplemented by photographic, petrographic and geochemical research. The methods of study included the following:

1) Regional mapping at a scale of 1:15,840 to outline major stratigraphic trends, structural geology and lithofacies,

2) Measurement of stratigraphic sections (1 cm = 80 cm) in critical areas of exposure,

3) Detailed descriptions of clast and matrix components within pyroclastics, epiclastics and laharic breccias,

4) Estimates of crystal fragment components within pyroclastic and flow deposits; also crystal grading within the pyroclastic deposits,

5) Photographic descriptions of well exposed stratigraphy, cross cutting relationships (intrusive or extrusive), sedimentary structures, and clast deformation within the pyroclastics and interesting features of the regional geology,

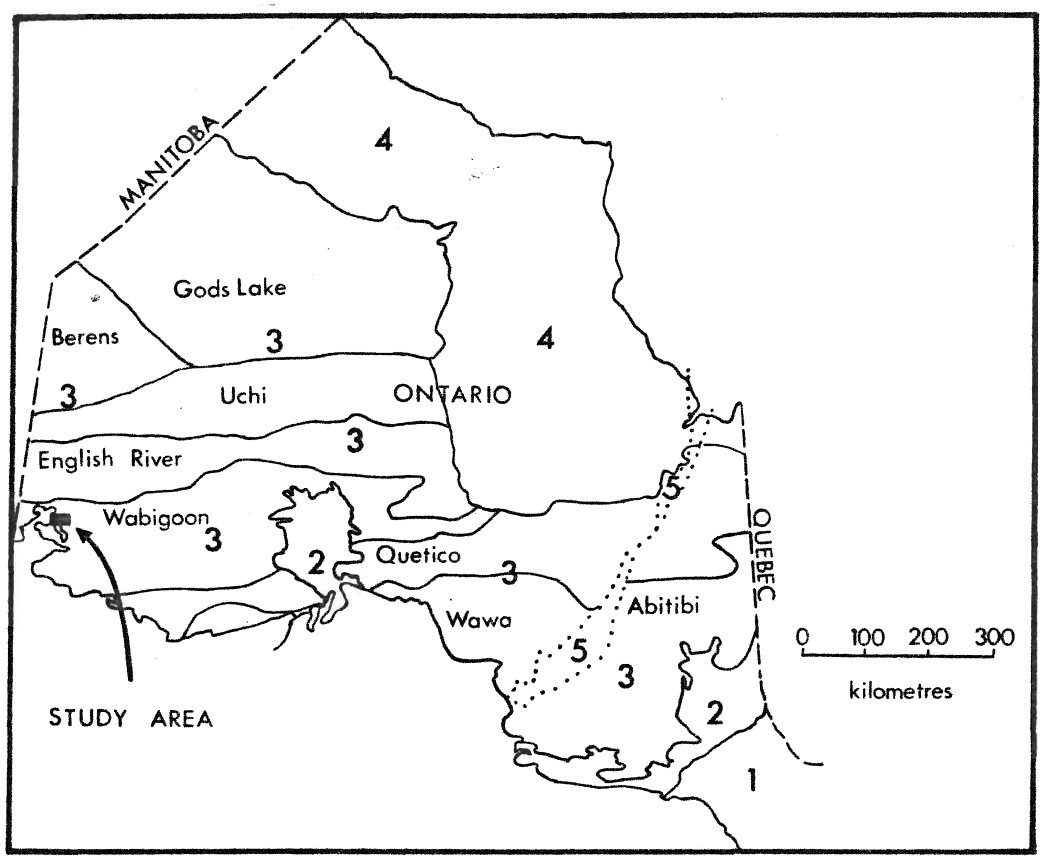

Figure 1. REGIONAL MAP OF ONTARIO NOTING THE ARCHEAN SUBPROVINCES OF THE SUPERIOR PROVINCE. STUDY AREA IS LOCATED IN THE WESTERN WABIGOON SUBPROVINCE IN THE EASTERN LAKE OF THE WOODS

6) Petrographic descriptions of 315 thin sections for mineralogy (relict and metamorphic), texture (extremely important for recognition of microvesicular fragments i.e. pumice) and deformation features (foliation, overgrowths, mylonitization, polyphase schistosity surfaces),

7) 47 samples were analyzed by xray fluorescence methods for 1Ø major and 1Ø trace element analyses,

8) 312 hand samples were selected from all of the rock types in the Sioux Narrows Greenstone Belt. Slabs were cut and polished from all samples with slab photography of selected examples of primary textures , clast heterogeneity and deformation structures.

ACKNOWLEDGEMENTS

Field research was completed while the author was employed by the Ontario Geological Survey, whom I wish to thank for field assistance, geological base maps, and the opportunities for independent detailed mapping.

I am especially grateful for the direction of W.T. Jolly and H.R. Williams. They are thanked for financial support, the opportunity to speak at the GAC conference in Victoria, and their constructive criticism of early drafts of this paper. I fully appreciated their responses to the continuum of questions during my research.

I was constantly encouraged by W.T. Jolly, H.R. Williams and N. Davison. I can't thank you enough.

Special thanks to my wife, Nicki, for typing the early manuscript, reviewing my grammar, and her understanding and encouragement through the entire project.

I also wish to acknowledge: J. Pinder for providing XRF analyses, computer printouts and her patience during my numerous lab sessions, C. Kramer for polishing thin sections, P. Peach and J. Terasmae for the microscope photography equipment, and especially J. Burke for helpful instruction on the word processor.

The Royal Ontario Museum Invertebrate Palaeontology Department is thanked for access to their computer.

Lastly, I wish to thank G.A. McKay for his usual question. I finally did!

LOCATION AND ACCESS

The Berry Creek Complex comprises parts of MacQuarrie, McGeorge, Willingdon and Devonshire Townships in the District of Kenora, northwestern Ontario. The complex also extends eastward from the township boundaries through the Lobstick Bay-Dirtywater Creek area. The map area, located in the northeastern section of Lake of the Woods, is bounded by latitudes 93 degrees, 50 minutes North to 94 degrees, 15 minutes North and by longitudes 49 degrees, 22 minutes West to 49 degrees, 30 minutes West.

Access to the study area is from secondary roads and dry weather bush roads extending from Highway 71, which bisects the map area. The western portion of the map area is accessible via the Bug Lake and Witch Bay roads, as well as the Ontario Hydro powerline transecting the region in a north-south direction. The eastern parts of the map area are accessed by Roberts Lodge, Running and Maybrun roads with canoe and power boat access from Berry Creek, Berry Lake, Otakus Lake, Kenu Lake, No Name Lake, and Dirtywater Creek. Portages from Berry Lake to Kenu Lake, Kenu Lake to No Name Lake, and Berry Lake to Otakus Lake permit overland access to canoes. The southern portion of the map area is completely accessible from Adams River Bay, Long Bay, Lobstick Bay, Whitefish Bay, Regina Bay and Reed Narrows, all estuaries of Lake of the Woods.

PREVIOUS WORK

GEOLOGICAL MAPPING

The part of the Berry Creek complex north of Lobstick Bay was first mapped by Burwash (1933) as predominantly quartz porphyry rhyolite flows. Fraser (1943) mapped the entire Whitefish Bay area of Lake of the Woods including the western half of the Berry Creek complex. Fraser (1943) described the volcanic rocks as tuff, lavas, and agglomerates and their metamorphosed equivalents, sericitic to chloritic schists. The first notation of large clastic fragments with distinct grading were also indicated by Fraser (1943). Other early reports or mapping include Burwash (1934) and Davies and Watowich (1956), who interpreted the Warclub sediments to the east of the study area to be continuous with the clastic metasediments described here as Berry Creek derivatives.

A regional study of the Kakagi, Rowan, Pipestone Lakes, Lobstick Bay areas was conducted by Edwards (1979). He described a subvolcanic to volcanic porphyry complex, of probable dacitic composition, with homolithic breccias, tuff and tuff breccia during this reconnaissance study. The term "Berry Creek Complex" was first used by Edwards (1979).

The mafic-ultramafic sill complexes near Berry Lake and No Name Lake were mapped as mafic metavolcanics (Fraser 1943), as recrystallized greenstones by Burwash (1933), and as metavolcanics by Davies and Pryslak (1966). Edwards (1979) described the western extent of the complex south

west of Berry Lake as gabbroic intrusions and the eastern part near the Dryberry to No Name Lake region as recrystallized gabbros.

Recent mapping by the Ontario Geological Survey (see Figure 1) was initiated in 1981 as a three year regional mapping project at a scale of 1:15,480 (1" = 1/4 mile) (Johns and Richey 1981; Johns and Davison 1982). Results of the past two field seasons are outlined under General Geology.

GEOCHRONOLOGY

Zircon U-Pb age dating (see Krogh 1982) of a "quartz porphyry" from the Berry Creek Complex is discussed by Davis and Edwards (1982). The sample location (their sample number DD78-28, Davis and Edwards 1982) is within Lithofacies B (proximal dome breccia facies) in the southern part of the Berry Creek Complex (Hwy. 71 north of Reed Narrows-Lobstick Bay). Davis and Edwards (1982) also sampled the intermediate to felsic metavolcanics of the Kakagi Lake region. Figure 2 (adapted from Davis and Edwards 1982) outlines the regional geology and sample site.

The Berry Creek Complex was sampled to examine lithostratigraphic relationships across the Pipestone-Cameron Fault system. Ages from the Stephen Lake felsic tuff (2711 +- 1.25 Ma) agree within error limits with ages determined from the Berry Creek Complex (2713.9 +- 5 Ma).

The ages of the majority of the older Kakagi Lake

Group and the minimum age of the Katamiagamak Group basalts (probably coeval with Snake Bay basalts; Edwards 1978) of 2724-2727 Ma implies that a younger phase of volcanism is responsible for the Stephen Lake tuffs and younger dome breccia phase of the Berry Creek Complex. The significance of the age dates with the stratigraphy and evolution of the Berry Creek Complex will be discussed later in this paper.

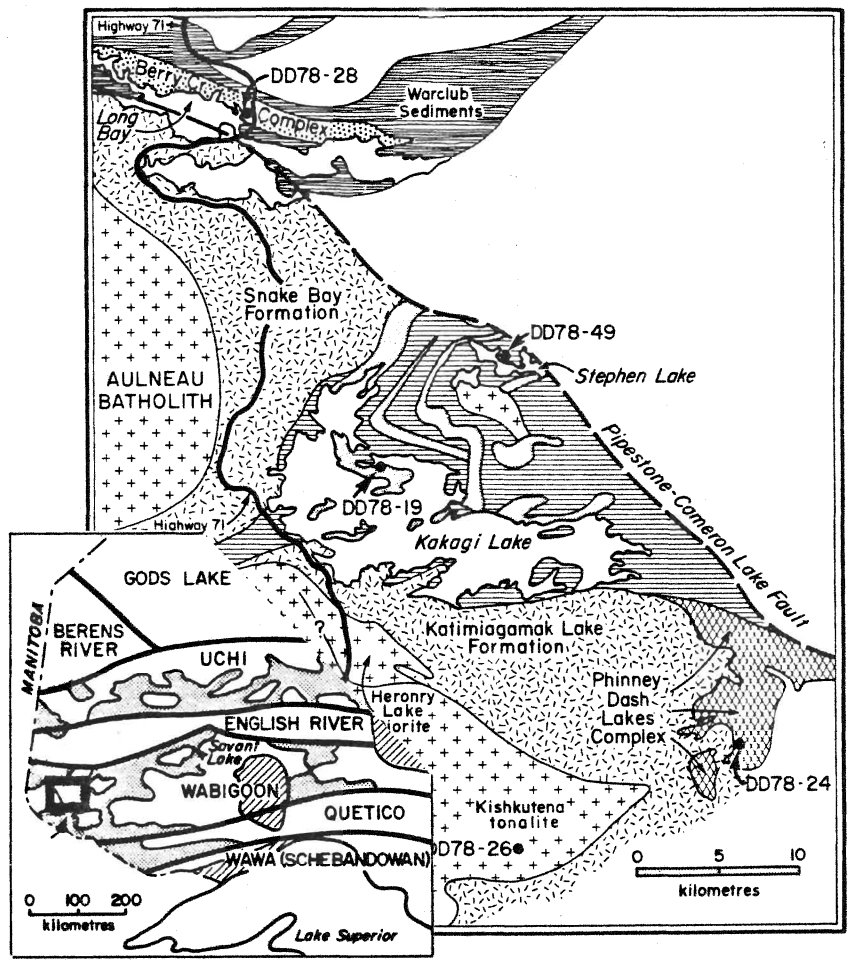

Figure 2. REGIONAL GEOLOGY OF THE SIOUX NARROWS-KAKAGI LAKE GREENSTONE BELT AND LOCATIONS OF ZIRCON U-Pb AGE DATES FROM THE BERRY CREEK COMPLEX AND THE CEDARTREE LAKE FORMATION-STEPHEN LAKE TUFF.

PHYSIOGRAPHY AND TOPOGRAPHIC ELEMENTS

The topography of the Berry Creek area typifies that of the Canadian Shield as it is characterized by rolling hills of low relief and dotted by abundant lakes with marginal swampy terrains. Rock outcrops are plentiful though local swampy terrain and glacial deposits substantially limit bedrock exposures. The shoreline of the abundant lakes, gravel pits and road cuts provide sufficient exposures but the former are again limited by the south facing overburden deposits. Islands are common with Long Bay, Lobstick Bay and Berry Lake ranging in size from 500 m in length to shoals exposed during the late season dry spells.

The shape of the lakes are controlled by bedrock, structural, and glacial features. Berry Lake, a large subcircular lake, is dominated by an antiformal structure with a granitoid core and rimmed by a gabbroic to peridotitic sill complex. The north shore of Berry Lake is probably fault controlled by NE-SW and E-W trending faults parallel to the regional foliation. Long Bay, Lobstick Bay, Reed Narrows, Sioux Narrows and the eastern end of Regina Bay are also fault controlled by the locus of the Pipestone - Cameron Fault zone and attendant splay faults. Many of the elongate lakes or bays such as Otakus Lake and Adams River Bay roughly parallel lithological units and are subparallel to the regional foliation. Many of the smaller lakes display no obvious lithological or structural controls and may be related to deposition of Pleistocene

tills and associated glaciofluvial deposits.

Fault scarps are locally found within the Dryberry Batholithic Complex, parallel to its margin north and west of Berry Lake, and near the Kishquabik Lake syenodiorite complex. The cliffs may reach heights of 30-50 m. Linear ridges of outcrop controlled by lithology are limited to the Keweenawan diabase dikes which transect the map area in a NW-SE direction. Late stage faults are located by apparent offsets in the ridges.

Glacial striae found throughout the map area indicate a south to southwest (190 degrees to 225 degrees) trend for ice flow direction. Till deposits are usually, but not always, found blanketing the north shore of the larger lakes while the south shores are scraped clean by the glaciers. Till thicknesses are highly variable and were not observed to exceed 10 m along lake sections and in gravel pits. Several gravel pits exploit the glacio-fluvial deposits within the map area.

GENERAL GEOLOGY

INTRODUCTION

The Lake of the Woods - Sioux Narrows greenstone belt is located within the Wabigoon Subprovince (see Figure 1), a lithostructural subdivision of the Superior Province of the Canadian Shield (Stockwell 1964; Wilson et al. 1975, 1976, 1977). The Sioux Narrows greenstone belt occupies a northwest to southeast trending area surrounded by several lobate to arcuate batholithic complexes (see Figure 3; regional geological compilation).

The greenstone belts of the western Wabigoon Subprovince are transected by major fault systems (Figure 4, Blackburn 1981, p.65; Blackburn et al. 1982 ;see Figure 5,Structural Geology). The fault and shear

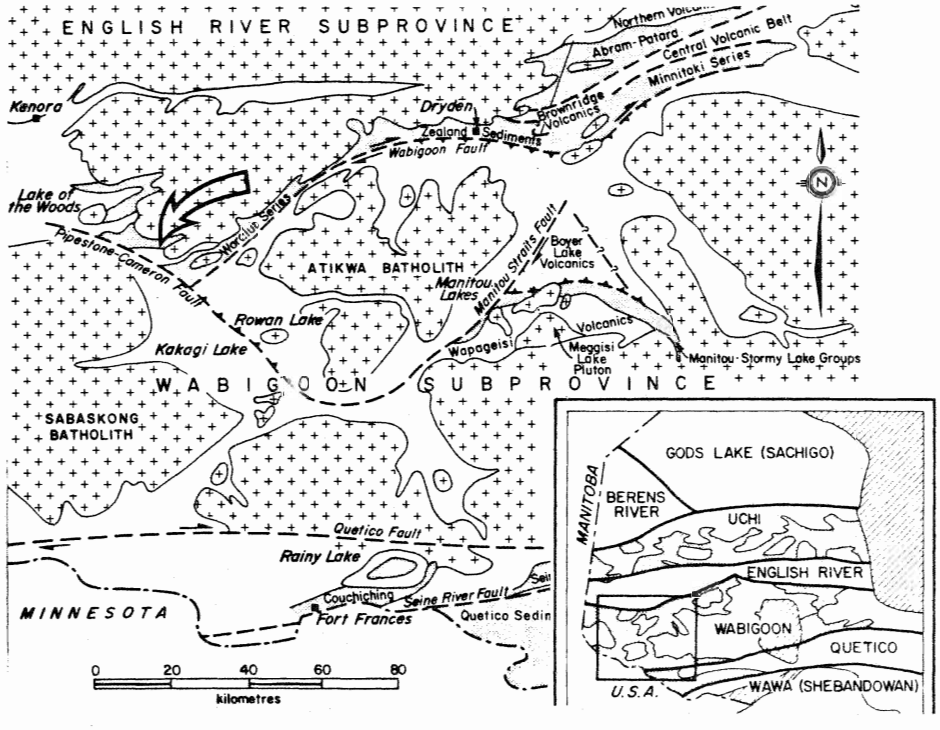

Figure 4. MAJOR FAULT SYSTEMS OF THE WESTERN WABIGOON SUBPROVINCE (PIPESTONE - CAMERON, MANITOU STRAITS,WABIGOON).

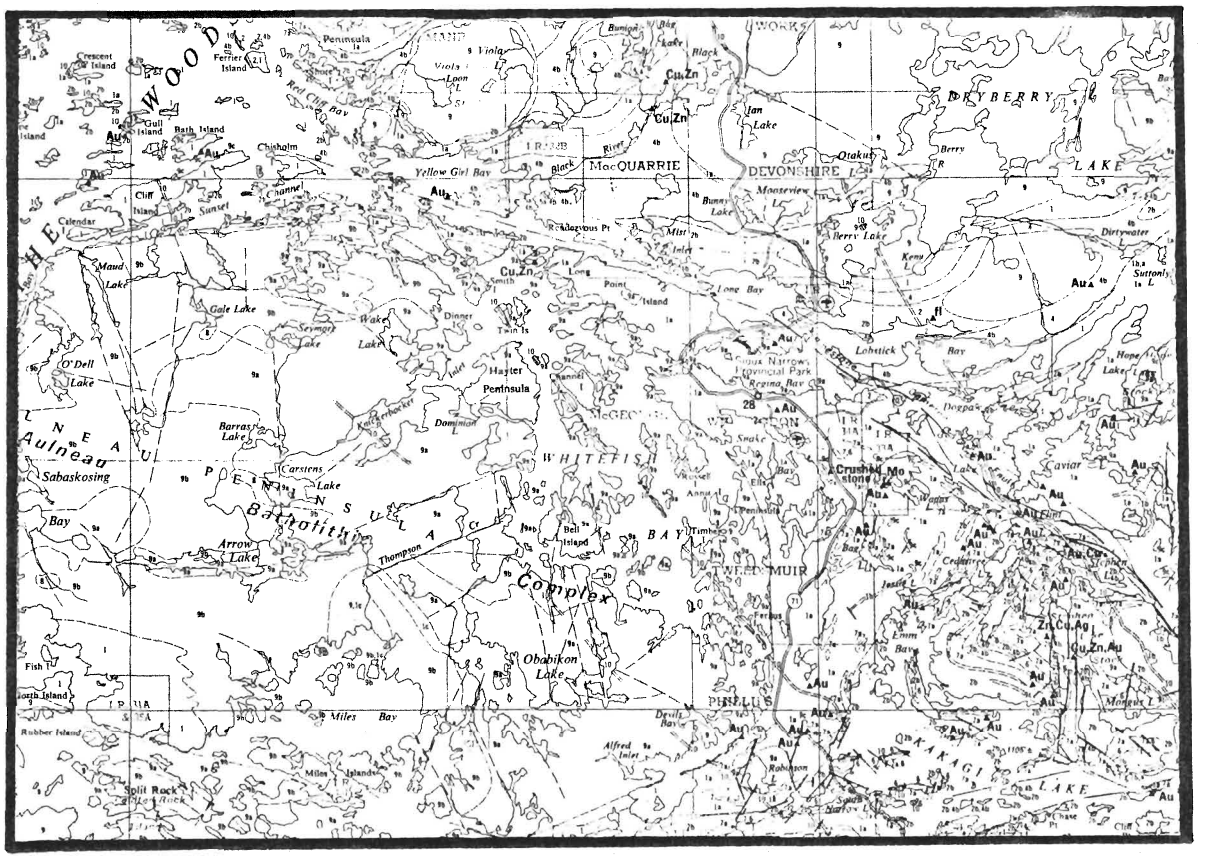

LEGEND

PHANEROZOIC

CENOZOIC

QUATERNARY

PLEISTOCENE AND RECENT

Sand, gravel, clay.

UNCONFORMITY

PRECAMBRIAN

MIDDLE TO LATE PRECAMBRIAN

MAFIC INTRUSIVE ROCKS

10 — *10 Diabase dikes.*

INTRUSIVE CONTACTS

EARLY PRECAMBRIAN[a]

FELSIC AND INTERMEDIATE INTRUSIVE ROCKS

9 — *9 Unsubdivided.*
9a Massive to foliated, equigranular and porphyritic, quartz monzonite, granodiorite, trondhjemite, quartz diorite, and granite.
9b Gneissic to foliated trondhjemite, quartz monzonite, granodiorite, quartz diorite.
9c Quartz and feldspar porphyries.

8 — *8 Unsubdivided equigranular and porphyritic monzonite, syenodiorite, syenite, diorite and quartz diorite.*
8a Monzonite syenodiorite, syenite.
8b Diorite, quartz diorite.

METAMORPHOSED MAFIC AND ULTRAMAFIC INTRUSIVE ROCKS

7 — *7 Unsubdivided mafic intrusive rocks.*
7a Gabbro, norite, diorite.
7b Anorthosite, anorthositic gabbro.

6 — *6 Peridotite, pyroxenite.*

INTRUSIVE CONTACTS[b]

METASEDIMENTS

CHEMICAL METASEDIMENTS

5 — *5 Unsubdivided ironstone.*
5a Magnetite ironstone.
5b Pyrite ironstone.
5c Chert.

CLASTIC METASEDIMENTS

4 — *4 Unsubdivided.*
4a Pebble and boulder conglomerate.
4b Sandstone, siltstone, argillite, and derived schists.
4c Migmatite metatexite.

METAVOLCANICS

ALKALIC MAFIC METAVOLCANICS

3 — *3 Unsubdivided.*
3a Flows[c].

FELSIC TO INTERMEDIATE METAVOLCANICS

2 — *2 Unsubdivided.*
2a Flows[d].
2b Tuff, agglomerate, and breccia[e].
2c Migmatite.

MAFIC METAVOLCANICS

1 — *1 Unsubdivided.*
1a Massive and pillowed flows.
1b Tuff, agglomerate, and breccia.
1c Amphibolite, amphibolite gneiss, and migmatite.

Figure 3. REGIONAL GEOLOGY OF THE SIOUX NARROWS - KAKAGI LAKE - LAKE OF THE WOODS GREENSTONE BELT.

zone systems envelop large areas of the granitoid-greenstone terrains and commonly form the margins of major subprovinces (Wilson et al. 1977).

Locally the boundaries of the subprovinces are subject to great debate (e.g., Blackburn and Mackasey 1977; review by Davis and Edwards 1982). The northern domain of the Sioux Narrows greenstone belt, i.e., north of the apex of the Pipestone - Cameron and Wabigoon Faults, contains the Berry Creek Metavolcanic Complex. The pyroclastic to epiclastic sequence overlies the lower mafic metavolcanics and appears to be contemporaneous with the Warclub metasediments (Davies and Pryslak 1967; Trowell et al. 1978), resulting in a regional metavolcanic-metasedimentary unit that is exposed along the southern margin of the Dryberry batholithic complex, and that terminates in the south against the western extension of the Wabigoon fault zone (Blackburn 1979, 1980). The implications of the temporal correlation was not realized until Breaks et al. (1978) and Davis and Edwards (1982) suggested that the Warclub, Zealand and Minnitaki metasediments were lateral equivalents along the southern margin of the English River Subprovince. The contemporaneous deposition of parts of the Berry Creek and Warclub metasedimentary-metavolcanic assemblage in the Sioux Narrows area suggests that the inferred boundary between the Wabigoon and English River Subprovince may be transitional on the basis of volcanosedimentary facies (Davis and Edwards 1982).

TABLE 1. TENTATIVE CORRELATION OF ROCK STRATIGRAPHY. (ADAPTED FROM TROWELL ET AL. 1982)

Southern Domain Sioux Narrows Belt	Northern Domain Sioux Narrows Belt	Manitou-Wabigoon Lakes Area
	Lobstick Bay	Boyer Lake
Stephen Lake	Berry Creek	Upper Wabigoon
Rendezvous Point	Warclub	
Long Bay		
Sammons Bay		Stormy Lake
Kakagi Lake		Manitou
Kakagi Metasediments		Kawashagamuk
	Kenu Lake	
Snake Bay	Black River	Wapageisi
Katamiagamak	Adams River Bay	Lower Wabigoon

The southern domain of the Sioux Narrows greenstone belt, (wholly confined to the Wabigoon Subprovince) south and southwest of the Pipestone - Cameron fault, contains the Snake Bay mafic metavolcanics, Long Bay intermediate metavolcanics, Rendezvous Point metavolcanics and the Sammons Bay metaconglomerate. Tentative correlations between the southern domain (extended southeast through the Kakagi (Crow) Lake region), the northern domain and the Wabigoon-Manitou Lakes area are shown in Table 1 (adapted after Trowell et al. 1982). The correlations are based on lithostratigraphic, geochemical and zircon U-Pb radiometric data (see Table 2). Aspects of the correlations are discussed by Blackburn (1980), Davis and Edwards (1982) and Trowell et al. (1982). Geochemical and radiometric data are discussed elsewhere in this paper.

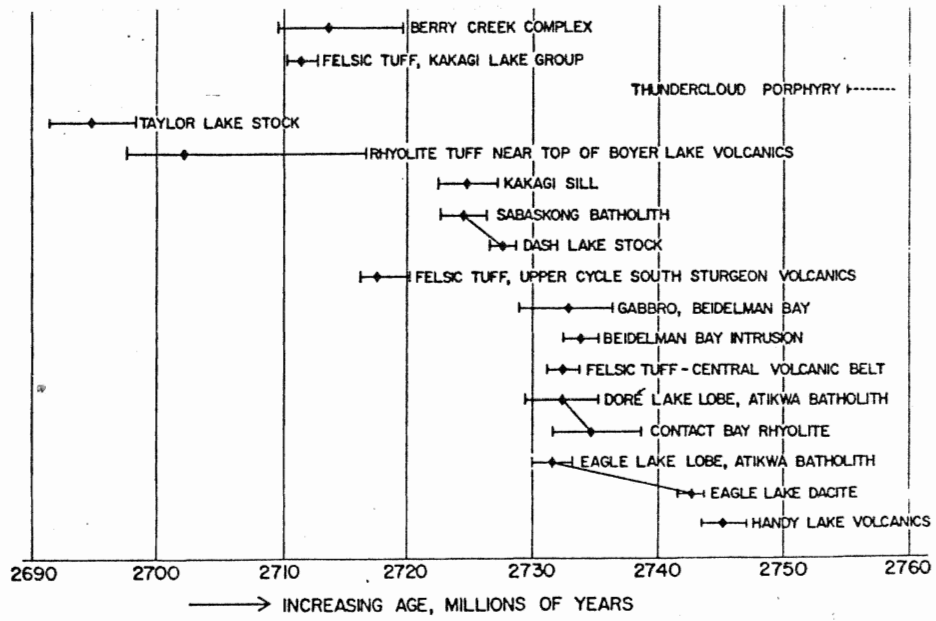

Table 2. ZIRCON U-PB AGE DATA CORRELATION FROM THE WESTERN WABIGOON SUBPROVINCE (ADAPTED FROM BLACKBURN ET AL. 1982)

GENERAL GEOLOGY

REGIONAL SETTING

The Lake of the Woods - Sioux Narrows - Kakagi Lake greenstone belt comprises a linear to cuspate series of isoclinally folded synclinoria surrounded by synkinematic massive to gneissic granitoid domes and diapirs. The regional geological compilation map is shown in Figure 3.

Except for several Middle to Late Precambrian diabase dikes, all rock types are Early Precambrian (Archean) in age (Johns and Davison 1982; Davis and Edwards 1982).

Each sector of the greenstone belts is characterized by inward facing (toward the center of the belts away from the marginal granitoids) stratigraphic cycles, similar to the idealized sequences described by Goodwin (1977).

Locally the ratio and importance of the chemical compositional groups varies markedly; a calc-alkaline or tholeiitic andesite division is commonly absent. Discontinuities (physical and geochemical) between the lower mafic cycles and the overlying acid to intermediate assemblage are discussed by Smith (1980), Goodwin and Smith (1980), and Hallberg (1978). The significance of the dual evolutionary cycles will be discussed later.

The Sioux Narrows Greenstone belt is transected by the regional Pipestone - Cameron and the Wabigoon Fault systems and divides the area into two domains: one north of the two fault zones and another south and southwest of the Pipestone - Cameron Fault (Figures 3 and 5, regional and structural geology).

The southern domain is characterized by the homoclinal, vertical to northerly dipping Snake Bay mafic metavolcanics. The Snake Bay basalts (sensu stricto) are overlain by a mixed metasedimentary to metavolcanic sequence containing the Rendezvous Point, Long Bay - Reed Narrows and Sammons Bay depositional groups. The latter Sammons Bay conglomeratic unit overlies the Snake Bay basalt along the south east shores of Regina Bay, while the former two groups are exposed along the northern shores of Long Point Island and extends west of Rendezvous Point. These groups contain intermediate to felsic tuff, ash flows, and related volcanogenic sediments intercalated with mafic flows.

The underlying Snake Bay basalts are comprised of

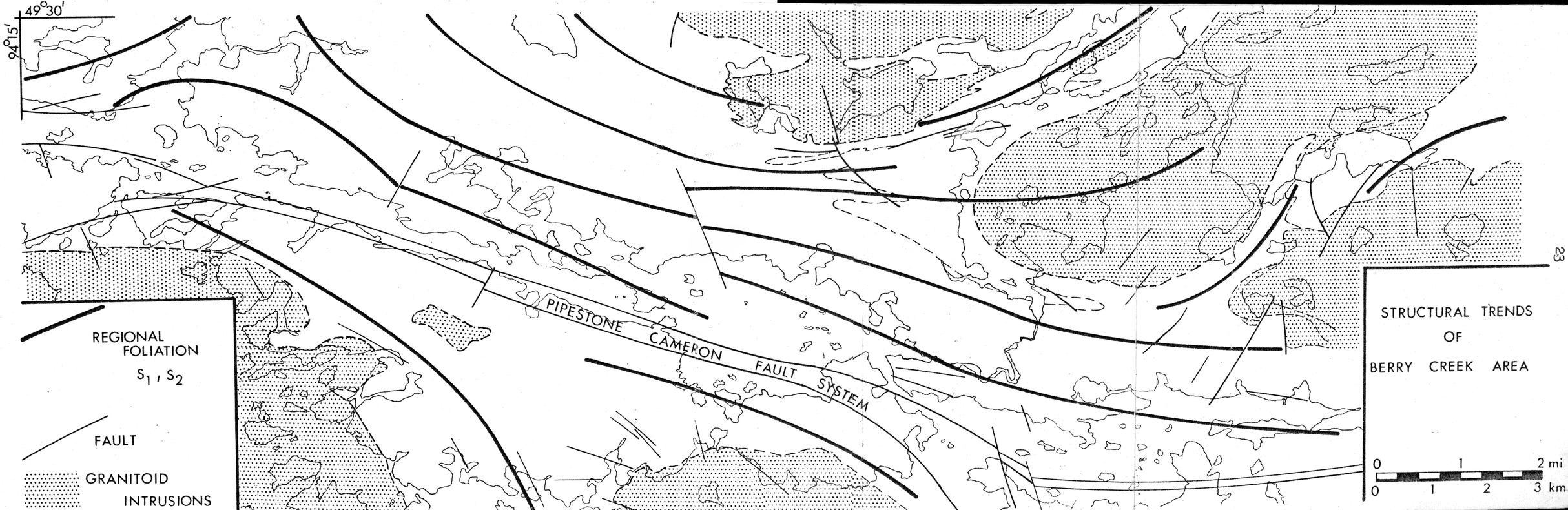

Figure 5. STRUCTURAL TRENDS AND FAULT ZONES WITHIN THE BERRY CREEK AREA.

massive to pillowed, commonly feldspar phyric, lava flows and locally intercalated chemogenic metasediments. Higher in the stratigraphic section, the lava flows become vesicular to locally amygdaloidal (often in radiating groups of pipe vesicles), contain cooling fractures, linear fissure feeder dikes, and dominantly pillowed flows. Hyaloclastic and interpillow breccias are common. Intercalations of the upper mafic fragmentals and mafic derived epiclastic metasediments are common. Locally, intermediate tuff units of the Reed Narrows - Long Bay groups are present at the top of the southern domain.

The northern domain is characterized by three major groups of metavolcanics and metasediments: the lower Adams River Bay mafic metavolcanics, Black River mafic metavolcanics, Kenu Lake mafic metavolcanics (all probably contiguous, as erosional remnants of an early mafic effusive stage); the Berry Creek felsic to intermediate metavolcanics and the upper Lobstick Bay mafic to felsic metavolcanics and metasediments.

The lower mafic metavolcanic sequence comprises massive to pillowed lava flows, tuff, tuff breccia and derived amphibolites. The mafic pyroclastics occur near the Adams River Bay area and have a limited vertical and lateral extent. The mafic metavolcanics transect the northern domain, west of the Dryberry batholith. Felsic to intermediate volcanics occur on both sides of the Black River antiformal structure. The northern sequences are probably coeval with the southern Berry Creek Complex. The

former are discussed by Trowell et al. (1979) and will not be discussed further.

The Berry Creek metavolcanics dominate the northern supracrustal domain to the south of the Black River antiform. The complex consists of felsic to intermediate tuff, tuff breccia, coarse pyroclastics, lava flows, autoclastic flow breccia, and epiclastic metasediments. The Berry Creek deposits are overlain by mixed metavolcanics, clastic metasediments, and chemogenic metasediments of the Lobstick Bay depositional group. The latter group terminates in the south against the Wabigoon fault extension, while the former is transversed by the Pipestone - Cameron Fault system.

The lower mafic metavolcanics and the early intermediate metavolcanics and metasediments are intruded by concordant, layered to podiform, gabbro, pyroxenite and serpentized dunite sills. The sills of the Berry Lake Layered Sequence are pretectonic and are isoclinally folded along with the metavolcanic-metasedimentary succession.

Quartz and/or feldspar porphyry sills and dikes, comagmatic with the extrusive metavolcanics, intrude the Berry Creek Complex and the overlying Lobstick Bay assemblage.

The entire supracrustal succession is intruded by syntectonic, multiphase, granitoid batholithic complexes (Johns and Davison 1982; Trowell et al. 1978). The northern domain is intruded by the Dryberry core complex, a

foliated to gneissic trondhjemite-tonalite-granodiorite pluton, and several satellitic granodiorite lobes. The latter are comprised of the Viola Lake stock, the Bunion Lake stock, the Otakus Lake - Berry Lake, Bunny Lake - Mooseview Lake, and the Sanford Lake lobes. The southern domain is intruded by the multiphase Aulneau batholithic complex.

The Regina Bay tonalite - granodiorite - trondhjemite stock intruded the Snake Bay mafic metavolcanics adjacent to and west of the Pipestone - Cameron Fault System (see south central granitoid intrusion, structural trends Figure 5). The Regina Bay stock, a syntectonic to post-tectonic intrusion, probably occupies a conjugate fault zone of the regional fault system. The Stephen Lake diorite to the south was interpreted in a similar manner (Edwards 1979).

The post-tectonic, compositionally zoned, Kishquabik Lake syenodiorite -syenogabbro intrudes the eastern periphery of the Berry Creek metavolcanics and the adjacent Warclub metasediments.

Strongly carbonatized lamprophyric dikes (sill, generally concordant to regional foliation) intruded the Berry Creek and Lobstick Bay supracrustals. The dikes range in composition from biotite gabbro to biotite - carbonate schists with the latter generally within the proximity of the regional fault systems.

DETAILED GEOLOGY

BERRY CREEK COMPLEX

Introduction, Classification

The Berry Creek metavolcanic and metasedimentary sequence can be broadly subdivided into three major groups according to mode of occurrence: 1) fine to coarse primary and secondary pyroclastic deposits; 2) epiclastic and turbiditic derivatives of volcanogenic tephra; and 3) proximal lava flows, domes, talus and scree deposits (crumble breccia) and subvolcanic porphyry intrusions.

The strata of the area are classified using the criteria of Fisher (1960, 1961, 1966) and Parsons (1969). All fragment sizes are based on the framework of Fisher (1961, 1966). Table 3 (Parsons 1969) outlines the volcanoclastic rock types found in the Sioux Narrows greenstone belt. it is important to note that all rock types and processes are gradational.

Deposits of pyroclastic tephra are classified according to relative abundance and size distribution of clasts and matrix within individual depositional units. The pyroclastic deposits were subdivided for mapping purposes into the following six lithotypes: 1) tuff consisting of ash size material only; 2) crystal tuff consisting of crystals and/or phenoclasts of any type, size or abundance within an ash tuff matrix; 3) lapilli tuff consisting of lapilli of any type within an ash tuff or crystal tuff matrix, (lapilli from 0-80% of mode); 4) lapillistone (as above but lapilli from 80-100% of mode);

TABLE 3. VOLCANOCLASTIC ROCK TYPES OF THE SIOUX NARROWS METAVOLCANIC-METASEDIMENTARY BELT (Modified after Parsons 1969).

1) AUTOCLASTIC
   a. Friction
      i. Flow breccia
      ii. Crumble breccia
   b. Explosion

2) HYALOCLASTIC

3) PYROCLASTIC
   a. Primary
      i. Subaerial
         - Vulcanian
         - Surtseyan
         - Plinian
         - phreatomagmatic
         - phreatic
      ii. Subaqueous
   b. Secondary
      i. Mass Movement
         - Lahar
         - Slump

4) EPICLASTIC
   a. Mass movement
      i. Lahar
      ii. Slump
      iii. Turbidite
      iv. Debris Flow
   b. Fluvial-Littoral

5) tuff breccia consisting of lapilli and blocks in varying proportions within an ash tuff or crystal tuff matrix (clasts from 0-80% of mode); 6) pyroclastic breccia (as above but clasts from 50-100% of mode).

Components

The Berry Creek pyroclastic deposits consist of lithic, vitric or pumiceous and crystal components set, in varying proportions, in a tuffaceous matrix.

The dark blue grey, often glassy, matrix of the

intermediate to felsic tuffaceous deposits consists of finely comminuted ash, crystal and vitric material. The white (altered feldspar to kaolinite) weathered, exposed surface is characteristic of the primary tuffaceous matrix. The fine tuff units commonly exhibit a recessive weathering pattern which can be used to distinguish between tuff and aphyric to sparsely aphyric lava flows (Buck 1978). Complications of this method are produced by incipient silicification, irregular weathering and development of deformational fabrics. In many of the fine tuff units, the distinctions are made by field relationships, lateral or vertical distribution grading or crystal component variations. Primary textures of the vitric ash are unrecognizable in the strongly recrystallized, metamorphosed and deformed pyroclastics. Laminations, bedding, cross bedding, and parallel stratification are the dominant mesoscopic features (see Lithology and Stratigraphy sections).

Tuffaceous deposits of mafic compositions also occur within the Berry Creek Complex. Fine to medium grained, pale green to dark green mafic ash, now consisting of amphibole and Fe - Ti oxides, occur as discrete beds of 1-10 cm thickness, and as mixed deposits with the primary or secondary intermediate to felsic pyroclastics and reworked tuff. Quartzofeldspathic sand and silt (epiclastic debris from fine tuff) is mixed with mafic ash in some laharic deposits (see Secondary Deposits). The discrete mafic ash units display normal distribution grading and often have

very sharp basal contacts. Mixing, to varying degrees with the overlying epiclastic deposits is common. Many "primary" pyroclastic deposits also contain a mafic ash matrix supporting intermediate lapilli and blocks. These deposits may contain monolithic or heterolithic clasts (see Secondary Deposits).

The crystal components of the tuffaceous deposits consist of quartz, feldspar and minor amphibole with accessory apatite, magnetite and tourmaline. Quartz crystals (phenoclasts) form 1-10 mm dipyramidal euhedra (alpha pseudomorphs after beta quartz) to resorbed, embayed and deformed anhedra. White and clear quartz phenoclasts are prevalent although blue quartz is common. The ratio of blue quartz to total quartz within single flow units varies from 10-75% and averages about 35-45%. Euhedral to subhedral plagioclase feldspars form 1-10 mm, white to light green (saussuritized) phenoclasts. Epidotization is patchy to pervasive. Skeletal feldspars were not observed. Fragmentation of the feldspar phenocrysts ranges from low to moderate, similar to that observed by Dimroth and Demarcke (1978). The distinction between the crystal tuff, porphyritic dacite and subvolcanic porphyry intrusions is difficult when based on crystal morphology. Many plagioclase phyric tuff units contain abundant euhedral phenoclasts, but can be distinguished from flows by size, composition and distribution grading of the phenoclast components. The transition from matrix phenoclasts to

plagioclase phenocrysts within partially vesiculated lithic and pumiceous fragments is commonly observed (see Dimroth and Demarcke 1978). A similar size, composition and morphology range occurs within both matrix and clasts. In some tuffaceous deposits, the crystal components showed a marked variation between the lithic clasts and the matrix. Pumiceous "skins" around unbroken euhedral plagioclase feldspars (Dimroth and Demarcke 1978) were not observed, although similar pumiceous rims are observed around feldspar phyric lithic clasts (see description and Plate 4 in Lapilli tuff, Tuff breccia section). Many of the small vitric shards and pumiceous clasts (less than 1 cm length) contain plagioclase crystals and minor quartz.

The small porphyritic vitric clasts, which probably form by a similar mechanism to that described by Dimroth and Demarcke (1978), may also be interpreted as pumiceous rims. Crystal components found within the pumiceous fragments are generally of euhedral to subhedral forms. This corroborates the observation of Dimroth and Demarcke (1978) that crystal fragments are not coated by pumiceous skins. Original crystal faces are rimmed while the broken fracture surfaces lack rims.

Primary amphibole crystals, now consisting of secondary minerals, are rare. Euhedral to subhedral, 1-3 mm rhombic microphenocryst cross sections are prevalent. Accessory phases such as magnetite, apatite, and pyrite occur as randomly distributed euhedral to anhedral grains. Magnetite is commonly associated with the mafic ash tuff

deposits.

Tourmaline is disseminated within porous tuffaceous deposits and the massive dacite breccias related to the Lobstick Bay dome breccia. Black to dark green 1-8 mm subhedral prisms of tourmaline range from trace amounts to a maximum of 10% in some fine tuffs. Tourmaline also occurs as a garbenscheifer phase i.e. radiating arrays parallel to the micaceous foliation of the intermediate to felsic metavolcanics.

Subangular to subrounded lithic clasts, measured in least deformed rocks, range in size from lapilli to blocks with a maximum long axis dimension of 1.5 metre. The majority of the lithic clasts exhibit lensitic to elliptical sections parallel to the schistosity plane due to pervasive flattening deformation ($0 < k < 1$, Flinn 1965; Wood 1973; Ramsay 1967). Length to width ratios vary with size, composition, matrix abundance, and intensity of deformation. Measured ratios range from 2 : 1 to 25 : 1 on the two dimensional outcrop surfaces. Exposures with extremely attenuated clasts, suggest that clasts have been deformed beyond the maximum measured ratios of 25:1 (X : Z). Plate 1 displays the shape of deformed clasts characteristic to the coarse pyroclastic deposits.

Massive quartz and feldspar phyric dacite and vesiculated pumiceous fragments are the dominant juvenile to accessory lithoclast types. Other accessory clast types include the following: nonporphyritic felsite, pink and

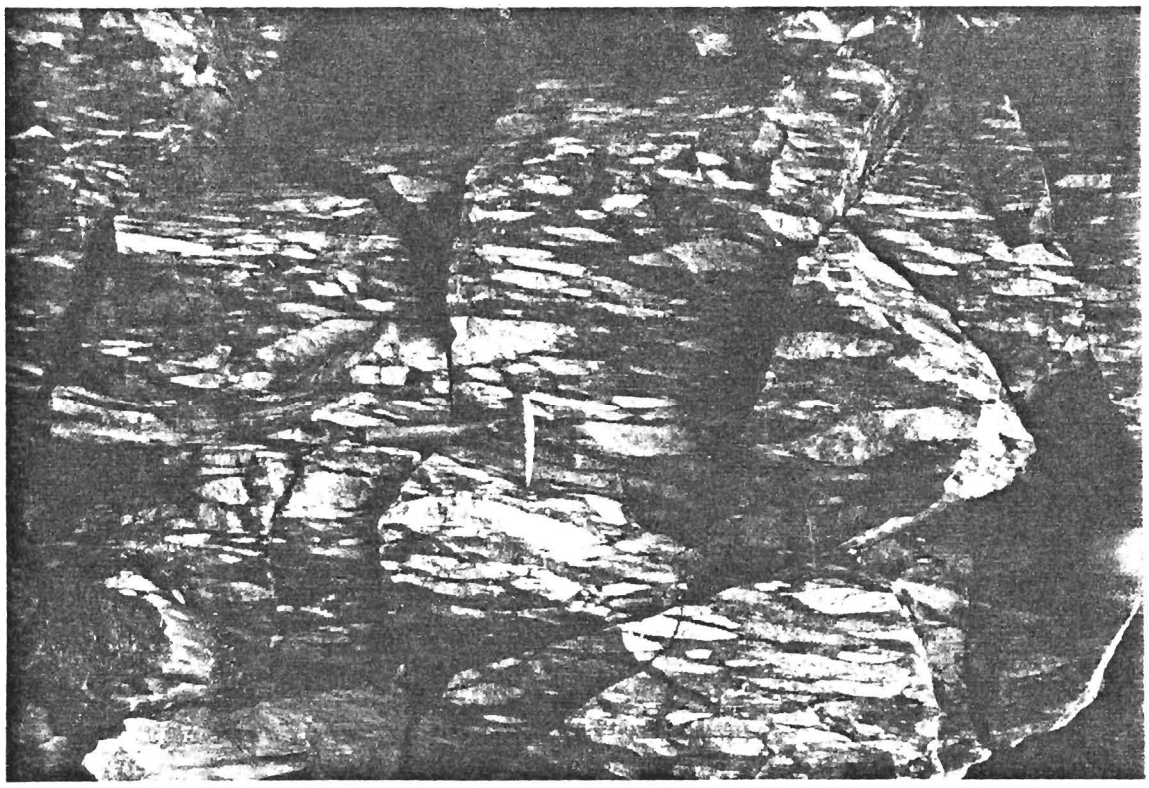

Plate 1. DEFORMED MONOLITHIC CLASTS FROM FRAMEWORK DEBRIS FLOW, RUNNING ROAD SECTION, BERRY CREEK METAVOLCANICS

orange quartz feldspar porphyry, light and/or dark blue grey feldspar porphyry, recessive weathering porphyritic dacite to andesite tuff, fine grained grey feldspathic wacke and quartzose wacke, quartz feldspar wacke and arenite, mafic tuff and fine grained massive dark green mafic metavolcanics (probably massive flows).

The dacite contains euhedral to subhedral quartz (alpha after beta quartz common) and feldspar in an aphanitic glassy groundmass. In outcrop, the distinction between the porphyritic dacite and porphyritic partially vesiculated pumiceous clasts is rarely observed. Normally, the pumice fragments are dominantly feldspar phyric while the dacite porphyry contains both quartz and feldspar. Relative abundances of pumice and dacite porphyry have been

estimated from large polished slabs of the hand samples. The pumice fragments are highly variable in both morphology and distribution. The vitric fragments range from fine ash to lapilli sized shards to pumiceous blocks with long axis dimensions of greater than one metre. Length to width ratios of 3 : 1 and higher , though common, may be further increased by tectonic attenuation of the pumiceous fragments.

The preservation of pumiceous fragments is commonly extremely poor in many Archean greenstone belts due to extensive recrystallization, devitrification, synvolcanic erosion and reworking, deformation, pressure solution and metamorphism. Fisher (1969) notes that the recognition of pumiceous fragments is critical for accurate assessment of pyroclastic depositional styles. In the Berry Creek deposits, observation of discrete pumice fragments is also limited by similarities with porphyritic dacite, low degrees of vesiculation, which is partially minimized by compaction and flattening deformation, and strong recrystallization, especially in the fine fraction.

Where possible, pumice can be recognized in the following manner: 1) recessive, often porphyritic, highly porous clasts (Apache Landing Section); 2) irregular particles of slightly recessive clasts with clots and/or slightly filled void spaces containing chlorite, amphibole and minor quartz and carbonate (Lobstick Bay); 3) irregular chloritized lapilli with swallow tail or

bifurcated terminations (Maybrun Section); 4) white to green, undulating, ash to fine lapilli shards (only observed on weathered surfaces and polished slabs where colour contrast between shards and chloritized matrix is significant)(Rendezvous Point); and 5) pale green pumiceous lapilli to blocks set in a dark green pumiceous ash matrix (displays pseudoeutaxitic texture).

The recognition of pumice fragments in polished slabs permits detailed morphological evaluation. Elliptical to lensitic pumice fragments are dominant. Rounded to oblate patches of vesiculated and partially vesiculated pumice are common. Pumiceous shards (less than 2.5 cm long axis dimension) are very fine grained to aphanitic, aphyric, elongate with undulating to wispy shapes and displaying rapid thickness variations (see Plate 17 in Petrography section) due to differential compaction by competent phenocryst (phenoclast) components. The grain boundaries of the pumice are generally ragged with multiple bifurcated or swallowtail terminations (see Plates 2 and 3). These ragged grain boundaries of the unreworked pumice fragments are commonly deformed into parallelism with the long axis of the fragment in the plane of the schistosity.

The majority of the pumiceous lapilli and blocks are aphanitic or sparsely phyric (quartz and/or feldspar) and can contain elongate lenses of quartz, chlorite, epidote, mica, and Fe-Ti oxides. The lenses probably represent original, now deformed and infilled, pore space in the vesiculated pumice. Estimation of original pore space is

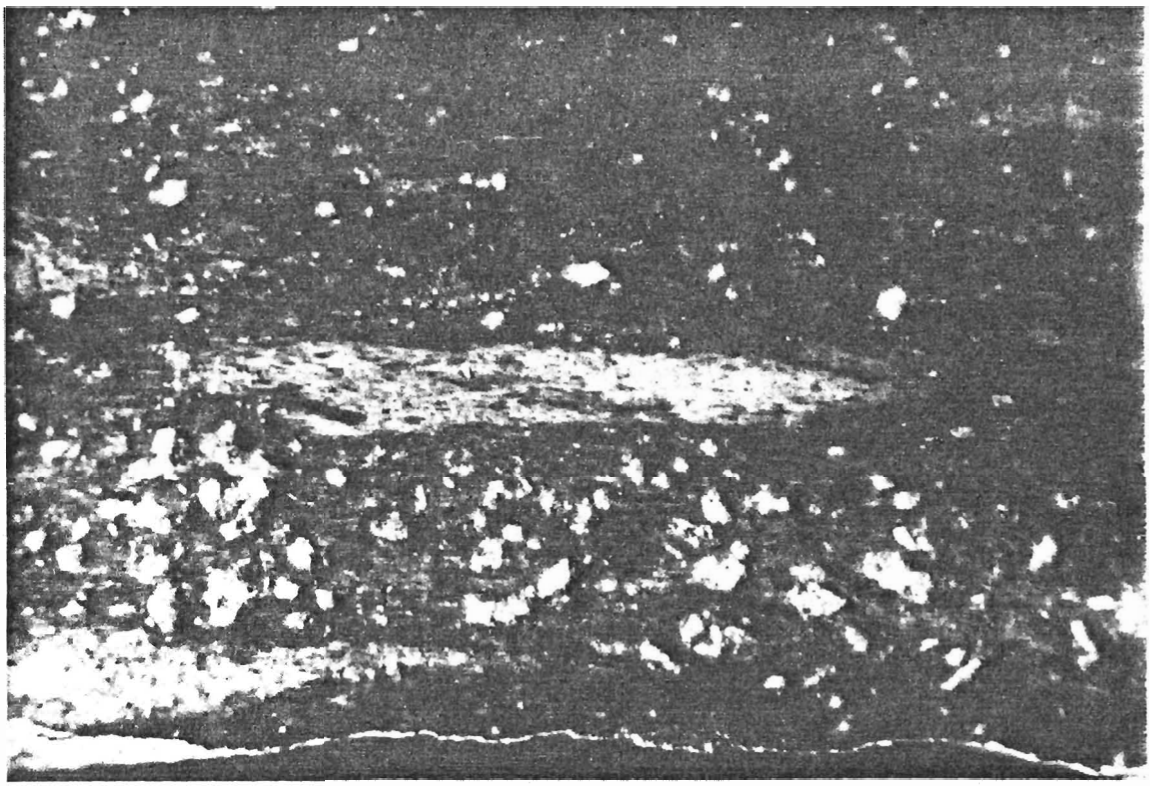

Plate 2. POLISHED SLAB OF PUMICE FRAGMENT, RUNNING ROAD SECTION. NOTE BIFURCATIONS, LACK OF PHENOCRYSTS, RELICT PRIMARY TEXTURES, AND ALIGNMENT WITH REGIONAL FOLIATION.

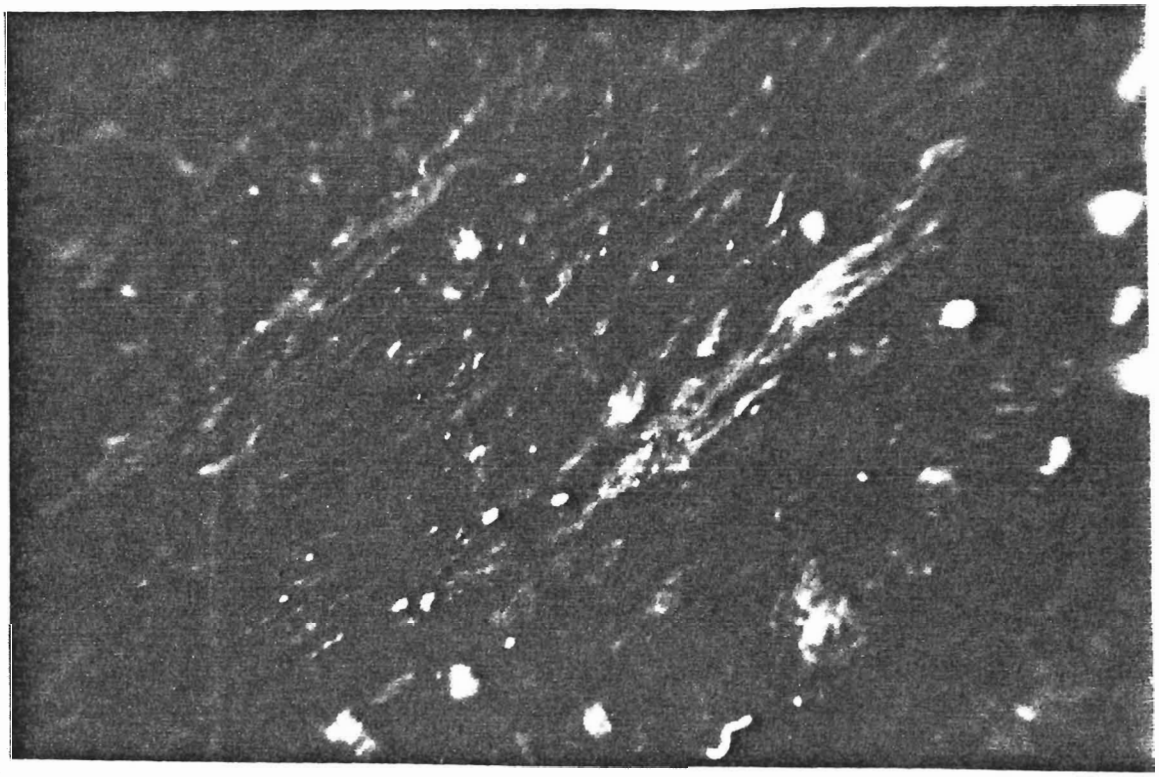

Plate 3. POLISHED SLAB OF PUMICEOUS FRAGMENTS, VITRICLASTS, SHARDS FROM DEBRIS FLOW, LONG BAY, NEAR WHITE MOOSE LODGE. NOTE BIFURCATIONS, MICROPHENOCRYSTS AND PSEUDOEUTAXITIC TEXTURE.

difficult due to recrystallization and deformation. In the least strained pumice from near Lobstick Bay, chlorite and amphibole account for greater than 60% of porous highly vesiculated pumiceous clots. Field and petrographic measurements of vesicularity in the Berry Creek pyroclastics suggest that the porosity ranges from almost nil to a miximum of 70%. The degree of attenuation of the pumice clasts appears to be directly related to the vesicularity, but also shows relationships with the competency of the matrix, the matrix abundance (i.e. matrix or clast support) and abundance of a phenocryst component.

Many of the pumice fragments are feldspar phyric. Resorbed quartz phenocrysts are less common. Euhedral to subhedral, 1-10 mm dipyramids of quartz (alpha after beta quartz) occur in the pumice of the upper parts of the pyroclastic sequence. The quartz phenocrysts in the pumice clasts from the lower part of the Berry Creek Complex range in size from 0.2 to 1 mm and usually occur as resorbed lenses (deformed from subhedral phenocrysts). The deformed quartz phenocrysts are accompanied by pore-filling silica and both phases are similarly deformed and recrystallized. Discrete quartz phenocrysts rarely exceed 3-5% of the pumice fragments.

The plagioclase phenocrysts form euhedral to subhedral, 1-10 mm laths. The abundance of plagioclase feldspars in pumice is directly related to: 1) size of the pumice fragments i.e. fine shards are usually aphyric while lapilli and blocks of pumice often contain 5-35%

phenocrysts, 2) the vesicularity of the pumice i.e. crystal abundances decrease with increasing vesicularity (highly vesicular pumice dominantly aphyric to sparsely quartz phyric), and 3) the stratigraphic level of the pumiceous deposit (feldspar to quartz ratios decrease upward in the stratigraphic section).

Within single exposures, pumice fragments display marked variability in both size and phenocryst content. Large pumiceous blocks contain 30% feldspar and quartz phenocrysts while the associated shard population, of similar composition, are aphyric or contain less than 5% feldspar and/or quartz phenocrysts.

The internal fabric and external morphology of the pumice fragments are distorted by the presence of phenocrysts in the matrix and within the pumice fragments. Wrap around deflection textures are very common (see Plates 17 and 19 in Petrography). Eutaxitic and pseudoeutaxitic textures characterize the highly pumiceous deposits. Samples collected from pumiceous ash flows (debris flow) in Long Bay display the relict texture of primary compaction following deposition. Similar eutaxitic textures have been observed by Hallberg et al. (1976) from the Marda Complex in Australia (see Figure 3-27 in Condie 1981). However, pseudoeutaxitic textures are commonly produced by subsequent tectonic deformation. Highly attenuated pumice fragments found in the White Moose section (see Figure 6) suggest that perhaps both mechanisms affected the Berry

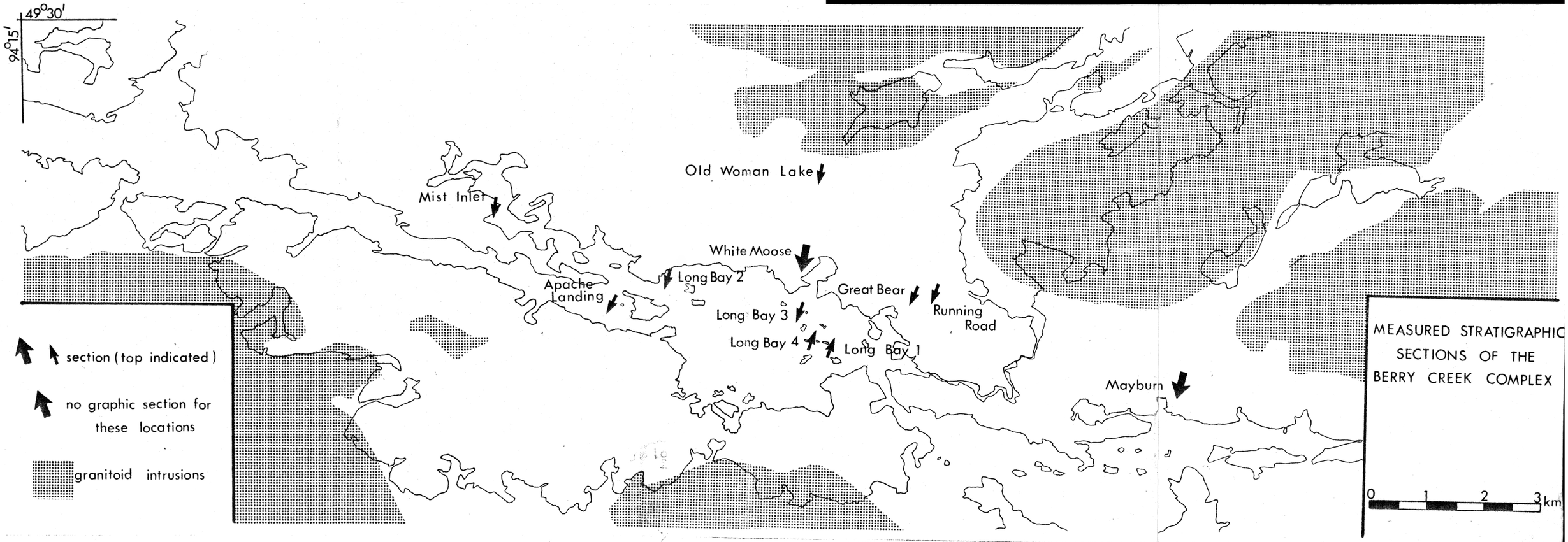

Figure 6. LOCATION MAP OF MEASURED STRATIGRAPHIC SECTIONS IN THE BERRY CREEK AREA.

Creek pyroclastic flows. Lithic clasts, which exhibit considerably more competence than the vitriclasts, are similarly elongated by oblate deformation, though to a lesser degree.

Lapilli tuff, Tuff breccia

Lapilli tuff and tuff breccia are the most common pyroclastic deposits of the Berry Creek Complex. These units consist of lapilli and block size clasts set in a tuffaceous matrix of not less than 20% modal volume. Those deposits containing less than 20% matrix components (lapillistone, pyroclastic breccia) are coarse matrix poor extensions of the former units and will be discussed in the following section. The tuffaceous and pyroclastic units are clearly gradational with each other in both lateral and vertical dimensions.

The majority of the fragmental pyroclastic deposits are monolithic, although some heterolithic and mixed monolithic to heterolithic deposits were observed. Lapilli tuff and tuff breccia units consist of subangular to subrounded fragments of quartz and feldspar dacite, accompanied by varying proportions of pumiceous fragments. Distinction between the two types of clasts in the field is difficult to impossible, due to **oblate** deformation, low vesicularity and abundant phenocrysts within the pumice fragments.

The primary heterolithic pyroclastics consist of the

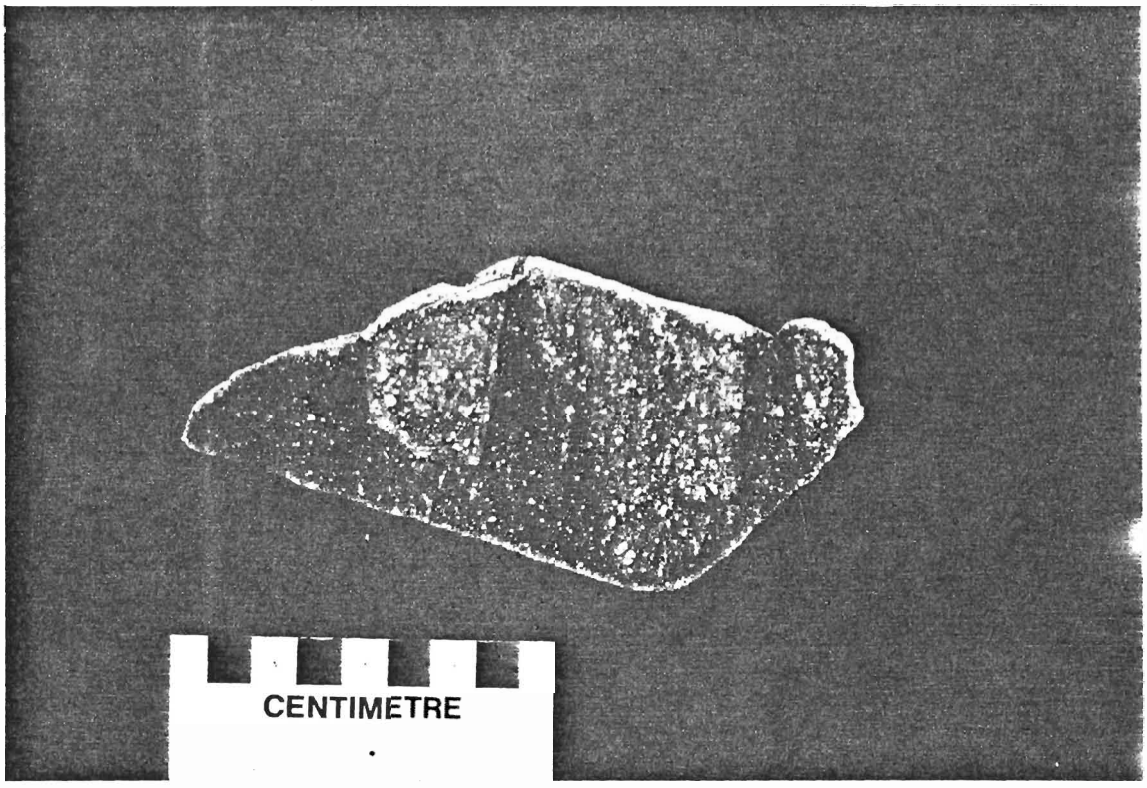

Plate 4. POLISHED SLAB OF LITHIC CLASTS OF DACITE PORPHYRY WITH THIN PUMICEOUS SKIN. NOTE ABSENCE OF PHENOCRYSTS IN OUTER RIM ZONE.

above fragment types and are supplemented by the following: 1) accessory fragments i.e., those produced by previous eruptions from the same vent and usually consist of several types of vesiculated to poorly vesiculated pumice and/or porphyritic dacite; 2) accessory to accidental fragments i.e., those clasts derived from vent fall back (vent talus) and from the inner vent walls from previous eruptions; and 3) accidental to exotic fragments i.e. derived from the paleosurface surrounding the eruption area (volcanic or nonvolcanic provenance).

In the case of vent derived fragments (Type 2), recognition is often based upon the presence of a skin of pumice or reaction rim coating the accidental lithic clasts (Dimroth and Demarcke 1978; Teng, p. comm. 1981). Plate 4

shows a porphyritic dacite clast from a tuff breccia in Long Bay. The presence of an aphyric pumiceous rim suggests contact with a melt phase. Although clasts of this type are probably common, recognition is difficult (without polished slabs) due to compositional and textural similarities between the fragment and its rim. In the case of exotic fragments, derived from transport over the paleosurface, pumiceous rims or weathering rinds are absent.

The lapilli tuff and tuff breccia units occur as debris flow deposits ranging in thickness from 15 cm to 50 metres (usually 2-10 m). The majority of the individual tuffaceous units cannot be traced due to lack of outcrop, faulting and similarities between depositional units. Some of the pyroclastics form discrete mappable horizons traceable over 1-2 km along strike length while lensitic, valley form, channel deposits occur over less than 10 m strike length. The lensitic deposits are often characterized by rapid lateral fining and vertical coarse tail grading from the depositional centre of the channel.

Of the sedimentary or depositional structures present, by far the most common is grading of the clasts. Several types of clast grading were observed. These include: coarse tail grading (normal and inverse), frequency grading, compositional grading and distribution grading. In general, facing directions are based on normal coarse tail grading of blocks and large lapilli. Many of the

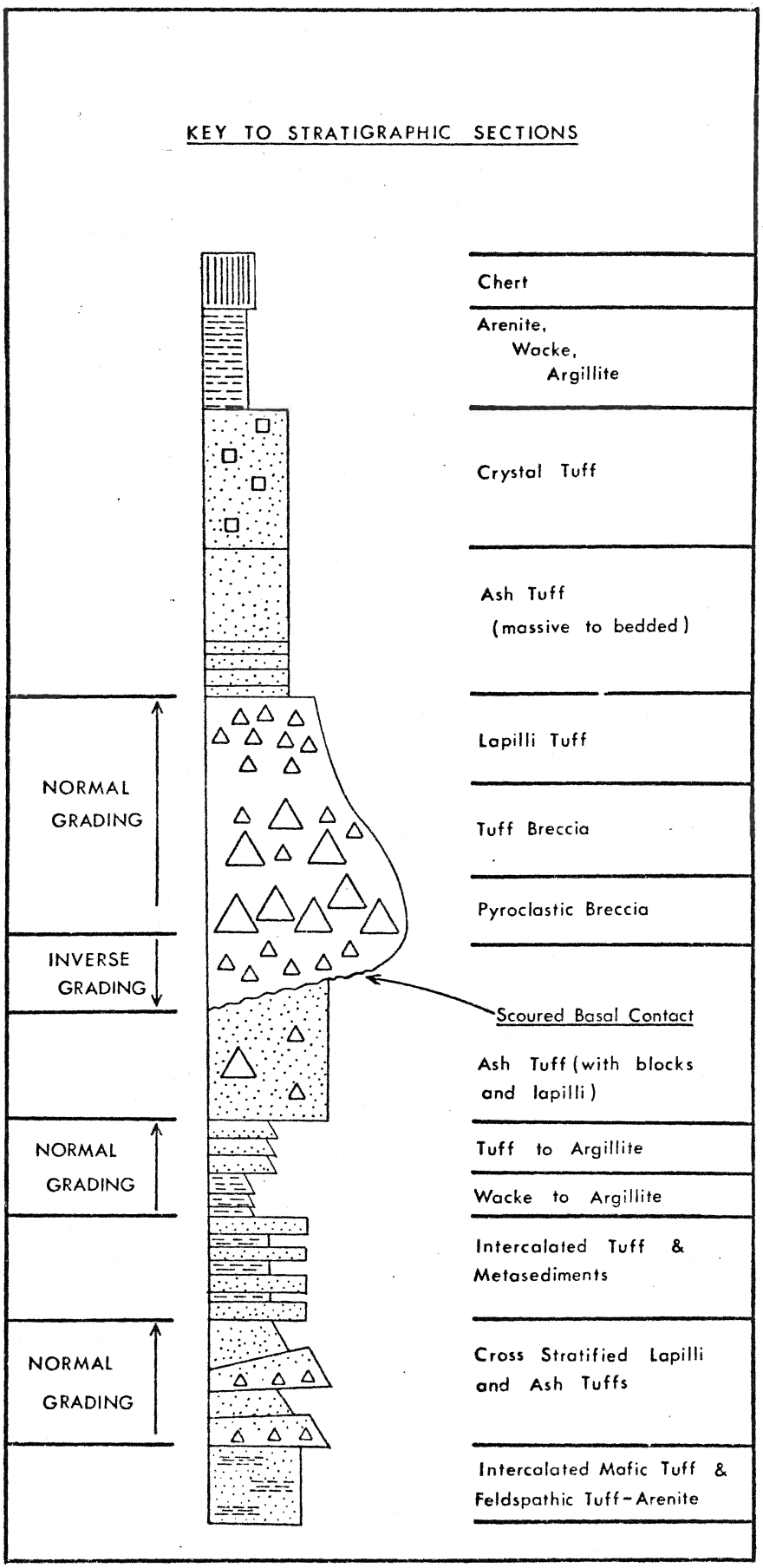

Figure 6a. KEY TO STRATIGRAPHIC SECTIONS.

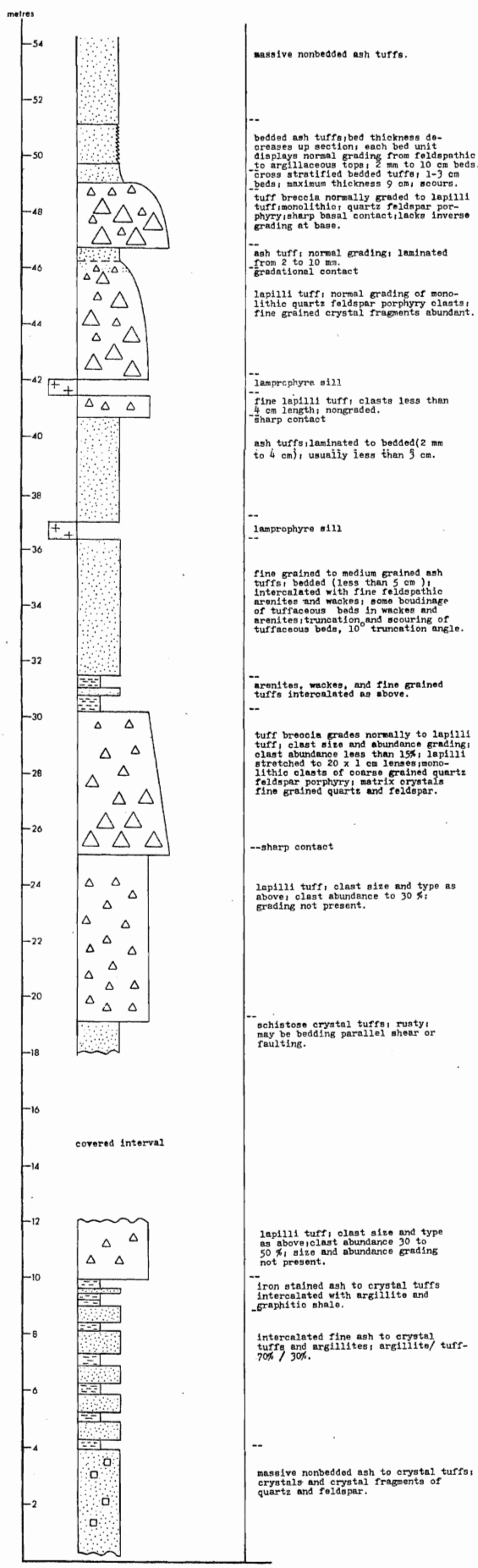

Figure 7. RUNNING ROAD STRATIGRAPHIC SECTION (PART 1).

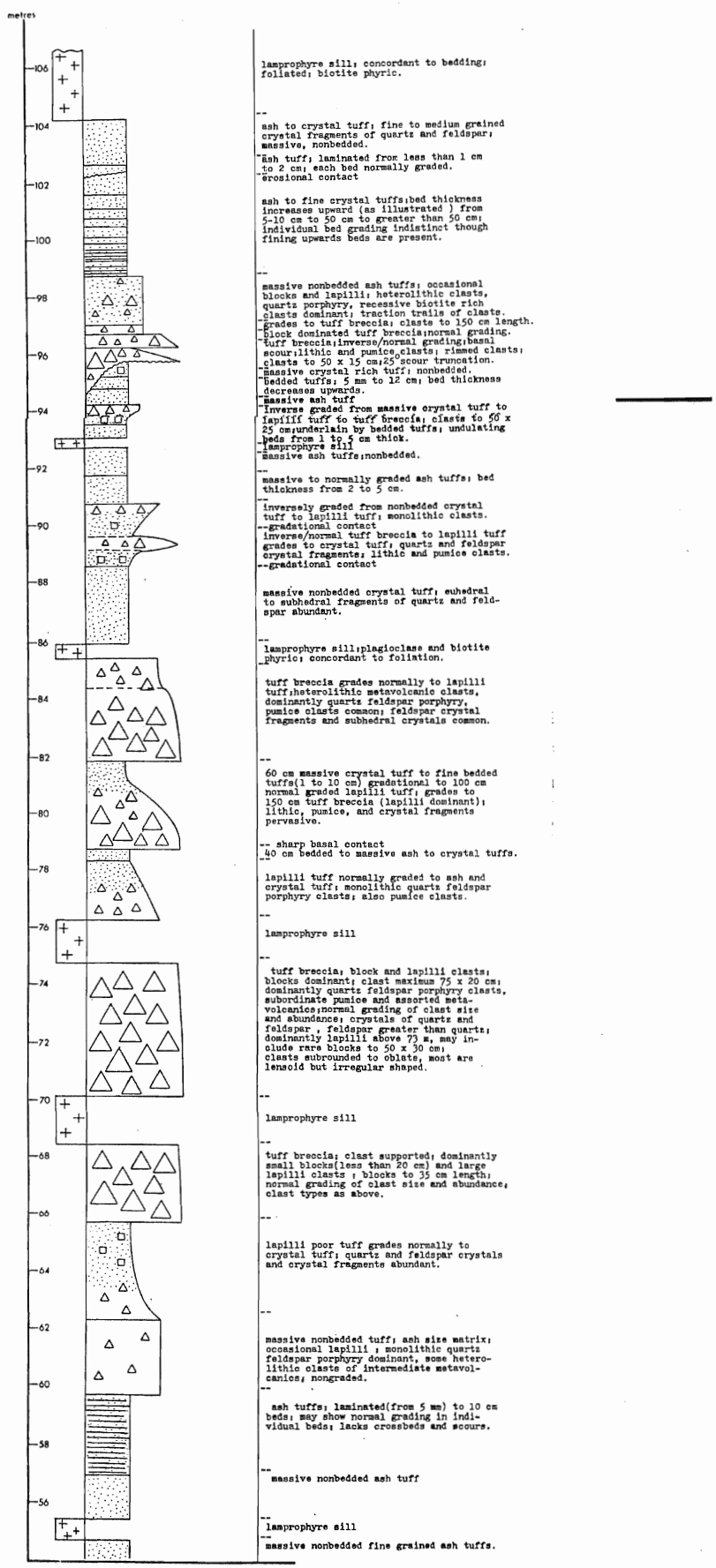

Figure 8. RUNNING ROAD STRATIGRAPHIC SECTION (PART 2).

pyroclastic deposits display a basal inversely graded zone, the 2a subaerial pyroclastic flow subdivision of Sparks et al. (1973) and Sparks (1976). The presence of the inversely graded zone is related to several factors (see discussion of inverse grading). Inversely graded zones were observed within the Berry Creek Complex, but show a sparse distribution. The coarsening upwards basal layers range in thickness from 20-75 cm and are dominantly crystal lapilli tuff although fine crystal tuff are also observed. The basal inversely graded layers appear to be discontinuous along strike although their occurrence shows no direct relationship with the thickness of the flow units. Flow deposits of less than 2 m thickness (see Figures 6 and 8, Running Road Section, 89 and 96 m) display basal 2a layers. The key to the measured stratigraphic sections is shown in Figure 6a. In some tuff breccia deposits, the lower inversely graded 2a zone is gradational from the underlying deposit (see Figure 6, Long Bay 4, Apache Landing Section, Figures 13, 24-28 m; 9, 3-4 m.) and also grades into the overlying flow (subunit 2b of Sparks 1976).

The basal contacts of tuff breccia and lapilli tuff deposits are commonly sharp and apparently nonerosive. Locally tuff breccias exhibit strongly erosional, undulating to channel form, basal surfaces. Locally an erosional base is followed by the 2a subunit of the tuff breccia to lapilli tuff flow units (see Figure 8, 94-96 m). Localized or channel deposition is well developed in the

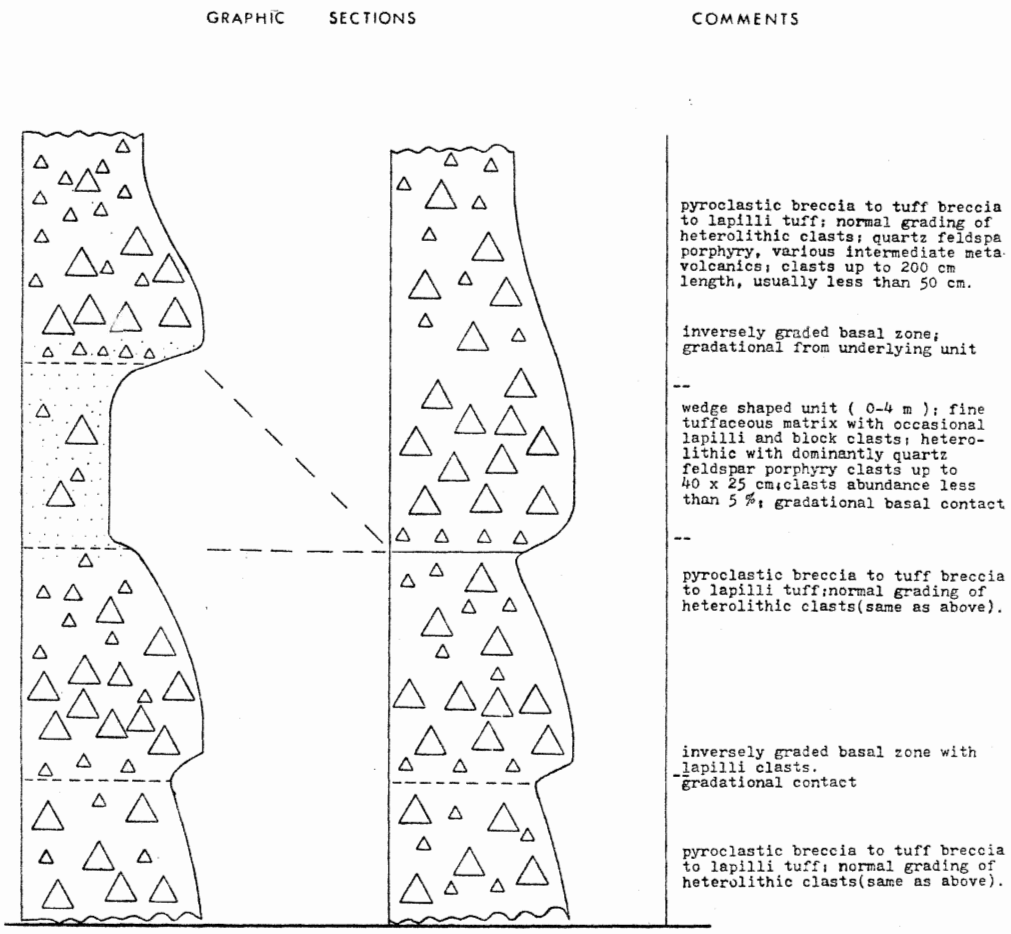

Figure 9. APACHE LANDING STRATIGRAPHIC SECTION.

Apache Landing measured section from an island in Long Bay (Figures 6 and 9). Flow unit 3 (8-12 m east section) is absent in the west section; the sections were measured less than 10 m apart. Apparent sharp nonerosional contacts between the basal 2a layer and the underlying debris deposits can be observed in Figures 8 (88m) and 14 (29 m). In the latter section, the fine upper division of the underlying debris unit has been preserved by a lack of erosive ability of the overriding flow unit. Development of a heterolithic

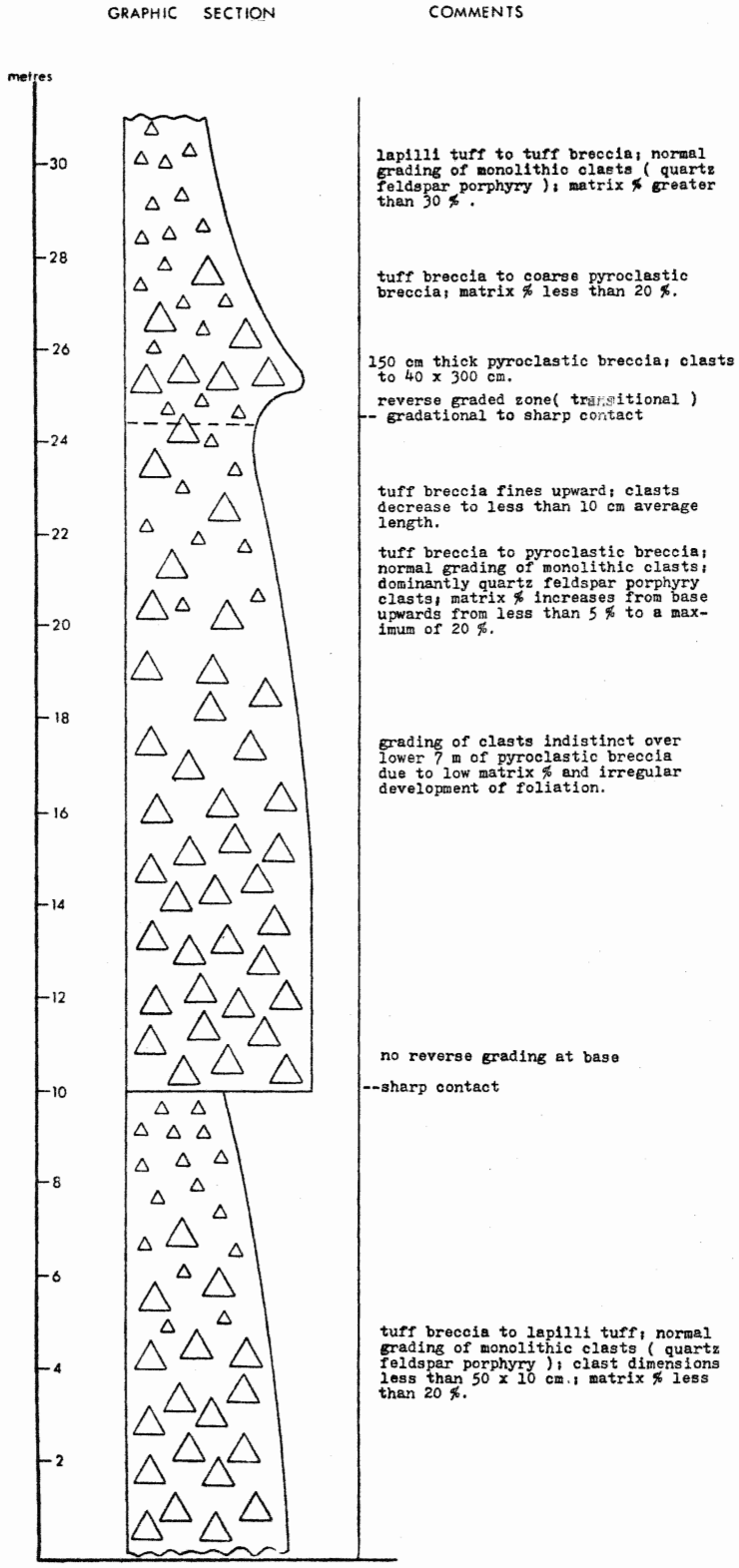

Figure 13. LONG BAY 4 STRATIGRAPHIC SECTION.

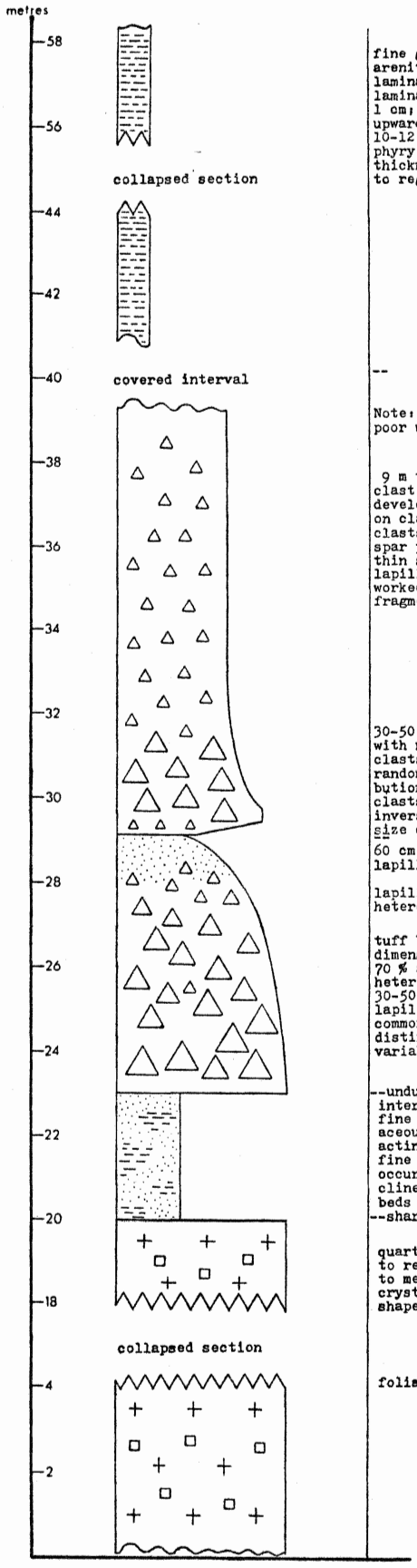

Figure 14. OLD WOMAN LAKE STRATIGRAPHIC SECTION.

coarse basal layer containing exotic and accessory rip-up clasts is common.

Although the distribution of heterolithic clasts within single debris flwo units is generally random (see Plate 5), some flow units exhibit a basal heterolithic zone and are transitional to monolithic to slightly heterolithic debris flows. Similar compositional clast grading has been observed by Buck (1978). Along the Maybrun Road section (see Figure 6), fine grained mafic clasts display normal distribution grading while the intermediate to felsic,

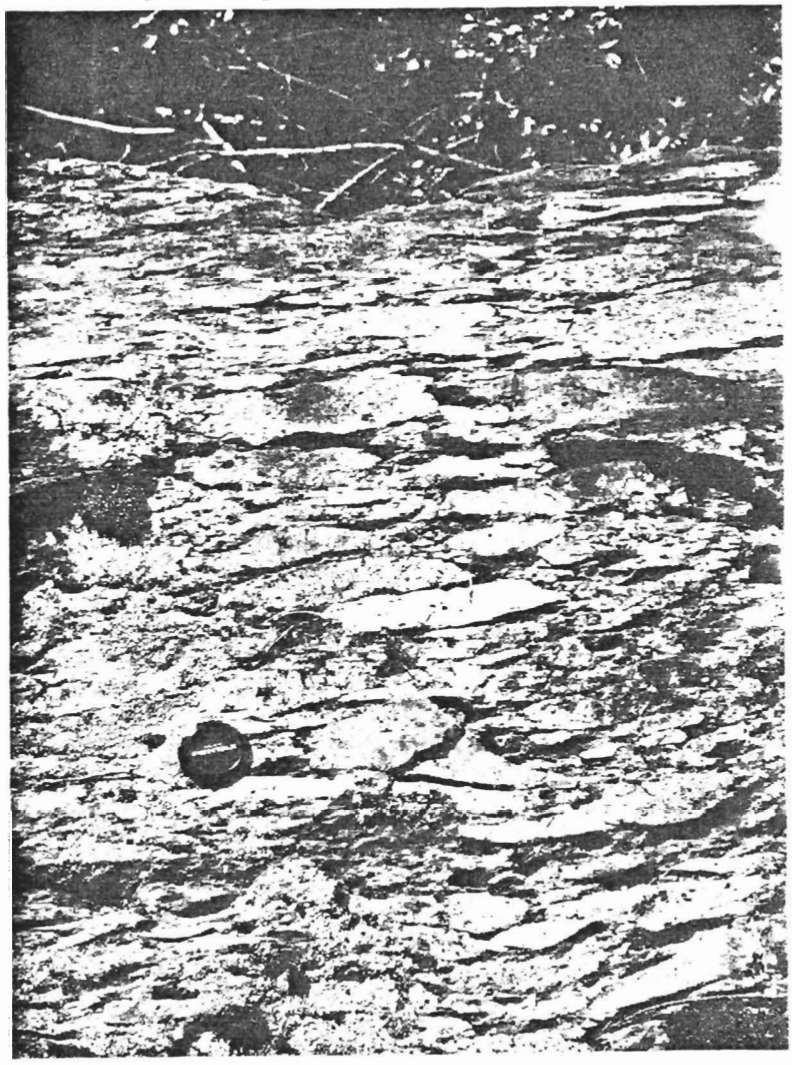

Plate 5. HETEROLITHIC FRAMEWORK DEBRIS FLOW, NORTH OF ROBERTS LODGE, LOBSTICK BAY.

porphyritic dacite clasts show a relative increase in abundance upward within the flow unit. Overall, the unit displays poor coarse tail grading. The basal contact was not exposed. Hornblende and garnetiferous mafic clasts occur in lensitic patches or zones ranging from isolated clasts to 15% of the flow unit.

In general, the lapilli to block size clasts show considerable overlap in any interval (less than 1 m generally) although normal coarse tail grading is commonly recognized. The increase in matrix percentage up section characterizes the normally graded deposits. Most of the tuff breccia and lapilli tuff units are matrix supported with clast abundances ranging from 15-65% of the unit volume. Figures 13 (10-25 m) and 8 (66-78 m) display thick tuff breccia deposits with massive nongraded to very poor coarse tail grading of lithic and pumice clasts.

Typical moderate rate of grading are exhibited in Figure 16 (9-19 m). In contrast, Figures 15 (12-14 m), 16 (26-33 m), and 14 (33-38 m) show rapid, coarse tail grading from block dominant tuff breccia to lapilli tuff or finer deposits. In the Old Woman Lake Section (30-38m), the rate of grading decreases sharply after depletion of components coarser than lapilli. Above 32.5 metres, the deposit displays frequency grading of lapilli clasts. In several tuff breccia and lapilli tuff units, rapid upward frequency and distribution gradients (i.e. fining of clasts and matrix to ash size particles only) occur over a vertical

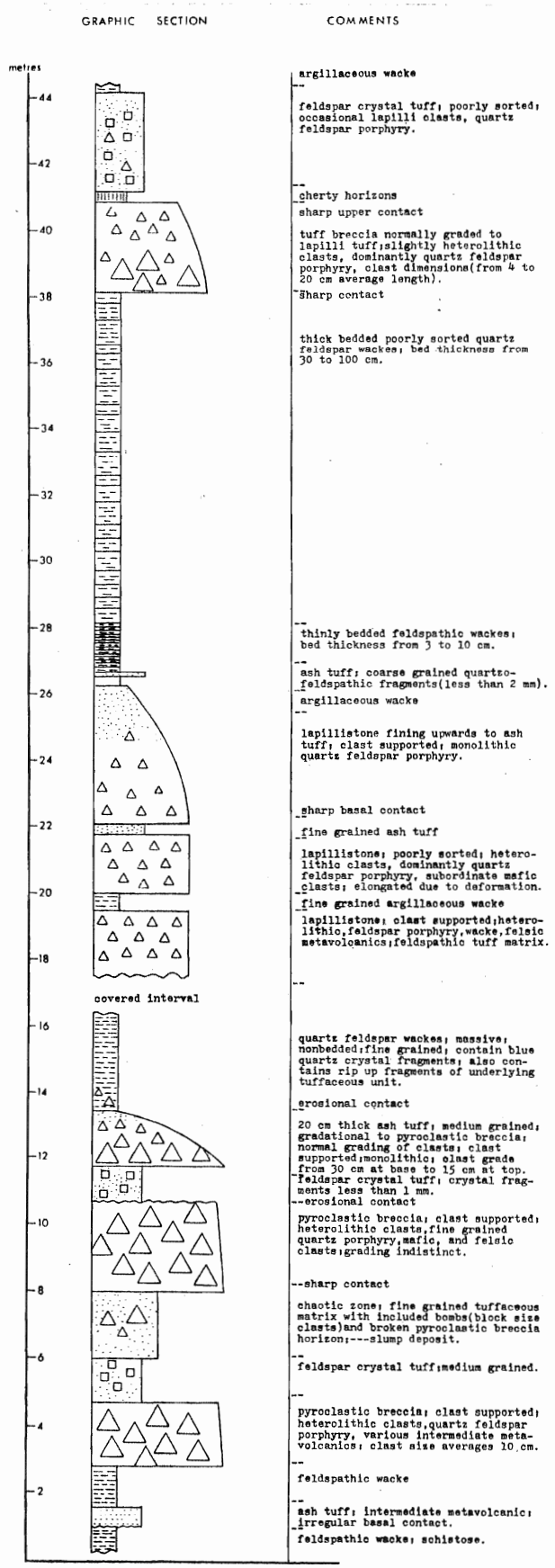

Figure 15. MIST INLET STRATIGRAPHIC SECTION.

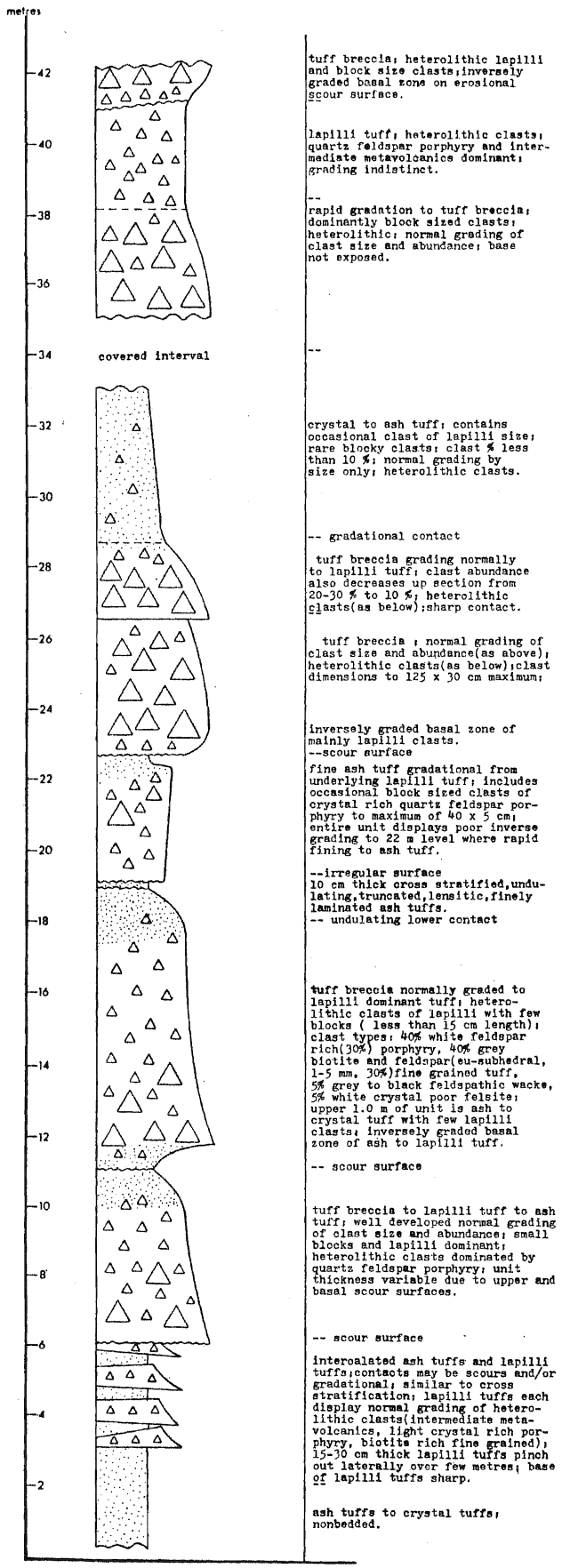

Figure 16. GREAT BEAR STRATIGRAPHIC SECTION.

thickness of 5-10 cm (see Figures 8, 81-82 m; 7, 46-47 m; 16, 22-23 m). The fining trend defines a sharp change in the depositional behaviour of the specific flow unit. The gradation over 5-10 cm intervals from the underlying deposits suggest temporal continuity of deposition. This trend of rapid fining over several centimetres was also observed in a single inversely graded lapilli tuff deposit (Figure 16, 22-23 metres). The fine tuff units are massive and nonbedded or laminated to thin bedded (3 mm to 3 cm, see Figure 10, 6-6.5 m). Normal distribution grading analogous to the a2a3 zones of the modified Bouma cycle is common.

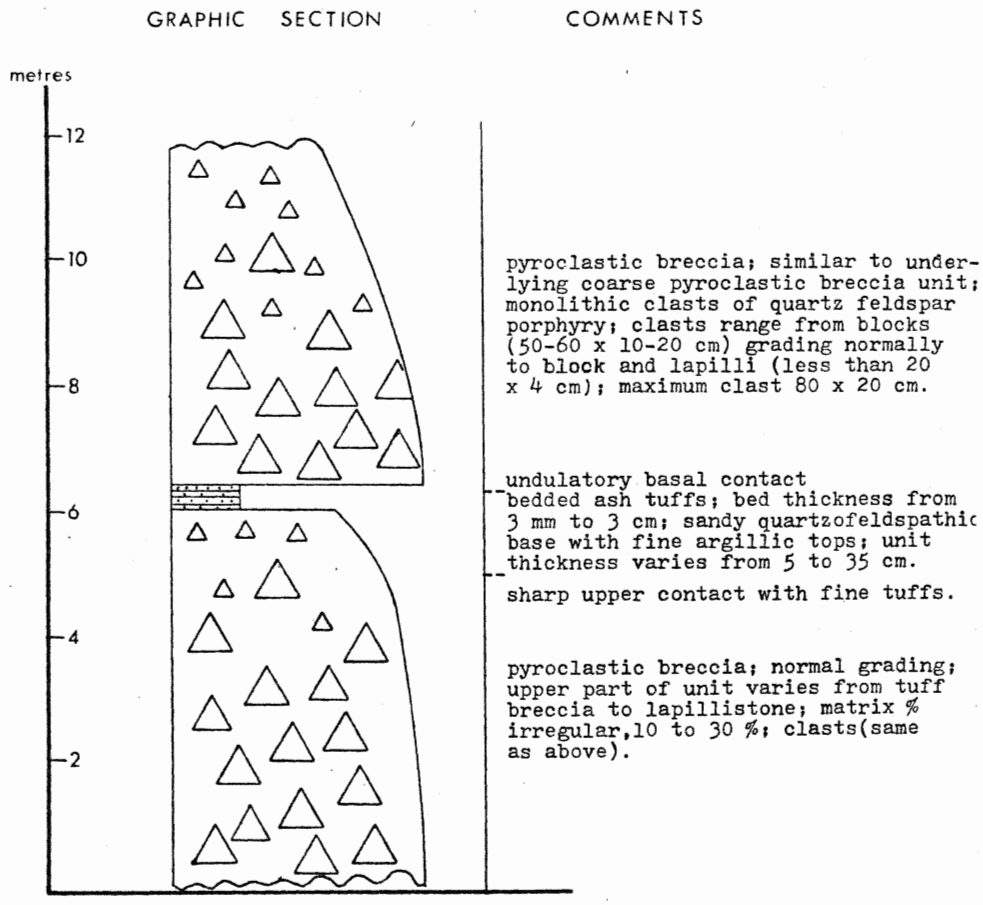

Figure 10. LONG BAY 1 STRATIGRAPHIC SECTION.

Tuff, Crystal tuff

Tuff occurs as massive or graded lenticular to sheetform deposits varying in thickness from several centimetres to a few tens of metres, although single tuff units rarely exceed 2-3 metres. Dark, blue-grey, intermediate to felsic ash tuff predominates, but fine to ultrafine feldspathic to argillic tuff is composed of fine fragmented feldspar crystals or pale to dark green saussuritic components, respectively. Ash size fragments in the tuff are subangular to subrounded with poor to moderate sorting. The fine, inequigranular, crystal fragments (broken and commonly very angular) provide a framework support in the coarse crystal rich ash tuff. Angular to subrounded blue quartz phenoclasts (0.5-1 mm) occur throughout the fine tuff deposits.

At Reed Narrows, couplets of feldspathic to feldspar phyric ash to crystal tuff grade to fine to ultrafine argillic tuff. Individual beds range in thickness from 0.5 to 10 cm commonly with normal distribution grading. The entire bedded to laminated sequence exhibits a well developed double grading pattern (Fiske and Matsuda 1964). The feldspathic tuff to argillic tuff ratio decreases systematically with increasing stratigraphic height (see Plate 6). The distribution grading is common and exhibited in normally graded, fining upwards, ash to crystal tuff throughout the Berry Creek Complex. The upper bed unit is characterized by ash

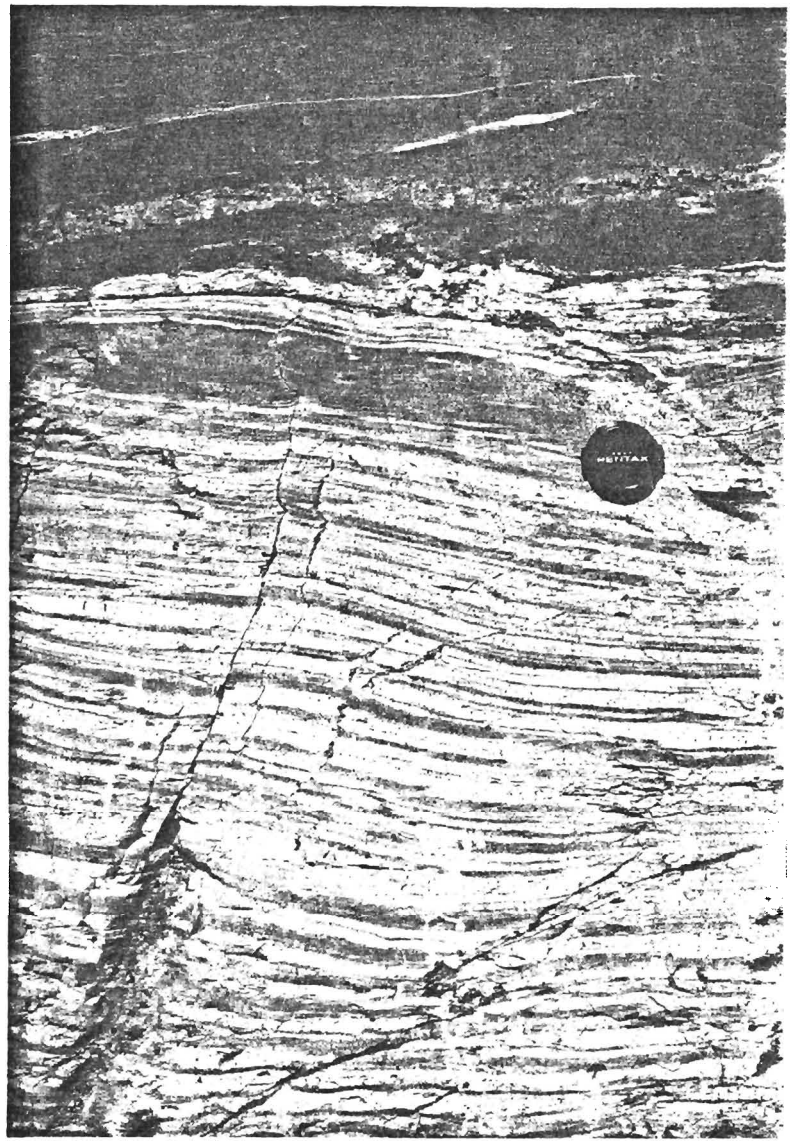

Plate 6. DOUBLY GRADED SEQUENCE OF FINE TO ULTRAFINE TUFF AND ARGILLITE, REED NARROWS. SECTION YOUNGS UPWARD.

tuffaceous material with minor coarse ash or phenoclast component in matrix support. The grading patterns are analogous to those described by Cas (1979) for a2, a3,e subdivisions of the revised Bouma sequence.

Bedding and laminations with the fine ash tuff beds are locally well developed. Beds range from 1-5 cm, although thickly bedded (30-100 cm) sequences are also observed (see Figures 8 and 11, Running Road and Long Bay

2 Sections). The frequency of the bed thicknesses within ash tuff sections are either **random** or exhibit a gradual thinning up-section. Parallel stratification is the dominant bedform (see Plate 7), although oblique stratification and cross bedding are common (see Plate 7). The stratification occurs as 1-35 cm beds or fine laminae from 2-10 mm thick. Stratification is easily recognized due to recessive upper bed units formed by preferential

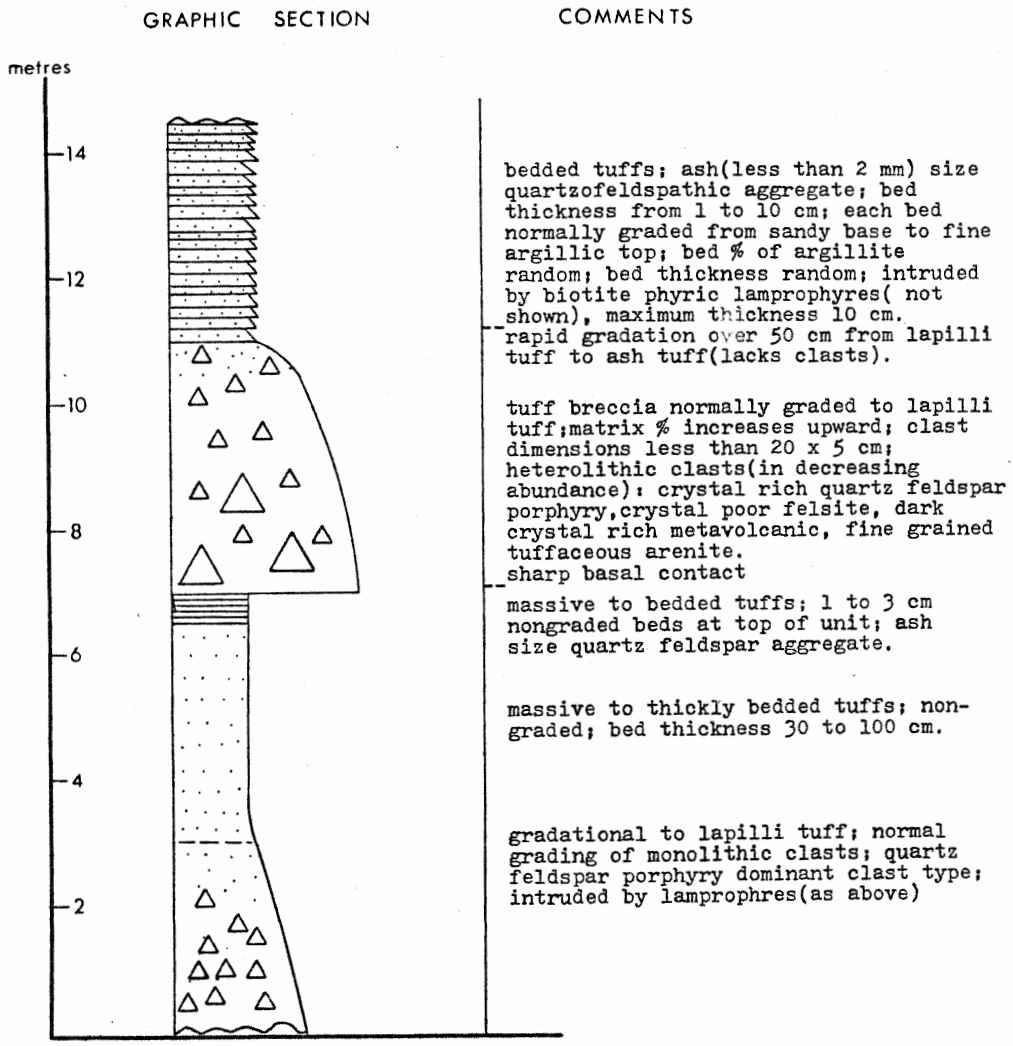

Figure 11. LONG BAY 2 STRATIGRAPHIC SECTION.

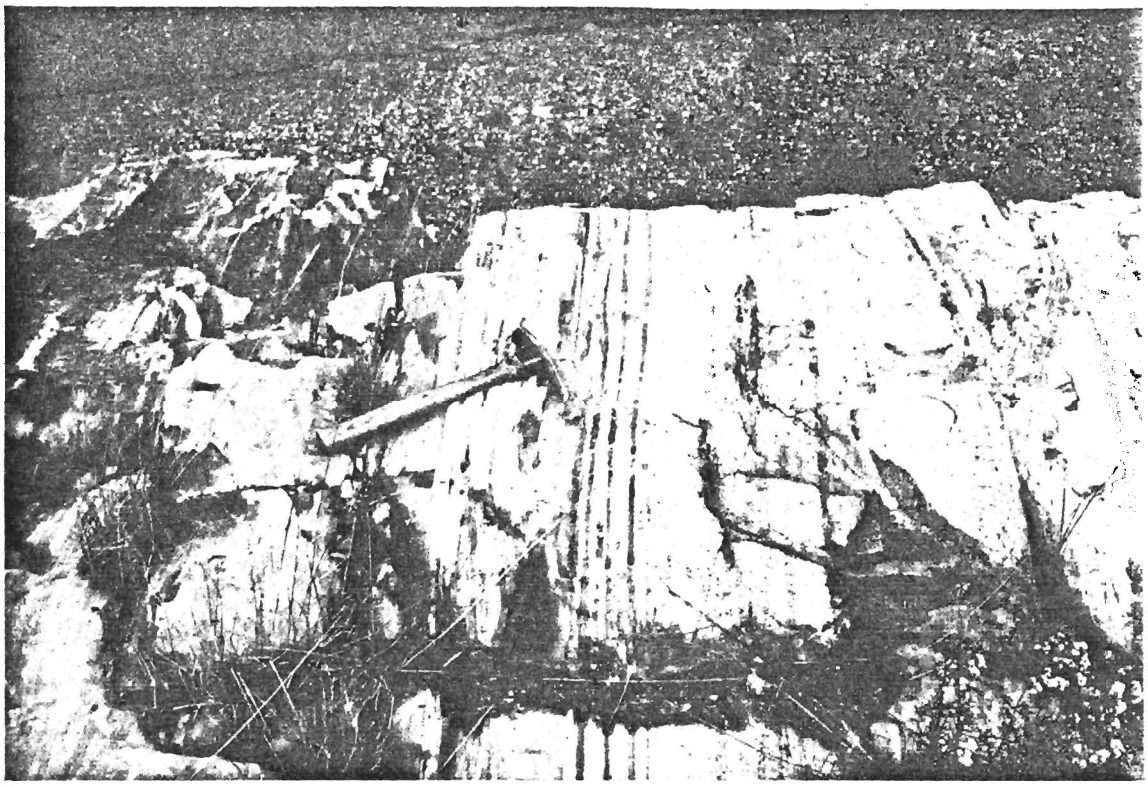

Plate 7. BEDDED TUFF, RUNNING ROAD SECTION. TUFF UNITS ARE NORMALLY GRADED WITH RECESSIVE UPPER ZONES LOCAL EROSION AND CROSS BEDDING.

weathering of the fine ash components (see Plate 7). Tasse et al. (1978) suggested that the interlayering of fragments of different sizes and specific gravities produced bedding parallel grading or parallel stratification. The oblique stratification generally forms by distribution grading oblique to the bedding (Tasse et al. 1978), and is most commonly observed as troughs or cross beds with normal grading of lapilli to ash size fragments. Beds within the crossbedded units of the Great Bear section (see Figure 16, 3-6 m) maintain thicknesses from 15-40 cm. The intercalated basal lapilli tuff displays basal scour contacts and poorly developed frequency grading of heterolithic clasts. The beds appear

to pinch out laterally over several metres.

Fine tuffaceous deposits commonly occur between coarse debris flow units (dominantly tuff breccia and lapilli tuff units) (see Plate 8, from Long Bay 1 section, Figure 1Ø). Bedforms of these tuffs include massive and nonbedded units, as well as finely laminated to finely bedded (less than 3 cm) units which rarely display macroscopic distribution grading.

Plate 8. THIN BEDDED TUFF BETWEEN TWO DEBRIS FLOWS, LONG BAY 1 SECTION, NOTE BIPARTITE STRUCTURE AND POOR GRADING OF MONOLITHIC CLASTS.

The crystal tuff units are gradational to fine ash tuff with fining upwards trends. They form composite deposits with, and are gradational from, lapilli tuff and tuff breccia. Discrete crystal tuff units vary in thickness from 10-50 cm to tens of metres. It is commonly difficult to isolate individual thick deposits from several amalgamated tuff units. A 40 metre thick crystal tuff along Highway 71 near Running Road displays well developed vertical compositional grading from a feldspar phyric base (25 m thick) through a transition zone (approximately 10 m thick) to a quartz phyric upper layer (minimum 8 m thickness). Frequency and distribution grading, though common in the quartz and feldspar phyric crystal tuff of the Berry Creek Complex, were not observed.

Crystal tuff occurs as crystal rich basal layers (2a subunit of Sparks 1973) within pyroclastic flow deposits. Such units exhibit massive nongraded or inverse (frequency) grading. The upper contacts are usually gradational over 5-30 cm to lapilli tuff and tuff breccia. Examples of these trends are shown in Figure 8 (89 m). The crystal tuff units are laterally discontinuous over a few metres and never exceed 40-50 cm in thickness. Exposures of such basal layers are rare in the Berry Creek Complex. Sparks (1973) notes that the basal 2a layer is absent or maintains a patchy discontinuous distribution at many locations.

Finely laminated to finely bedded, fine to ultrafine tuff exposed west of Apache Landing in Long Bay, exhibit an abundance of primary sedimentary and synsedimentary

deformation structures, which were subsequently modified by tectonic deformation of a brittle nature. Preservation of primary bedding features are commonly obscured by penetrative fabrics (incipient to pervasive mica-chlorite foliations). The fine tuff beds characteristically display a stronger fabric than the adjacent coarse fragmental debris flow deposits. Interpretations of the fine deposits are commonly masked by secondary fabrics, especially within the immediate proximity of the Pipestone - Cameron Fault Zone. The Apache Landing tuff is glassy with well developed conchoidal fracture and is extremely brittle. Early soft sediment structures include graded bedding and laminae, flame and load structures and rare dewatering structures. The fine beds show distinct colour changes with grain size and range from yellow, brown, grey and locally black. Plate 9 displays fine synsedimentary deformational structures and modifications by tectonic stresses. On outcrop scale, the tuff is locally massive, but changes rapidly over several centimetres to a predominantly slump folded sequence of thin bedded tuff. The 1-5 cm S-shaped slump folds display a parasitic east-west vergence (see Plate 10). Thickening at hinges and thinning slightly oblique to fold limbs accompanies the nonpenetrative spaced cleavage. Microfaulting along the cleavage is common (Plate 9).

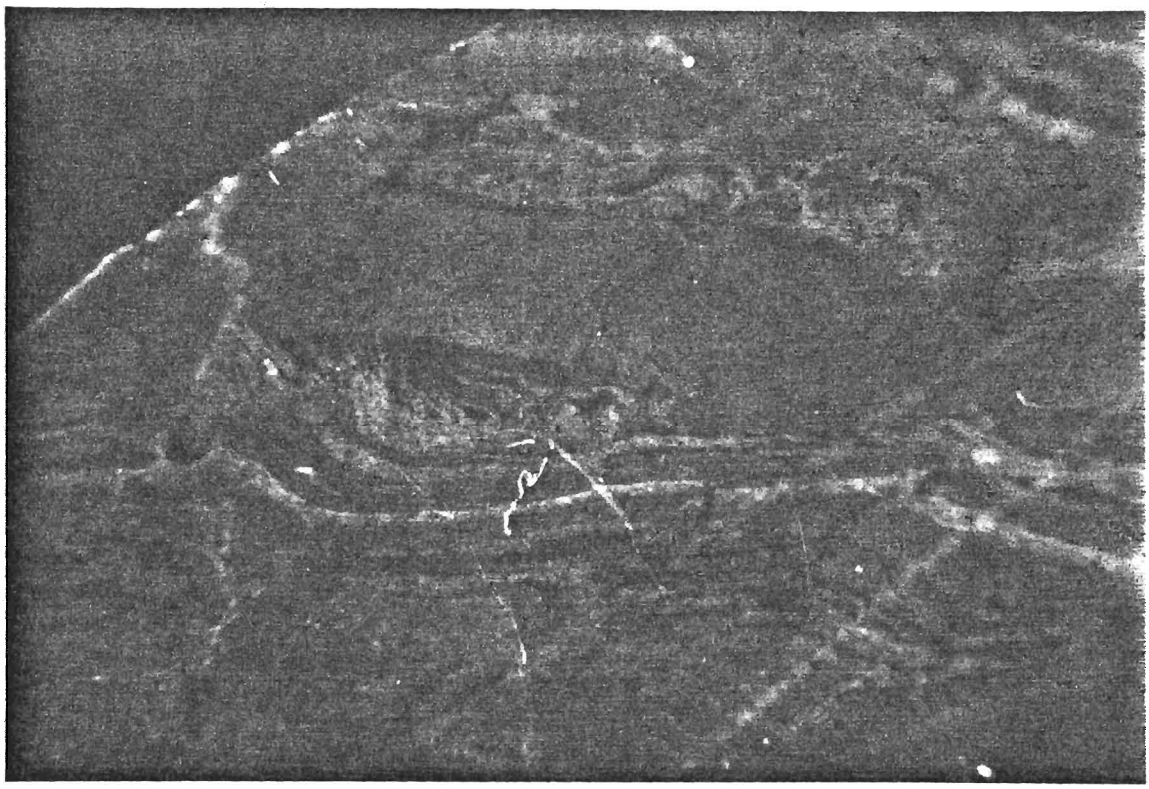

Plate 9. FINE BEDDED TO LAMINATED TUFFACEOUS SEDIMENT, WEST OF APACHE LANDING, LONG BAY. NOTE THIN LAMINAE, DEWATERING STRUCTURES, MICROFAULTING.

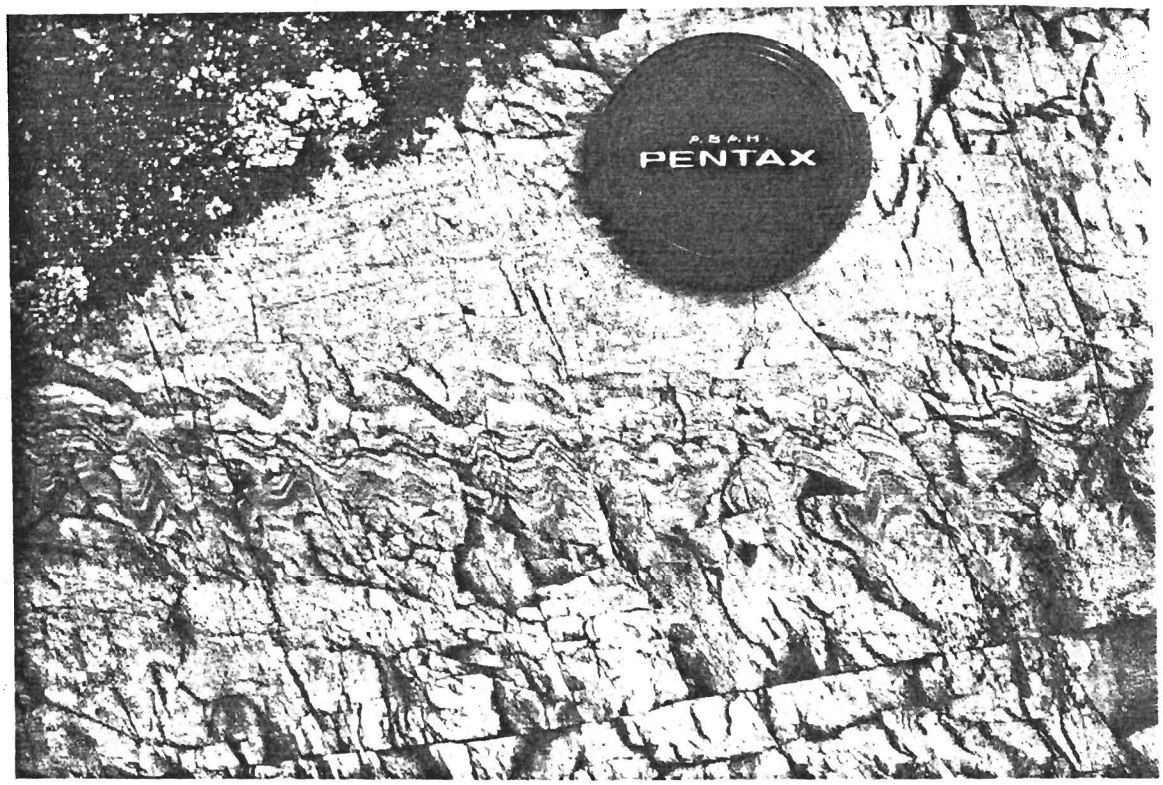

Plate 10. EXPOSURE FROM WEST OF APACHE LANDING, SAME LOCATION AS FIGURE 9, NOTE FOLDING BY SYNDEPOSITIONAL SLUMPING.

Lapillistone,Pyroclastic breccia

Lapillistone and pyroclastic breccia comprise the framework (matrix poor) equivalent of lapilli tuff and tuff breccia, respectively. These deposits, although less commonly observed than the matrix supported tuff, normally form the lower portion of the basal 2b layer (Sparks et al. 1975; Sparks 1976) of a debris flow unit (see Figure 8). The majority of the pyroclastic breccia and lapillistone units are monolithic deposits containing lithic and pumiceous clasts of porphyritic dacite. Heterolithic, low matrix deposits are sporadically distributed (see lahars in Secondary Deposits section). The matrix poor, clast supported (framework) deposits are lenticular to channel form in distribution. They are related to localized coarse debris flows which are topographically controlled and rarely sheetform deposits. Measured clast supported units range in thickness from 1-10 metres.

Figures 12 (0-8 metres) and 13 (10-20 metres) show a typical transition from the clast supported to matrix supported deposition by the following: 1) size distribution grading; 2) frequency grading; 3) coarse tail grading; 4) any combination of the above. The matrix component shows an increase from less than 5% in many deposits to 25% in the upper transition zone of the clast supported deposit. Continuous increases in the matrix content through the matrix supported 2b layer characterize a normally graded flow unit.

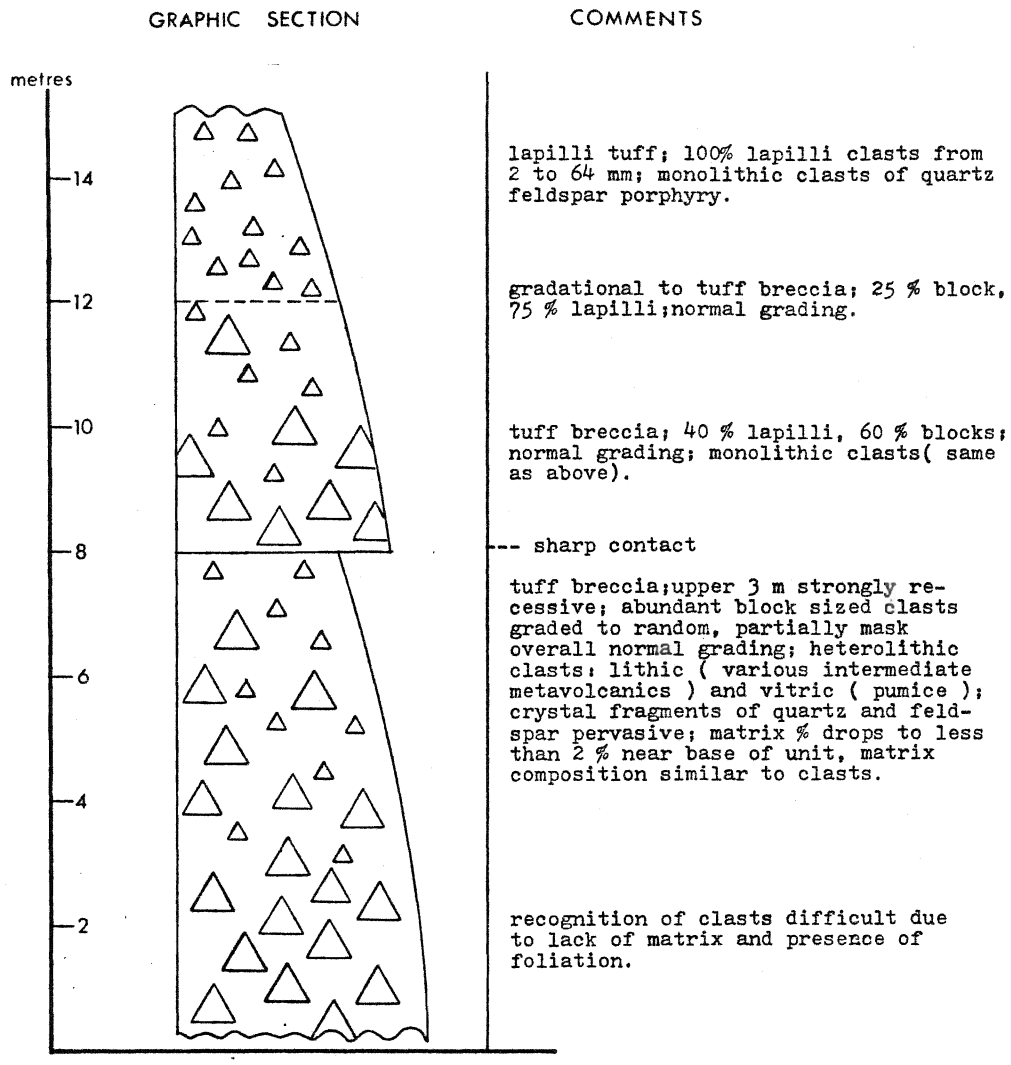

Figure 12. LONG BAY 3 STRATIGRAPHIC SECTION.

The upper portion of the 2b normally graded layer is commonly gradational into the overlying layer 3 (Sparks et al. 1973); a fine ash to crystal tuff. However, the sharp change from the underlying coarse debris flow (subunit 2b) to the overlying layer 3 can be observed in Plate 8. The erosional slightly undulose basal contact of the subsequent coarse debris flow is also exposed. Locally, the transition from layer 2b to layer 3 consists of a sharp

contact (Figures 7, 46-47 metres, 8, 81-82 metres) or very rapid gradation (Figure 10, 6-6.5 metres) over less than 30 cm to a 10-50 cm thick ash to crystal tuff.

As was observed in the tuff breccia and lapilli tuff units, conflicting facing directions due to local changes in size distribution grading are common in the coarse matrix poor deposits. In Long Bay, at least five units with completely gradational inverse/normal graded zones occur over a 75 metre section. Younging directions were obtained from a single, lapilli dominant, pyroclastic breccia which contained exotic rip-up clasts in the coarse basal 2b layer. Distinction of single clasts, their dimensions and margins, is difficult in the matrix poor deposits.

Much of the monolithic tuff breccia (matrix supported) is gradational from the coarse pyroclastic breccias and/or lapillistones. In many areas, where a gradation can be traced, the basal 2b layers are: 1) massive with no discernible fragments; 2) massive with a splay-type foliation which may outline primary clast; or 3) a clast supported fragmental deposit with recognizable matrix between the clast components. The splay-type foliation consists of sericite-muscovite +- chlorite +- epidote displaying an incipient to locally pervasive penetrative fabric. The foliation is characterized by shallow arcuate surfaces which commonly mimic the lensitic shape of deformed clasts. Problems exist because the low matrix monolithic pyroclastic breccia types cannot be

distinguished from crystal tuff or lava flow breccias unless grading of fragments is observed. The splay-type foliation, characteristic of relatively homogeneous volcanic deposits (Poulsen, p. comm. 1982), may occur within any of the forementioned types, precluding the rapid recognition of the splay foliation as primary clast boundaries.

Tuff (plus blocks and lapilli)

Variations in the simple normal graded patterns are observed in several depositional units. Fragments of lapilli and blocks occur together with a progressive upward increase in the lapilli/block ratios. In the lapilli zone (upper 2b of Sparks et al. 1973) of debris flows, lapilli can be accompanied by 2-5% blocky clasts. The blocks are randomly distributed and may persist into the layer 3 flow unit. Gradations of this type are observed in Figure 16, (29-33 m), where lapilli and blocks comprise 5-10% of the unit mode.

A second type of deposits are essentially nongraded with sparse lapilli and/or blocks. The scattered clasts have been observed in Figure 9 (8-12 m, eastern section) which exhibits the wedge from of a valley filling deposit. Several of these units were observed on the islands in Long Bay. The clasts are commonly heterolithic although quartz and feldspar phyric dacite is predominant. Subordinate grey porphyritic dacite, minor sediments and pumiceous

fragments are present. In the latter, fragments observed in the Great Bear section (Figure 16) and Long Bay sections have the morphological features of silicified shards in an aphyric groundmass.

Lava Flows

Intermediate to felsic lava flows of the Berry Creek Complex are exposed near Dirtywater Creek, along the southern margin of the Sanford Lake granodiorite lobe of the Dryberry Batholith, and also along the north shore of Lobstick Bay. The latter extends from the mouth of the Berry River to the eastern end of Lobstick Bay. Each of these two areas displays unique and markedly contrasting textural, mineralogical and morphological features.

The Dirtywater Creek lava flow parallels an east-west trending linear ridge between Dirtywater Creek to the south and the underlying amphibolite and metasedimentary horizons of the Warclub Group. The maximum thickness of the flows reaches 65 to 75 metres with an observed lateral extent of 250 to 300 metres. Field mapping has not yet delineated the maximum eastward extent of the lava flows; present mapping suggests that the flow either pinches out to the west, as suggested by the orientation of flow laminae, abut against the granitoid intrusions, or is bounded by a north-south trending fault zone (Johns and Davison 1982).

The lavas consist dominantly of pink to buff quartzo-feldspathic domains, intercalated with thin buff, dark green and greenish-black domains. The latter are strongly

recessive on the weathered surfaces, and are composed of chorite (after biotite), biotite, quartz and feldspar. The domains average 0.5 to 1 cm in thickness, but range from less than 1 mm to a maximum of 4 cm. Each domain probably represents relict flow layering developed during extrusion and lateral flowage.

Three distinct layering types were observed: 1) chlorite, biotite, quartz and feldspar, 2) quartz and feldspar (feldspar greater than quartz) and 3) quartz with minor feldspar. The feldspathic layers are characterized by incipient sericitization and kaolinization. The layers can be traced over tens of metres although each layer may vary considerably in thickness. Primary flow folding of the flow layers has resulted in asymmetric, complex fold patterns. Systematic flow fold variation across the flow sequence was not observed.

Tectonic deformation complicates the primary layering pattern by isoclinal folding and layer transposition. Thickening and thinning of flow layers within fold hinges and limbs, respectively, also disrupts spacing and dimensions of primary flow layering.

The Lobstick Bay - Maybrun lavas consist of massive to brecciated, highly porphyritic dacite associated with an apron of cogenetic fragmental deposits (see also Secondary Deposits). The lavas are comprised of 10-40%, euhedral to subhedral, 1-10 mm quartz and feldspar phenocrysts (quartz more abundant than feldspar) set in a white to buff

weathering, dark blue grey to greyish black glassy groundmass. Flow laminae are strictly absent from the Lobstick Bay flow sequences.

Within flow units the lavas contain lobes of fragmented quartz feldspar porphyry (massive lava flows) clasts in a hyalotuffaceous matrix of finely comminuted porphyritic dacite. The lobes vary in size from less than one metre diameter to tens of metres. Boundaries between massive and brecciated lobes of porphyritic dacite vary from sharp to gradational over tens of centimetres. Clasts of quartz and feldspar phyric dacite range from subrounded to subangular in shape and generally exhibit the effects of flattening deformation. In the matrix support lapilli tuff and tuff breccia units, subrounded to rounded clasts maintain their original dimensions. Clast dimensions within the lobes grades from fine lapilli to blocks up to 25 cm. Individual lobes can be described as lapilli tuff, tuff breccia and pyroclastic breccia (OGS classification, 1982) based on relative size and abundance of clasts and matrix.

Difficulties in assessment of the distribution pattern is hindered by lack of recognition of flow boundaries. Problems also arise due to the compositional similarities between the clasts and matrix. Recognition of clasts in low matrix, clast supported lobes can be facilitated by use of polished slabs. In outcrop, the presence of an incipient to pervasive splay foliation inhibits the distinction of the boundaries of clasts. In some rocks,

the foliation, within low matrix, clast supported breccia, follows a preferred path within the matrix and around the periphery of the clasts. The monolithic fragmental lobes show a massive nongraded character. Clast dimension variations are restricted within individual lobes though clast dimensions within flow sequence is extremely variable.

The lower part of the flow sequence is gradational to massive quartz feldspar porphyry subvolcanic intrusions. Brecciated flow lobes decrease in abundance northeastward toward the Kishquabik syenodiorite complex. Phenocryst content increases towards the subvolcanic sill zone with 40-55% quartz with subordinate feldspars. The porphyritic intrusions grade into quartz phyric granodiorite. Mafic xenoliths are common in the subvolcanic porphyry intrusions and the margins of the granodiorite. The granodiorite is similar in appearance and composition to the granodiorite lobes of the Dryberry batholithic complex.

Monolithic debris flow deposits and hyalotuff characterize the upper and distal sections of the Lobstick Bay flow sequence. These deposits display a microbreccia matrix containing quartz and feldspar phyric dacite clasts derived from massive and brecciated lava flows. Hyalotuff and mass flow deposits are distinguished from the flow lobes by: 1) normal distribution of the clasts, size sorting of the clasts (lapilli dominant or block dominant deposits are common), and 2) extensive lateral distribution

of the deposits (up to 10 km extending from the core of the flow sequence). The thickness of the deposits ranges from 1-20 metres.

In the near vent region, these mass flows are amalgamated into thick deposits, while the more distal deposits are commonly intercalated with metasediments and pyroclastic ash and debris flows. A massive porphyritic dacite is exposed along Lobstick Bay from Roberts Landing west to Long Bay between Reed Narrows and Berry River. The deposits, texturally and compositionally, resemble the massive flows near the Maybrun Road section. Locally, sorted and graded, clast supported lenses and the lack of distinctive flow lobes suggest an origin by ablation and deposition of a hyalotuff, derived from the advancing and slumping lava flows (massive and brecciated) (Walker 1979; and others). The association with, and gradation from, adjacent debris flows of flow lava derivation are consistent with this interpretation. The thickness of the hyalotuff and debris flow deposits increases westward from the flow front zone. The massive to locally fragmental dacite may represent the distal equivalent of the coarse hyalotuff and monolithic debris deposits common in the eastern sector of Lobstick Bay.

Tectonism of these deposits consists of: 1) narrow intensely brecciated zones, generally less than 1 metre with an apparent random spacing (contains fragments of quartz feldspar porphyry in iron stained tectonic microbreccia) and 2) incipient to pervasive splay foliation

subparallel to the strain zones.

Lineated and garbenschiefer arrays of tourmaline are common along the sericitic and muscovitic schistosity planes. Thin (< 3 cm) veinlets of quartz and tourmaline intrude the massive dacite breccia. Dark green to black tourmaline occurs as 1-5 mm radiating clusters. The discordant veinlets commonly display right lateral offsets and detached fold limbs with displacement parallel to the regional splay foliation.

Secondary Deposits

The secondary pyroclastic deposits consist of laharic and slump deposits derived from mass flowage of primary volcanogenic material. As Buck (1978) noted, no single criterion can be used to distinguish between primary and secondary deposition. In the Berry Creek Complex, the laharic units maintain a number of features common to the primary debris flows. These include: 1) monolithic to heterolithic clast types; 2) presence of normal distribution and frequency grading of clasts; 3) a matrix composed of quartzofeldspathic material with a minor micaceous component; 4) erosional basal contacts; and 5) occurrence as sheetform, lenticular or channelform (valley fill) deposits.

Features, exclusive to laharic and laharic - epiclastic deposits, commonly include: 1) marked compositional contrasts between clasts and matrix; 2) mafic

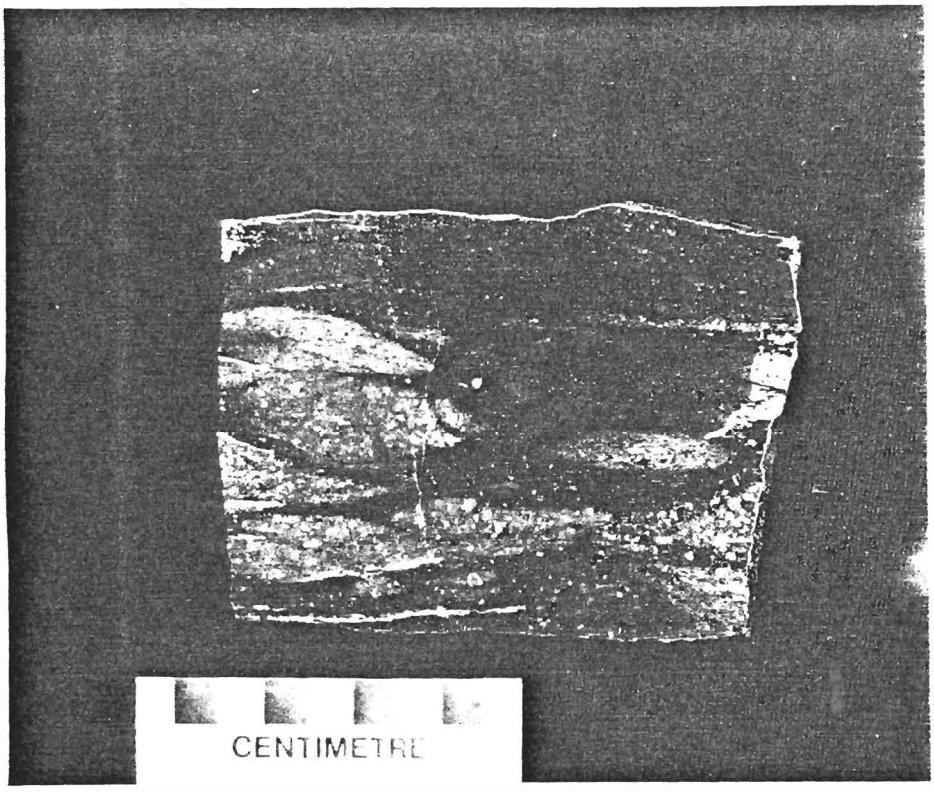

Plate 11. HETEROLITHIC DEBRIS FLOW CONTAINING A VARIETY OF PUMICE FRAGMENTS AND LITHIC CLASTS, LONG BAY, NOTE PRESERVATION OF PRIMARY TEXTURES.

ash with monolithic and/or heterolithic clasts; 3) combination of mafic ash with epiclastic or tuffaceous matrix plus heterolithic clasts; and 4) absence of pumice fragments. The latter is less restricted since Sparks (1976) has interpreted pumice fragments in mudflows. Reworked lahars are usually devoid of pumice shards and clasts.

Distinction between depositional types can be based on variations with the forementioned criteria. In regard to clast and matrix evaluation, three specific examples from the Berry Creek metavolcanics can be illustrated. In the Long Bay islands, several heterolithic deposits contain as many as four varieties of pumice and several lithic clasts within a single flow unit. Pumice types display a wide

variety of colour, morphology and degree of vesiculation. Plate 11 shows a slab of the heterolithic laharic deposit. Although the primary debris flows may be heterolithic, a laharic origin is suggested by : 1) variety of pumice clasts; 2) variety of lithic clasts; 3) high percentage of heterolithic clasts relative to porphyritic dacite (lithics and pumice; dominant component of primary pyroclastics); 4) hematite dusted matrix (possibly inclusive of muddy component from paleosurface)and 5) lack of glassy dacitic rims on the clasts (precludes vent origin; see section of rimmed clasts in primary pyroclastics).

Similarly a coarse lahar in the Maybrun stratigraphic section (see Figure 6) contains lapilli to blocky clasts. The lahar contains a high proportion (greater than 65%) of fine grained, olive green, mafic clasts with subordinate metasediments and aphyric to porphyritic dacite in a mafic ash to sandy, feldspathic arenite matrix. The laharic deposit consists of three subunits showing a matrix gradation from predominantly mafic ash with minor sediment, to a mixed zone, and finally to a upper zone of predominantly sandy arenite. The upper subunit probably represents the transition from mass flow deposition to epiclastic reworking of the volcanogenic debris. Although this laharic deposit displays a crude normal fining upwards of clasts similar to primary pyroclastics, a secondary origin is indicated by : 1) high percentage of mafic clasts and metasedimentary clasts, 2) mafic and metasedimentary

Epiclastic Deposits

The clastic metasedimentary assemblage of the Berry Creek Complex consists of feldspathic and quartzo-feldspathic arenite, wacke, and argillite. The metasediments occur as sheetform deposits derived by reworking of proximal to distal volcanogenic debris. Intercalation with and lateral gradations between primary and secondary pyroclastics and sediments are common. Locally the metasediments are intercalated with mafic ash tuff, flows and hyaloclastite, and magnetite ironstone.

The sediments weather a pale brown to tan colour from dark brown to bluish grey fresh surfaces. The transition from slightly reworked arenite to strongly reworked wacke is accompanied by a colour transition from blue-grey (white to dark grey weathered surface) to yellow brown (tan to brown weathered surface), respectively. The colour changes allow for rapid evaluation of sedimentary facies and relative degree of reworking. The argillite beds, exibiting variations based on composition and alteration, are pale to dark grey, pale brown or locally pale green on exposed surfaces.

Although colouration provides some criteria for facies assessment, the distinction between pyroclastic and epiclastic sequences include the following: 1) rounding of crystal and lithic fragments; 2) lack of vitric shards and pumiceous fragments; 3) granular matrix with rare preservation of phenoclasts; 4) sedimentary structures

arenite matrix; 3) distinct lack of pumiceous clasts; and 4) presence of subrounded clasts. The Maybrun lahar is a very lenticular unit, in the exposed section, consisting of a valley fill deposit bounded by monolithic debris flows. The unit shows a maximum thickness of 24 metres with a lateral dimension of less than 8-10 metres. The lahar cannot be traced laterally for more than 25-30 m. The channel margins in the underlying pyroclastic breccia are steep and range from 60 degrees to 80 degrees dip toward the centre of the channel.

Although monolithic deposits characterize the primary debris flows, secondary deposits can be observed along the north shore of Lobstick Bay. The slump or lahar deposits consist of quartz and feldspar phyric nonvesiculated massive dacite varying from lapilli to blocks. The matrix is composed of fine grained porphyritic quartzofeldspathic debris.

These slump deposits range in thickness to tens of metres and in lenth to approximiately 3 km from the apparent source area. The lahars form lenticular to sheetform deposits similar to the primary debris flows. The distinction between primary and secondary deposition of these slumps is based upon facies relations within the Facies B dome complex. Slumping probably occurred by oversteepening of talus deposits by dome growth (see lava flow descriptions, also Facies B descriptions).

i.e., commonly load, slump and flame structures; 5) turbidity current Bouma cycles; 6) sheet form depositional units; and 7) metamorphic assemblages characteristic to pelitic and psammitic sediments.

The grain size of sediments ranges from fine sand to fine silt and mud. Measurement of grains is inhibited grain size modification by metamorphic recrystallization. Coarse pebbles and boulders are rare and were only observed from a single conglomerate horizon near the upper part of the Snake Bay Formation. A local intraformational conglomeratic breccia, possible a result of synsedimentary slump faulting, is exposed near Mist Inlet (see location map, Figure 6). The 30 cm thick lag breccia beds contain rounded clasts within a pyritic argillite matrix. The breccia occurs within thin to thick bedded (3-100 cm) fine grained wacke.

Reworking of the pyroclastic debris rapidly contributes to a marked decrease in the abundance of vitric shards and pumice. The glassy vesicular clasts are readily destroyed by subaerial to subaqueous transport and reworking (Heiken 1972; Ayres 1982). Although vitric clasts have been recognized in epiclastic sequences of volcanogenic sediments (Stoeser 1975; Cas 1979; Rodolfo and Warner 1980), the accumulations are considered to be products of rapid deposition. The recognition of fine vitriclasts in the Berry Creek metasediments is masked by extensive recrystallization, metamorphism and deformation.

The metasediments are subdivided into several associations based on outcrop relationships and presence of various sedimentary structures. These three associations consist of the following: 1) massive to thick bedded (beds greater than 30 cm thick), tuffaceous and reworked arenite and quartzofeldspathic wacke; 2) graded arenite and wacke of varying bed thickness (usually less than 1 metre); and 3) graded couplets of arenite to wacke and argillite. The distinction between arenite and wacke is based upon visual estimates of the modal abundance of biotite (arenite < 15%, wacke > 15%).

The proximal metasediments are characterized by sharp bedding contacts, poorly developed bedding, and the presence, locally, of deformed lapilli clasts of quartz and feldspar phyric dacite. Neither clast nor matrix size grading was observed. The presence of single beds or multiple amalgamated beds and the lack of grading characterizes beds in the a2 subunit of the revised Bouma cycle (Cas 1979). Recognition of single beds is hindered by similar composition, lack of clasts, lack of fine interbedded argillite and intrusion of bedding parallel, quartz feldspar porphyries.

Graded arenite and wacke display bedding thicknesses from 1 -100 cm but most commonly 3-30 cm. Bed thickness varies with local facies changes. Partial Bouma cycles i.e., a2, a3, characterize the sandy arenite and wacke beds. Normal size grading can be observed and may be reflected in colour transitions i.e., darker towards the

fine grained part of the bed.

Bouma cycles of a more complete pattern i.e., A-E cycles, are present within the arenite to argillite and wacke to argillite couplets. The basal contacts of each Bouma cycle are sharp to undulatory with flute marks and load casts from overlying coarse sandy units into the fine argillite bed of the underlying cycle. The a2 and a3 divisions display sharp or transitional contacts with the overlying argillite layer (Bouma E division). The majority of the cycles are characteristic of the AE (a2, a3, e), middle absent, Bouma sequence. The proportion of sandy to argillic beds within a multicycle sequence may exhibit double grading as the ratio of argillite to wacke plus arenite increases up section. Progradational (coarsening upwards) cycles are also present.

Ball and pillow structures, of less than 3 cm length, are found within fine argillite beds. The structures are poorly defined, commonly include flame and/or dewatering structures (see Plate 9), and are, in most examples, offset by microfaults.

Facing reversals, interpreted from size grading, are common due to bedding parallel intrafolial folds and transposition of layers. The reversals vary in scale from microscopic (several parasitic folds in single thin section) to outcrop scale. Single beds or groups of beds exhibit tight isoclines, commonly rootless, within numerous parasitic limb folds. Interbedded garnetiferous mafic ash

tuff and metasediments (see Figure 14, 20-23 m., Old Woman Lake section) provide the best visual contrast for observation of small scale facing reversals. Garnets display a well developed normal frequency grading from the mafic ash tuff into the overlying metasediments.

Thin bedded sulfide rich siliceous to graphitic siltstone, arenite, and argillite form discontinuous thin lenses between basaltic flows of the Snake Bay Formation and are also intercalated with quartzofeldspathic metasediments of the Berry Creek Complex. Lenses of graphitic shale up to 2 m thick, occur within feldspathic arenites, in Lobstick Bay. Bed thickness ranges from 10-130 mm (average 40mm). Soft sediment deformation consisting of highly contorted folds and minor slump structures are common. Boudinage of siliceous beds within the graphitic horizons are the predominant feature of tectonic deformation.

Thin chert beds are rarely observed in the Berry Creek Complex. Bed thickness ranges from 4 mm to 40 cm. The thickest chert horizon occurs within the Mist Inlet stratigraphic section (see Figures 6 and 15). The chert beds are also intercalated with quartzofeldspathic tuff. In Figure 15, the chert bed occurs above a normally size graded heterolithic tuff breccia (lahar). The sharp basal contact of the cherty tuff with the underlying tuff breccia is characteristic of the chert horizons suggesting deposition during quiescent ponding or juxtaposition by slumping.

Tectonic deformation affects many of the chemogenic and epiclastic beds in the proximity of the Pipestone - Cameron Fault. Beds are offset by right lateral shear movements oblique to bedding orientation. Small isoclinal to transposed folds were observed in some chert layers. Granulation and alteration of the cherty beds (silica, kaolinization) occurred in the major shears on the north shore of Long Point Island.

BLACK RIVER, KENU LAKE, ADAMS RIVER BAY,SNAKE BAY MAFIC METAVOLCANICS

The bulk of the Black River mafic metavolcanics are massive to pillowed lava flows. Pillow breccia, autoclastic and pyroclastic deposits are locally present especially in the upper part of the mafic sequences.

Fine to coarse pyroclastic horizons outcrop along the shores of Adams River Bay and Yellow Girl Bay. The pyroclastics consist of subangular to angular, grey to black, vesicular lithics of lapilli to blocks; ash to lapilli, scoriaceous to pumiceous clasts with highly irregular boundaries; and euhedral to anhedral, 1-5 mm, dark green amphibole phenoclasts set in a fine to aphanitic chloritic ash groundmass. Fine tuffaceous to epiclastic horizons are intercalated with the coarse pyroclasts. Crystal and clast size and frequency grading were observed.

Mafic pillowed flows near the Bug Lake Road contain well developed to irregularly shaped, subcircular balloon

pillows with abundant interpillow breccia. In the eastern part of the map area, the basalts are strongly amphibolitized, especially peripheral to the Dryberry granitoid complex. Preservation of primary textures is poor. Enclaves of the amphibolites are common within the satellitic granodiorite stocks and locally within the foliated trondhjemite-tonalite. The amphibolitized basalts are characterized by lineated to foliated hornblende and plagioclase feldspars. Grain size of the amphibolites increases toward the granitoids.

The upper part of the Black River - Kenu Lake metavolcanics are intercalated with fine grained dark grey, green to black chloritic argillite and feldspathic wacke. The metasediments are thinly to thickly bedded, moderately sorted sandstone and massive to laminated argillite. Graded bedding is common in thin bedded wacke - argillite couplets as well as soft sediment folding and flame structures. The sediments are derived by reworking of hyaloclastite and tephra of the underlying volcanics.

The Snake Bay Formation consists mainly of pillowed to massive basalt. Fragmentals increase in abundance toward the top of the formation and consist of coarse flow breccia, commonly pillowed, interpillow brecccia, epiclastic wacke, argillite, and minor felsic to intermediate tuff.

The olive green to greenish grey basalt flows are subdivided into four categories. These include pillowed, massive to gabbroic, vesicular, and porphyritic flows.

Combinations of two or all types are present. Pillowed flows contain balloon, mattress and irregularly shaped pillows ranging from several centimetres to several metres in average length. The smaller pillows are generally buds from large pillows and/or lava tubes. Single flow units may contain pillows of similar or highly variable dimensions. Reentrant selvages (budding pillows) similar to those described by Hargreaves and Ayres (1979) are locally well developed (see Plate 12) south of Sioux Narrows and west of Dogpaw Rapids. Discrete feeder dikes within the pillowed flows are rare (see Plate 13).

Pillows are commonly deformed into elliptical or subrounded oblate shapes with length/width ratios in the 3:1 to 10:1 range. Extreme attenuation of pillows was observed in areas of high strain, particularly the Pipestone - Cameron Fault zone. Pillow structures are commonly destroyed and replaced by pseudobedded pale green shaly horizons locally intercalated with very thin (high length to width ratio, often greater than 100:1), deformed pillow relicts. Lensitic relicts of epidote cores were observed south east of Apache Landing. The cores are preserved within a strongly altered and foliated chloritic schist.

Pillow selvages are less than 3 cm thick and are commonly chloritized and foliated. They are preferentially weathered compared to the pillow cores. East of Sioux Narrows, where basalts are metasomatized by the Regina Bay

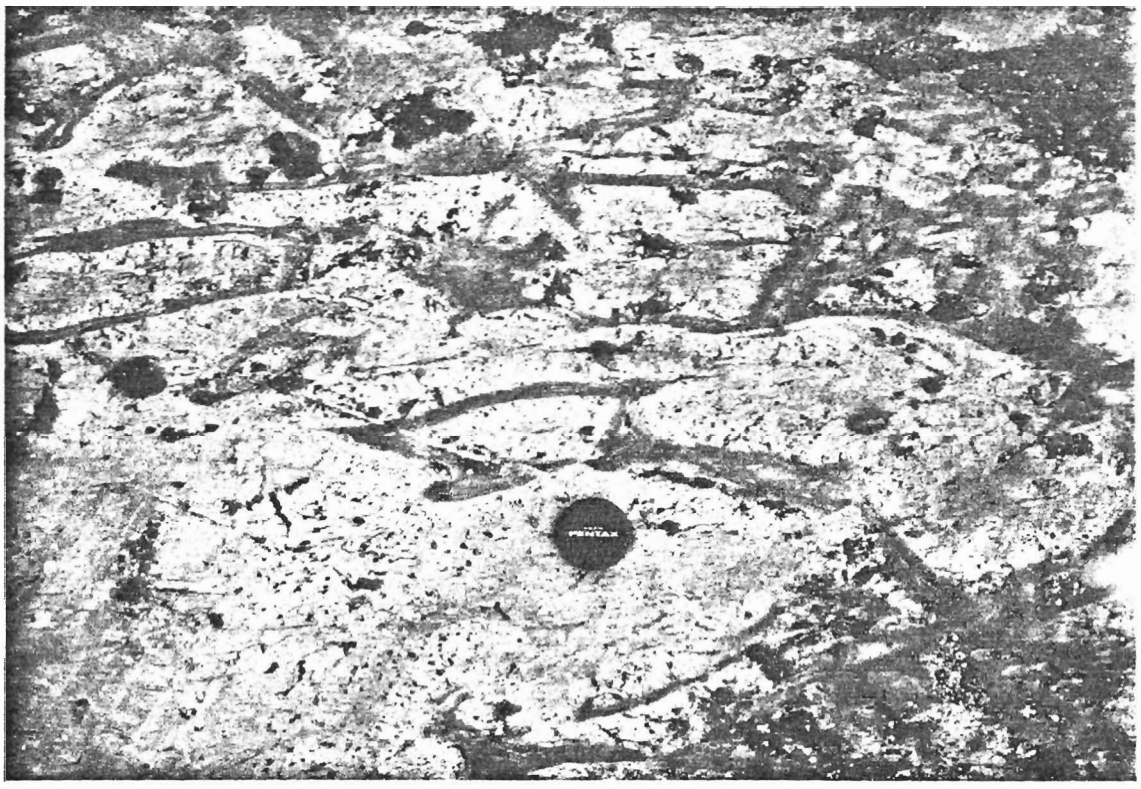

Plate 12. BUDDING PILLOW BASALT FLOWS, UPPER SNAKE BAY FORMATION.

tonalite. Recrystallization to coarse grained hornblende and epidote characterized the pillow margins. Pillow buds are totally recrystallized while large pillows are recrystallized within several centimetres of the selvage zone.

Central pods of epidote produced by autometamorphism and/or metasomatism (Dimroth and Lichtblau 1979; Jolly, p. comm. 1983) are present (see Plate 14). Pervasive, though patchy epidotization is recognized in massive flows. The epidotized massive flows are light to pale green compared to the darker green, less altered flows. Massive flows are commonly gradational to coarse grained gabbroic zones. Coarse grained amphiboles are intergrown with fine to medium grained plagioclase feldspars. Pillowed flows are

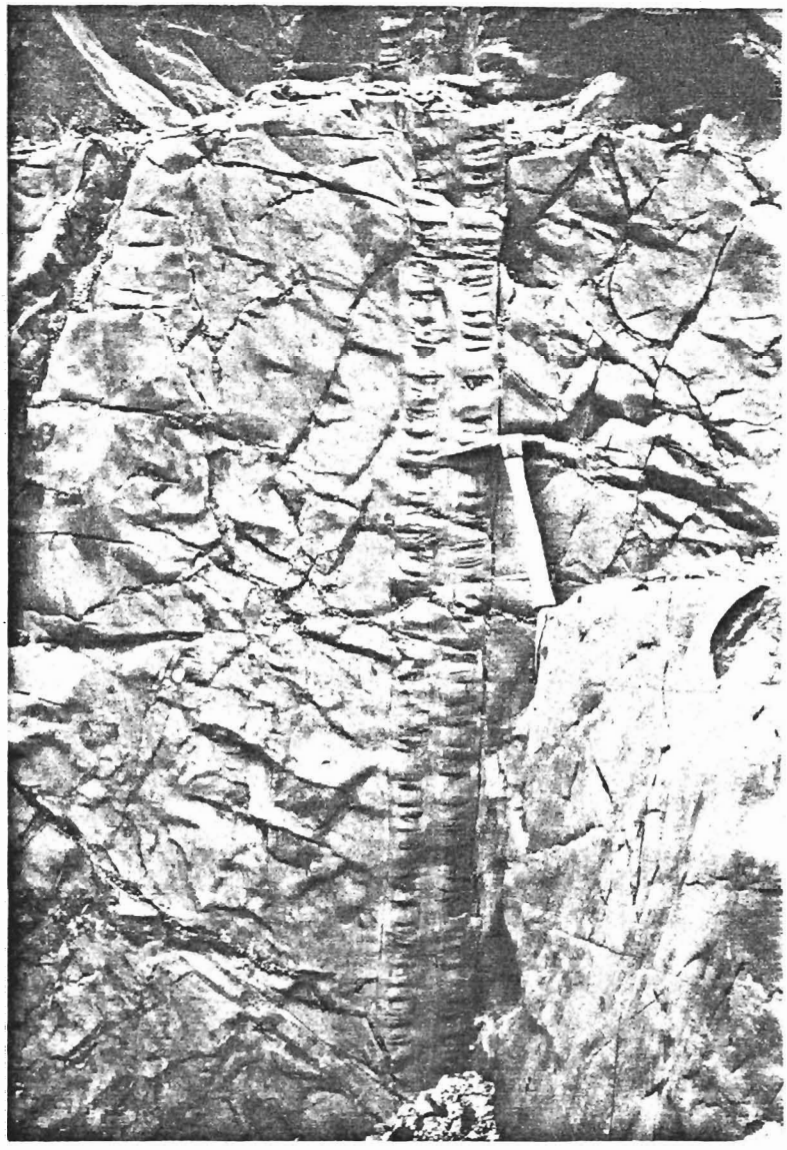

Plate 13. PILLOWED FLOWS INTRUDED BY FEEDER DIKE, UPPER SNAKE BAY FORMATION.

interlayered with and/or part of the adjacent gabbroic to massive flows.

Porphyritic to glomeroporphyritic basalts and basaltic andesites recognized by Fraser (1943) and termed "leopard rock" are common along Long Point Island. White to pale green translucent plagioclase feldspars form single crystals or glomerocrysts. Euhedral to anhedral forms are

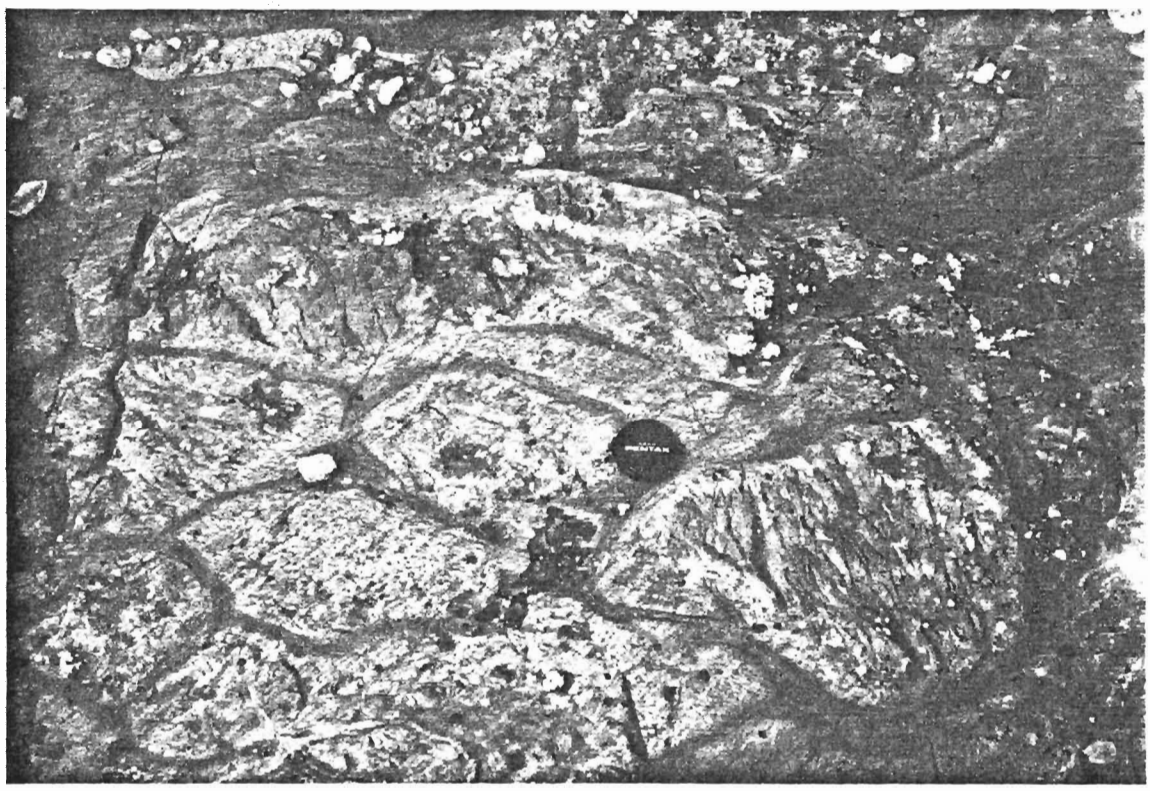

Plate 14. EPIDOTE PODS WITHIN PILLOWED BASALT FLOWS, UPPER SNAKE BAY FORMATION.

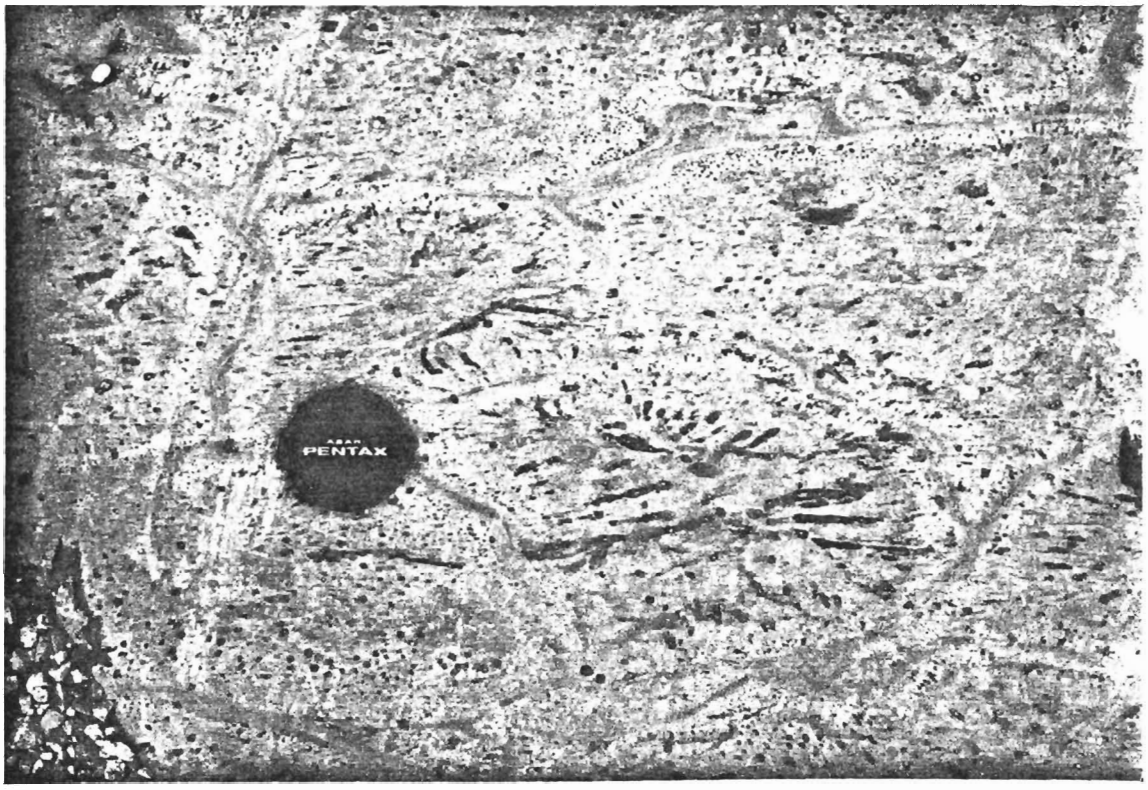

Plate 15. VESICULAR PILLOWS, UPPER SNAKE BAY FORMATION.

present. The proportion of feldspar phenocrysts is highly variable. Phenocrysts and glomerocrysts (1-15 cm diameter) range in abundance from 5-40%. In highly sheared rocks, the relative abundance of the competent feldspars ranges from 60-80% within a highly schistose matrix, especially along the north shore of Long Point Island.

The vesicular basalts are restricted to the northeastern area of the Snake Bay Formation, south of Regina Bay. Vesicles occur in irregular masses, radial patterns and commonly form vesicular rims and/or cores in the pillowed basalts. Plate 15 shows the distribution and relative abundance of vesicles in pillowed flows found southwest of the Whitefish Bay Indian Reserve. Vesicles are rounded to oblate and locally form pipe vesicles.

Fragmental sequences in the upper Snake Bay Formation are common. Interflow argillite, graphitic shale, and minor tuffaceous horizons occur between flows in all parts of the Snake Bay Formation.

BERRY LAKE LAYERED SEQUENCE

Exposures of dunite, peridotite, gabbro, pyroxenite and anorthositic gabbro are exposed along the margins of the Berry Lake granodiorite lobe. Large enclaves of the layered complex are present within the granodiorite, especially north east of Berry Lake. Several pods of pyroxenite and gabbro are scattered through the metasedimentary sequence west of Highway 71. Compositional changes are sharp to gradational and form layered to

podiform cumulate horizons. Cycle thicknesses range from 50 cm to tens of metres. A small boudin of the layered intrusion, within metasediments south of Berry Lake, grades from pyroxenitic gabbro to anorthositic gabbro over 1.5 metres. Repetition of dunite and gabbro layers are well exposed along Highway 71, west of Berry Lake.

The main lithological types found in the sequence are described as follows: 1) serpentinized dunite (pale green to whitish exposures, strongly foliated, fine to medium grained); 2) coarse grained dunite (coarse cumulate phases, olivine and pyroxene phenocrysts, dominantly secondary mineralogy, yellow brown exposures, dark brown green fresh exposures); 3) gabbro (fine to medium grained, massive amphibolitized, grades to pyroxenite and/or anorthosite, dark green to black exposed and fresh surfaces); 4) pyroxenite (dark green, strongly foliated to massive, fine to medium grained); 5) mica peridotite (coarse grained, large mica (phlogopite or biotite) flakes, euhedral amphibole, minor feldspar, gradational into syenitoid complex); 6) peridotitic gabbro (associated with mica peridotite but contains 15-20% feldspar).

RENDEZVOUS POINT SEQUENCE

Gabbro, pyroxenitic gabbro, quartz gabbro, and perodotite are exposed in the west end of Long Point Island, south and southwest of Rendezvous Point. The sills

are intruded into a mixed sequence of tuff, fragmentals and basalt.

Discrete compositional variations are present and are comprised of: 1) medium to coarse grained dunite to peridotite, 2) fine to coarse grained gabbro; 3) pyroxenite to dunite, gradational into gabbro; and 4) pyroxenitic gabbro containing blue quartz phenocrysts (see Petrography for details of phenocrysts) and minor feldspar.

QUARTZ FELDSPAR PORPHYRY INTRUSIONS

Porphyritic intrusions are common within the Berry Creek Complex and adjacent rocks of the Sioux Narrows greestone belt. Contact relationships are concordant (parallel to regional foliation) and discordant. The sills and dikes range in width from 30 cm to 5 m although the majority are between 50 cm and 1 metre. Contacts are very sharp with local intrusive brecciation. Accidental fragments from intrusion margins are very angular and were observed only in discordant dikes. Fragments range from several millimetres to metres and fragmentation along apophyses is common.

The buff to light blue grey weathering porphyry and felsitic dikes and sills have a dark blue grey to pale grey glassy to aphanitic groundmass. Pervasive saussuritization of the feldspathic groundmass in feldspar quartz porphyries east and south of the Regina Bay tonalite is common. The pale green groundmass contains waxy saussuritic folia. Near the contacts of the intrusions, within the Snake Bay

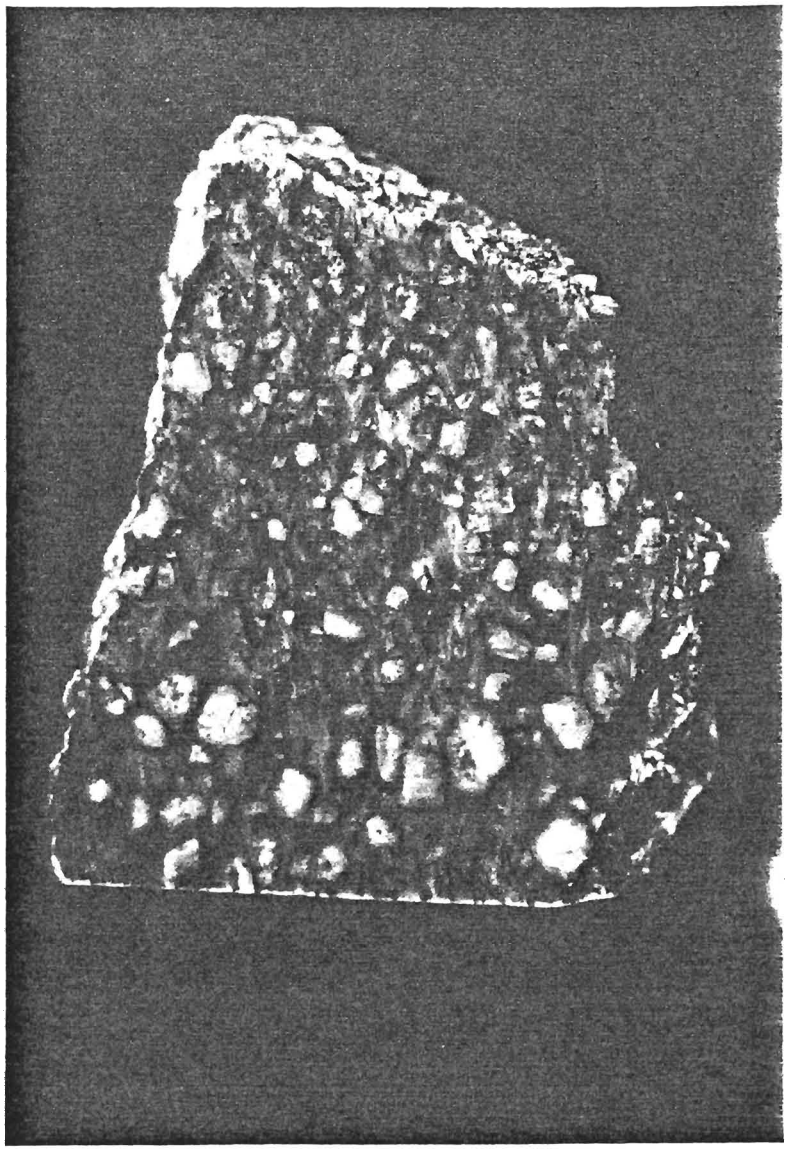

Plate 16. FELDSPAR PHYRIC PORPHYRY INTRUSION, LONG POINT ISLAND NEAR RENDEZVOUS POINT.

basalts, the porphyries exhibit reddish (iron) discolouration along the margins.

Phenocrysts constitute 5-50% of the observed dikes and sills. The felsitic dikes and sills are nonporphyritic. Buff, white, grey and light green 1-10 mm plagioclase feldspars are euhedral to subhedral forms (see Plate 16). Locally the feldspars form glomeroporphyritic clusters up to three discrete phenocrysts. Most of the feldspars are

equant and rarely aligned with the regional foliation. Feldspars, which have altered to clays, are preferentially weathered from the exposed surfaces, especially from glassy intrusive margins, to produce a pockmarked appearance.

Clear, rarely blue, 1-8 mm quartz phenocrysts form subhedral dipyramids to anhedral crystals. Resorption of phenocrysts was common. The ratio of quartz to feldspar in the porphyritic dikes and sills was highly variable. Many of the quartz phenocrysts are deformed into lensitic forms lineated along the regional foliation surface. Microphenocrysts of chlorite, after amphibole, are rarely present within the feldspar porphyries.

The foliation is commonly defined by undulatory patches or blades of biotite and chlorite. Fine grained masses of muscovite and sericite are common on the schistosity plane.

GRANITOIDS

Dryberry batholith, Regina Bay tonalite

The multiphase Dryberry batholithic comples intruded the north and northeastern margin of the supracrustals. The complex consists of variably foliated tonalite, trondhjemite and granodiorite. The latter generally occurs as satellitic lobes of massive to poorly foliated, fine to medium grained granodiorite e.g., Berry Lake, Viola Lake, Bunion Lake, Bunny Lake, Sanford Lake. Locally, the deformed tonalite-trondhjemite exhibits a gneissic to augen gneissic fabric. Cross cutting relationships suggest

several phases of intrusions. Foliated tonalite-trondhjemite is intruded by several, often crosscutting, phases of granite, granodiorite, felsite, pegmatite and quartz veins.

The Regina Bay tonalite intrudes the Snake Bay basalts and the upper fragmental sequences east of Sioux Narrows. The intrusion consists of massive to locally schistose tonalite gradational to a core zone of quartz phyric granodiorite-trondhjemite. Several small tonalitic to granodioritic plugs associated with the Regina Bay tonalite intrude the supracrustals west of Sioux Narrows. Intrusive brecciation was common along the margins of the tonalite. Zones of recrystallized and metasomatized xenoliths were observed along the south margin of Regina Bay.

SYENITOIDS

Kishquabik Lake Pluton

The Kishquabik Lake Pluton consists predominantly of a central syenodiorite phase with locally observed marginal phases of gabbro. Complex relationships between gabbro, granite, diorite and porphyries was observed at the southwestern margin of the intrusion.

Megacrysts of euhedral to subhedral potash feldspars characterize the syenodiorite. The 5-20 mm feldspars display a translucent blue-grey-white or pinkish-white colouration. The groundmass is fine to medium grained with minor hornblende and/or biotite phenocrysts and

interstitial growths. Mineralogical layering of hornblende and/or feldspars in layers up to 5 cm wide were observed. The layering is parallel to the contact between the gabbro and syenodiorite. The transition from homogenous syenodiorite to gabbro covers a range of 75 to 100 metres.

PETROGRAPHY

BERRY CREEK COMPLEX

Tuffaceous Deposits

Thin section examination of the pyroclastics and related volcanoclastic deposits reveals sufficient preservation of primary textures to describe in detail, the morphology of crystal, lithic and pumiceous components within the tuffaceous matrix.

Pumice is commonly observed as one of the three following types: 1) very fine grained quartzofeldspathic aggregates set in a coarser quartzofeldspathic and micaceous groundmass; 2) elongate aggregates of granular epidote with minor quartzofeldspathic material; and 3) aphanitic to very fine grained quartz-feldspar-mica patches containing vesicles filled by chlorite, hornblende, and calcite.

Pumice is usually recrystallized and recognition of pumiceous fragments within the quartzofeldspathic matrix is commonly based on grain size and relict outlines of shards. Although embayments by the matrix are common, the elongate ragged pumice fragments still exhibit multiple bifurcations and swallowtail terminations (see Plate 24). The wispy pumice fragments and shards display rapid thickness variations due to compaction by crystal and lithic components (see Plates 17, 18 and 19). Wrap around features (pumice around crystals) are also observed where intra-pumice crystals are common. The abundance of crystals (phenoclasts or phenocrysts) within pumice is

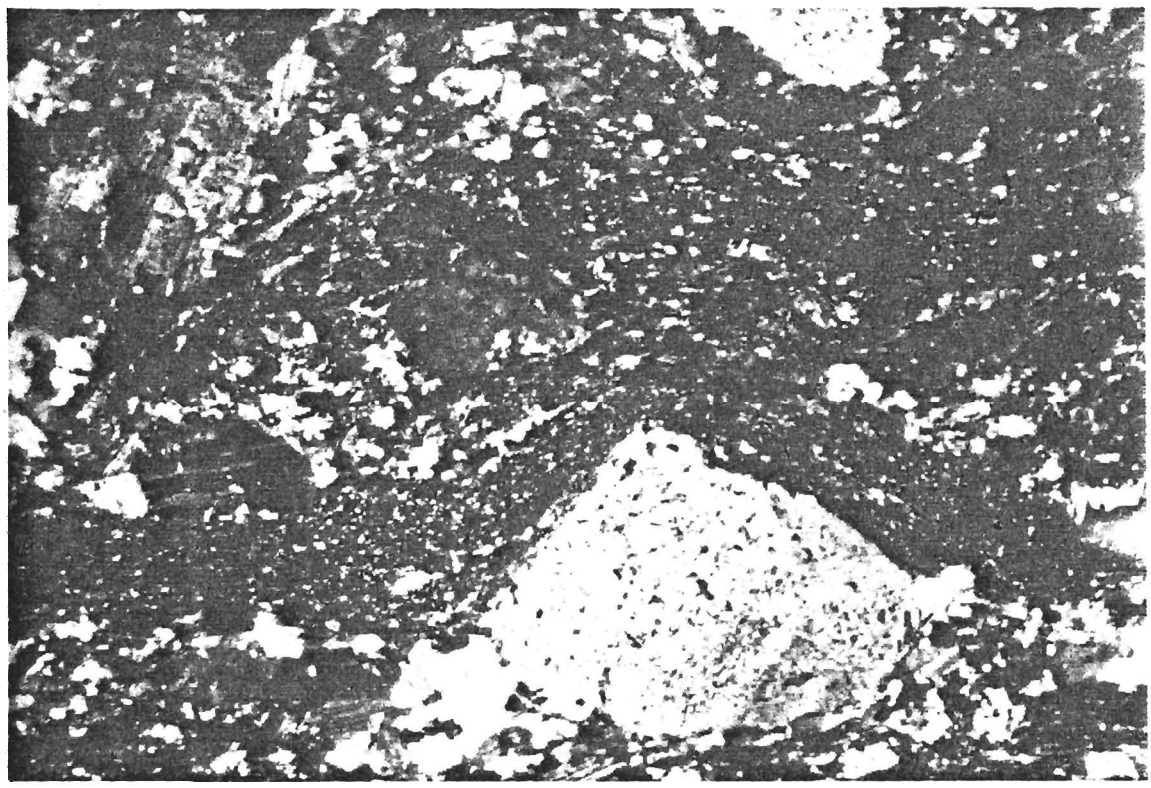

Plate 17. MICROGRAPH OF PUMICE AND SHARDS IN DEBRIS FLOW, LONG BAY. NOTE CRYSTAL DEFORMATION, RECRYSTALLIZATION, AND RELICT MORPHOLOGIES.

widely variable (0-50%). In crystal rich units, recognition of individual pumice shards is difficult due to pressure solution between pumice shards and extensive crystal-pumice deformation. Pseudoeutaxitic textures are present but are possibly the result of tectonic deformation. However, eutaxitic textures found in a single sample (#267)(see Plate 20) are identical to textures described by Hallberg et al. (1976) from the Marda Complex in Australia.

Crystals (phenocrysts) in pumice fragments are usually confined to pumice lapilli and blocks, while pumice shards are generally aphyric. However, the porous vesicular pumice lapilli and blocks (Type 3) found in the upper mixed sequence (Facies E) is also aphyric. The epidote rich

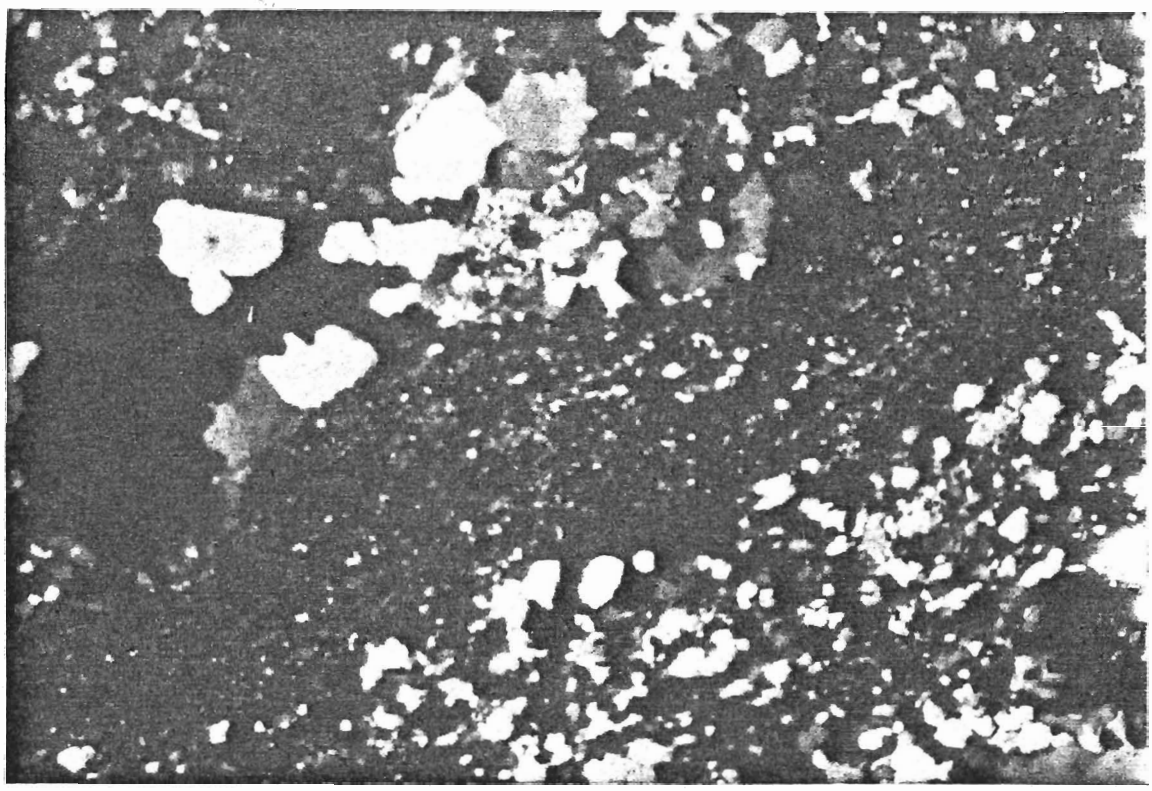

Plate 18. MICROGRAPH OF PUMICE, LONG BAY AREA, NOTE BIOTITE AND MUSCOVITE FILLING ORIGINAL PORE SPACES WITHIN PUMICE CLAST. NOTE GRAIN SIZE DIFFERENCE BETWEEN PUMICE AND MATRIX

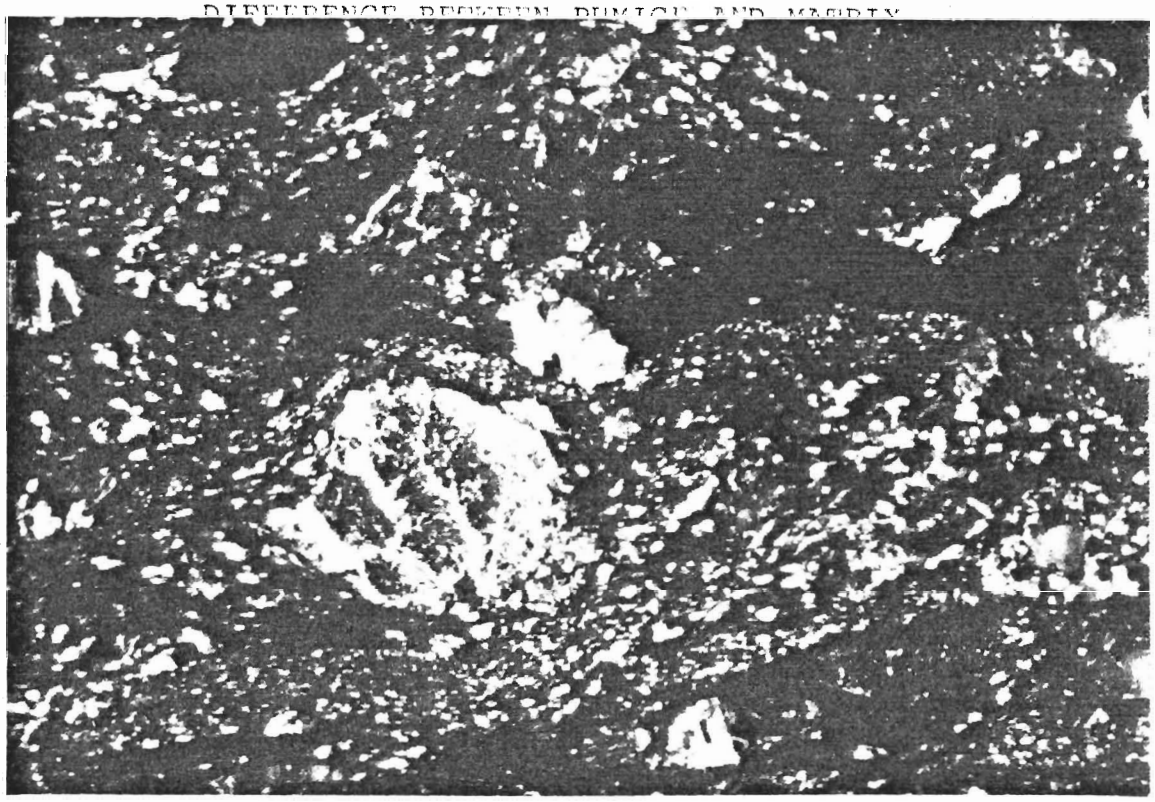

Plate 19. MICROGRAPH OF PUMICE FROM RUNNING ROAD SECTION, NOTE RECRYSTALLIZATION, AND REPLACEMENT OF ALBITIC FELDSPAR BY SERICITE AND CALCITE.

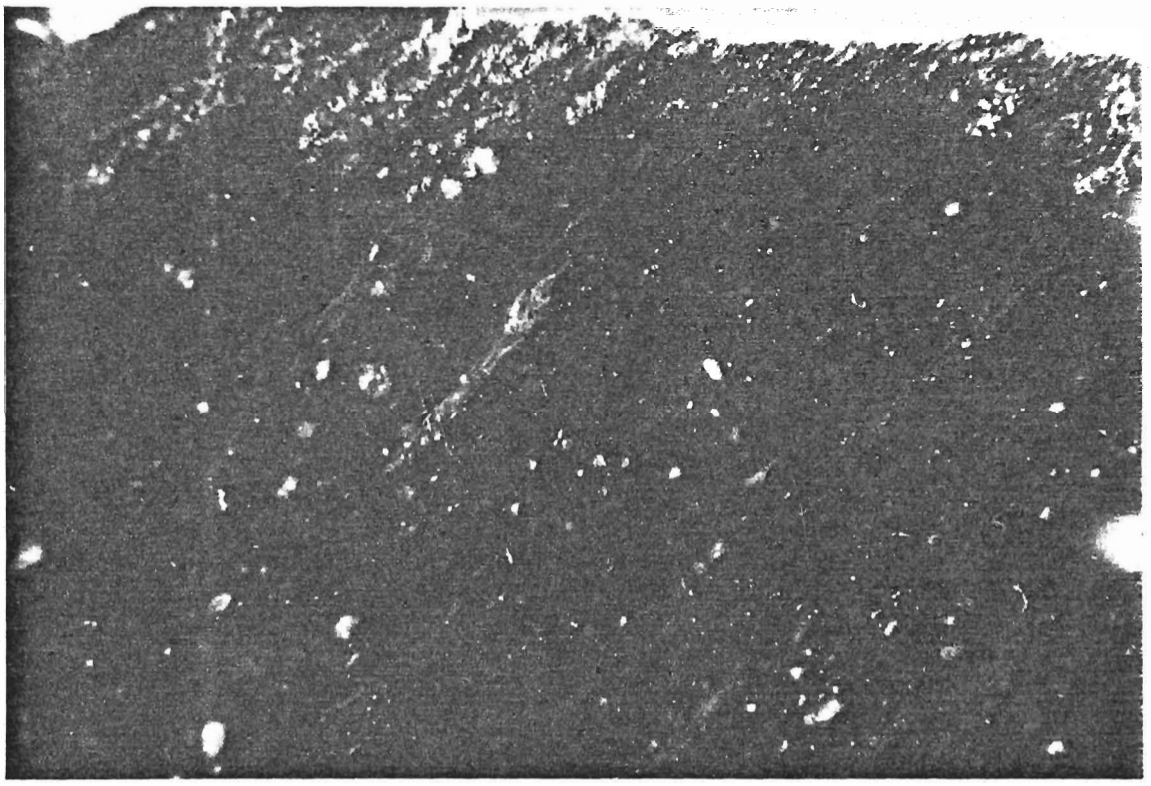

Plate 20. POLISHED SLAB OF LONG BAY DEBRIS FLOW. NOTE PSEUDOEUTAXITIC TEXTURE.

pumice (Type 2) is dominated by euhedral to subhedral plagioclase phenocrysts while quartzofeldspathic pumice (Type 1) contains both plagioclase and quartz phenocrysts in varying proportions. Fine grained pseudoeutaxitic pumice, observed near the White Moose section (see Figure 6), contains quartz phenocrysts and patches of chlorite, the latter possible replacing a ferromagnesian phase.

Initial porosity or vesicularity within pumice fragments is difficult to estimate due to deformation. Narrow lenses of quartz, calcite, epidote, sphene, biotite, muscovite, pyrite and Fe-Ti oxides probably represent initial pore space (see Plate 21). In relatively undeformed pumice near Lobstick Bay, pore spaces exceeding 50-70% are filled by chlorite, hornblende, calcite and

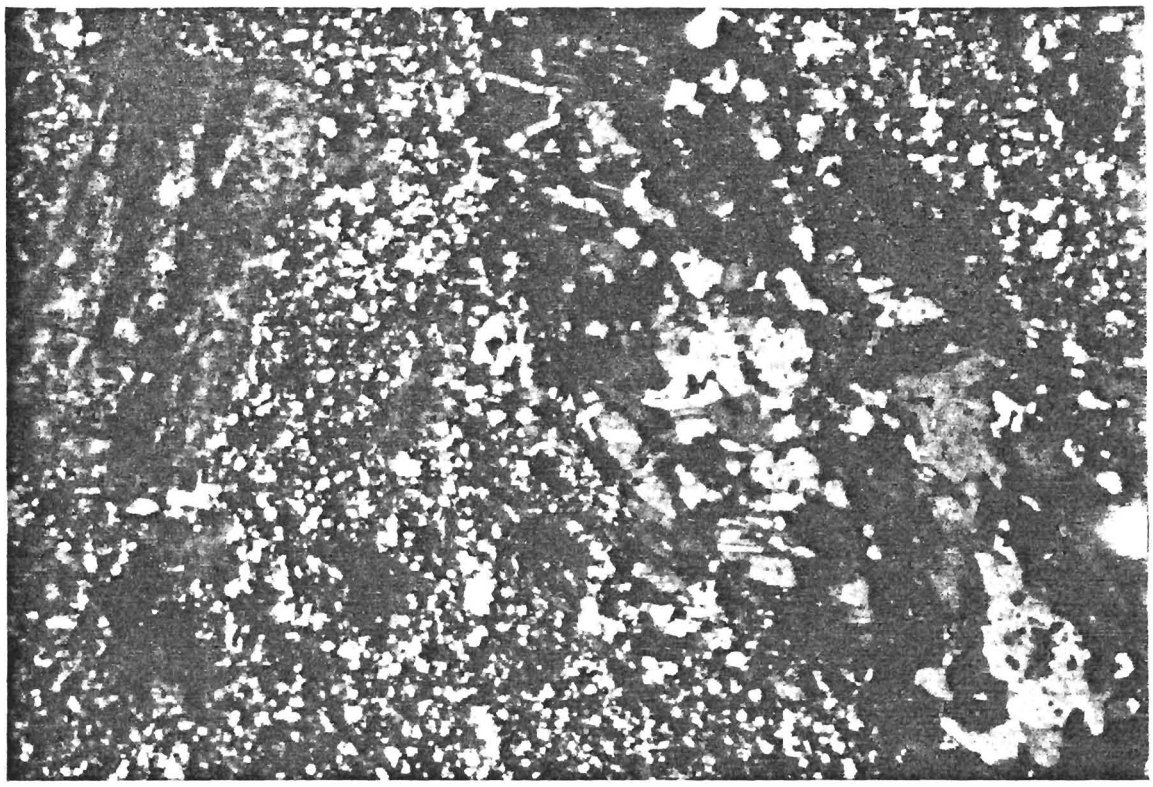

Plate 21. MICROGRAPH OF PUMICEOUS DEBRIS FLOW, RUNNING ROAD SECTION. NOTE INFILLING OF VOID SPACE BY CALCITE, EPIDOTE, SPHENE, SERICITE, AND BIOTITE.

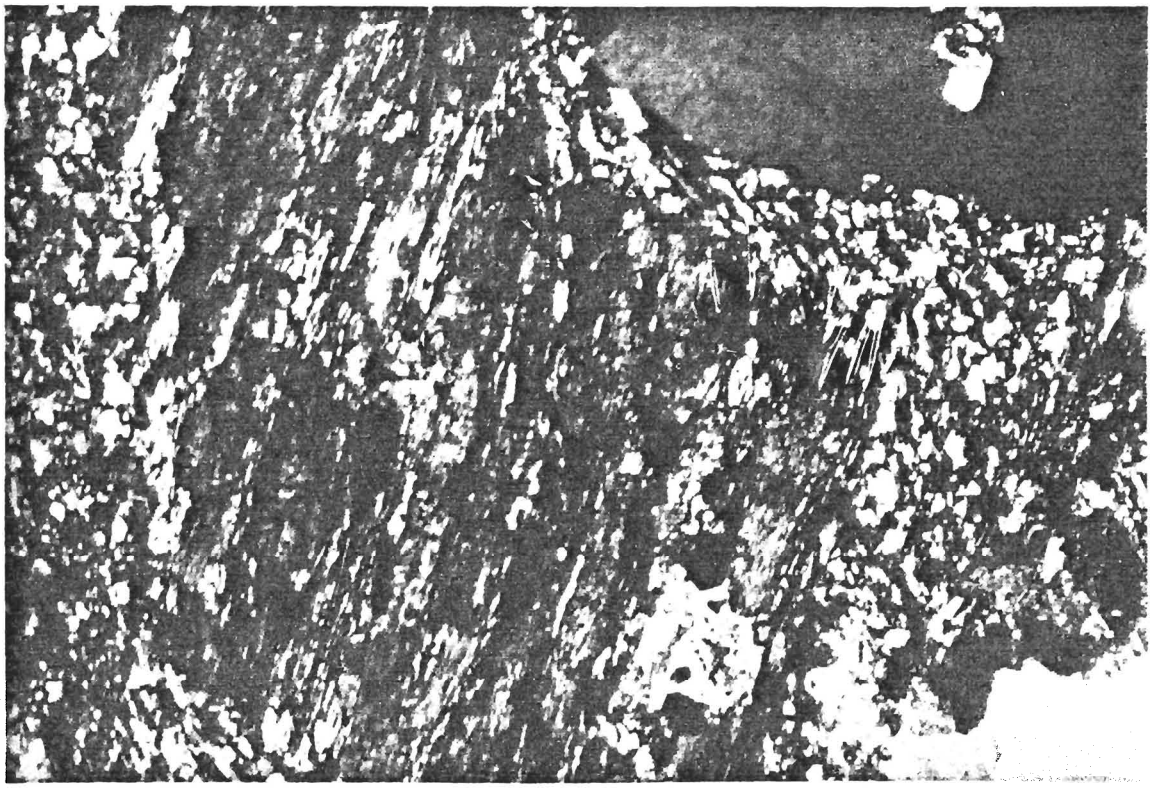

Plate 22. MICROGRAPH OF CALCIC FELDSPAR REPLACED BY EPIDOTE, CALCITE, ALBITE, SERICITE AND QUARTZ.

quartz. Yellow-green to blue-green hornblende forms poikiloblasts which are partially retrograded to equant and radiating, acicular pseudomorphs of calcite, chlorite and chloritoid.

There is an obvious continuum between crystals in the pumiceous and lithic fragments and the matrix of the pyroclastic deposits. The Berry Creek pyroclastics contain mainly quartz and feldspar phenoclasts although minor mafic phenoclasts are present. Individual phenocrysts and glomerophenocrysts of both quartz and more commonly plagioclase feldspars were observed in the tuffaceous deposits. Euhedral to anhedral (broken), 1-10 mm plagioclase feldspars display Ab twins (distinct, partial or discontinuous patches), Carlsbad twins, minor pericline twins, and locally curved deformation twins. Plagioclase compositions from Albite twins range from albite to calcic oligoclase. Compositions range from oligoclase to calcic andesine occur in highly metamorphosed tuffaceous deposits. Albitization of plagioclase feldspars is extremely common and subsequent pseudomorphic replacement by sericite, muscovite, calcite, zoisite, epidote and pistacite range from 5-95% completion. Plagioclase grain boundaries and twin planes commonly display albitic subgrains with irregular, sutured (lobate to angular) and straight to curved loci. Grain boundary types vary with unit porosity and metamorphic grade. Calcic feldspars found in several thin sections show pervasive replacement by pistacitic

epidote with minor albite and quartz (see Plate 22). Normal zoning and concentric oscillatory compositional zoning are common in plagioclase feldspars. Zoning was often deduced from concentric rings of sericite alternating with rings of twinned to untwinned clear albite.

Euhedral to rounded, 1-10 mm quartz phenocrysts display zoned extinction, variable polygonization and subgrain development and extensive embayments. As with feldspars, subgrain boundary types vary with metamorphic grade and proximity to high strain regions. Deformation of quartz phenocrysts into lensitic grains with rounded edges, polygonized pressure shadows and wavy extinction is common. Rare mafic phenocrysts form equant to prismatic subhedra characteristic to amphibole. Retrogression to chlorite (penninitic), calcite, sphene, Fe-Ti oxides and epidote is commonly complete.

Lithic fragments in the Berry Creek pyroclastics consist mainly of quartz and/or feldspar phyric dacite. Lithic fragment boundaries are distinct only where marked compositional differences exist between fragments and the adjacent matrix. Sharp to embayed or sutured boundaries are common. The elliptical, subrounded to angular blocks and lapilli contain embayed to euhedral quartz phenocrysts (blue, white or clear) and/or euhedral to subhedral plagioclase feldspar phenocrysts similar to those previously described. The groundmass of the dacite clasts consists of a fine to medium grained, quartzofeldspathic aggregate with muscovite, biotite, chlorite, epidote,

calcite and Fe-Ti oxides.

The distinction between the dacite clasts and a matrix of similar composition is recognized by the following parameters: 1) increased abundance of micaceous minerals within the matrix; 2) differences in phenocryst assemblage (crystal type, shape, abundance, alteration); and, 3) development of foliation (foliation more developed in matrix). Rarely, biotite content of lithic clasts is higher than biotite content within matrix. Otherwise recognition of porphyritic dacite clasts within a crystal bearing matrix of dacitic composition is impossible.

Accessory lithic fragments are less common but far easier to recognize due to compositional contrast. Mafic tuff clasts were the only type of accessory fragment observed in thin sections. The mafic clasts consists of hornblende and actinolite, in equant to acicular, radiating clusters; biotite, dark brown euhedra in decussate intergrowths; garnet, subhedral to euhedral with helicitic trails of Fe-Ti oxides and interstitial feldspar; and plagioclase of albite-oligoclase composition. A full description of the mafic tuff clasts is found in the section on mafic metavolcanics.

The matrix of the tuffaceous units consists, in varying proportions, of quartz, feldspar, muscovite, biotite, chlorite, chloritoid, calcite, garnet and epidote with accessory sphene, apatite, tourmaline, zircon and Fe-Ti oxides. Quartz and feldspar occur as fine grained

aggregates with irregular, sutured or straight grain boundaries. The larger grains of quartz and feldspar show subgrain development. Quartz grains are commonly embayed and have undulose extinction. Albitized feldspars are dusted by sericite, calcite and muscovite.

The mica components within the matrix vary with composition and metamorphic grade. The characteristic assemblages include: muscovite-chlorite, green biotite - chlorite - muscovite, brown biotite to green biotite +- muscovite, and brown biotite. The micas and chlorite occur as fine platy to acicular grains which define the planar fabric of the tuff units and are also locally developed to prismatic or bladed micropoikiloblasts. Clear to green penninitic chlorite occurs as both retrograde poikiloblasts and porphyroblastic phases after biotite and muscovite in the dacitic matrix and is commonly retrograde after biotite, hornblende, and actinolite in the andesitic to mafic matrix. Yellow to green pleochroic chloritoid also occurs as a retrograde phase after biotite blasts. However, chloritoid locally forms primary metacrysts as well as a secondary phase after patches of tourmaline. The mica and chlorite component define grain size and compositional grading within thin bedded tuff. Mica dominant (pelitic) and quartzo- feldspathic dominant (psammitic) layers occur within tuff-argillite (psammite-pelite) and normally size graded tuff, respectively.

Epidote commonly occurs as 5-20% (mode %) disseminated granular crystals and aggregates. Euhedral to

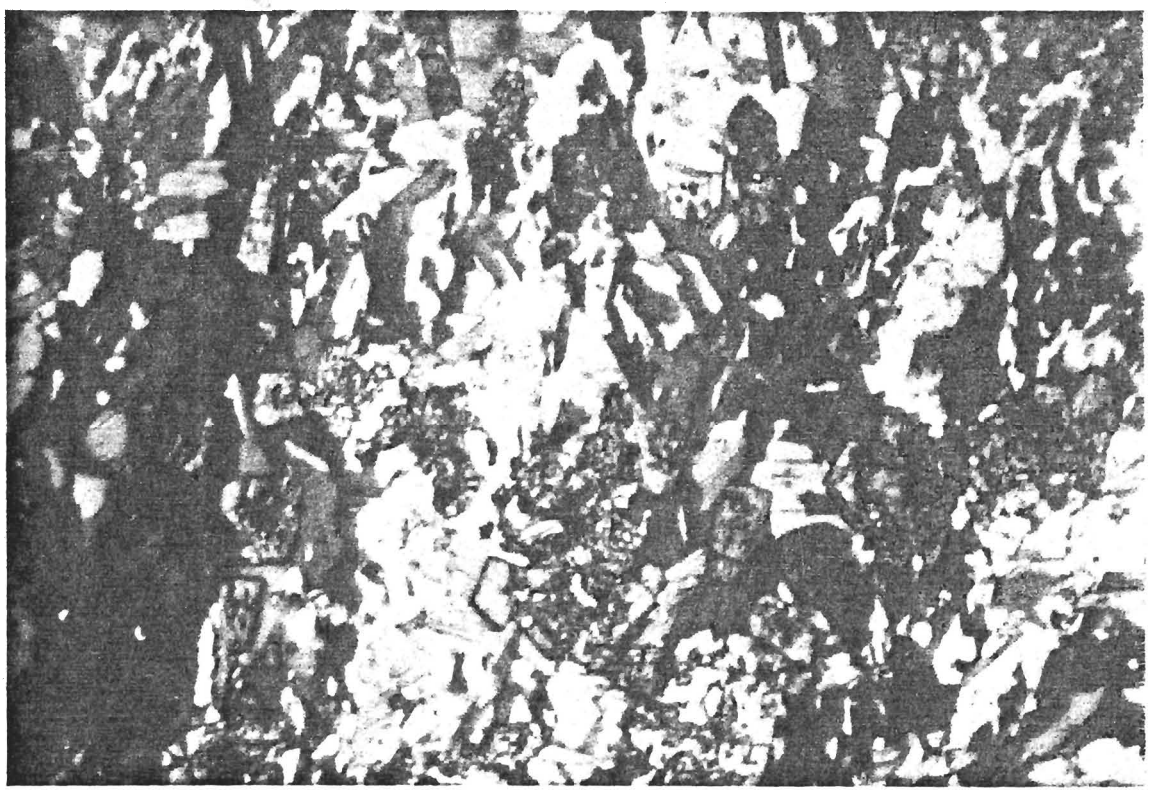

Plate 23. COARSE GRAINED EUHEDRAL EPIDOTE, BROWN BIOTITE, AND SPHENE FROM AMPHIBOLITE ZONE,BERRY CREEK METAVOLCANICS,NO NAME-KENU LAKE AREA.

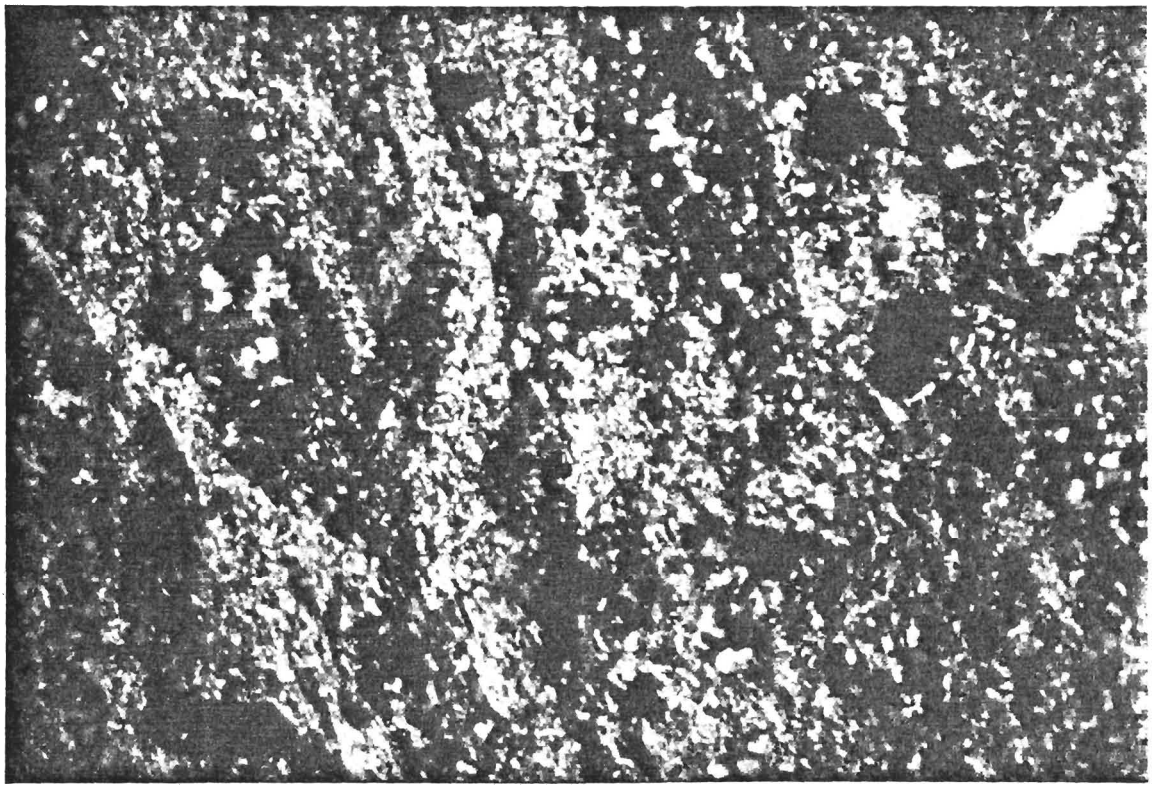

Plate 24. MICROGRAPH OF LENTICULAR TO CUSPATE RELICT SHARDS IN MICACEOUS MATRIX.

subhedral epidote crystals form in the highly metamorphosed tuffaceous units (see Plate 23). Patchy pistacitic epidote rich domains were observed in several exposures of altered tuff. The presence of garnet within the dacitic and andesitic pyroclastic types was rare and was only observed in a single thin section. The garnets are pervasive throughout the matrix and also within several dacitic clasts. The poikiloblasts are anhedral, rounded to elongate (in the plane of foliation) and include quartz, feldspar, epidote and calcite inclusions. Quartzo-feldspathic **anhedra** (partially from retrogression of the garnet), which ring the garnets, are also elongated in the plane of the foliation.

Calcite is a common secondary mineral after feldspars and is disseminated as fine granular anhedra. Many of the porous tuff units are moderately carbonatized such that calcite forms as irregular patches with well developed twin planes. Strong carbonatization associated with faulting is accompanied by albitization of feldspar and chloritization of biotite. In such sections, calcite, albite, and chlorite are equally distributed throughout the matrix.

Apatite prisms (commonly subrounded), euhedral to subhedral zircon, and euhedral to anhedral magnetite, pyrite and hematite are randomly distributed in the groundmass. Tourmaline is a common accessory mineral and occurs as both detrital subhedral to anhedral prisms and large subhedral to anhedral patches (often several

interlocking prismatic blasts)(see Plate 25). Clear to blue and blue to green pleochroism characterizes the metamorphic tourmaline prisms while the detrital tourmaline shows a clear to pale green pleochroism. Large patches of tourmaline are altered to chloritoid, muscovite and chlorite.

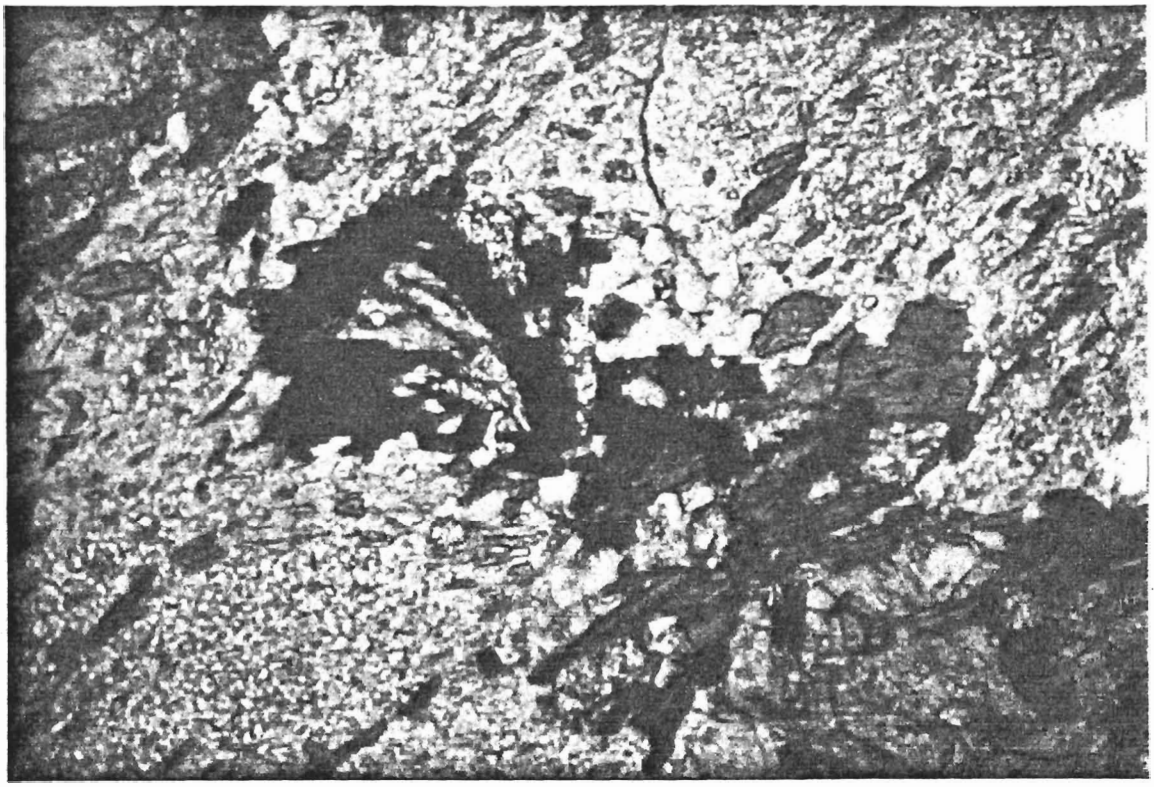

Plate 25. RADIATING PRISMS OF TOURMALINE WITHIN METASOMATIZED BERRY CREEK TUFF, NORTH OF LOBSTICK BAY.

Flows, Dome Complex

The Berry Creek lava flow types can be subdivided texturally into two groups for descriptive purposes: 1) generally nonporphyritic to very weakly porphyritic dacitic to rhyolitic flows displaying obvious flow laminations; and 2) massive to locally fragmental, moderately to strongly

porphyritic rhyolite to dacite.

The laminated flow consists of a granoblastic quartzofeldspathic aggregate displaying fine to medium grained laminae. Adjacent laminae vary in both grain size and composition. Individual layers consist of quartz; quartz and feldspar; and quartz, feldspar, chlorite and epidote. The recrystallized flow, from the highly metamorphosed zones near Dirtywater Creek, contains quartz and feldspar with straight to curved grain boundaries. The plagioclase feldspars may display Albite and Carlsbad twinning, normal compositional zoning (single cycle), have calcic oligoclase compositions and show incipient to pervasive clay and sericite alteration. Epidote occurs mainly as subhedral to anhedral, fine grained clots but locally as 1-3 mm, euhedral to subhedral prisms. Fine anhedral apatite prisms, subhedral to anhedral crystals and aggregates of sphene, calcite and hematite constitute the accessory phases. Very pale green penninite forms a pervasive replacement of biotite along some flow layers.

The massive porphyritic rhyolite to dacite consists of euhedral to subhedral quartz and feldspar phenocrysts in a groundmass of quartz, feldspar, muscovite, biotite, chlorite and accessory minerals. The massive dacite is petrographically similar to the porphyritic intrusions, crystal tuff and the porphyritic dacite clasts characteristic of the majority of the tuffaceous deposits.

Epiclastic Deposits

The metasedimentary deposits of the Berry Creek Complex are described under three groupings: arenite and wacke, argillite and mixed mafic tuff and metasediment deposits. The arenite and wacke units are characterized by phenoclasts of quartz and feldspar in a matrix of fine grained quartz, feldspar, biotite and chlorite with accessory detrital apatite, tourmaline and zircon. Quartz phenoclasts are subhedral to anhedral, display irregular fractures, sector zoning, wavy extinction, embayments, and are usually recrystallized into subgrains. Subgrain boundaries vary from sutured to straight with an increase in metamorphic grade. Feldspar phenoclasts display incipient to pervasive albitization, varying degrees of sericitization (also muscovite), and locally preserved albite twins. Plagioclase compositions are generally albite to oligoclase but increase to Ca-oligoclase, andesine, and possibly labradorite with increase in the metamorphic grade.

The matrix of the arenite and wacke units is dominated by a quartzofeldspathic aggregate. Biotite occurs as prismatic, stubby to bladed elongate crystals generally aligned with the regional foliation. Pleochroism of biotite varies from brown to pale grown, green to pale green and shades of yellow to green. Deflections of biotite clusters or layers around quartz and feldspar phenoclasts are common. Pressure shadows also contain abundant biotite. The presence of graded bedding is also

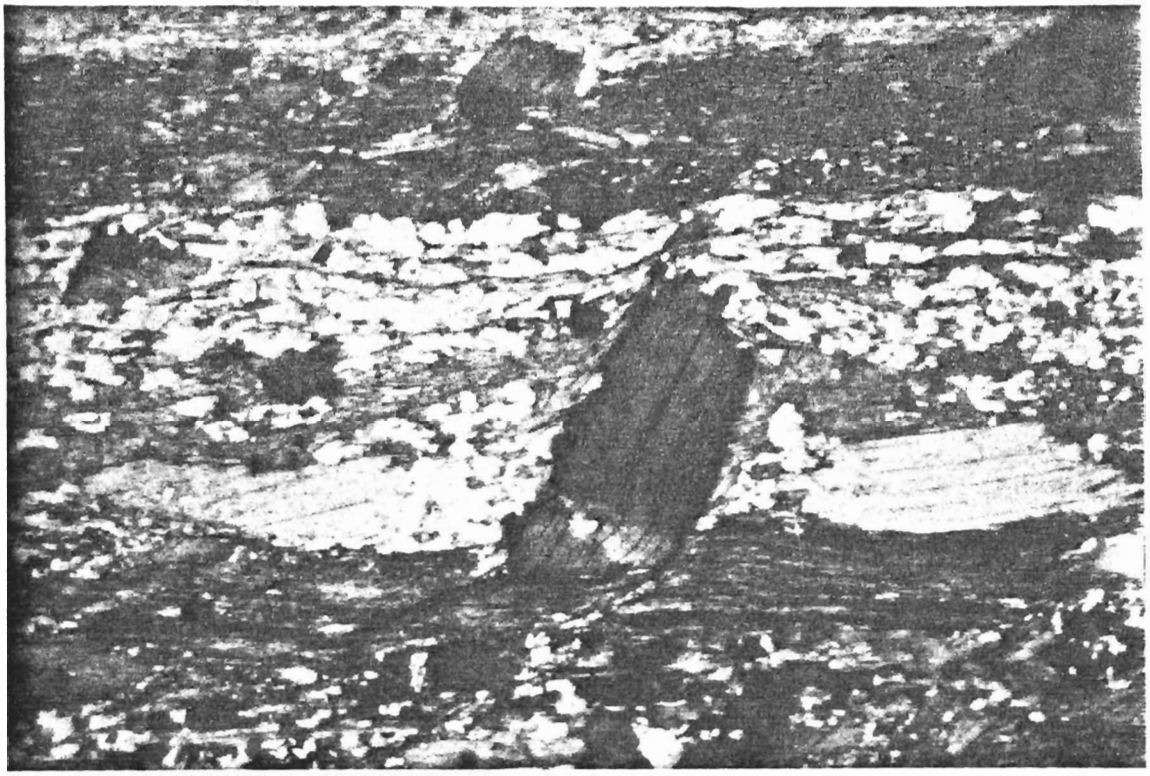

Plate 26. MICROGRAPH OF GRADED BEDDING IN TURBIDITE, NORTH OF LONG BAY, PLANE POLARIZED LIGHT, QUARTZO-FELDSPATHIC AND PELITIC LAMINAE.

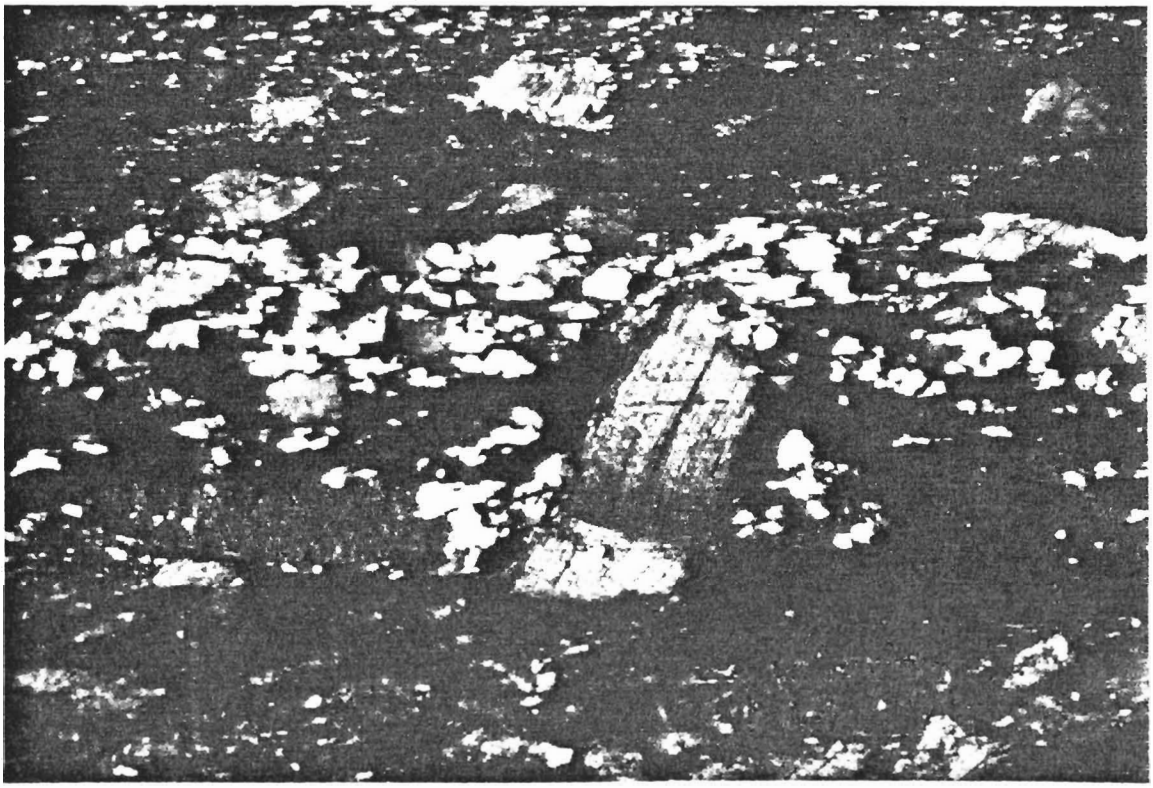

Plate 27. SAME AS PLATE 26. CROSSED NICOLS. NOTE THE CRENULATIONS IN BIOTITE BLASTS.

determined by variations in the abundance of biotite from arenite to wacke to pelitic zones (see Plates 26 and 27). Coarsening of the biotite is coincident with pelitic compositions, and also with an increase in metamorphic grade.

Pistacitic epidote and zoisite generally occur as fine granular masses (common in pressure shadows) or disseminated throughout the matrix. Euhedral to subhedral epidote (and zoisite) are abundant within highly metamorphosed quartzofeldspathic arenite and wacke (see Plate 23). Clear to green pleochroic chlorite occurs as a retrogressive phase after biotite. Rare orange-yellow-brown acicular stilpnomelane was observed. Microcline, with crosshatch twinning; anhedral apatite; anhedral to euhedral prismatic tourmaline (green or blue pleochroism) and euhedral to anhedral disseminated pyrite, magnetite and hematite are accessory minerals in the matrix. Zircon with well developed halos are common within the brown biotite blasts.

Pelitic horizons of argillite are characterized by high proportions of biotite and chlorite with minor quartzofeldspathic grains. Laminations and bedding are locally preserved by the elongate platy minerals (see Plate 26). Undulations in the biotite foliation are common. The mixed assemblage of mafic tuff and sediments are characterized by the presence of hornblende or actinolite. Radial sprays of hornblende/actinolite (see Plate 28) are common within a quartzofeldspathic aggregate. Quartzo-

feldspathic clasts can occur in a matrix of hornblende and actinolite. The abundance of hornblende/actinolite decreases in the metasediments within 3-5 cm of the bed contacts in areas of slight reworking. Garnet poikiloblasts, which are common in the mafic tuff, decrease markedly in size and abundance where tuff grades to metasediments (wacke, arenite).

Blasts of garnet, biotite, staurolite, andalusite and possibly cordierite were observed in the metasediments. The majority of the metamorphic blasts are confined to pelitic wacke and argillite. Garnets are commonly strongly poikiloblastic anhedra with round to oblate outlines (elongated parallel to foliation). Porphyroblastic garnets were rarely observed. Biotite porphyroblasts (pale to light brown pleochroism) are euhedral to subhedral, have ragged terminations, are partially retrogressed to pennintic chlorite and/or chloritoid, and are oriented oblique to the regional foliation. Crenulations with the large, obliquely oriented blasts are common (see Plate 27).

Staurolite occurs as rounded to subhedral porphyroblasts and weakly poikilitic blasts. Yellow pleochroism was characteristic of the staurolite blasts and minor retrogression to chloritoid was observed. Patches of andalusite or cordierite (now retrogressed to micaceous aggregates) form late poikiloblasts which include staurolite, garnet and biotite blasts. Slight crenulations were observed within the retrogressed poikiloblasts. The

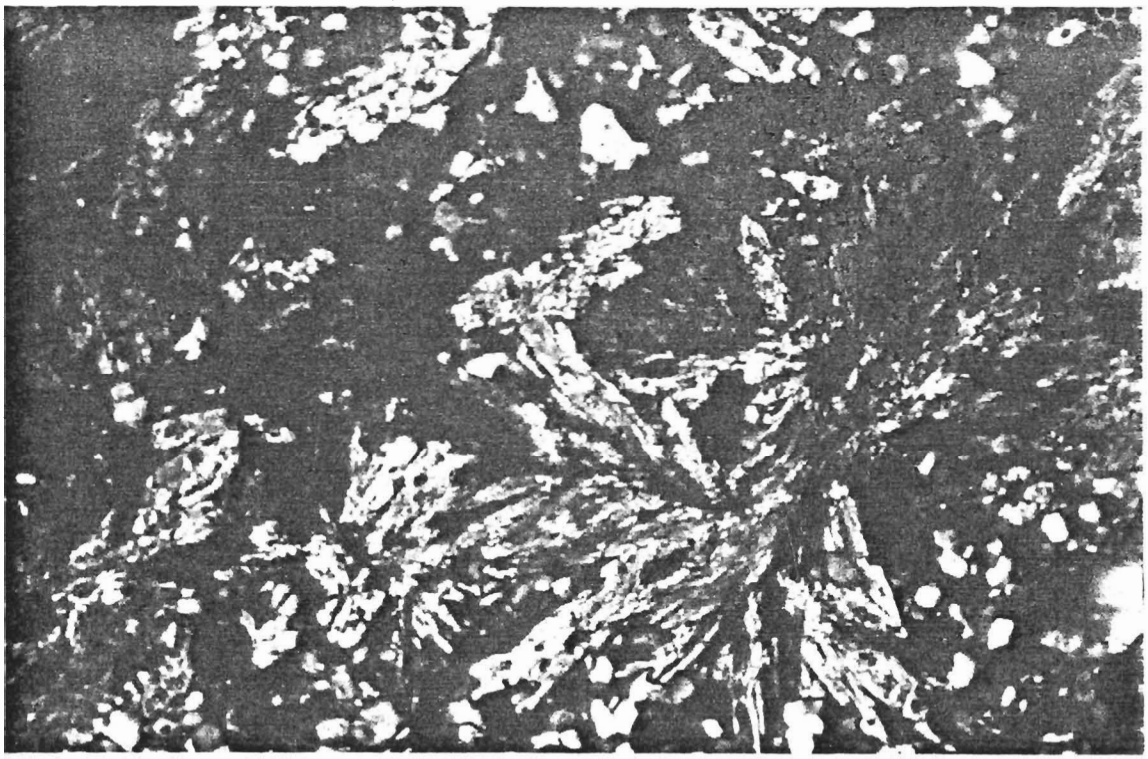

Plate 28. RADIATING SHEAVES OF HORNBLENDE/ACTINOLITE IN QUARTZOFELDSPATHIC MATRIX, MAYBRUN ROAD SECTION.

presence of andalusite was noted by Johns and Richey (1982). The presence of cordierite has been suggested by Johns and Richey (1982). Yellow to green, porphyroblastic to weakly poikiloblastic, metacrysts of chloritoid were observed in several thin sections. Lamellar twinning (similar to albite twins of plagioclase) of the acicular to prismatic blasts are common. Chloritoid generally occurs as an alteration product of biotite, muscovite, staurolite and tourmaline.

Porphyry, Dikes, Sills

The porphyries consist of 1-10 mm quartz and/or feldspar phenocrysts set in a mosaic of fine quartz, feldspar, epidote, calcite, chlorite, sphene, Fe-Ti oxides, apatite and zircon. Muscovite and biotite define a

foliation within most porphyry intrusions. Feldspar phenocrysts, of albite to oligoclase compositions, form euhedral to anhedral crystals with Carlsbad and Albite twins. Normal, oscillatory and transgressive oscillatory zoning are common. Zone boundaries, in the latter, form straight to curved and irregular patterns, suggesting partial resorption by the liquid phase. Octagonal and rounded boundaries are common. Up to twelve zones have been observed in a single phenocryst. Glomeroporphyritic feldspars are common in feldspar porphyries. Sericite, kaolinite, calcite and muscovite dust the majority of the feldspars. Subhedral to anhedral quartz phenocrysts are commonly embayed and recrystallized into sutured subgrains. Rare mafic microphenocrysts are pseudomorphed by chlorite, calcite and epidote.

Biotite (green or brown pleochroism) forms clusters of blades and laths, locally exhibiting a radiating spray parallel to the foliation. Micas also form in aggregates with calcite, apatite, sphene, zircon, and leucoxene. Aggregate assemblages form in shadow zones behind the competent quartz and feldspar phenocrysts. Many zircons are twinned parallel to the long axis of the crystal (similar to Carlsbad type).

Mafic Metavolcanics

For descriptive purposes, the mafic metavolcanics are subdivided into three categories: 1) pillowed and massive

flows (Snake Bay and Lobstick Bay); 2) coarse pyroclastics (Adams River Bay); and 3) mafic tuff (Berry Creek).

All flows are characterized by mixed assemblages of greenschist to lower amphibolite facies metamorphism (Winkler 1979) consisting of actinolite, hornblende, chlorite, albite, oligoclase, calcite and epidote. A massive porphyritic basalt flow includes euhedral to subhedral glomeroporphyritic, 5-25 mm, oligoclase to labradorite plagioclase feldspars set in a fine grained pilotaxitic felted groundmass of actinolite and plagioclase microlites (see Plate 29). The phenocrysts exhibit albite,

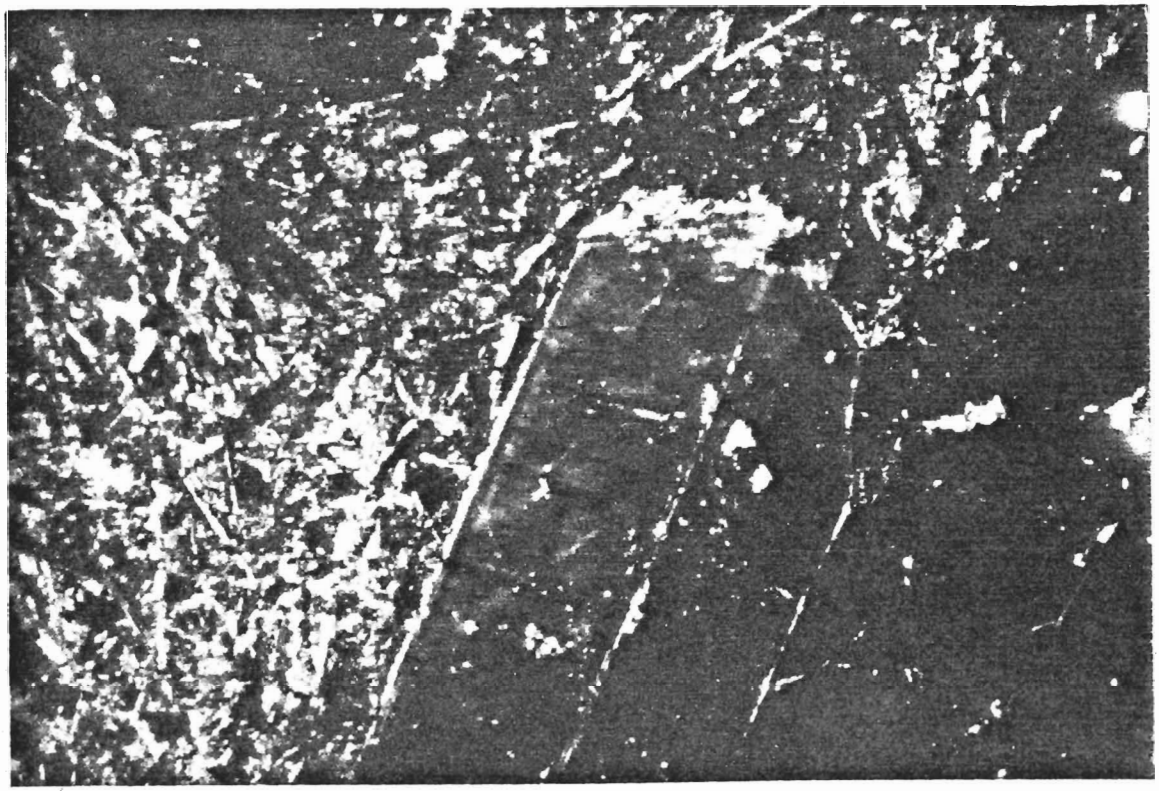

Plate 29. PLAGIOCLASE PHYRIC BASALT, SNAKE BAY FORMATION, LONG POINT ISLAND, GROUNDMASS OF PLAGIOCLASE MICROLITES, EPIDOTE, ACTINOLITE AND CHLORITE.

Carlsbad and pericline twins and contain abundant inclusions of zoisite, calcite, sericite, clinozoisite and muscovite. Oscillatory compositional zoning combined with inclusion trails is common. The plagioclase microlites display embayed to skeletal euhedra with Carlsbad twins and continuous compositional zoning. Actinolite displays pale to green pleochroism and wavy extinction in prismatic laths. Acicular actinolite is also common. Abundant inclusions of fine grained secondary minerals are common. Patches of actinolite and chlorite may pseudomorph mafic phenocrysts.

Pillowed flows display discrete mineralogical domains from the pillow core to the hyaloclastic interpillow breccia zones. The inner pillow zone contains matted intergrowths of stubby to acicular actinolite. The pillow matrix also contains chlorite, epidote, pale to brown biotite, calcite and albite feldspar. Round and pipe vesicles are filled with calcite and penninitic chlorite. The plagioclase feldspars are recrystallized to clear albite with incipient twins. Polygonization of the feldspars is common. Recrystallized pillows along the contact of the Regina Bay tonalite contain 1-1Ø mm poikiloblasts of bright green to olive green or brown to dark green, pleochroic, anhedral to equant hornblende. The marginal zone of pillows is characterized by foliated, fine grained actinolite, chlorite and epidote +- feldspars +- calcite. The relative abundance of epidote (zoisite, clinozoisite, epidote, pistacite) shows a marked increase

from the pillow core (15-20%)to margin (35%) to interpillow breccia (ranges from 20-80%). Interpillow breccias also contain 30-40% acicular actinolite, 10-20% calcite, with accessory albite, chlorite, leucoxene, sphene and Fe-Ti oxides.

In the coarse pyroclastics of the Adams River Bay metavolcanics, lithic, pumiceous and crystal fragments occur in a groundmass of quartz, epidote (locally pistacitic), chlorite, plagioclase feldspar, hornblende and actinolite, and calcite. The groundmass feldspars are albite to andesine compositions (based on albite twins), contain pericline twins and numerous inclusions of epidote and chlorite. Crystal fragments include euhedral to anhedral, equant to prismatic hornblende with pale green to dark green or yellow brown to green pleochroism. Biotite is present as an alteration of hornblende. Epidote (fine grained masses) is common as rims around hornblende phenocrysts.

Lithic fragments are angular, of lapilli size to locally blocks, and are predominantly hornblende and feldspar. Fragments resembling pumice are randomly distributed lapilli with irregular boundaries. Epidote is the dominant accessory phase and is found as granular masses. Plagioclase phenocrysts within the pumice fragments are epidotized, range in composition from albite to oligoclase and contain numerous inclusions. These epidote - plagioclase +- quartz domains are discrete zones

as compared to the groundmass of hornblende, actinolite and plagioclase.

Mafic tuff, of the Berry Creek metavolcanics, is composed of hornblende, actinolite, garnet, biotite, quartz, feldspar and magnetite. The metamorphic assemblage is directly related to the degree of mixing between the mafic tuff and associated metasedimentary sequence. Unmixed tuff contains 25%, poikiloblastic, subhedral to anhedral garnet, poikiloblastic hornblende, and associated biotite, plagioclase, quartz with minor Fe-Ti oxides.

The garnets contain 10-70% inclusions of quartz, plagioclase, biotite, calcite, epidote and chlorite. Small garnets (< 2 mm) are subhedral, rarely embayed and sparsely poikiloblastic to porphyroblastic. Embayments, inclusions, and anhedral outlines characterize large garnets (10-40 mm length by 5-20 mm width) which are commonly aligned parallel to the plane of the S1S2 foliation. Helicitic inclusions are recognized in some garnets. Garnets may be retrogressed to chlorite, calcite, biotite, hematite, and magnetite. Equant to prismatic, subhedral to anhedral hornblende is pleochroic as follows: pale green to dark green, pale brown to green to dark brown, pale blue to dark blue to green. Sector zoning is common in clusters of hornblende prisms. Alteration to biotite (green to brown pleochroism) along margins is pervasive.

Magnetite is locally abundant (maximum 10-15%) in mafic tuff horizons. In thin section, magnetite occurs as lenses or discrete, euhedral to anhedral, grains up to 5 mm

diameter.

Mixed mafic tuff and metasediments contain a similar assemblage, but with the addition of quartz and feldspar as an important groundmass and fragmental (lithic clast) component. The abundance of garnet and hornblende shows a marked depletion to between 30-50% of the mode. Acicular pale to light green actinolite occurs as radiating clusters (see Plate 28). The radiating sprays and decussate intergrowths of hornblende and actinolite are surrounded by and locally penetrative into lithic clasts of quartzofeldspathic arenite and wacke. Gradations from hornblende-garnet-actinolite zones to biotite-garnet-feldspar +- garnet zones are common in the mixed zone between the epiclastics and the tuff units.

Berry Lake Layered Sequence

Thin section examination of the gabbro-dunite-pyroxenite sequence reveals assemblages of actinolite, olivine, serpentine, talc, chlorite, plagioclase, hornblende, biotite, and accessory magnetite, hematite, muscovite, calcite, apatite and quartz. Preservation of primary textures and mineralogy is poor although pseudomorphs of olivine, pyroxene and plagioclase are common.

Actinolite is the dominant mafic phase and occurs as acicular needles with spiky terminations or blocky prisms (see Plate 30). Actinolite may pseudomorph pyroxene.

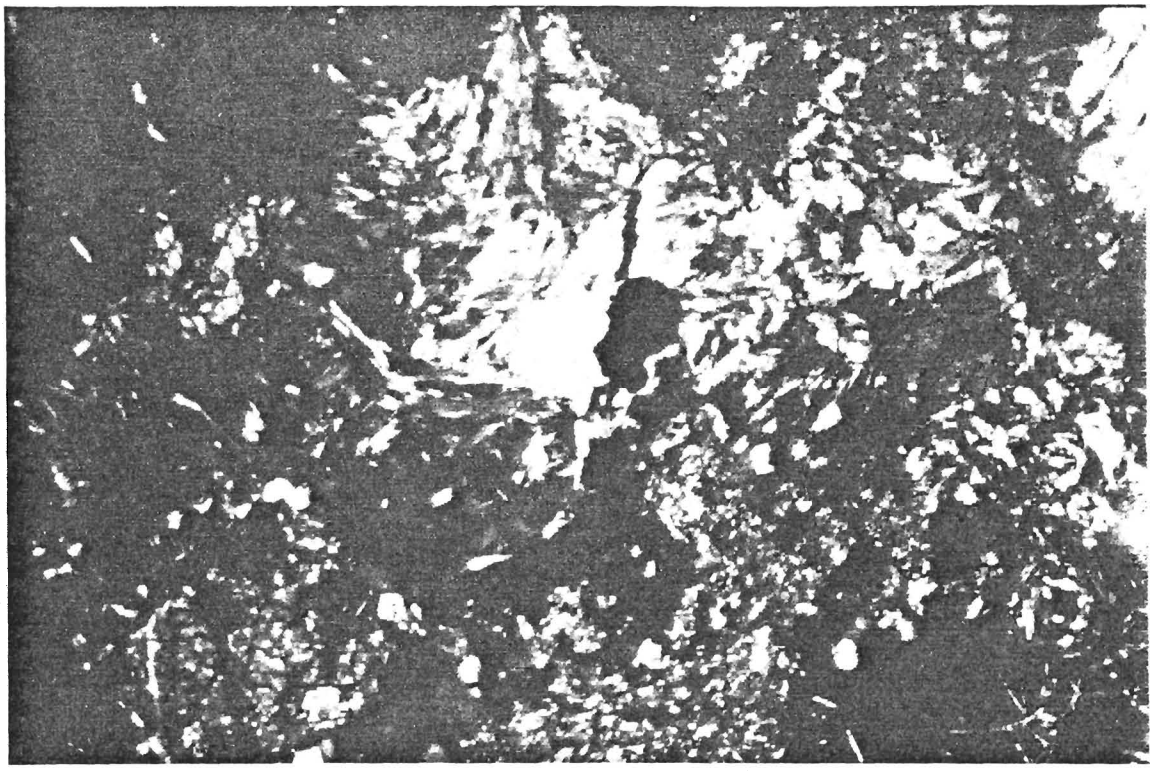

Plate 30. MICROGRAPH OF ACICULAR TO SPIKY ACTINOLITE IN PYROXENITIC GABBRO, BERRY LAKE SILL, MINOR PROGRADE OLIVINE.

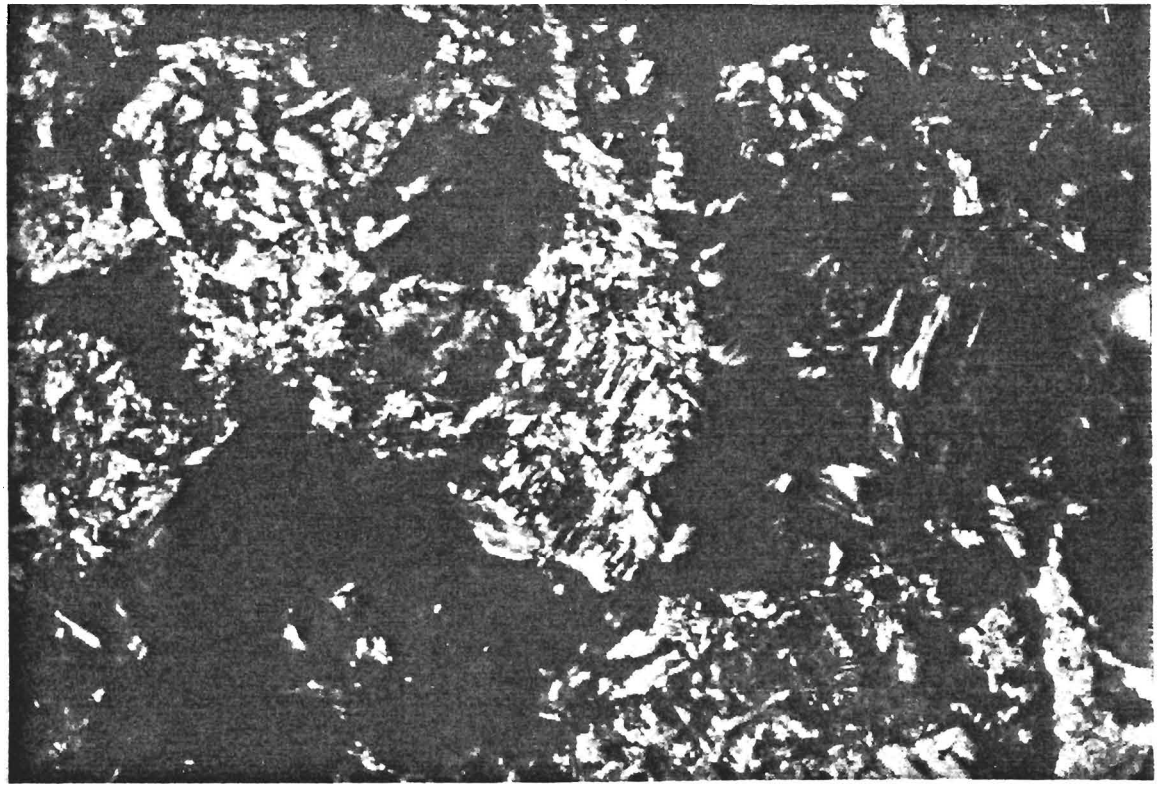

Plate 31. MICROGRAPH OF SERPENTINE, TALC AND CHLORITE PSEUDOMORPHS AFTER OLIVINE IN PYROXENITIC DUNITE, BERRY LAKE SILL.

Needlelike actinolite and chlorite form a felted groundmass intergrowth in the gabbros and pyroxenites. The pale to green actinolite has commonly retrogressed to chlorite plus oxides and chloritoid. Compositional zoning and Carlsbad sector twins were observed in the coarse actinolite prisms.

Blue green to bright green and yellow brown to dark green hornblende is locally common and is probably transitional from the actinolite. Talc, chlorite and serpentine form pseudomorphs after olivine in the highly foliated, serpentinized dunites and peridotites (see Plate 31). Chlorite occurs as fibrous clear to green penninite or greenish to brownish varieties and forms matted pseudomorphs floating in islands of talc and serpentine. Actinolite, olivine, and secondary minerals dominate the peridotitic layers.

Coarse grained biotite occurs locally within the peridotite zones. Pale greenish brown biotite flakes are also common in the gabbroic zones. Fe-Ti oxides are randomly dispersed and also occur along cleavage traces within hornblende metacrysts. Muscovite and calcite replace feldspars in gabbroid horizons.

Plagioclase feldspar in the gabbro and amphibolite layers have compositions of sodic andesine, display poor to well developed albite twins, minor pericline twins, and deformation lamellae (Augustithis 1979). Bands of irregular subgrains follow twin planes and phenocryst

margins. Quartz occurs as fractured recrystallized masses of polygonized grains with slightly undulose extinction.

Granodiorite

The granodiorites are allotriomorphic to hypidiomorphic granular seriate and are locally porphyritic with quartz and/or feldspar. Phenocrysts are set in a groundmass of quartz, feldspar (microcline perthite, albite), biotite, hornblende and epidote. Accessory minerals include hematite, magnetite, chlorite, zircon, apatite, and sphene.

Quartz (phenocryst and groundmass) is anhedral, has resorbed outlines, irregular cracks, and numerous inclusions of biotite, sphene and zircon. Resorbed quartz is commonly found inside plagioclase laths. Intergrowths of quartz and feldspar exhibit myrmeketic textures. Ribbons, blebs and heiroglyphs of quartz are present within alkali feldspars and vice versa. The intergrowths are commonly found as marginal growths around large phenocrysts or as interstitial to the large crysts.

Alkali feldspars occur as microcline perthites, twinned and untwinned albite. Phenocrysts and microphenocrysts of microcline perthite exhibit cross hatch twinning. In some samples, twins are only found in interstitial microcline. The lamellae are discontinuous, ribbon or spindle types. The alkali feldspars are untwinned and contain abundant inclusions of sericitized

calcic feldspar, biotite, chlorite, zircon and epidote. Plagioclase compositions (measured from Albite twins) are of calcic oligoclase. Twinning is moderately preserved with Albite, Carlsbad and pericline twins present. Twins become indistinct toward the sericite-muscovite cores of normally zoned plagioclase. Normal (marginal), normal continuous (from core to margin), oscillatory and transgressive oscillatory zoning were observed. The latter describes resorbed margins with single feldspar phenocrysts when melt resorption precedes growth stages (Phillips et al. 1981). The widths of compositional bands (i.e. sodic, calcic) are variable and display no overall compositional trends.

Biotite flakes are euhedral to anhedral with pale to strong green pleochroism. Chlorite after biotite is patchy. Epidote occurs as prismatic, equant, or euhedral crystals within the groundmass. Pistacitic compositions are common. Hornblende, a pale yellow green variety, occurs as anhedral groundmass grains, inclusions, and locally as microphenocrysts. Fe-Ti oxides occur as anhedral interstitial grains. Apatite prisms and euhedral to subhedral sphene are common with biotite and hornblende in the groundmass. Subhedral zircons are ubiquitous within the granodiorite.

Tonalite

The tonalite, from the Regina Bay pluton, is hypidiomorphic, granular, seriate with coarse 1-4 mm

euhedral to subhedral plagioclase phenocrysts, and minor amphibole microphenocrysts, the latter consisting of secondary minerals including chlorite, epidote and calcite. Plagioclase compositions are indistinct due to pervasive (30-80%) sericitization (also includes patchy muscovite and chlorite). Normal zoning is suggested by the lower percentage of alteration around phenocryst margins. The groundmass consists of quartz (anhedral, zoned, fractured), apatite (euhedral to anhedral prisms), chlorite, calcite, biotite (brown flakes), sphene, and leucoxene. Sagenitic rutile needles and zircon were observed within the biotite flakes.

Syenitoids

Examination of three thin sections from the Kishquabik Lake Pluton includes two samples from the pluton and one sample from a hypabyssal sill intruding the Berry Lake layered sequence at No Name Lake. The hypidiomorphic seriate syenodiorite is strongly porphyritic with euhedral to subhedral laths of microcline and microperthites. Tartan twinning is well developed in the ribbon (lamellae) and patch microperthite. Patch antiperthite was also observed with irregular patches of twinned microcline within albitic phenocrysts. The plagioclase is albite to oligoclase in composition and displays albite, pericline and Carlsbad twins. Continuous zoning was observed in a few plagioclase phenocrysts.

The groundmass consists of green to yellow brown, euhedral to subhedral hornblende (compositionally zoned), euhedral to anhedral apatite prisms, euhedral to anhedral sphene, magnetite, hematite, pistacitic epidote, biotite, euhedral zircon, and feldspar (albite, microcline and microperthite). In the hypabyssal dike/sill, the groundmass is mainly hornblende and epidote with accessory minerals. Feldspars are restricted to the phenocryst phase. The feldspar phenocrysts exhibit a trachytic flow alignment within the mafic (hornblende rich) groundmass.

STRUCTURAL GEOLOGY

The supracrustal succession occurs in triangular to linear belts rimmed by granitoid batholithic complexes. The supracrustals are generally steeply dipping (80 +- 10 degrees dip) and normally face away from the batholiths. An overall synformal basin structure (Ayres 1977) with a northwest trending axis characterizes the Sioux Narrows greenstone belt. Deformation broadly follows the margins of the batholithic complexes (see Figure 5). Schwertdner et al. (1979) suggested a syntectonic relationship between the diapiric granitoids and the regional deformation within the supracrustals. However, Ayres (1977) and Brown (1976, 1977) suggested that a period of deformation and/or metamorphism may have preceded granitic plutonism.

A regional study of the structural geology of the eastern Lake of the Woods area is in progress (Brown, p. comm. 1982). The structural evolution of the Berry Creek area is illustrated in Table 4 (modified after Brown 1976,1977). Brown (1976, 1977) recognized two major deformational stages. The earliest deformation consisted of upright, easterly trending, isoclinal folds (see Figure 17, Brown 1977). The F1 folds are recognized by following facing indicators: size and composition grading of clasts within pyroclastics; size (distribution) grading within tuff, metasediments (turbidites); Bouma cycles in turbidites; double grading of tuff couplets and tuff argillite couplets; flame and other load structures in turbidites; rip-up clasts at the base of debris flows

TABLE 4. FABRIC EVOLUTION AND STRUCTURAL GEOLOGY OF SIOUX NARROWS GREENSTONE BELT.

Deformation	Folding	Fabric	Metamorphism	Intrusion	Comments
		SØ			Deposition of supracrustals
DØ					Syndepositional slumping
			MØ		Synvolcanic fumaroles
				IØ	Subvolcanic sills
D1	F1	S1			E-W isoclinal folds planar fabric?
			M1		Pre-synkinematic regional metamorphism
D2	F2				E-W marginal rim folding N-S interference folding
			M2	I1	Diapirism and emplacement of granitoid complexes-folds and metamorphism
D2,3					Initiation of shear zones
		S2			Regional foliation (superimposed coaxial to oblique to S1)
		S2a			Foliation of marginal plutonics and aureoles
		S2b			Foliation of shear zones
				I2	Emplacement of tonalite, local marginal foliation
D3	F3				Kink and conjugate folds, chevron folds, crenulations
			M3		Retrograde metamorphism near shear zones, alkali + Fe + CO2 metasomatism
				I3	Post-tectonic syenitoid complex
			M4		Syn-post syenite potassic metasomatism
D4					NW faults temporally associated with late Precambrian diabase
D5					NE faults offset late Precambrian diabase

(primary and secondary types); crystal compositon grading in tuff; pillow cusp orientations in pillowed basalts; erosional channels and cross bedding in the pyroclastic

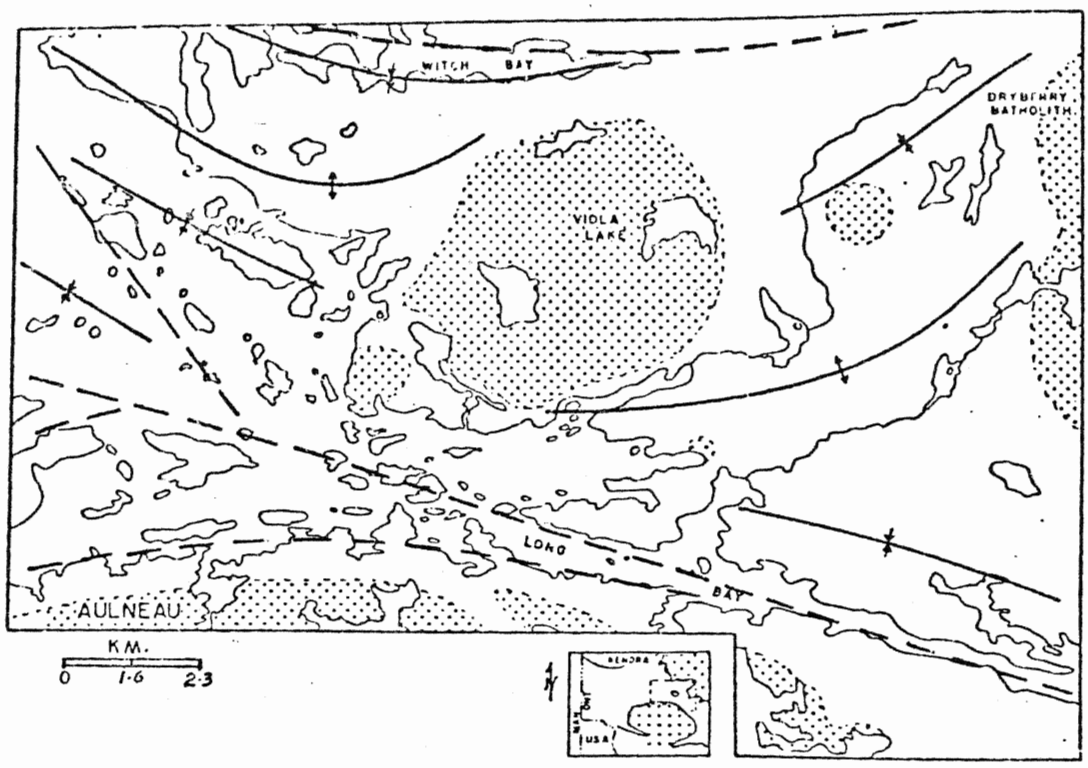

Figure 17. F1 FOLD STRUCTURES AND FAULT ZONES, WESTERN BERRY CREEK AREA (Brown 1977).

deposits; and compositional layering within cumulate zones of the Berry Lake layered sequence. Orientation and abundance of vesicles within pillows provided only regional younging trends. Alteration patterns, specifically chloritization, locally observed at the base of volcanogenic units (felsic flows overlying mafic argillite), also contributed facing directions. Bedding is commonly parallel to the regional foliation although angular relationships are present (see Plate 32).

The regional geology maps (see maps in pocket) display the numerous facing reversals with the Berry Creek metavolcanic and metasedimentary units. The long axes of clasts commonly parallel the F1 regional axial planar foliation (see Brown 1976, 1977). The F2 fold phase

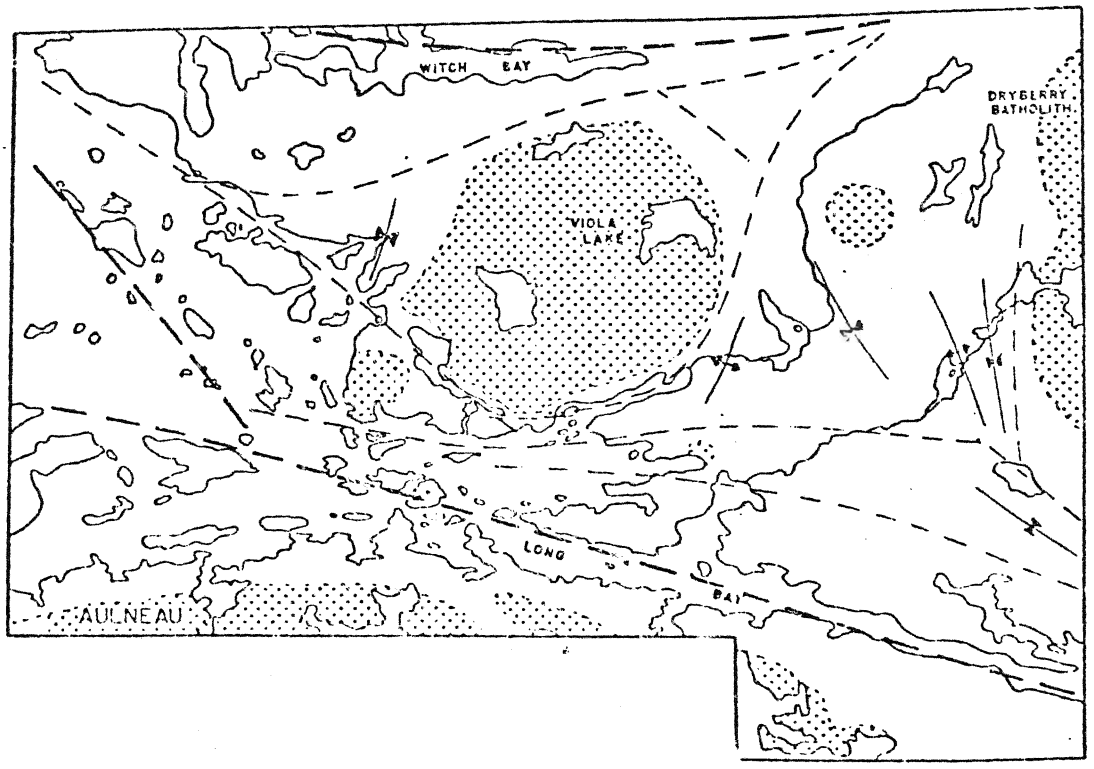

Figure 18. F2 FAULT AND FOLD STRUCTURES IN THE WESTERN BERRY CREEK AREA (Brown 1977).

accompanied the emplacement of the granitoid plutons. Figure 18 outlines the loci of the major F2 fold trends in the western half of the Berry Creek area.

In Figure 5, the distinction between F1 and F2 folds has not been interpreted due to : 1) lack of obvious crosscutting fabrics or refolded clasts; 2) common parallelism of F1 and F2 fabrics along the southern parts of the Berry Creek metavolcanics; and 3) the incipient, commonly microscopic, development of secondary minerals across S1 foliations. Mappable cross folding was only observed southeast of the Viola Lake stock near Yellow Girl Bay and Adams River Bay. The nonpenetrative F2 structures

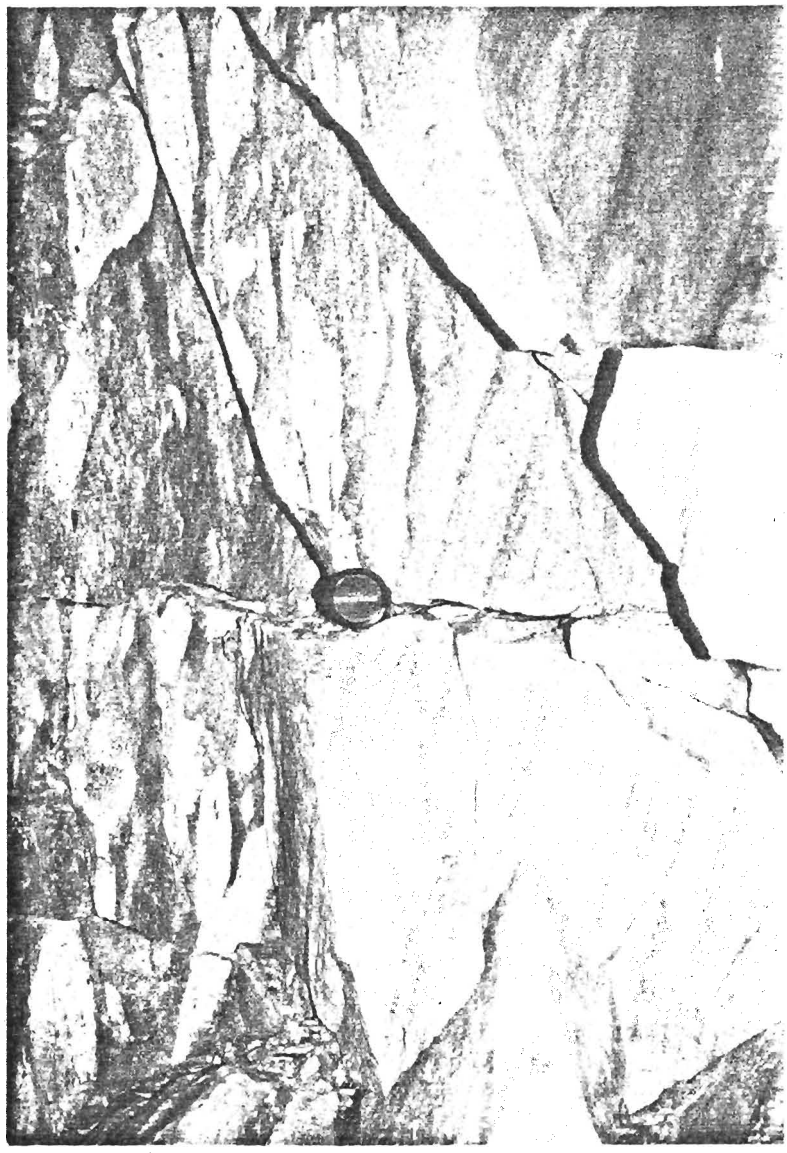

Plate 32. BEDDING/FOLIATION INTERSECTION, RUNNING ROAD SECTION, CLASTS ARE FLATTENED ALONG REGIONAL FOLIATION AT 15 DEGREES TO ORIGINAL BEDDING IN TUFF UNITS.

offset S1 foliations and locally fold S1 surfaces within elongated clasts.

The roughly north - south trends of F2 folds dominate the region between the Viola Lake Stock and the Dryberry batholith. However, south of the Dryberry batholith the S2 foliation has been overprinted on the F1 fold pattern (Brown 1977). Brown (1977) noted that the F2 folds reach a

maximum development proximal to the batholiths and rapidly decrease in intensity away from the margins. Some F1 structures are truncated against the granitoid batholiths, e.g., Black River antiform (see maps in pocket).

The deformation contrasts sharply between the two domains separated by the regional fault. The Snake Bay basalts are characterized by a generally north facing homocline forming a single limb rim synform around the Aulneau Batholith. Similarly the lower volcanic sequence of the northern domain forms a regional antiformal structure (Black River Antiform) which is later modified by cross folding and faulting. Conversely, the Berry Creek Complex and Berry Lake layered sequence are characterized by numerous shallow to moderately plunging vertical to slightly overturned (+- 15 degrees from vertical) isoclinal folds. Small scale parasitic folds and subsequent facing reversals are commonly observed within single exposures. Bedding parallel, transposed isoclinal folds are ubiquitous within finely layered sediments and mafic tuff. The multiple folds of the upper mixed sequence and homoclinal structures of the lower basaltic sequence also occur with the Kakagi Lake region (Edwards 1979, 1982) and are typical of many greenstone belts (see review by Condie 1981).

Other macroscopic structures associated with the regional foliations (F1, F2, S1, S2) include: boudinage of quartz veins, porphyritic intrusions, and layered gabbro to anorthosite sills within the Berry Creek metasediments;

tight to isoclinal folding of discordant intrusions; transpositon of folded layers; and development of rootless isoclines with thickened hinge zones. The latter occur within: 1) mafic tuff plus sediment assemblages; 2) mafic and felsic tuff assemblages; 3) disaggregated zones within layered pyroxenites (clasts of peridotite within strongly folded pyroxenite to peridotite matrix); and 4) attenuated mafic pillows.

Shear zones, pseudotachylytes, and faults range in scale from microscopic dislocations with minor displacements to large zones of intense strain. Many of these zones are associated with diapirism and exhibit a direct relationship with the D2 deformation. However, displacements are probably episodic throughout the D3 deformation (Brown 1977). The batholiths are surrounded by numerous faults and shear zones which roughly parallel the margins (Johns and Davison 1982). Thin (< 2 cm), discontinuous, pseudotachylyte zones were observed along the south western margin of the Mooseview granodiorite lobe of the Dryberry batholith. Plagioclase feldspar glomerophryic basalts locally display flattening, attenuation and stretching of phenocrysts proximal to shear zones at the margin of the Aulneau batholith.

The map area is dominated by the Pipestone - Cameron Fault System, a regional fault (see Edwards 1979) along Long Bay and south east into Dogpaw Lake (see structural geology, Figure 5 and maps in pocket). Edwards (1979)

suggested that the locus of the Pipestone - Cameron Fault along Long Bay represents the sheared out axial zone of the regional synform. As Edwards (1979) mentioned, the maximum deformation should coincide with the synclinal core. The structural facing and younging directions from the north and south domains supports this conclusion. The western extension of the Wabigoon regional fault probably transects Lobstick Bay (north of the Whitefish Bay Indian Reservation) and intersects the Pipestone - Cameron Fault near Regina Bay. Intense cataclasis covers a 1-2 km wide zone. Splay faults from the major zones are common. The F2 S2 crenulation cleavage is developed within tuffaceous units on the northern margin of the Pipestone - Cameron Fault zone. Numerous shear zones related to the fault system occur near Rendezvous Point and south east of Reed Narrows. It is possible that emplacement of the Regina Bay tonalite occurred during or between movements along splay shear zones (Edwards 1979) in a mechanism similar to that of the Stephen Lake pluton. Shear zones along the south shore of Regina Bay predate and post date the intrusion of the Regina Bay tonalite.

The D3 deformation is characterized by small scale microscopic to mesoscopic crenulations and kink folds. Development of the S3 crenulation cleavage, superimposed over S1 and S2 fabrics, reaches a maximum within Ø.5 km of the northern margin of the regional fault system. The chloritic metasediments along the south shore of Lobstick Bay display steeply plunging, conjugate, box type folds.

Brown (1977) suggested that the fabric developed in these zones displays a strong vertical component.

Microcrenulations are commonly observed in lamprophyric dikes and sill, schistose metatuff units, and mylonitized metasediments and mafic metavolcanics in Long Bay and Lobstick Bay.

The D4 and possibly D5 deformations consist of faulting in a northwesterly trending direction and in a northeasterly trending direction, respectively. Brown (1977) suggested that the D4 deformation is associated with the regional en echelon diabase dike intrusions. The dikes are offset by NE - SW faults and locally by E - W trending faults (Berry Lake). Northwest trending left lateral drag and release (kinking) structures and northeast trending tension gashes occur in chloritized metasediments.

METAMORPHISM

The supracrustal rocks of the Sioux Narrows greenstone belt have been regionally metamorphosed to upper greenschist, lower amphibolite and epidote-hornblende hornfels facies rank.

Metamorphism has destroyed the majority of the primary mineralogy, but textural features are normally preserved. The presence of pseudomorphs after primary phases and the relicts of microcline feldspar phenocrysts suggest that the metavolcanics have not attained bulk rock equilibrium (Jolly 1980, 1982). Plagioclase feldspars display pervasive albitization, although primary albite, Carlsbad, and pericline twins are preserved. Quartz phenocrysts typically display octahedral forms as alpha pseudomorphs after beta quartz. Microcline feldspars occur as patchy zones (similar to patch perthites) within albitized feldspar blasts. Serpentine, talc, and chlorite also form as pseudomorphs of primary olivine crystals within cumulate dunites of the Berry Lake layered sill (see Plate 3). Jolly (1982) noted that pseudomorphs are commonly obliterated by amphibolite grade metamorphism. The relict pseudomorphs are commonly embayed by biotite, albite, actinolite, hornblende, and sphene. Plagioclase feldspar phenocrysts (blasto-porphyritic albite, Studemeister 1983) are generally embayed by plates of medium to coarse grained muscovite.

Metamorphism has resulted in the growth of porphyroblasts to poikiloblasts of garnet, staurolite,

biotite, actinolite, hornblende, chloritoid, epidote, andalusite and cordierite. Garnet, hornblende, and staurolite contain numerous inclusions of quartz, feldspar, and accessory minerals. Prograde forsteritic olivine was observed within the amphibolite grade serpentinized dunites of the Berry Lake layered sill (see Plate 30).

Porphyroblasts of garnet are common within mafic tuff of the Berry Creek metavolcanics and within interpillow hyaloclastite breccias of the Black River metavolcanics. Plagioclase feldspars range in composition from albite to andesine and rarely labradorite. Anorthite content increases towards the granitoid intrusions. Actinolite commonly forms rims of elongate needles around hornblende blasts (see Studemeister 1983). Epidote occurs as subrounded to irregular pods within pillowed mafic metavolcanics. Primary epidote commonly forms as pillow cores (Ayres 1969; Dimroth et al. 1983), but is usually preserved only at below lower greenschist grade.

Mafic to ultramafic sills are mineralogically similar to the mafic metavolcanics with abundant actinolite, hornblende, olivine, chlorite, serpentine, albite, and minor talc. Biotite, sphene and magnetite form the accessory assemblage. Pyroxenites are characterized by actinolite with accessory chlorite (see Plate 30). Serpentinized dunite, containing serpentine, talc and chlorite with actinolite, forms a greenschist assemblage due to chemical constraints.

The intermediate to felsic Berry Creek metavolcanics and immature arenitic metasediments contain polygonized quartz and plagioclase feldspars with green to brown biotite, muscovite, epidote group minerals (pistacite, zoisite, epidote), sphene, and tourmaline. The low abundance of andesine plagioclase within amphibolite grade metatuff probably reflects compositional ranges of the primary feldspar crystals. Porphyroblasts of chloritoid and garnet are restricted to several units of the metavolcanic suite. Garnet, chloritoid, and tourmaline found north of Lobstick Bay are related to synvolcanically altered (MØ fumarolic metasomatism) metatuff. Pistacitic epidote metadomains are developed adjacent to the Keweenawan diabase dykes. The remaining metadomains, modified by high pCO_2, pO_2, Fe_2O_3, and K_2O, are characterized by calcite, sericite, epidote and chlorite.

Pelitic horizons are characterized by aluminous porphyroblasts including garnet, staurolite, biotite, subordinate andalusite and cordierite. Although andalusite was not observed by the author, reports of tiny blasts are discussed by Johns and Richey (1982) and Edwards (1979). Andalusite also occurs within the nearby Manitou Straits area (Blackburn, p.comm. 1982).

Retrograde metamorphic phases are widespread (see Condie 1981) and include the following: chloritoid after biotite, muscovite, actinolite, hornblende, and staurolite; muscovite, sericite, saussurite, and carbonate after plagioclase feldspar; albitic plagioclase after garnet;

and minor chlorite, sphene and magnetite after forsterite, serpentine and hornblende.

Retrogressive phases are commonly associated with structural breaks, such as the Pipestone - Cameron fault, while biotite and chlorite, are ubiquitous throughout the map area. Carbonatization and sericitization are restricted to faults and late stage (D3, D4, D5) folds, kink bands, and conjugate fractures.

The degree of annealing (recrystallization) increases toward the granitoid intrusions. Grain boundaries range from sutured to granoblastic. Phenocrysts of plagioclase (albite) and quartz commonly show marginal to complete polygonization. Epidote and sphene display a morphological progression from granular aggregates to idioblastic and subidioblastic porphyroblasts. The latter are extremely common near No Name Lake (see Plate 23). Hornblende exhibits compositional changes from yellow-brown-green to dark bluish green within basalts adjacent to the Regina Bay tonalite and the Berry Lake granodiorite lobe. Jolly (1980) noted that brown biotite blasts occurred within the aureole of alkalic intrusions. The introduction of K_2O-rich fluids probably occurred in the dark brown to orange biotite zone found peripheral to the Kishquabik syenodiorite and the Mooseview granodiorite lobe.

Hornblende and actinolite display various morphologies consistent with both static and dynamic domains. Oriented laths characterize the tightly folded amphibolites while

acicular, commonly radiating, sheaves of actinolite and hornblende form clusters within intermediate intrusions and mafic tuff. The latter are commonly mixed with felsic metatuff and metasediment (see Plate 28). The radiating hornblende and actinolite develop during post-tectonic growth or within static domains (Studemeister 1983; Condie 1981; Williams, p. comm. 1982) i.e., peak of metamorphism outlasts deformation. Random growths of amphiboles occur away from contact aureoles and zones of tectonic activity (Jolly 1982).

Brown (1976) reported rotated blasts of garnet and staurolite. Straight helicitic trails (Spry 1969) were observed within garnet and hornblende poikiloblasts north of Lobstick Bay and from the Maybrun road stratigraphic section.

The field and petrological observations indicate that the assemblages formed during a prolonged episode of regional contact metamorphic conditions. Reactants and products of the specific reactions have been reported from the upper greenschist to amphibolite transition zone (Reymer 1983). The reactions indicated in Table 5 and Figure 19 provide critical limitations on the pressure-temperature conditions (Jolly 1980, 1982; Winkler 1979; Turner 1968; Reymer 1983; Holdaway 1971; Richardson et al. 1969). Ayres (1972, from Goodwin et al. 1972) noted that the assemblages around large granitoid batholiths of the Superior Province correlate with low or low to intermediate pressure facies series similar to regional facies. The

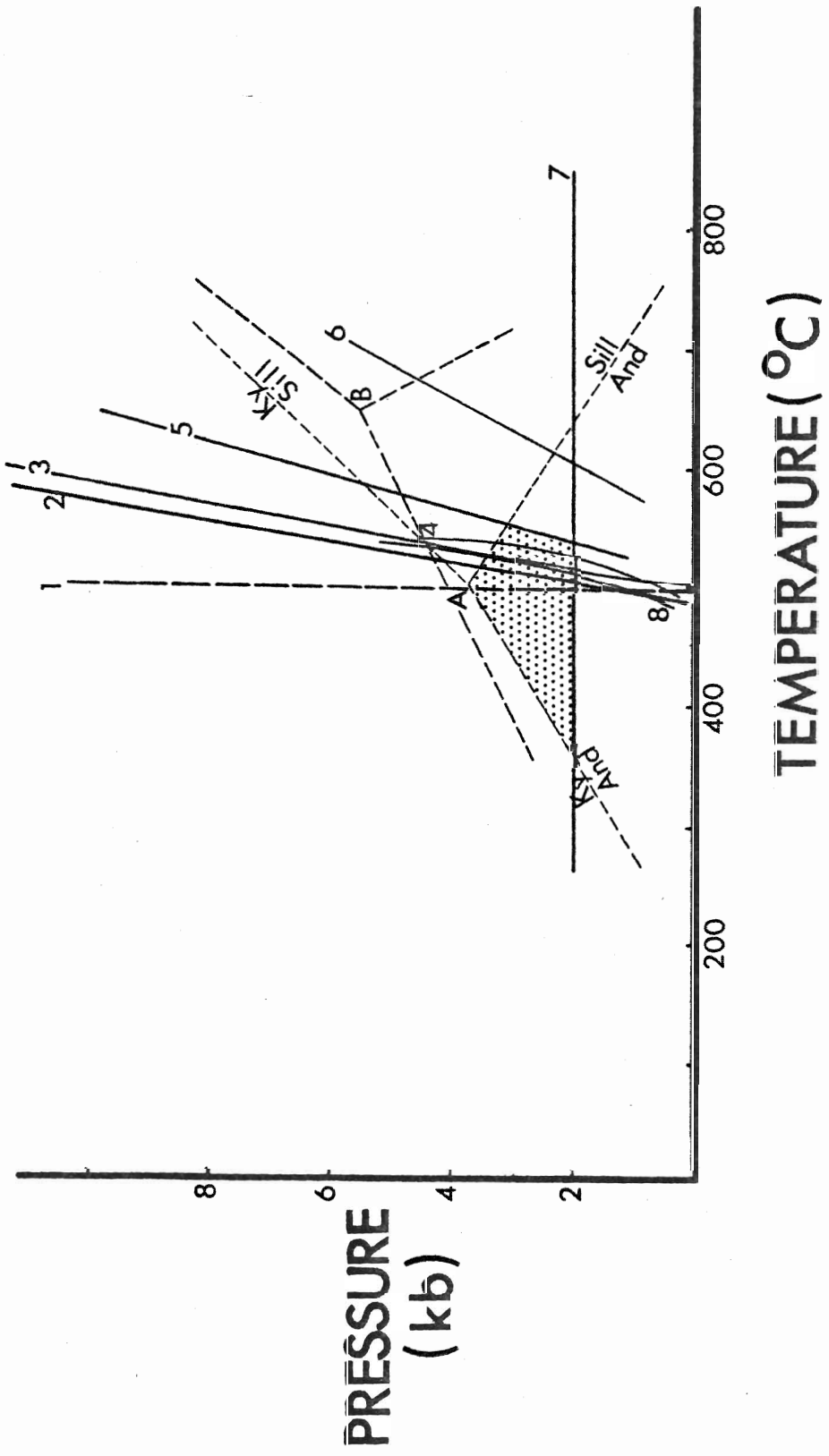

Figure 19. P-T DIAGRAM AND METAMORPHIC REACTION CURVES IN THE BERRY CREEK AREA.

TABLE 5. METAMORPHIC REACTANTS AND PRODUCTS OF THE BERRY CREEK AREA.

1) Actinolite -----> Hornblende

2) Pelites Almandine In
Mafics An17 + Hornblende In

3) Serpentine -----> Forsterite + Talc

4) Chlorite + Muscovite -----> Cordierite

5) Epidote breakdown

6) Staurolite -----> Cordierite + Andalusite + Muscovite + Garnet

7) P > 2 kb Cordierite + Staurolite + Almandine
P < 2 kb Cordierite + Staurolite

8) Chloritoid + Chlorite + Muscovite -----> Staurolite

A) Al2SiO5 triple point -- Holdaway (1971)

B) Al2SiO5 triple point -- Richardson et al. (1969)

recognition of contact aureoles, specifically hornblende hornfels, may be difficult in areas where the overall grade is upper greenschist to amphibolite facies (Ayres 1972).

The metamorphic assemblage, containing garnet, staurolite, andalusite, cordierite and hornblende, can be reconciled with an equilibrium, low to intermediate pressure, epidote amphibolite to amphibolite facies series (Miyashiro 1973; Reymer 1983; Winkler 1979; Condie 1981). Geochemical constraints, e.g., Fe/Fe + Mg ratios, are favourable for the associations of staurolite, cordierite, garnet, and andalusite (Turner 1968; Miyashiro 1973; Winkler 1979).

Miyashiro (1973) reports the coexistence of staurolite, garnet, and aluminosilicates within medium pressure contact aureoles; specifically near the aluminosilicate triple point. Cordierite and almandine may coexist over wide pressure ranges in the upper greenschist - amphibolite facies (Turner 1968; his Figure 40-6). Ramsay and Kamineni (1977) suggested that garnet predominates over cordierite at pressures greater than 3 kb. Reymer (1983) reported the almandine garnet, staurolite, andalusite, cordierite assemblage at approximately 3 kb under lower amphibolite conditions. Andalusite and Fe-cordierite may coexist at pressure of less than 3.5 kb (Richardson 1968; Reymer 1983). Variations in the field size of andalusite depending upon the position of the triple point and the overlapping reaction field suggest that andalusite will remain to pressures of 4 kb (Reymer 1983; Turner 1968).

Staurolite may possibly break down to produce cordierite, andalusite and muscovite at temperatures exceeding 500 degrees C within the lower pressure regime (Turner 1968, see reaction 6, Figure 19). Garnet may be involved in the reaction at higher pressures.

Condie (1981), Ramsay and Kamineni (1977) and Breaks et al. (1978) suggested that pressures may have been reduced during synkinematic diapirism. Early regional medium pressure metamorphism is probably superimposed by a lower pressure regional contact metamorphism. Metamorphism

within the Norseman-Wiluna greenstone belt is related to synkinematic intrusions (Condie 1981).

The abundance of garnet within the Sioux Narrows belt suggests that a moderate pressure facies series has preceded the lower pressure staurolite, cordierite and andalusite assemblage. The presence of undeformed and non-rotated garnet porphyroblasts suggest that the decreasing pressure during diapirism and M2 metamorphism remained within the garnet stability field (greater than 2.5 kb). Transitional regional to contact metamorphism has been reported by Reymer (1983) and Miyashiro (1973).

The metamorphic history of the Berry Creek area (see Table 4) is similar to the sequence of events proposed for the English River Subprovince by Breaks et al. (1978, their Table 5). Textural relations of the porphyroblasts suggests that deformation D1, D2 and metamorphism M1, M2 are probably contemporaneous although the M2 metamorphism outlasted the D2 deformational stage. A modification to the above sequence includes the presence of local static domains within competent lithologies.

Matrix coarsening occurred during and after development of the incipient S2 fabrics (see Plates 26 and 27). Minor rotation of biotite porphyroblasts was also observed. Late stage post-tectonic metamorphic products include the M3 metasomatic effects of alkalic intrusions and M4 retrogressive alteration related to D3, D4 and D5 structures (see Table 4).

ARCHEAN STRATIGRAPHY

The problems and advantages involved in the detailed analysis of Archean stratigraphy have been discussed by Ayres (1977, 1982), Buck (1978), Car (1976) and many others. The analysis is hampered by a combination of structural, physical, lithological and erosional factors. Although the Archean sequences are deformed by isoclinal folds, occasionally polyphase, similar erosional cross sections are not available in modern subaqueous volcanoes. Studies of subaqueous volcanics, especially komatiites, are commonly restricted to Archean terrains.

Problems within the Archean exposures include the following: 1) loss of primary structures, textures, and sedimentary features by greenschist to granulite facies metamorphism; 2) complex fold structures involving flattening, rootless isoclines, transposed and deformed facing indicators, lineations and telescoping beds; 3) faulting (synvolcanic, syn to post-deformational) producing missing sections, local unconformities, repetition of sequences; 4) assimilation by granitoids and subvolcanic intrusions; 5) poor outcrop, till coverage, and lack of three dimensional exposures; 6) absence of marker beds; 7) presence of lenticular beds; and 8) problems locating vent zones and position of exposed stratigraphy within the volcanic centre. Facies analysis is most useful in the pyroclastic and epiclastic assemblage due to the possible abundance of measureable variables (Tasse et al. 1978; Ayres 1977, 1982; Parsons 1969; Heiken 1972).

STRATIGRAPHY

LITHOFACIES

The Berry Creek Metavolcanic Complex has been subdivided on the basis of facies and stratigraphic mapping (see Tasse et al. 1978; Lajoie 1979; Ayres 1977, 1982, 1983; Hendry 1978; Dimroth and Demarcke 1978; Buck 1978; Gordanier 1976) into eight lithofacies types (Table 6, Figure 20). Each lithofacies is characterized by a specific deposit or group of deposits displaying distinct spatial, genetic and/or temporal associations. Based on lateral variations in each lithofacies types, proximal (central), medial and distal members have been recognized within several lithofacies. The facies boundaries are generally gradational and commonly are interdigitated with the adjacent lithofacies type. Given the scale of mapping, the lithofacies broadly outline the lateral and vertical lithologic associations. Boundaries between primary pyroclastic and sediments are defined by trends of progradational volcanic deposition and/or cessation of volcanism coupled with extensive sedimentary reworking of tephra.

Facies A

The proximal lava flow facies occurs in the eastern end of the map area near Dirtywater Creek (Figure 20). Subaqueous flow laminated lava consists of laterally continuous flow layers and highly contorted laminations. Brecciation was not observed at the basal contact with the

TABLE 6 . LITHOFACIES TYPES OF BERRY CREEK COMPLEX AND ASSOCIATED METAVOLCANICS AND METASEDIMENTS

A. Proximal Flow Facies - flow laminated lavas.

B. Proximal Dome Breccia Facies - massive and brecciated lava, scree and talus, crystal tuff, hyalotuff, debris flows, subvolcanic porphyries.

C. Pyroclastic Facies - Proximal to Distal Members - debris flow, ash flow tuff, reworked tuff, turbidites, lahars, ash tuff.

D. Lower Mixed Facies - lahars, debris flows, arenite and wacke, reworked mafic to felsic tuff, ash flow tuff.

E. Upper Mixed Facies - debris flows, ash flow tuff; Lobstick Bay metavolcanics - massive to pillowed flows, mafic tuff; greywacke, argillite turbidites intermediate to felsic tuff/crystal tuff, sulphide iron formation, chert, feldspathic chert.

F. Pyroclastic to Epiclastic Facies - Medial to Distal Members - tuff, ash flow tuff, turbidites, debris flows.

G. Epiclastic Facies - greywacke, argillite (turbidites), arenite, iron formation, minor mafic to felsic tuff, reworked tuff.

H. Lower Lava Plain Facies - amphibolites, mafic lavas, tuff, argillite, greywacke (mafic provenance).

underlying mafic argillite (Facies H) although significant alteration characterizes the lower few metres of the lava flow. The lateral extent of Facies A terminates at the Berry Lake - Sanford Lake granodiorite lobe. Several remnants occur as pendants within the granodiorite to the

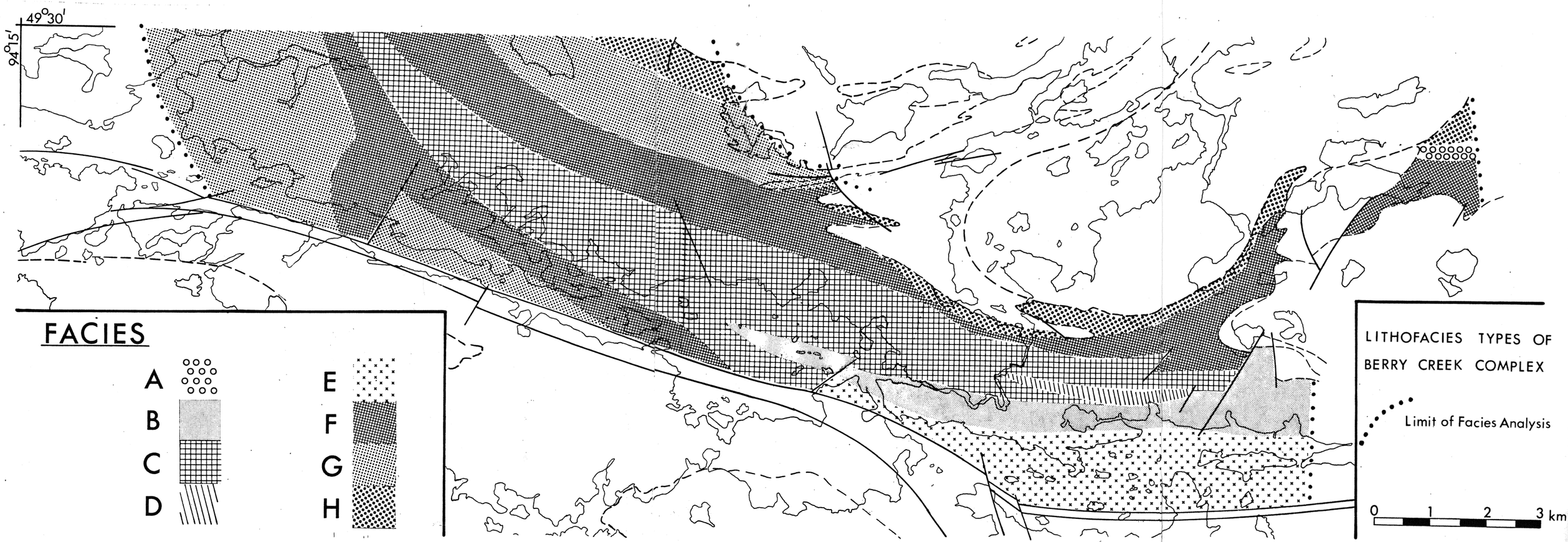

Figure 20. LITHOFACIES TYPES OF THE BERRY CREEK COMPLEX.

east of the Kenu River. The upper facies boundary with Facies F was not observed due to granitoid and syenitoid intrusions and the Dirtywater Creek valley.

Facies B

The proximal to medial dome breccia facies (see Figure 20) parallels the north shore of Lobstick Bay to the centre of Long Bay. The maximum western extent of Facies B is probably gradational with the underlying Facies C and overlying Facies E. Determination of boundaries is hindered by the similarity of Facies B and C monolithic breccias and the lack of outcrop (small islands only). Since pumiceous fragments, common to Facies C, are not recognized in the outcrop, the boundary has been approximated. Similarly, monolithic breccias of Facies E are associated with a later stage of mixed volcanism and sedimentation. These monolithic breccias, equivalent to those of Facies B, are derived from further degradation of the central dome complex.

The proximal member of the dome breccia consists of massive and brecciated lavas, debris flows, pyroclastics and minor sediments. The proximal porphyry and lava member also contains numerous synvolcanic porphyritic intrusions associated with the extrusive lavas and fragmental deposits. Granitoid and late syenitoid stocks intrude the porphyry dome complex. The monolithic breccias are adjacent to brecciated lava flows consisting of lobes or

tongues of massive to brecciated rhyolite with occasional pockets of lapilli tuff. Fragment grading in the brecciated lavas was not observed in the lower proximal member. However, the upper proximal member and the medial member are dominated by normally graded and inverse to normally graded monolithic debris flows commonly intercalated with pumiceous pyroclastic flows. Nongraded fragmental deposits, both monolithic and heterolithic, are also present. The upper proximal and medial members also contain a thick succession of tuff which overlies and is gradational from normally graded debris flows. The massive crystal rich deposits are exposed between Berry River and Reed Narrows, from west of Roberts Lodge to the central part of Long Bay, south of White Moose Lodge.

Facies C

The pyroclastic facies encompasses the majority of the primary and resedimented pyroclastics of the Berry Creek Complex. The deposits consist of normally graded, inverse to normally graded, massive, graded stratified and minor inversely graded debris flows intercalated with minor tuff, sediments and reworked volcanics (including lahars). Proximality indicators based on clast size and distribution have been discussed by Walker (1979), Hein (1979), Hendry (1978), Lajoie (1979), Tasse et al. (1978), Nemec et al. (1980) and Long (1977). Lateral variations in the Berry Creek deposits are comparable with deposits described in Figure 21 by Tasse et al (1978) and Lajoie (1978).

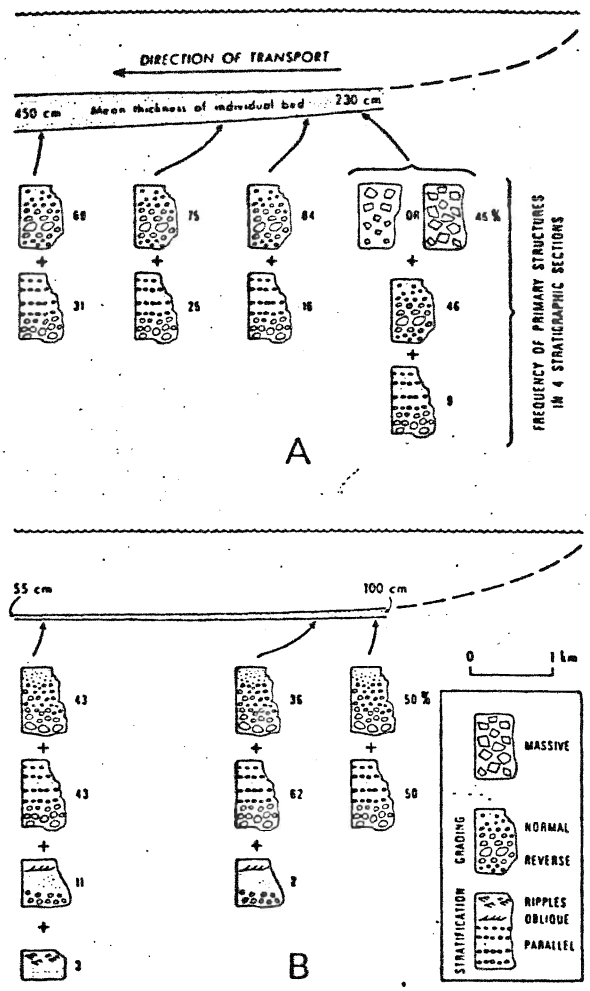

Figure 21. LATERAL VARIATIONS, GRADING AND BED THICKNESS, PRIMARY STRUCTURES IN DEBRIS FLOWS AND TURBIDITY CURRENTS (Tasse et al. 1978, Lajoie 1979)

The proximal pyroclastics are typically inverse to normally graded coarse fragmentals with upper fine grained tuff deposits. The coarse debris flows are overlain by the subsequent coarse volcanoclastics without the intervening fine grained suspension deposits. This is particularly evident in Figures 10 and 12. The proximal coarse flows may exhibit erosive bases as shown by scour channels and rip up clasts (see Figures 8 and 16).

The proximal members can be analyzed by local stratigraphic variations based on the grain size and clast

dimension as well as sedimentary textures. On a local scale, sequences contain progradational bed units defining coarsening upward profiles and similarly fining upward cycles defining a decrease in the supply of volcanogenic detritus. Development of these cycles is discussed under Facies Models.

Simply stated, the distal to medial members of the pyroclastic Facies C are equivalent to the upper proximal members of abandoned or fining upward lobe cycles. These members are characterized by normally graded debris flows, commonly containing pumiceous fragments, graded stratified debris flows with pebbly layers (see Figure 22) and fine grained tuff deposits. The evolution of the fining upwards cycle shown in Figure 15 is essentially similar to the characteristic lateral variation in the distal and medial members. The medial to distal members may contain erosive bases but usually lack a basal **inversely**graded zone. The Mist Inlet stratigraphic section (Figure 15) contains several normally graded debris flows intercalated with sedimentary units. The debris flows of these medial and distal members are thinner, contain finer clast sizes, and are commonly matrix supported with relatively thick tuff subunits. Intercalations of fine tuff and reworked volcanics with turbidite sediments are common at the base of the proximal pyroclastic Facies C and in the medial and distal members. The lower part of the Running Road section

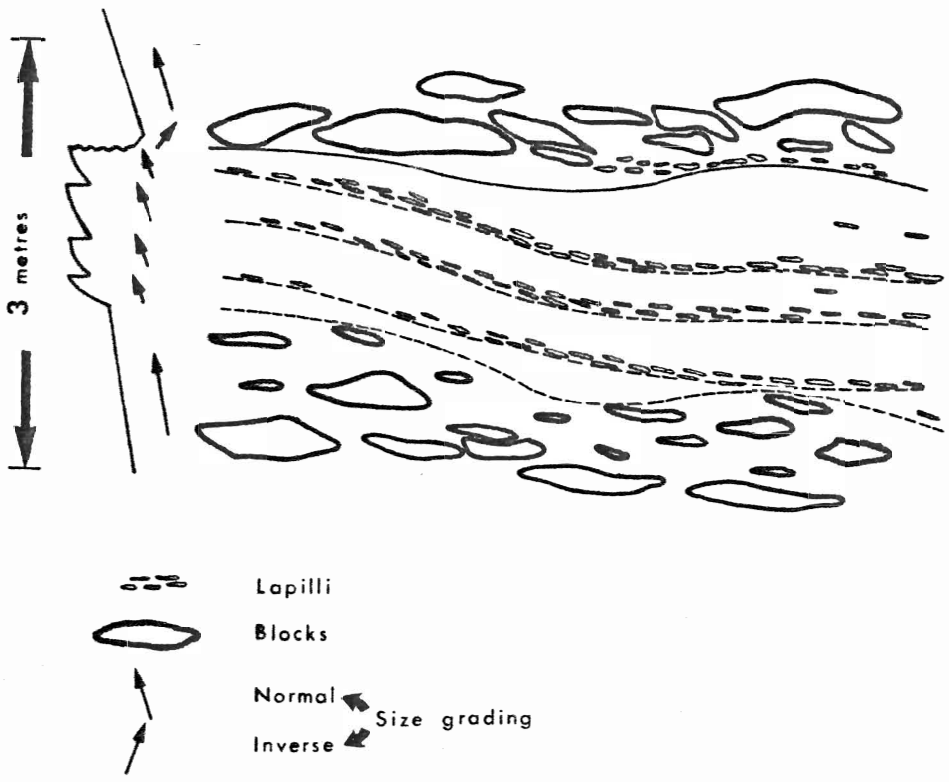

Figure 22. GRADED STRATIFIED DEBRIS FLOW FROM RUNNING ROAD SECTION. LAPILLI ALIGNED ALONG BASE OF UPPER BEDS. NOTE EROSIONAL BASE AND INVERSELY GRADED LAYER OF OVERLYING DEBRIS FLOW.

(Figure 7) overlies a sedimentary assemblage of proximal turbidites from Facies G.

Facies D

The lower mixed facies consists of a variety of sedimentary and volcanic deposits (Table 6). This facies is exposed subparallel to the Maybrun Road and contains deposits from the lower section of the Maybrun stratigraphic section (see location, Figure 6). These deposits of reworked tuff, sediments (proximal turbidites and mass flow wacke) and mafic tuff are laterally intercalated with ash flow tuff and monolithic breccias

from Facies C and B. The laterally restricted facies may have been deposited in a basin associated with collapse following the temporary cessation of pyroclastic volcanism. The presence of mafic tuff and lahars containing rounded mafic clasts suggests a sediment source from a topographic high adjacent to parts of the central volcanic complex (see depositional model, Figure 43, Stage 4). The laharic deposits occur within steep sided narrow channels.

The proximal wackes and AE turbidites are interbedded with fine mafic tuff and grade laterally into the reworked lahars. Although the lahars imply subaerial derivation (Ayres 1977; 1983; Bailes 1980; Attoh 1981), all deposition has occurred within a relatively shallow subaqueous environment.

FACIES E

The upper mixed facies (also termed Lobstick Bay metavolcanics) consists of deposits formed during the late stages of volcanism. These deposits (see Table 6, Figure 20) include: debris flows; tuff; crystal tuff; massive, pillowed and brecciated mafic lava flows; mafic tuff; chert; feldspathic chert; sulphide iron formation; argillite (pelagic deposits) and turbidites. The latter consists of greywacke and argillite couplets. All of the Facies E deposits occur in the Lobstick Bay area and show a western extent to Laughing Water Lodge, west of Reed Narrows. A northeasterly trending fault terminates the mixed sequence. The southern boundary of the facies is

controlled by the Wabigoon and Pipestone - Cameron fault system (see Figures 5 and 20). The eastern (proximal) deposits include monolithic to heterolithic breccias derived from the Facies B dome complex. The breccias commonly have fragments of sulphide iron formation and the matrix is stained by iron metasomatism. The southern and western deposits are characterized by products of quiescent sedimentation. Chert and feldspathic chert are intercalated with argillite near the north shore of Lobstick Bay. Turbidite sedimentation consisting of AE couplets and doubly graded tuff-arenite to argillic tuff (see Plate 6) dominate the upper members of the upper mixed facies. Some of the upper Facies E deposits are contained within fault slivers parallel to the Pipestone-Cameron fault along Long Bay. Correlation of the Facies E units near Reed Narrows and similar deposits south and east of Apache Landing is uncertain.

Facies F

Lithofacies F is essentially a transitional zone between Facies C and E (see Figure 20). The deposits include debris flows (normally graded, may be stratified), crystal tuff, tuff, and turbidite sediments. Depositional structures are similar to those described for the Mist Inlet stratigraphic section (Figure 15). This facies is also recognized in the Old Woman Lake section (Figure 14). The background turbidite sediments are periodically intercalated with distal or lateral facies equivalents of

controlled by the Wabigoon and Pipestone - Cameron fault system (see Figures 5 and 20). The eastern (proximal) deposits include monolithic to heterolithic breccias derived from the Facies B dome complex. The breccias commonly have fragments of sulphide iron formation and the matrix is stained by iron metasomatism. The southern and western deposits are characterized by products of quiescent sedimentation. Chert and feldspathic chert are intercalated with argillite near the north shore of Lobstick Bay. Turbidite sedimentation consisting of AE couplets and doubly graded tuff-arenite to argillic tuff (see Plate 6) dominate the upper members of the upper mixed facies. Some of the upper Facies E deposits are contained within fault slivers parallel to the Pipestone-Cameron fault along Long Bay. Correlation of the Facies E units near Reed Narrows and similar deposits south and east of Apache Landing is uncertain.

Facies F

Lithofacies F is essentially a transitional zone between Facies C and E (see Figure 20). The deposits include debris flows (normally graded, may be stratified), crystal tuff, tuff, and turbidite sediments. Depositional structures are similar to those described for the Mist Inlet stratigraphic section (Figure 15). This facies is also recognized in the Old Woman Lake section (Figure 14). The background turbidite sediments are periodically intercalated with distal or lateral facies equivalents of

ash flow tuff (debris flow). In both of the above sections, the lower coarse debris flows exhibit rapid normal grading of the clasts to a fine lapilli tuff and are overlain by extensive turbidite deposits. The local coarsening to fining cycles characterizes the distal or peripheral areas of the depositional aprons. The scattered debris flows are not confined to channels interpreted in the proximal suprafan and midfan facies.

Facies G

The epiclastic facies (Table 6) consists of greywacke and argillite associated with reworked tuff, arenite, mafic tuff and iron formation. The distribution of Facies G (see Figure 20) follows the proposed periphery of the volcanic apron. Subaqueous deposition by turbidites, supplemented by minor chemical sedimentation, comprise the dominant assemblage. Rare exposures of tuff, arenite, and mafic tuff are associated with distal facies of upper debris flow subunits. Tuff/arenite units generally contain abundant crystals of quartz and feldspar.

Facies H

This facies comprises the lower lava plain assemblage of massive to pillowed mafic flows, mafic tuff and pyroclastic deposits, and sediments of mafic provenance. The flows are locally exposed as amphibolites along the southern margin of the Dryberry batholithic complex (Figure 20). Although the basalts outcrop as a curvilinear

antiform from Bunny Lake to Adams River Bay, only a cursory examination of several small areas was conducted. The Adams River Bay tuff and tuff breccia contain essential pumiceous fragments (scoriaceous), large mafic clasts and abundant mafic crystals. Bedding features and associated pillow basalt suggest subaqueous deposition. Detailed facies analysis was not completed on these deposits.

The eastern amphibolites locally are tectonically intercalated with the basal debris flows and arenite/tuff units of Facies C (see Figure 14, 20-23 m). The amphibolites and mafic argillite of the Dirtywater Creek area directly underlie lava flows of Facies A. In all other sequences, the mafic flows are separated from the primary pyroclastics by sediments and reworked volcanic deposits of Facies G.

DEPOSITIONAL CHARACTER

Pyroclastics and Tuffaceous Deposits

The majority of the Berry Creek metavolcanics exhibit textures, structures, components and facies associations similar to those described for subaqueous pyroclastic flow deposits e.g., Fiske and Matsuda 1964; Fisher 1963; Niem 1977; Tasse et al. 1978; Cas 1979; Carey and Sigurdsson 1980. Detailed studies of the internal fabric of the volcanics, the association of specific textures, motifs, units and sequences, and their proximity to sedimentary facies suggest that the pyroclastics were subaqueously

deposited by downslope mass flow mechanisms. Evidence will be given to compare primary and secondary deposition and the effects of the morphology and components on the volcanosedimentary assemblage. Deposition has occurred by ash flow tuff, debris flow, grain flow, turbidity currents and secondary derivatives including ash clouds, slumps, collapse structures, and lahars.

The criteria for recognition of these deposits and their paleoenvironmental associations include: grading (several varieties), textural motifs (Nemec et al. 1980), fragment or clast lithology and morphology, crystal components, primary sedimentary structures and Bouma style bed unit sequences (Cas 1979).

Many of the above factors can be directly related to the fluid mechanics involved in the transport of the tephra such as laminar versus turbulent flow or a combination of the two flow types (Lowe 1982; Fisher 1983; Nemec et al. 1980; Sparks 1976; Fisher and Heiken 1982; Sheridan 1979; Eriksson 1981). In practise, most of the subaqueous currents or flows display a lateral and commonly vertical transition from laminar (proximal) to turbulent (upper and/or distal) suspensions (Fisher 1983; Tasse et al. 1978,1982; Cas 1979; Morton and Nebel 1983; Wilson 1980). Flow types defined by Wilson (1980), Tasse et al. (1978) and Nemec et al. (1980) closely parallel the lateral facies changes observed in the Berry Creek pyroclastic deposits. Although the modelled flows provide two end

member styles, the majority of the debris flows display transitional behaviour.

The degree of turbulence depends upon the particle density (clast concentration) within the head and body of the moving flow (Sparks 1976; Nemec et al. 1980; Fisher and Heiken 1982; Hein 1982; Lowe 1982). Several authors, e.g., Tasse et al. (1978), Lowe (1982), and Fisher and Heiken (1982) suggest that the high density flows are essentially laminar. Grading of clasts and matrix should be inhibited by the high particle concentration and dispersive pressures due to clast collisions (Fisher and Heiken 1982; Cas 1979; Lowe 1982). Massive or nongraded beds may also result from rapid deposition (Cas 1979; Hein 1982). The high particle density (high viscosity) effectively damps out turbulence (Morton and Nebel 1983).

In subaerial and subaqueous flows, the turbulence is maximized at the flow head, commonly a cleft and lobe form, by ingestion of air and water, respectively (Wilson and Walker 1982; Simpson 1972; Fisher 1977). The influx of water in the subaqueous flows lowers the flow density, reduces the effectiveness of dispersive pressure and matrix strength for clast support and generally initiates the onset of traction and suspension sedimentation of the coarse clasts (Lowe 1982; Sparks 1976; Druitt and Sparks 1976). Lowe (1982) noted that flow unsteadiness combined with the velocity decrease often caused rapid dumping of the coarse particles. The separation of a flow into laminar and turbulent components may occur by gravity

(density separation) and/or by mixing with the upper and peripheral zones of the flow body (Fisher 1983; Walker 1979). Laminar and turbulent flows commonly coexist as basal and upper zones, respectively (Sparks et al. 1980; Sigurdsson 1982). These zones occur in subaerial and subaqueous ash flows (Sparks et al. 1980; Fisher 1982). The turbulent ash cloud in subaerial environments (due to air ingestion and elutriation of the fine particles) (Sparks and Walker 1977) is recognized in subaqueous flows by similar coarse fragment depleted tuff horizons overlying the basal debris flow (Sparks et al. 1980).

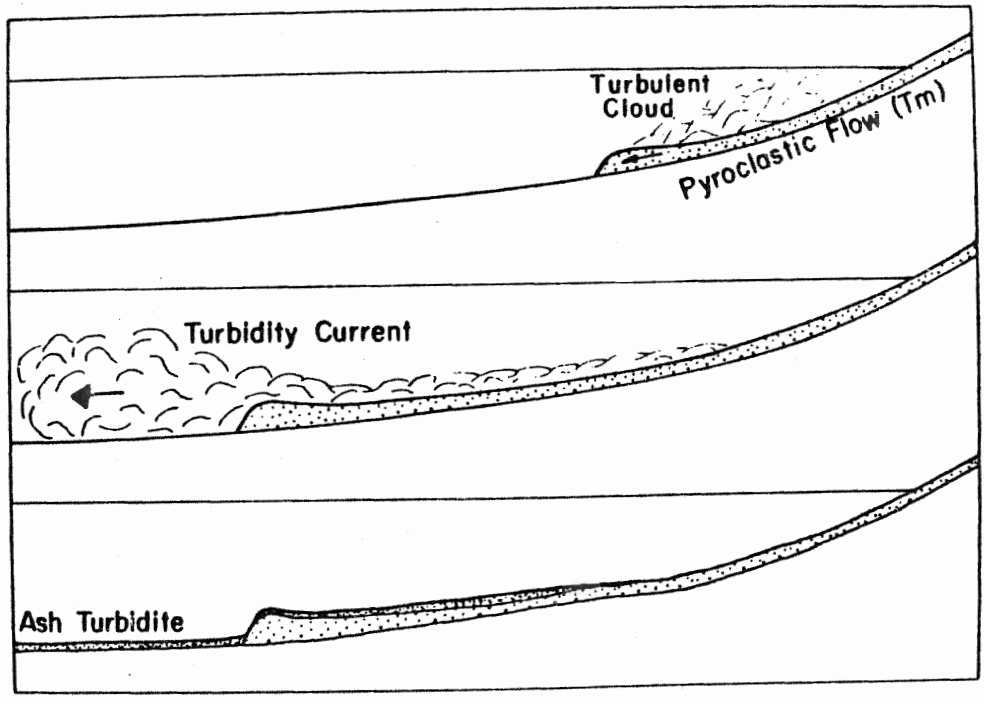

Figure 23. FLOW SEPARATION WITHIN MOVING SUBAQUEOUS DEBRIS FLOW-TURBIDITY CURRENT (Sparks et al. 1980).NOTE OVERRIDING EFFECT OF FINE LOW DENSITY CURRENT.

Figure 10, the Long Bay 1 measured section contains the separation units, upper and basal zones described by Sparks et al. (1980) and Nemec et al. (1980). The Sparks et al. (1980) model is shown in Figure 23. The flow separation is comparable to the ash cloud surge and secondary block and ash flow phases of subaerial environments (Figure 24, Fisher 1982, Sparks and Walker 1977). Although the Berry Creek metavolcanics commonly display the subaqueous bizonal sequence of Fiske and Matsuda (1964) (Figure 7, 47-51 m), it is apparent that the textural motifs of the Berry Creek metavolcanics represent a continuum from the laminar deposits to bizonal deposits (laminar-turbulent combinations) to purely turbulent deposits.

The laminar deposits are recognized by high particle concentration, commonly framework or clast support, lack of

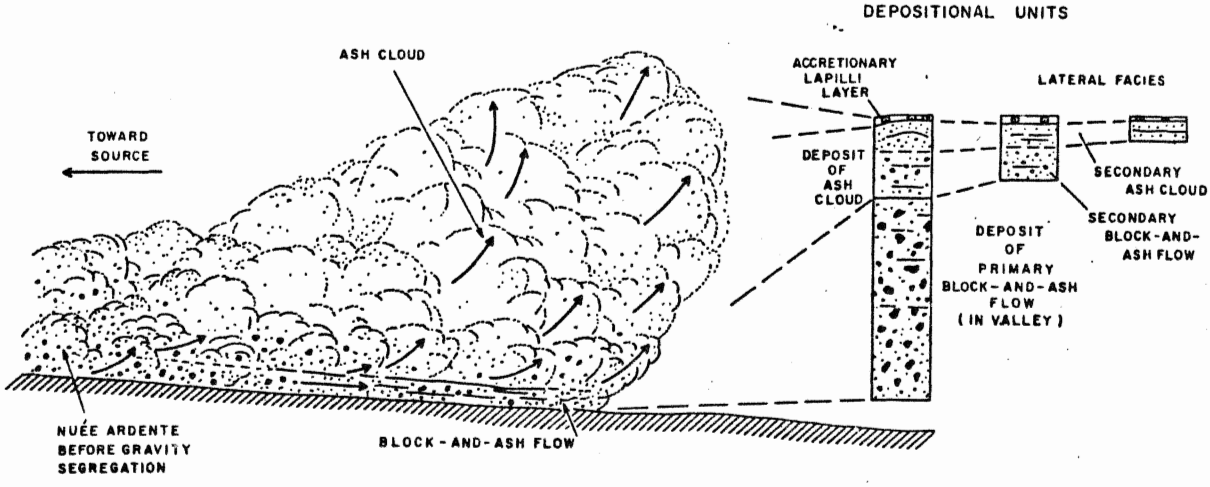

Figure 24. GRAVITY FLOW SEGREGATION OF TURBULENT SUBAERIAL ASH FLOW. SEPARATION INTO BLOCK AND ASH FLOW AND ASH CLOUD DEPOSIT (Sparks and Walker 1977; Fisher 1982).

clast grading, often the presence of a basal inversely graded layer, poor sorting with abundant lithic clasts and commonly reflect deposition within the proximal or vent zone (Fisher and Mattinson 1968; Fisher 1971; Sparks 1976; Morton and Nebel 1983; Long 1977; Tasse et al. 1978; Sheridan 1979; Lajoie 1979). Massive to poorly graded bed units predominate in the eastern end of the map area north of Roberts Lodge (Facies C) and also occur in Long Bay (Facies C,B). The framework deposits (see Plates 1 and 5) do not exhibit basal inverse grading but are extremely poorly sorted and grading of clast dimension or abundance was not observed. The heterolithic framework deposits may have undergone an earlier turbulent erosive phase (possibly on steep slopes) before turbulence was dissipated by high clast concentration. Since the yield strength of these deposits is probably lower than that of mudflows (Hampton 1972), the clasts are supported by dispersive pressure (Nemec et al. 1980; Sparks 1976). Subsequently, rapid deposition most likely occurs by traction carpet sedimentation (Lowe 1982) and/or frictional freezing (Lowe 1982; Fisher 1971; Sparks 1976). These coarse deposits of the Berry Creek metavolcanics are texturally similar to the proximal flow type A deposits of Tasse et al. (1978) and the Type one deposits of Wilson (1980).

The laminar-turbulent transitional flows probably best explains the textures of the graded Berry Creek deposits. Inverse to normally graded deposits of Facies C (proximal and medial members), characteristic of the proximal facies

of Tasse et al. (1978), Lowe (1982), Wood (1980), Walker (1975, 1979), Afifi (1981) and Nemec et al. (1980), are generally produced by a series of sedimentation patterns involving traction, traction carpet and suspension sedimentation from coarse grained moderate to high density subaqueous flows (Lowe 1982). The mass flow deposits are characterized by a number of grading patterns which are related to clast type and abundance, matrix compositon, channel geometry and proximality (Nemec et al. 1980; Walker 1975, 1977, 1979; Hein 1982; Tasse et al. 1978). The proximal deposits, as noted for laminar flows, commonly exhibit basal inverse grading (distribution and frequency types) of the suspended particles.

Inverse grading may be produced by one or a number of mechanisms including dispersive pressure from clast - clast collision, kinetic sieve effects, fluidization, shear stresses and traction carpets (Lowe 1982; Sparks and Wilson 1976; Naylor 1980; Sallenger 1979; Walker 1975; Cas 1979; Nemec et al. 1980; Middleton 1970; Fisher and Mattinson 1968). Avalanche deposits, talus or scree, and changing vent conditions may provide partial or completely inverse graded beds (Duffield et al. 1979; Thurston 1980). Lowman and Bloxam (1981) and Sparks (1976) suggested that flotation of low density fragments (vesicular pumice) may result in inversely graded beds.

Density inversion grading of the pumiceous fragments is common within subaerial ash flow tuffs (Sparks et al.

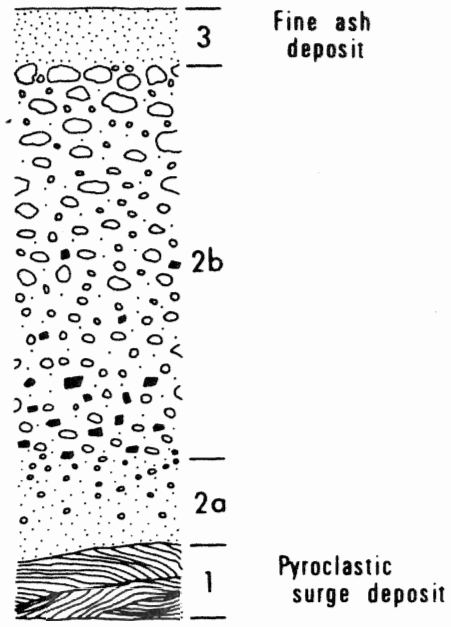

Figure 25. SEGREGATIONAL DEPOSITIONAL MODEL FOR SUBAERIAL ASH FLOWS (Sparks et al. 1973). 2a- NORMALLY GRADED LITHIC CLASTS; 2b- INVERSELY GRADED PUMICE CLASTS; 3- FINE ASH CLOUD ZONE.

1973; Ross and Smith 1961; Thurston 1980) but has been reported from subaqueous ash flows (Dimroth and Demarcke 1978; Nemec et al. 1980). The latter mechanism was probably not important within the Berry Creek deposits. Pumiceous fragments are commonly associated by size and frequency grading with the lithic clasts. The pumice density was not sufficiently low for flotation (absence of unconnected vesicles) or pumice became rapidly waterlogged due to the connected vesicle patterns. Pumice can separate by flotation and not be preserved in the flow deposit (Fiske and Matsuda 1964). Wilson and Head (1981) suggested that the presence of yield strength (non-Newtonian flow behaviour), coupled with high particle density concentration, common in the proximal to medial Berry Creek

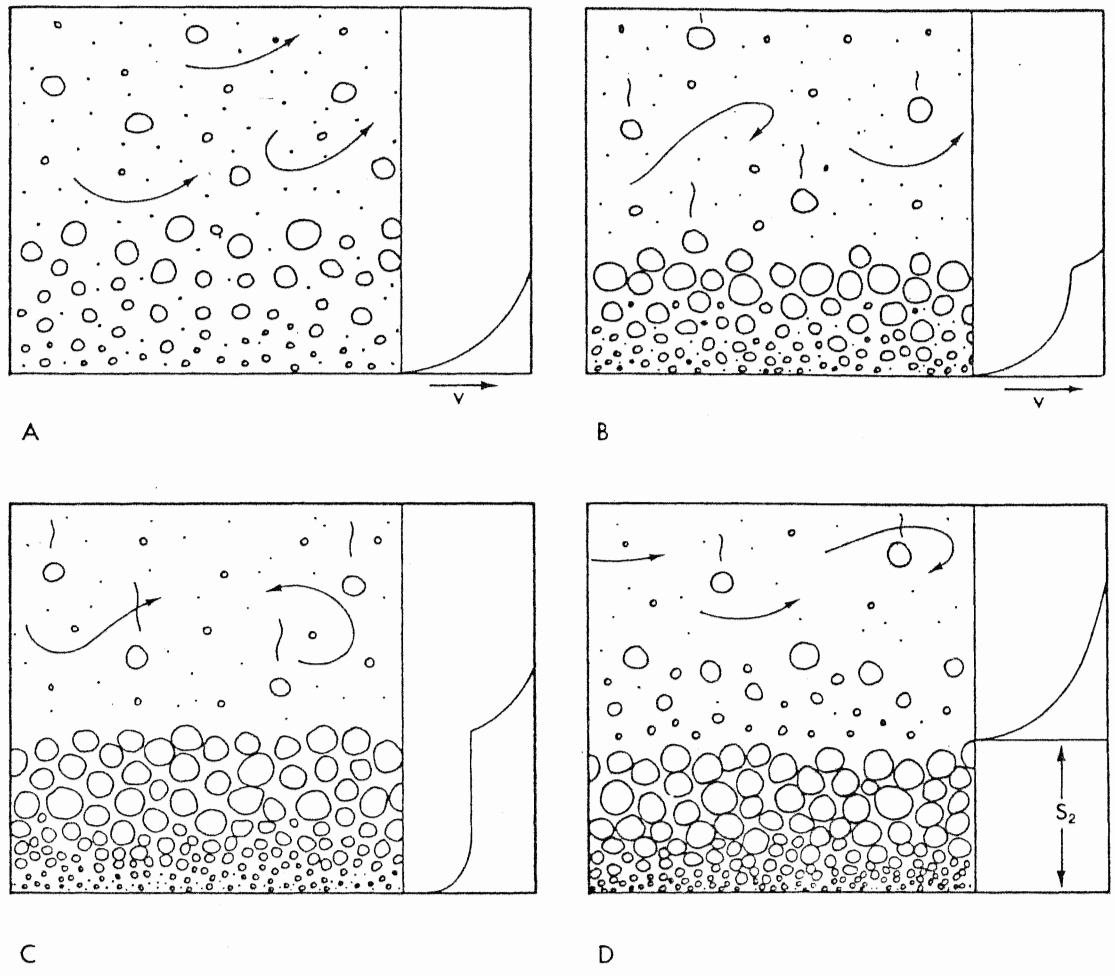

Figure 26. DEVELOPMENT OF TRACTION CARPET LAYER (Lowe 1982) A) INVERSE GRADED ZONE FORMS DUE TO DISPERSIVE PRESSURE; B) SUSPENSION FALLOUT AND INITIATION OF TRACTION CARPET; C) CONTINUED FALLOUT AND FREEZING OF TRACTION CARPET; D) INITIATION OF SECOND INVERSE GRADED ZONE. PROCESS REPEATS ITSELF.

deposits, may inhibit upward pumice flotation due to lack of proper density contrast. A similar mechanism involving rapid deposition of pumice in the laminar flow state is suggested by Tasse et al. (1978). Nemec et al. (1980) noted inverse grading of all components in the proximal laminar framework deposits. Similar patterns are common within high concentration mudflows (Schminke 1967; Fisher 1971; Sparks 1976).

Lowe (1982) suggested that traction carpet sedimentation produced basal inverse grading within coarse clastic flows. Figure 26 outlines the development of the traction carpet layer. Relatively low turbulence and the high clast density account for the rapid deposition of coarse clasts as dispersive pressures cannot maintain suspension and lateral motion (Lowe 1982). While sandy mass flows may exhibit basal traction sedimentation structures (Cas 1979; Lowe 1982), the coarse clastics commonly lack any evidence of the traction structures (Nemec et al. 1980; Bailes 1980; Lowe 1982; Walker 1975) (see discussion of sedimentary structures).

The transition from traction carpet to suspension sedimentation occurs in both lateral and vertical dimensions. The ratio of the thickness of inversely graded to normally graded zones decreases with distance from source due to increased turbulence and lower velocity. Eventually, the suspension sedimentation (normally graded) becomes dominant (Lowe 1982). Inversely graded zones are characteristically absent from the turbulent and/or distal bed units (Lowe 1982; Walker 1975,1977). Nemec et al. (1980) interpreted bipartite textures in inversely graded framework deposits as relatively proximal beds. Similar deposits from the Great Bear section (Figure 16, 19-23 m) generally contain a thick basal inversely graded zone (at least 2/3 of bed thickness, Nemec et al. 1980) overlain by a fine tuff horizon. These Berry Creek deposits are probably transitional between the Type II bipartite motif

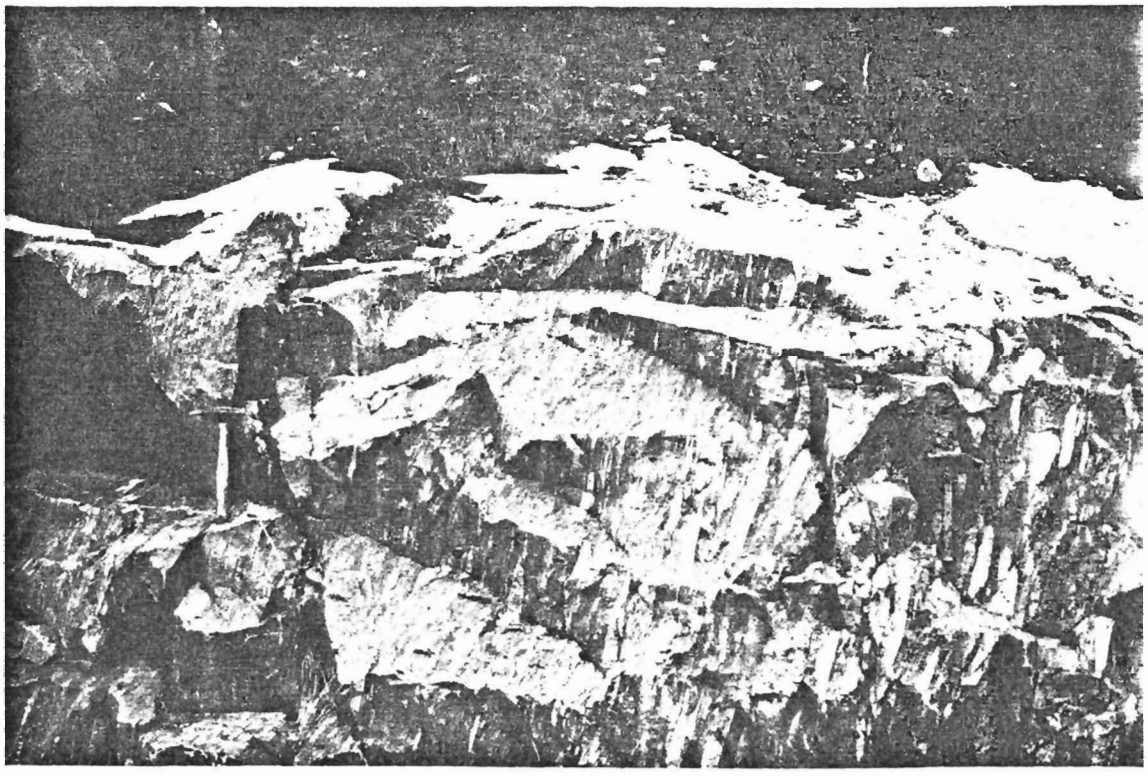

Plate 33. COARSE TAIL GRADING OF CLASTS WITHIN DEBRIS FLOW IN RUNNING ROAD SECTION. YOUNGING DIRECTION TO THE LEFT.

Nemec et al. (1980) and the Type I matrix supported clastics. Beds of the Running Road area are commonly matrix supported and locally contain framework supported basal zones.

As distance from the source increases, suspension sedimentation of the coarse clasts rapidly follows deposition of the traction carpet (Lowe 1982). The normally graded flows and the upper subunit of the inverse to normally graded flows of the Berry Creek volcanics are products of lower density turbulent currents (Cas 1979; Lowe 1982; Tasse et al. 1978; Nemec et al. 1980; Wilson 1980). Distribution or continuous size grading (Lowe 1982; Cas 1979) and coarse tail grading (Lowe 1982; Druitt and

Sparks 1982; Nemec et al. 1980) are subtypes of normal grading. Both varieties occur within the Berry Creek deposits. Coarse tail grading can be observed in Plate 33. Lowe (1982) suggested that coarse tail graded deposits developed from nonturbulent suspensions because fine settling of particles is commonly hindered by turbulence. Rapid deposition of the coarse fraction from partially turbulent flows can trap the fine fraction within the coarse lower subunits. Druitt and Sparks (1982), Rowley et al. (1981), and Kuntz et al. (1981) noted that coarse tail grading is common in ignimbrites (high particle concentration sediment flows) and is not reported from alluvial, flash flood or laharic deposits. However, coarse tail grading of laharic deposits transitional to stream flow deposits have been observed (Janda et al. 1981). Normally graded lithic clasts are typical of subaerial ignimbrites (ash flow tuff) (Sparks et al. 1973) and have been reported from basal coarse subunits from the Mount St.

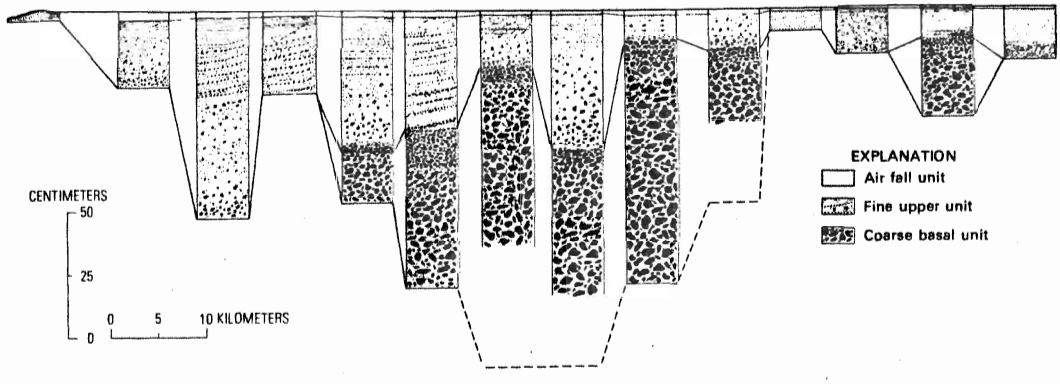

Figure 27. BIPARTITE DEPOSITION IN THE SUBAERIAL MOUNT ST. HELENS ASH FLOWS, SURGES AND CLOUD DEPOSITS. NOTE POOR GRADING OF BASAL ZONE AND STRATIFIED UPPER ZONE (Rowley et al.1981).

Helens deposits (Moore and Sisson 1981; Hoblitt et al. 1981) (see Figure 27). Coarse tail size and frequency grading, controlled partially by dispersive pressures and low turbulence, were also reported in subaqueous mass flows by Cas (1979), Rupke (1977) and Eriksson (1981). The fining upward, normally graded profiles shown in the debris flows, e.g., Figures 8 and 16, display a range of trends from gradational to very sharp transitions between flow subunits. The textural variability of the Berry Creek deposits compares well with interpretations of subaqueous conglomerates (Nemec et al. 1980). Subunit boundaries become more gradational as the distance from source (and relative matrix component) increases. Flow types A and B (Tasse et al.1978) develop normal grading of clasts in the distal facies (see Figure 21).

Incomplete normal grading of the complex inverse to normally graded flows and the distal or turbulent normal flows may result from partial or total upper subunit separation (Cas 1979; Fisher 1979; Wright et al. 1980; Wilson and Walker 1982). The mechanism is similar to the development of co-ignimbrite lag or ground veneer deposits and separation of ash clouds within subaerial ash flow tuff deposits (Walker 1979; Kuntz et al. 1981; Sparks and Walker 1973). The turbulent ash cloud, plume, or slurry overrides the basal deposit (Lowe 1982) (see Figure 23). In the proximal facies, the upper pelitic layer is absent (see Figures 13 and 16, note erosional upper surface and abrupt contacts with overlying debris flows).

Similarly, the residual ash deposits may deposit only a thin veneer over the subjacent basal flow zone ,e.g., the bipartite deposits of Nemec et al. (1980) and similar Berry Creek bedunits (see Figure 10). The laminated or thinly bedded tuff horizon may have been deposited by subaqueous elutriation and backstreaming in the turbulent upper regime (Morton and Nebel 1983).

The upper bed units of the complete cycles are commonly represented by traction structures and/or suspension sediments characterized by normal grading, stratification (oblique to parallel), pebbly layers, ripples and lamination (Belt and Bussieres 1981; Tasse et al. 1978; Cas 1979; Morton and Nebel 1983; Nemec et al. 1980; Walker 1975, 1977, 1979; Moore and Sisson 1981; Lowe 1982; Bailes 1980; Gelinas et al. 1979). The Berry Creek bedforms, shown in the stratigraphic sections, are produced by gradual deceleration, decreasing grain size, and increased turbulence of the lower density flows. Traction structures, including cross laminations and stratification, are also common in the distal to medial zones of the subaqueous turbidity currents (Lowe 1982; Tasse et al. 1978; Cas 1979). Pebbly layers, stratification, and normal grading have also been recognized in subaerial ash flow and surge deposits (see Figure 27). Hiscott and Middleton (1979), Cas (1979), and Allen (1970) noted that the basal residual currents exhibit numerous structures of the moderate flow regime. In contrast, the proximal coarse

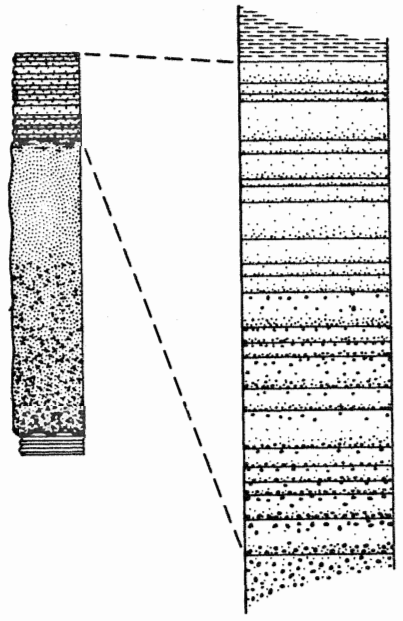

Figure 28. DOUBLY GRADED SEQUENCE COMMONLY FOUND IN SUBAQUEOUS PYROCLASTIC FLOW DEPOSITS (Fiske and Matsuda 1964).

debris flows rarely display lower traction sediments (Lowe 1982; Walker 1975, 1979). Cross stratified beds at the base of poorly graded, moderately coarse debris flows in the Great Bear Section (Figure 16) may have formed by traction sedimentation.

Complex graded sequences or doubly graded sequences (see Figure 28) are probably generated by surging low density flows, back streaming, slumping, and/or dissipating eruption clouds (Fiske and Matsuda 1964; Morton and Nebel 1983; Lowe 1982; Fisher 1963, 1969). Normally graded and inversely graded double graded sequences have been reported by Fiske and Matsuda (1964) and Lowe (1982). The former, recognized in the Berry Creek deposits (Plate 6, Figure 11), was formed by low density slurries. Figure 29 (Fiske and Matsuda 1964) outlines the development of

low density doubly graded sequences from subaqueous eruptions. The latter is the result of progressive traction carpet sedimentation (Lowe 1982, his Figure 5b, p. 284). Poorly developed, doubly graded sequences produced by subaerial deposits have been reported by Rowley et al. (1981) from the 1980 Mount St. Helens eruptions. The low yield strength ash flow tuff, where deposited on steep slopes, almost immediately slumps and flows. It is here

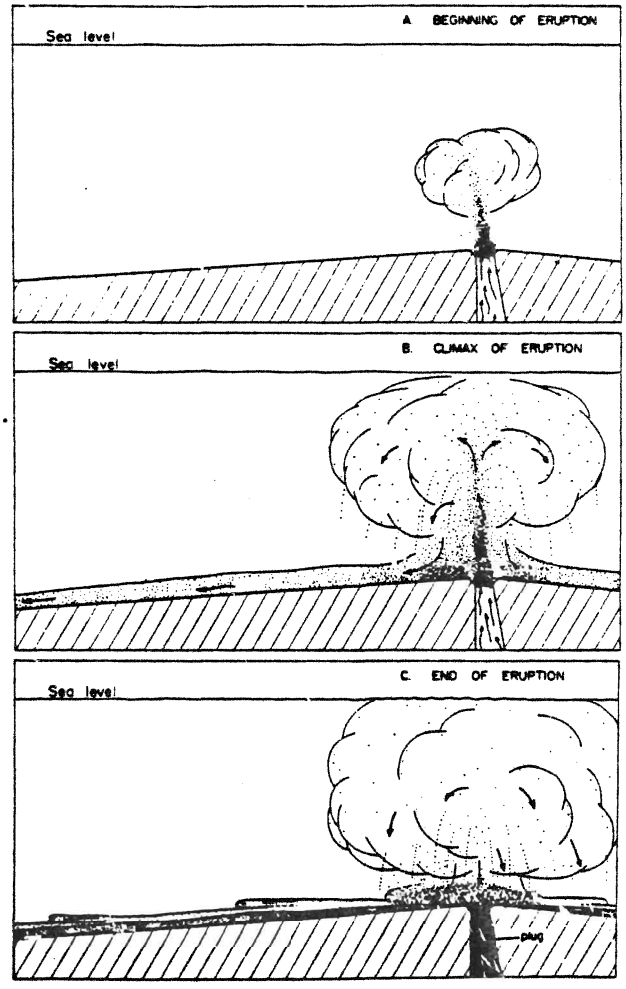

Figure 29. DEVELOPMENT OF DOUBLY GRADED SEQUENCES FROM SUBAQUEOUS ERUPTIVE COLUMN. AFTER CESSATION OF ERUPTION, SETTLING FROM PLUME AND NUMEROUS LOW DENSITY TURBULENT CURRENTS (Fiske and Matsuda 1964).

suggested that transitional subaerial to subaqueous flows may develop doubly graded sequences by progressive slumping, possibly from the littoral environment (Fornari et al. 1979; Cas 1983; Walker 1979), where fine grained ablation particles and crystal fragments have accumulated from low density pyroclastic flows. Fiske and Matsuda (1964) have suggested that flank sloughing of debris into deeper water was not likely to produce doubly graded sequences. Low density, interchannel debris flows and turbidites as well as channel bank collapse or slump debris may also produce crude doubly graded profiles.

Locally, bed units contain isolated large clasts ranging from blocks to lapilli (see Figure 9, lenticular nongraded bed). These deposits may represent sedimentation by frictional freezing involving matrix strength (Nemec et al. 1980; Lowe 1982), collapse or slump structures from the margin of depositional channels, or isolated clasts which outran the coarse facies of the debris flow into the distal suspension facies (Prior et al. 1982).

In an overall context, the mass flows (primary, secondary, sedimentary) contain many features consistent with modified Bouma style sequences (Cas 1979; Allen 1970) including AE cycles, cross beds, ripples, scours, ripup clasts, flute casts, load and flame structures (Hendry 1978; Cas 1979; Eriksson 1981; Henderson 1972; Turner and Walker 1973; Meyn and Palonen 1980; Afifi 1981; Wood 1980; Dunlop and Buick 1981; Barley 1980). Bouma cycles of the Berry Creek turbidity and grain flows are

characteristically top absent to middle absent. Cas (1979) recognized similar sequences within the Merrions Tuff and were interpreted as inner to middle fan deposits (see depositional models). The Bouma a division of the amalgamated sand beds and the AE turbidites locally contains a1, a2, and a3 subdivisions (inverse graded, massive, normally graded) (Middleton 1970; Cas 1979). Recognition of these structures in the Berry Creek epiclastics is complicated by penetrative foliation, metamorphic grain size changes (recrystallization) and blast growth.

High rates of deposition of the saturated debris is suggested by flames, load structures, penecontemporaneous erosion, Bouma divisions, and dewatering pipes (see Plate 9) (Hendry 1978; Cas 1979; Eriksson 1981; Meyn and Palonen 1980; Afifi 1981; Henderson 1972; Bailes 1980; Barley 1981; Middleton and Hampton 1976). Rapid deposition is also indicated by the preservation of fine shards, pumice and associated vitriclasts (Ricketts et al. 1982; Cas 1979, 1983; Carey and Sigurdsson 1980; Barley 1980,1981; Fisher 1969; Heiken 1972; Morton and Nebel 1983; Afifi 1981) and crystal components (Fisher 1969; Cas 1983; Dimroth and Demarcke 1978). Fisher (1969) suggested that the association of turbidites mixed with subaqueous coarse pyroclastics was indicative of rapidly deposited tephra. Nemec et al. (1980) and Carey and Sigurdsson (1980) concluded that the marked variations in grain size and clast dimensions as well as morphology of vitriclasts

suggested a derivation by primary flowage rather than secondary shoreline ablation zone slumping.

The Berry Creek pyroclastics are characteristic of highly mobile, relatively coarse deposits developed by subaerial to subaqueous eruptions and transported to subaqueous depocentres (Middleton and Hampton 1976; Carey and Sigurdsson 1980; Francis and Howells 1973; Lowman and Bloxam 1981; Dimroth and Demarcke 1978). Extensive mobility of the debris flows in the subaqueous environment is maintained by high velocity, high density, large grain size, low ablation rates and fluid pressure gradients (Sparks et al. 1980; Carey and Sigurdsson 1980; Padgham 1980; Sigurdsson et al. 1980; Tasse et al. 1978). Several critical conditions are necessary for emplacement of ash flow tuff units across the air-water interface. These include steep slopes, high flow rates, high density (dominantly juvenile lithic clasts), and probable lack of shoreline deposits (Sparks et al. 1980). High temperatures and mobility, due to steam absorption, can lower flow viscosity (Lowman and Bloxam 1981), although the flow front ablation by mixing with water (increased cooling rates) may inhibit forward transport, especially in the littoral zone (Walker 1979; Sparks et al. 1980). The Berry Creek pyroclastics are probably emplaced by cold state processes similar to the Merrions Tuff of New South Wales (Cas 1979). This statement is based mainly on negative evidence. The lack of **quench** crystals, as observed in the Dalembert Tuff

of the Noranda area (Dimroth and Demarcke 1978) or indications of subaqueous welding (Lowman and Bloxam 1981; Francis and Howells 1973) supports this conclusion. In the absence of the above criteria, NRM studies have been used to recognize hot subaqueous flows (Yamazaki et al. 1973). Initially hot debris flows can cool sufficiently to inhibit welding and minimize quench crystallization. Yamada (1973) and Dimroth and Demarcke (1978) have suggested transport of debris flows at high temperature but emplacement at low temperatures following rapid thermal depletion.

It is most probable that the primary pyroclastics of the Berry Creek volcanics were deposited by rapidly cooling subaqueous flows. However, secondary deposits including dome collapse flows were emplaced by the forementioned cold state mechanism.

Deformation of pumiceous shards and clasts, recognized in the Berry Creek pyroclastic deposits, can be attributed to nonpenetrative deformation. Relationships between tectonism and attenuation of pumice void spaces are similar to those described by Dimroth and Demarcke (1978) and Afifi (1981).

Primary and secondary processes involving crystal separation and concentration (e.g., primary flow segregation; flow front ablation zones; littoral flash explosions) may have played a small role in the development of the crystal rich tuff and arenite units (Cas 1979, 1983; Sparks and Walker 1977; Walker 1979; Carey and Sigurdsson

1980; Sigurdsson et al. 1980). The euhedral form, large grain size and abundances similar to the quartz and plagioclase/microcline phenocrysts of the associated intrusive porphyry complex corroborate this conclusion. Phreatomagmatic explosions associated with littoral concentration mechanisms produce finely comminuted debris inconsistent with the observed components of the Berry Creek deposits (Sparks and Walker 1977; Cas 1979, 1983).

Rhyodacitic Lava Flows

Lava flows of Facies A and B were probably deposited under deep water and shallow water conditions, respectively. The former, Facies A laminated flows, are of a similar morphology to low viscosity subaqueous flows described by Cas (1978), De Rosen-Spence et al. (1980) and Morton and Nebel (1983). Colour banding, defined by the metamorphic mineralogy and primary flow laminae, compare well with rhyolitic flows of the Wawa belt (Morton and Nebel 1983). Replacement of laminae by secondary minerals was also noted by Barley (1980). Armstrong et al. (1982) suggested that rhyolite flow banding is commonly obliterated by recrystallization. Flow layering has also been observed in the internal facies of lava domes (Self 1982) and as extensive, variable aspect ratio, flows of subaerial environments (Guest and Sanchez 1969; Teng, p. comm. 1981). Layered subaqueous flows are contained by the high ambient fluid pressure (Cas 1978; McBirney and Murase

1970) while subaerial lava effusions are commonly produced as passive events following significant outgassing by pyroclastic eruptions (Self 1982). Coherent flow patterns of the subaqueous flows are maintained by volatile suppression, reduced viscosity, and relatively lower degree of quench fragmentation, pillow formation, and peripheral flow brecciation (Cas 1978; McBirney and Murase 1970: Self 1982). DeRosen-Spence and Dimroth (1979) and DeRosen-Spence et al. (1980) have suggested that the flow laminations in some lava flows are produced by deformation of pumice by shear flow. The presence of pumice indicated shallow to subaerial conditions not consistent with the lithological associations found in the Berry Creek deposits. The flows from Facies A are associated with deep subaqueous argillic turbidites and derived amphibolites (mafic flows). Deep water flows, interpreted by Cas (1978), are commonly associated with flyschlike sediments.

The Facies B dome and breccia complex has the characteristic features of shallow subaqueous to subaerial lavas (Cas 1978; Self 1982; Morton and Nebel 1983; DeRosen-Spence et al. 1980). The typically fragmental, high aspect ratio profile of viscous rhyolite-dacite domes contains several internal facies (DeRosen-Spence et al. 1980; Morton and Nebel 1983; Goldie 1983; Tasse et al. 1982). The Berry Creek Facies B flows contain the massive to brecciated flow lobes, pods and pseudopillow forms observed in subaqueous deposits by DeRosen-Spence et al. (1980) and Tasse et al. (1982) (see Figures 30 and 31). Association of pyroclastic

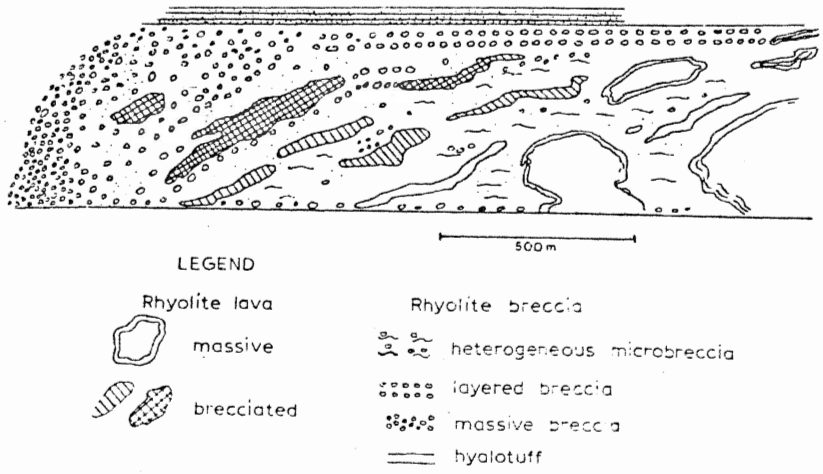

Figure 30. HETEROGENEOUS BRECCIA AND LAVA FACIES FROM SUBAQUEOUS RHYOLITE FLOW . NOTE PODIFORM DEVELOPMENT OF LAVA LOBES AND OVERLYING STRATIFORM HYALOTUFF DEPOSITS. (DeRosen-Spence et al. 1980).

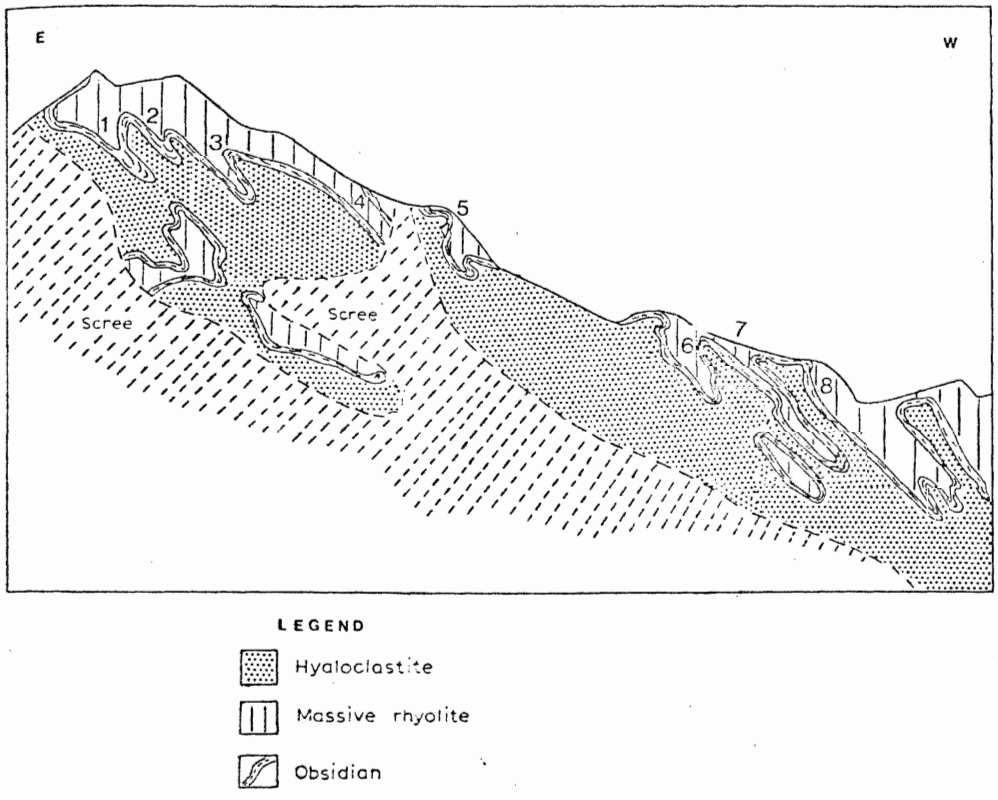

Figure 31. LAVA LOBES AND HYALOCLASTIC FACIES WITHIN SUBGLACIAL RHYOLITE FLOWS (DeRosen-Spence et al. 1980)

debris with the lava flow facies in the Maybrun section is comparable to the pyroclastite and autoclastite association of Tasse et al. (1982). This association is suggestive of shallow to subaerially derived detritus. Complex field relationships, observed in the Berry Creek sections, are similar to those of Tasse et al. (1982, Figure 1, p. 1338; see also Figure 32). Pockets of fine lapilli tuff or tuff breccia complexly intercalated with the massive and brecciated flow lobes are considered to have been generated by fragmentation along the margin of flow lobes or by later explosive fragmentation by gaseous explosions (flash expansion) (De Rosen-Spence et al. 1980; Dimroth 1977; Ayres 1981; Peloquin et al. 1981). Ayres (1981), Ferreira (1980) and Van Wagoner and Van Wagoner (1981) have suggested that the monolitnic tuff breccia, lapilli tuff and flow breccia deposits associated with lava lobes in the Amisk Lake belt are produced by deposition in a surf zone environment peripheral to a subaerially exposed dome complex. Comparisons with the Berry Creek deposits support a similar depositional environment.

Collapse breccias and talus aprons developed around dome buildups are commonly redeposited in deeper subaqueous environments by mass flows and turbidity currents (Barley 1980; De Rosen-Spence and Dimroth 1979; DeRosen-Spence et al. 1980; Lambert 1977; Wright et al. 1980; Goldie 1983; Fisher and Heiken 1982). The monolithic debris flows are explained by laminar to turbulent subaqueous flows similar

to those described for the associated pyroclastic flows (see previous section). The debris deposits commonly exhibit normal grading of the nonvesicular juvenile and cognate debris. Hyalotuff deposits produced by primary flow brecciation, quenching (thermal strain) and possibly phreatic or oceanic (littoral zone) flash explosions comprise a large proportion of the Facies B deposits (De Rosen-Spence and Dimroth 1979; De Rosen-Spence et al. 1980; Walker 1979; Van Wagoner and Van Wagoner 1981; Ayres 1981; Peloquin et al. 1981). Stratified tuffs have been reported in association with massive lava facies by Dimroth and Rocheleau (1979) and De Rosen-Spence et al. (1980).

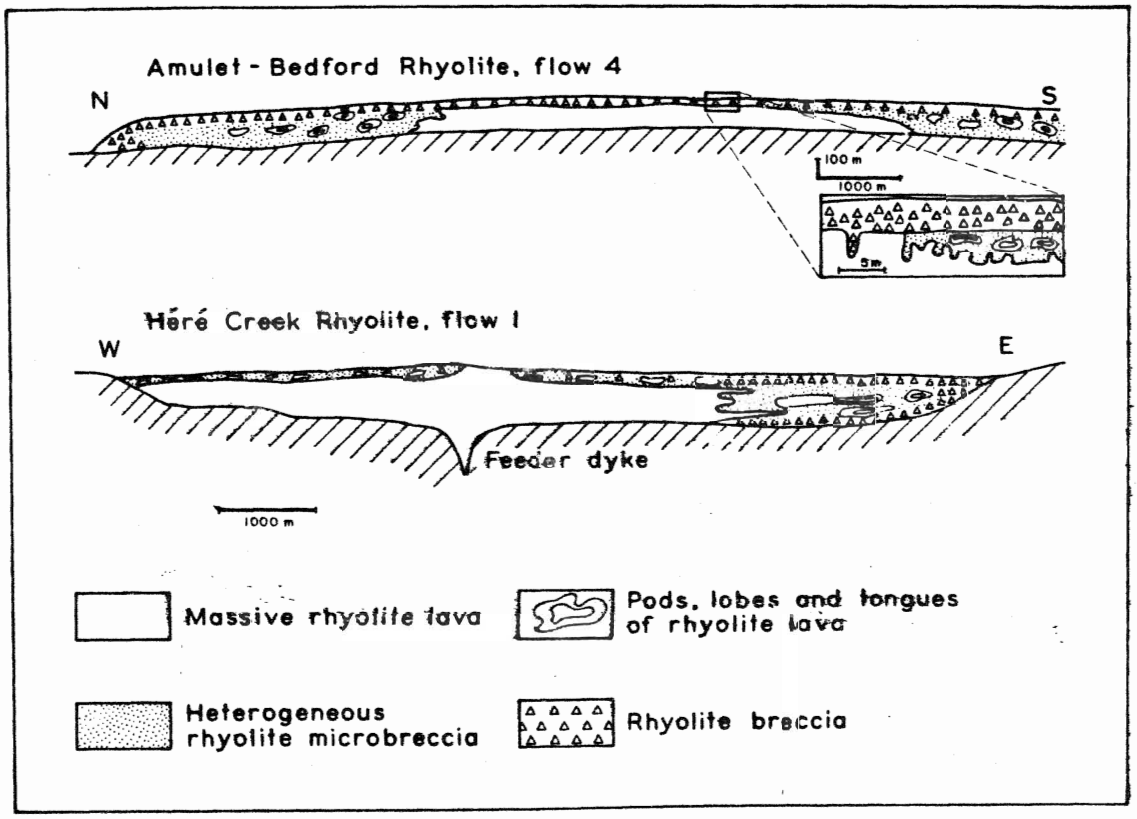

Figure 32. COMPLEX FIELD RELATIONSHIPS AND LATERAL FACIES VARIATIONS WITHIN SUBAQUEOUS RHYOLITE FLOWS (DeRosen-Spenceet al. 1980).

Proximality of the dome and breccia deposits (Facies B) is indicated by : 1) central zone comagmatic porphyries, massive flows, minor brecciated zone, minor pond sedimentation (Lambert 1977, 1978; Hallberg 1978; Barley 1981; De Rosen-Spence et al. 1980); 2) proximal and medial zones by an increase in brecciated lava lobes and less common occurrence of porphyries (De Rosen-Spence et al. 1980; Peloquin et al. 1981); and 3) medial and distal zones by hyalotuff, debris flow deposits, minor brecciated lava lobes (probably transported as whole blocks) and association with turbidity currents (DeRosen-Spence et al. 1980; Lambert 1978; Cas 1978, 1979; De Rosen-Spence and Dimroth 1979; Tasse et al. 1982).

The lateral and upward migration from the feeder zone (porphyry complex) to brecciated lenses, avalanche deposits, and massive banded rhyolite flows was reported from rocks of the Michipicoten Group by Goodwin (1983).

FACIES INTERPRETATION

Deposits interpreted as midfan to outer fan fringe facies of a subaqueous fan occur in the Berry Creek area. Recognition of the sedimentary environments is based upon numerous criteria including depositional cycles, sedimentary structures, degree of reworking, bed unit associations, and presence or absence of critical facies (Walker 1979; Tasse et al. 1978; Lajoie 1979; Turner and Walker 1973; Eriksson 1980, 1981; Normark 1978; and many

others). Archean examples of subaqueous fan deposition have been described by Hyde (1980), Turner and Walker (1973), Wood (1980), Teal and Walker (1977), Gordanier (1976), and Henderson (1972). The Berry Creek complex forms a composite group of deposits which partly belongs to the Resedimented Association of Turner and Walker (1973). Although the primary pyroclastic deposits found in the Berry Creek subaqueous fan display similar sedimentary structures, the mode of deposition may not involve reworking or redeposition. The primary ash flow tuff has been deposited from subaerially derived Plinian eruptions producing rapidly moving gas charged tephra (Car 1976; Ayres 1977, 1982, 1983; Carey and Sigurdsson 1980) (see Figure 33). These deposits penetrate the seawater

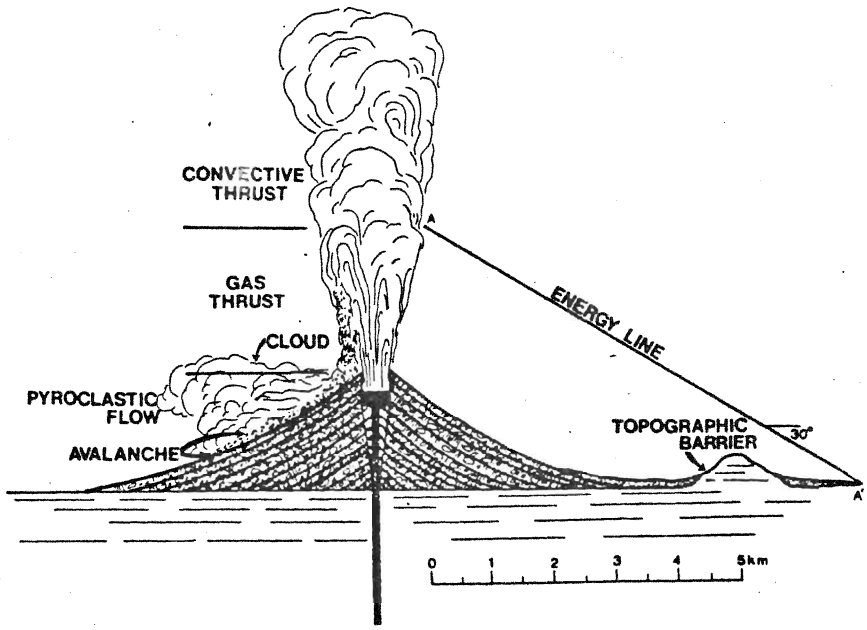

Figure 33. SUBAERIAL PLINIAN ERUPTION COLUMN WITH COLLAPSING PYROCLASTIC FLOW. PARTIAL UPWARD SEGREGATION OF ASH CLOUD BY CONVECTIVE THRUST AND SURGES ABOVE BASAL PYROCLASTIC UNDERFLOW DEPOSITS (Sheridan 1979).

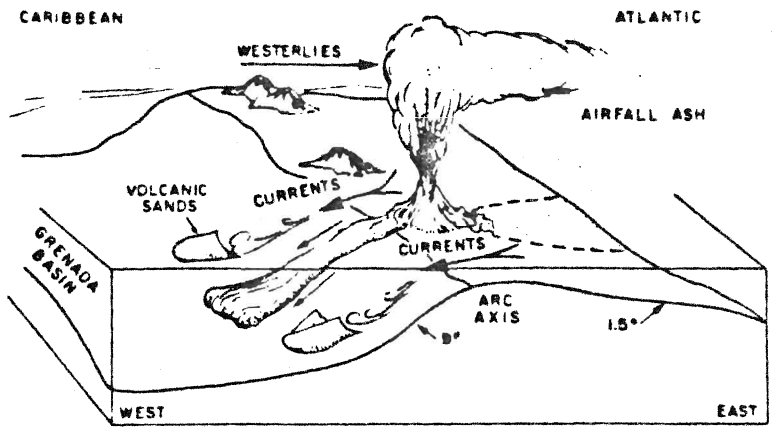

Figure 34. PYROCLASTIC FLOWS PRODUCED BY COLUMN COLLAPSE CROSS THE SEAWATER INTERFACE AND TRAVEL DOWN-SLOPE IN SUBAQUEOUS ENVIRONMENT. CONVECTIVE ASH CLOUD MAY SEPARATE BY PREVAILING AIR CURRENTS (Sigurdsson et al. 1980).

interface and subsequently move downslope into the subaqueous fan. Figure 34 shows the development and distribution of the subaerial to subaqueous debris flow-ash flow tuff combination (Carey and Sigurdsson 1980; Sigurdsson et al. 1980). Ayres (1977, 1982), Ricketts et al. (1982) and Armstrong et al. (1982) have reported volcanogenic debris (pyroclasts, vitriclastic fragments) which supplement the sediment supply into the depositional basin.

The association with background basinal sediments, dominantly fine grained turbidites and pelagic deposits, of the periodically deposited volcanogenic mass flows has been used as criterion for subaqueous deposition (Turner and Walker 1973; Ricketts et al. 1982; Padgham 1980). Reworking of volcanics may produce the quartzose and feldspathic turbidites (see also Ayres 1983; Niem 1977). The secondary volcanogenic deposits may be the product of

fluvial, alluvial or braided stream environments in stable to metastable volcanic islands (Ayres 1977, 1983; Rust 1981; Cas 1978, 1983). The preservation of primary vitriclasts in much of the Berry Creek deposits suggests that deposition occurred with a minimum of subaerial reworking. Many Archean analogues from the Canadian Shield are characterized by the rapid transition between subaerial and subaqueous deposits; specifically by the absence of shallow marine deposits or similar shoreline facies (Turner and Walker 1973; Wood 1980; Walker 1976; Hyde 1980). Rocheleau (1979) and Walker (1976) have suggested that rapid vertical changes are produced by tectonic activity. The narrow shelf may indeed have sufficient slope to inhibit deposition e.g., Yallahs Basin, Jamaica (Hyde and Walker 1977; Hyde 1980); slope minimizes beach facies. The presence of shallow water lava flows and reworked laharic deposits in the Berry Creek metavolcanics suggests that ablation and rapid redepositon in the sloping littoral zone produced poorly reworked debris flows containing primary fragments (Ricketts et al.1982; Lambert 1978).

The Berry Creek assemblage, belonging to the Modified Resedimented Association, contain proximal, medial, and distal (fan fringe) facies defined by relative proportions of primary pyroclastics, coarse mass flows, epiclastics and turbidity flows; and textural features of the mass flows and cycles within the flow unit assemblages (Dimroth et al. 1983; Tasse et al. 1978; Nemec et al. 1980; Teal and

Walker 1977; Walker 1979). Deposits of the Resedimented Association (Turner and Walker 1973) have been reported from many areas and are characterized by graded conglomerates and turbidity deposits (Ayres 1983; Gordanier 1976; Henderson 1972; Walker and Pettijohn 1971; Okado 1980; Meyn and Palonen 1980). The Minnitaki Group, temporally equivalent to the Berry Creek deposits, is also characterized by subaqueous deposition of graded coarse clastics and turbidity flows (Ayres 1983; Hyde 1980; Walker and Pettijohn 1971; Turner and Walker 1973; Davis and Edwards 1982). Facies associations are commonly complex and vary with fan morphology (Chan and Dott 1983; Walker 1979), source area, distributionary trends, flow magnitude and efficiency of the fan system (Ricketts et al. 1982; Ayres 1982, 1983; Chan and Dott 1983). Although typical fan profiles and models of Walker (1979) and Mutti and Ricci-Lucchi (1975) may be applicable, models involving restricted basins, possibly in volcanotectonic depressions, have been suggested by Chan and Dott (1983) (see Figure 35). The fan geometry is controlled by the rate of deposition (and eruption; primary subaqueous deposition of pyroclastics) and physical flow parameters (Sparks et al. 1980; Long 1981; Carey and Sigurdsson 1980). Comparison of the sedimentary structures between subaerial alluvial fans, fluvial and deltaic environments and subaqueous fans indicates that the former models can be ruled out as depositional environments for the Berry Creek Complex (e.g., Eriksson 1981; Walker 1979; Turner and Walker 1973;

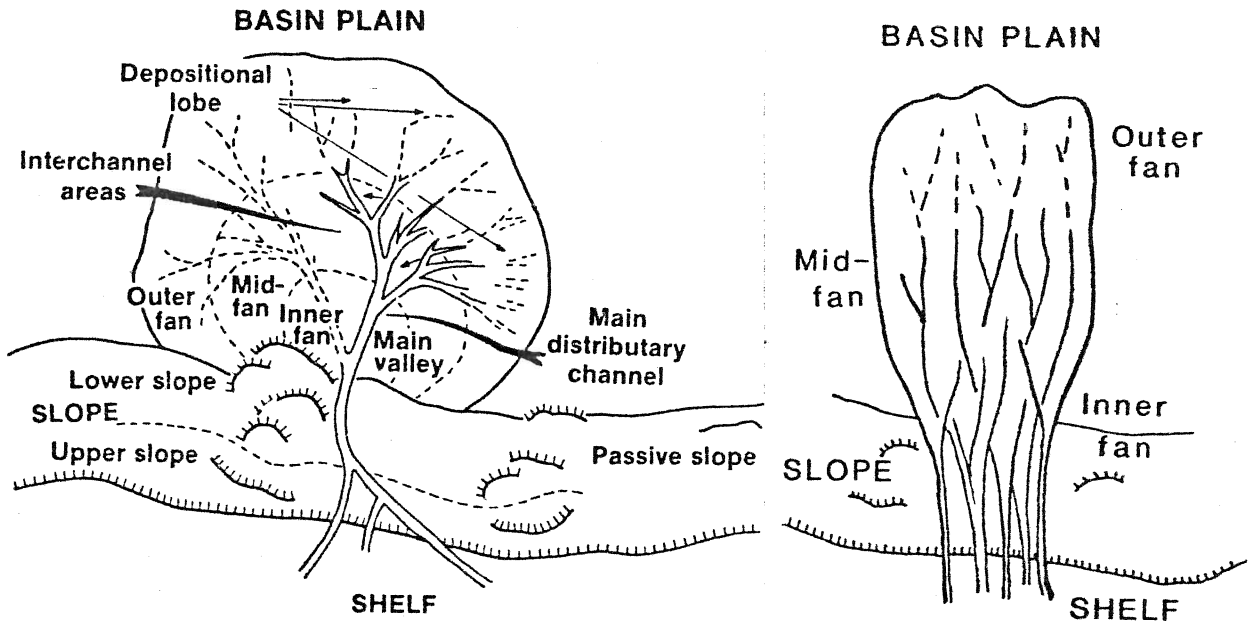

Figure 35. RADIAL FAN GEOMETRY COMPARED WITH SAND RICH FAN MODEL. RESTRICTED BASINS MAY PARALLEL THE LATTER (Chan and Dott 1983).

Rust 1981; Miall 1981; Bailes 1980; Galloway 1976; Dimroth and Demarcke 1978; Tasse et al. 1978; Carey and Sigurdsson 1980). Distinct similarities of the Minnitaki and the Berry Creek suggest similar depositional models (Turner and Walker 1973). The proximal facies of the Berry Creek Complex is composed of poorly channeled massive and inverse to normally graded ash flow tuff (debris flows) and minor reworked lavas and lahars. These deposits belong to the inverse to normally graded association of Walker (1978) (see Figure 36) and characterizes the inner to mid fan areas (Okado 1980; Lowe 1982) as well as the proximal suprafan lobe deposition (Pickering 1981, 1982; Belt and Bussieres 1981; Walker 1979). The proximal deposits are commonly interbedded coarse breccias, epiclastics and mafic tuff (see also Car 1976; Armstrong et al. 1982). The mixed

assemblage may involve a subaerial fluvial or laharic supplement of the shallow water or subaerially derived pyroclastic breccias (see also Buck 1978; Ayres 1977, 1983; Car 1976).

The proximal character of the sedimentary assemblage of the Berry Creek area is defined by the amalgamated sandy greywackes (AA, AB Bouma divisions) and AB greywacke-argillite couplets (Meyn and Palonen 1980; Henderson 1972; Turner and Walker 1973; Nemec et al. 1980; Belt and Bussieres 1981). The poorly graded to nongraded sandy deposits commonly form by en masse deposition within channel sequences (Chan and Dott 1983; Cas 1979; Afifi

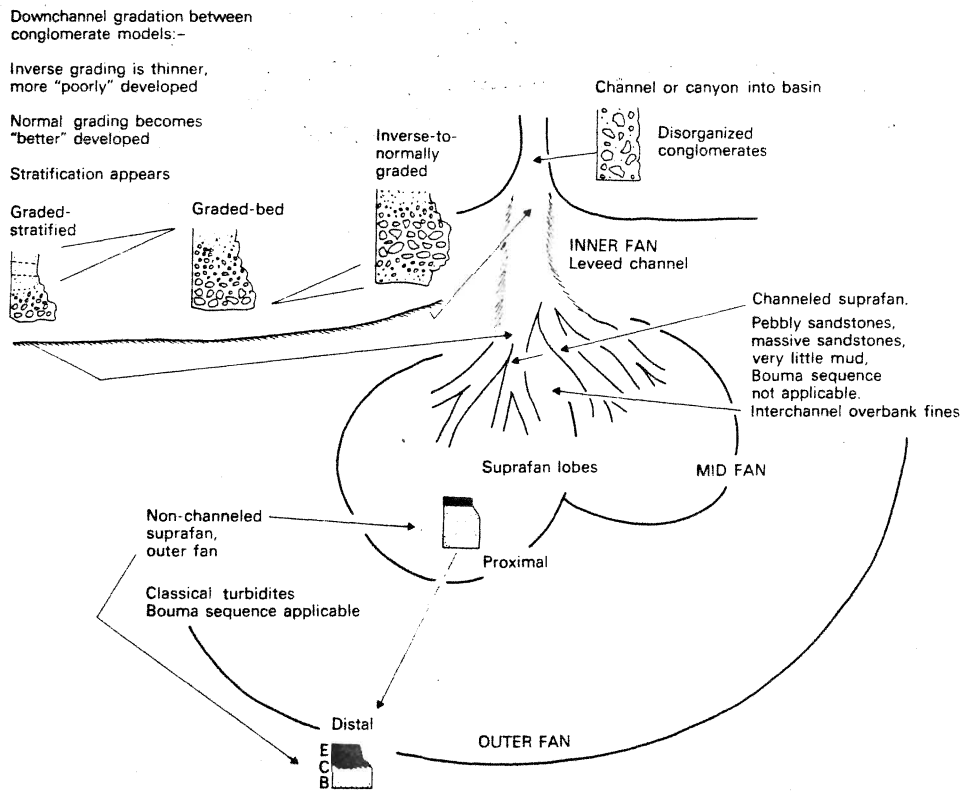

Figure 36. SUBMARINE FAN MODEL (Walker 1975,1977).

1981; Ghibaudo 1980) of the midfan, inner fan or suprafan facies (Eriksson 1981; Meyn and Palonen 1980). Nemec et al. (1980) also reported the absence of traction structures within the massive proximal turbidites (mass flows of Walker 1970; Turner and Walker 1973). Most of the primary pyroclastics are characterized by midfan to upper fan and suprafan lobe deposits. The proximal to medial associations of Walker (1979) include the inverse to normally graded, graded stratified, and massive Berry Creek pyroclasts. The high density currents associated with these flow units, characterized by framework (clast support), lack of traction structures, and commonly erosional bases, form the channeled inner facies of the prograding lobes (Walker 1976; Ghibaudo 1980; Nemec et al. 1980; Eriksson 1981; Lowe 1982; Afifi 1981). The flow units display lateral fining of grain size, traction to suspension sedimentation (normal grading of clasts) and stratified, commonly pebbly layers during deceleration across the outer lobe facies (Walker 1979; Normark 1978; Ayres 1982; Fiske and Matsuda 1964; Dimroth 1977). Morton and Nebel (1983) reported similar facies variations involving thinner and better graded medial beds containing fewer clasts and abundant sedimentary structures. Subaqueous structures interpreted by Niem (1977), Dimroth and Demarcke (1978), Ayres (1982), Dimroth (1977) and Tasse et al. (1978) are comparable to lateral facies variations in the Berry Creek pyroclasts.

The proximal currents gradually change to low density slurries forming distal and proximal to medial and suprafan interchannel deposits (Niem 1977; Tasse et al. 1978; Afifi 1981). The overbank and/or distal turbulent currents (Eriksson 1981; Afifi 1981) produce sheetform deposits within the upper to midfan terraces (Hein 1979) or interchannel regions (Henderson 1972; Eriksson 1981; Meyn and Palonen 1980) of the suprafans. Low density flows, commonly described as tuff, crystal tuff or mass flow arenite (Cas 1979, 1983) within the medial to distal Berry Creek region, characterize the shallow (lacking channels) outer suprafan lobes and fan fringe (Link and Nilsen 1981; Hiscott and Middleton 1979; Bailes 1980; Lowe 1982; Cas 1979). Chan and Dott (1983), however, reported sandy mass flows (turbidites) within the proximal facies of a poorly efficient, sand-rich subaqueous fan.

Interchannel and/or distal pelagic deposits of iron formation, black argillite and chert occur in Lobstick Bay and Long Bay (Eriksson 1981; Turner and Walker 1973; Ghibaudo 1980). Some outer fringe deposits, specifically very fine grained tuffaceous horizons, are probably derived from one of two mechanisms: 1) flow segregation by fluid shear such that the upper subunit forms thin distal layers after deposition of the proximal coarse subunit (Sparks et al. 1980); and 2) ash cloud deposits associated with co-ignimbrite ash falls (Wilson and Walker 1982). Mass slumping of these deposits was observed in Long Bay and probably added another downslope component.

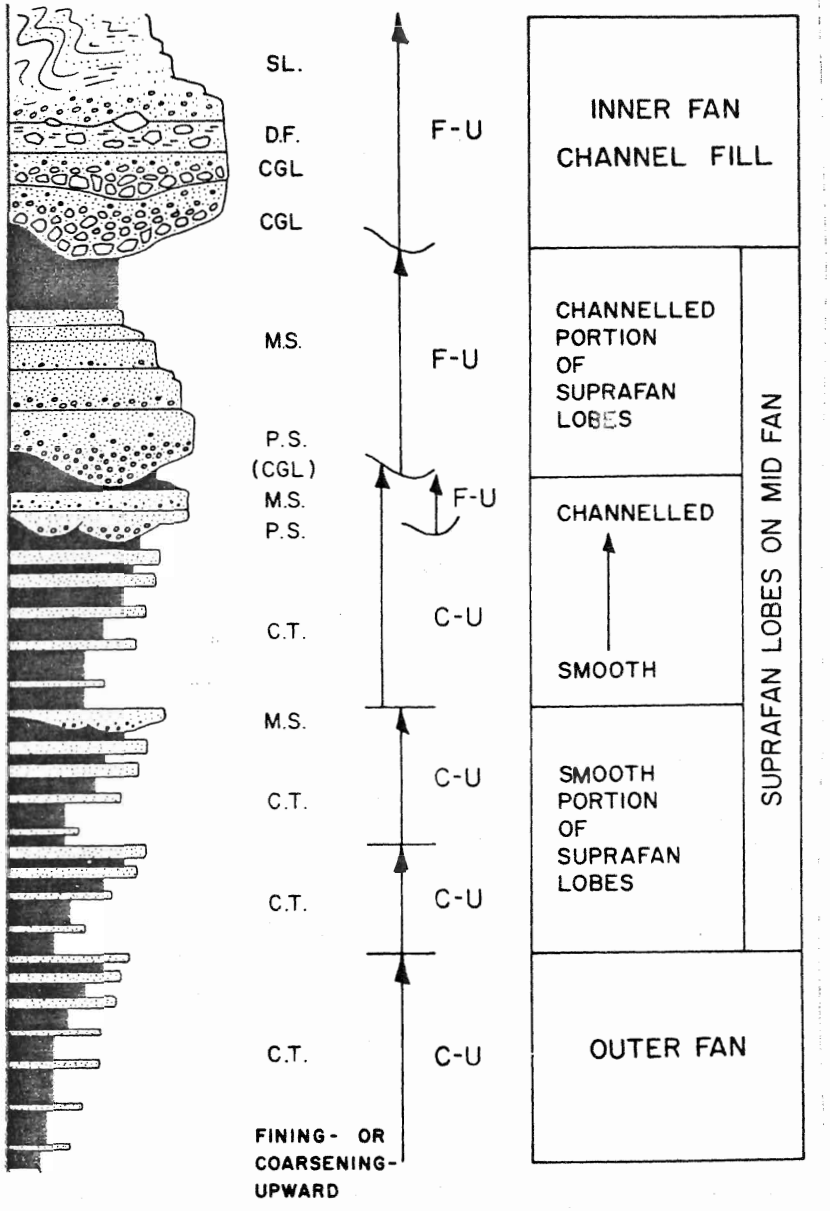

Figure 37. HYPOTHETICAL COARSENING AND THICKENING UPWARDS CYCLE COMMONLY PRODUCED BY SUPRAFAN PROGRADATION AND CHANNEL FILL DEPOSITION (Walker 1975, 1979)

Sedimentary cycles observed in the Berry Creek measured stratigraphic sections, particularly the Running Road and Mist Inlet section, Figures 7 and 15, contain coarsening upward and/or fining upward sequences (Walker 1979). The coarsening upward cycles, characteristic of lobe progradation (see Figure 37), are represented by

symmetrical to asymmetrical profiles (Pickering 1981, 1982; Normark 1978; Walker 1979). The latter cycles (Type II of Pickering 1981) probably represent the most common sequence in the outer suprafan deposits of the Berry Creek area. The high coarse fraction component and large flow volume of the primary pyroclastics commonly bypass the inner fan and form shallow channel deposits upon distal turbidites (Chan and Dott 1983; Sigurdsson et al. 1980; Carey and Sigurdsson 1980; Ricketts et al. 1982). The single coarse flow deposits are similar to avulsion deposits (Miall 1981) which are subsequently overlain by fine grained pelagic deposits. Belt and Bussieres (1981) noted that coarsening upward profiles are not observed in all suprafan lobes. These deposits are commonly top absent due to rapid channel migration, multiple source regions, bypassing by large flows, or simple cessation of volcanism (Link and Nilsen 1981; Chan and Dott 1983; Walker 1979; Belt and Bussieres 1981).

The channel type coarsening upward sequences in Figures 7 and 8 are probably comparable to the symmetrical, thickening upward progradational lobes of Bailes (1980), Mutti and Ricci-Lucchi (1975), Eriksson (1981) and Pickering (1982). The lower turbidite sequence (Figure 7) was rapidly overlain by progressively shallowing series of channel deposits. The volcanic sequence is intercalated with proximal massive AA turbidity mass flows. The shallow channels in the Running Road section (Figure 8) are characteristic of braided mid to outer suprafan deposits

Figure 38. DEPOSITIONAL TRENDS OF BERRY CREEK COMPLEX SHOWING THE WESTWARD PROGRADATION DIRECTION AND PROXIMAL, MEDIAL, AND DISTAL (LATERAL). ASSEMBLAGES. VENT ZONE PROBABLY LOCATED IN THE EASTERN BERRY CREEK AREA NEAR THE KISHQUABIK LAKE SYENITOID COMPLEX.

(Normark 1978; Walker 1976, 1979). In summary, the proximal lobes are characterized by symmetrical, coarsening-fining cycles while the lateral and distal lobes commonly contain individual volcanic flows (local coarsening) overlain by turbidites and pelagic sediments. Fans dominantly composed of suprafan lobes have also been interpreted by Link and Nilsen (1980).

The overall cycle of the depositional system in the Berry Creek Complex indicates a progressive shoaling trend followed by degradation or foundering of the central volcanic island complex similar to the models of Hyde (1980), Bailes (1980), and Ayres (1983). The rapid buildup of coarse pyroclastic debris, characterizing the Berry Creek deposits, may indicate a migratory system of relatively proximal suprafans fed by a number of sources. The probable westward progradation of the Berry Creek Complex is diagrammed in Figure 38. Preservation of the coarse fragments and glassy shards suggests rapid downslope motion similar to the canyon fed subaqueous systems interpreted by Normark (1978).

ENVIRONMENT OF VOLCANISM

The metavolcanics and metasediments of the northern domain of the Sioux Narrows greenstone belt are subdivided into several lithofacies describing the distribution and development of an Archean volcanic complex. Facies patterns and sedimentary cycles are consistent with a localized, rapidly shallowing upwards, intermediate to felsic edifice (tephra cone) built upon a lower mafic shield volcano (platform). Contemporaneity of volcanism and sedimentation characterize the growth and dispersal of Berry Creek volcanism.

A schematic reconstruction of the Berry Creek Complex and associated mafic metavolcanics is shown in Figure 39. The exploded diagram of the inferred local paleogeography outlines the types of lithologies, source areas, depositional modes, types of volcanism, lateral facies development, and distribution patterns of volcanogenic products during the active cycle of the Berry Creek volcanism. Figures 39 and 44 are shown during Stage 5 development of the Berry Creek edifice (see Figure 42). A plan view of the volcanic complex, illustrated in Figure 40 outlines another schematic approach to the distribution of subaqueous depocentres adjacent to the subaerial to subaqueous edifice complex (also modelled during Stage 5 development).

The generation of vast amounts of pyroclastic debris, during shallow water volcanism, is commonly characterized by progressive shallowing and growth of a subaerial tephra

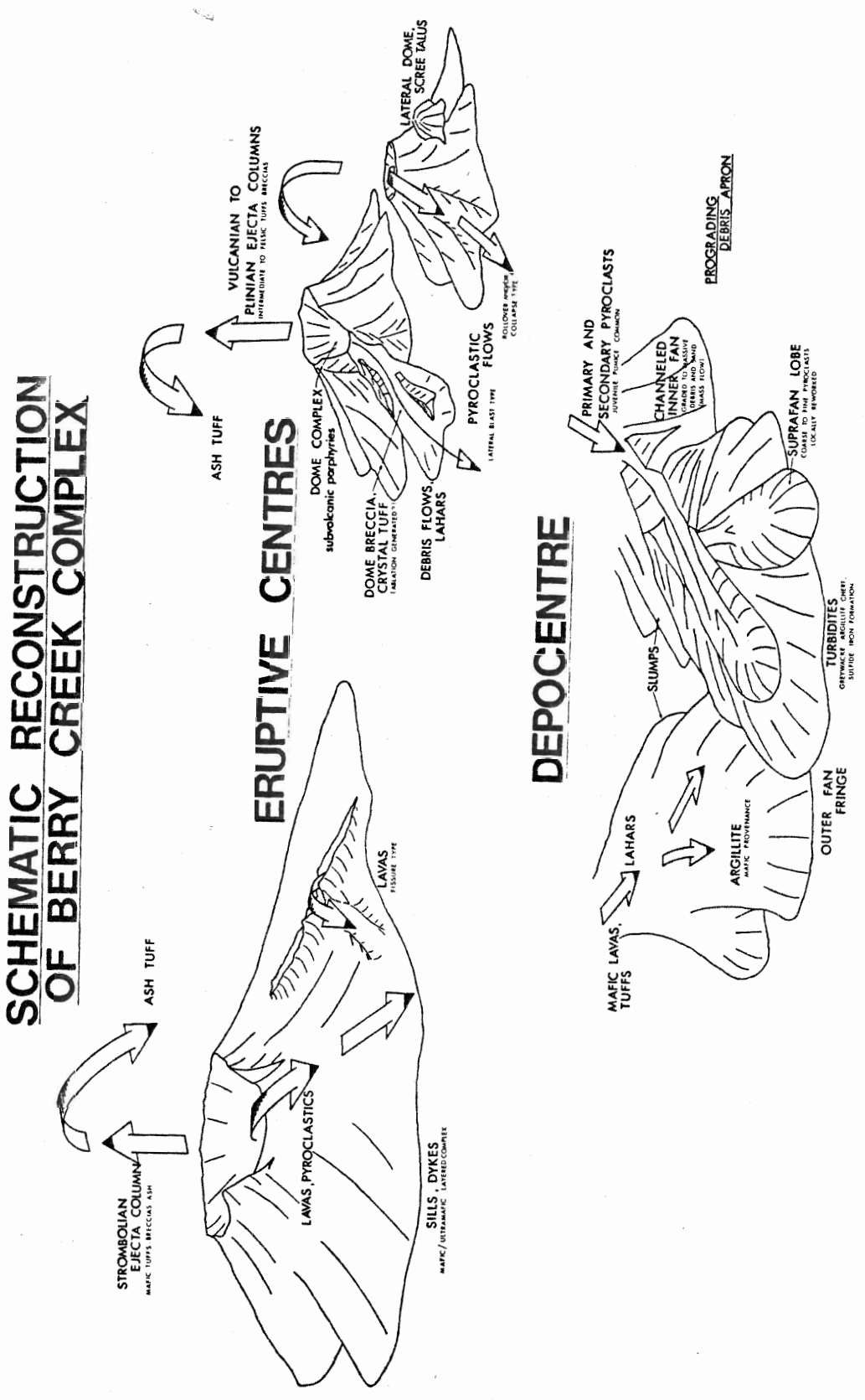

Figure 39. SCHEMATIC RECONSTRUCTION OF THE BERRY CREEK COMPLEX AND SUBJACENT MAFIC SHIELD VOLCANO (SHOWN DURING STAGE 5 DEVELOPMENT). EXPLODED DIAGRAM OF ERUPTIVE CENTRES AND DEPOCENTRES SHOWS SCHEMATICS OF ERUPTIVE STYLE, DEPOSITION, AND DISTRIBUTION OF VOLCANOCLASTIC PRODUCTS.

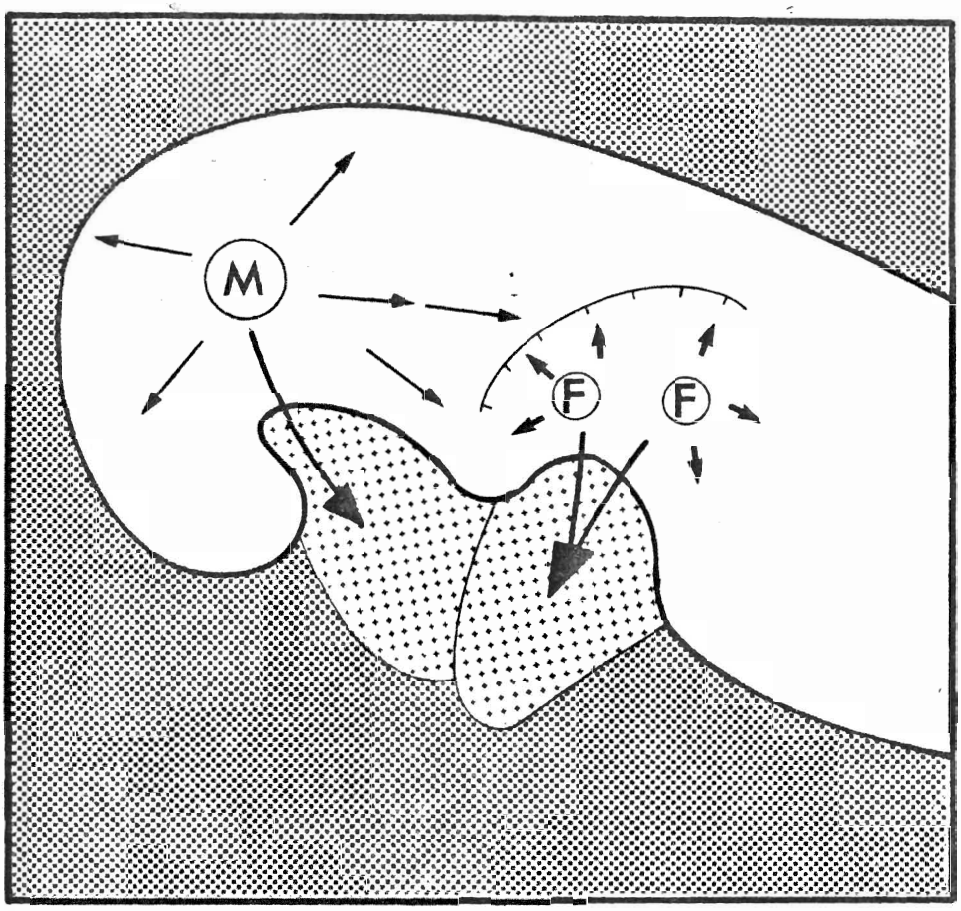

Figure 40. PLAN VIEW OF FIGURE 39. SUBAERIAL (UNSTIPPLED) MAFIC AND FELSIC VENTS WITH DISTRIBUTIONARY TRENDS OF TEPHRA. LARGE ARROWS INDICATE SEDIMENT MOVEMENT TO SUBAQUEOUS FANS. SECONDARY MASS FLOW AND AIR FALL DEPOSITS IN SUBAQUEOUS ENVIRONMENT OUTSIDE MAIN FEEDER ZONE (DARK STIPPLE). HASH MARKS REPRESENT VOLCANIC COLLAPSE DURING STAGE 4.

cone from the initially subaqueous vent zone (Buck 1978; Ayres 1977, 1982, 1983). The evolution of the Berry Creek Complex (see Table 7) also follows the eruptive growth cycle from Stages 2 - 5 (see Figures 41, 42 and 43). Similar evolutionary trends have been suggested for the Blake River Group of the Abitibi belt (Dimroth et al. 1982). Figure 45 (cf. Dimroth et al. 1982) closely parallels the physiographic parameters suggested for the Berry Creek complex. The contemporaneous development of the sedimentary aprons and the locally subaerial eruption

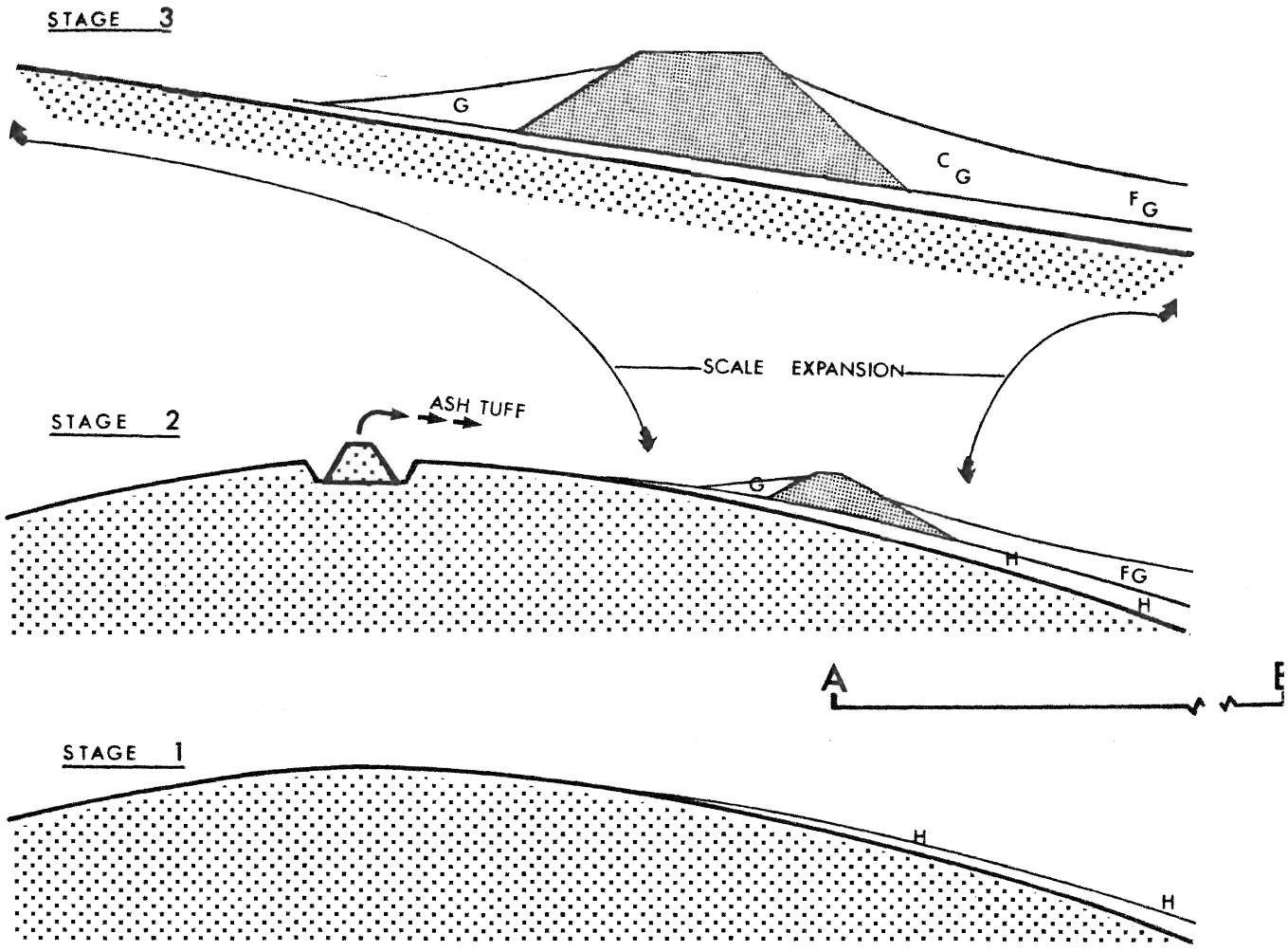

Figure 41. STAGES 1 - 3 IN THE DEVELOPMENT OF THE BERRY CREEK COMPLEX AND MAFIC VOLCANIC PLATFORM. "AB" SECTION SHOWN IN FIGURE 44. STAGES AND FACIES ARE DISCUSSED IN TABLES 6 AND 7.

columns is well illustrated.

Dimroth et al. (1982) suggested that the interfingering relationships between the primary and reworked deposits demonstrated the instability of the volcanic islands. Tasse et al. (1978), Ayres (1982), and Dimroth et al.(1982) noted that subaqueous volcanics and sediments comprise the majority of many Archean sequences. The presence of abundant pyroclastic debris, lahars, reworked volcanics, and strongly vesicular, massive and/or

TABLE 7. EVOLUTION OF BERRY CREEK COMPLEX

Stage 1. Deposition of lower mafic volcanic platform (facies H). Dominantly massive to pillowed lava flows and comagmatic gabbro to peridotite sills. Sedimentation of pelagic and suspension deposits (probably distal argillic turbidites). Eruption of minor mafic tuff, tuff breccia. Progressive shallowing indicated by vesiculation, selvages, pillow dimension, hyaloclastite.

Stage 2. Accumulation of facies A lava flows, facies C pyroclastics and mixed epiclastic-pyroclastic assemblages (facies F,G) in deep to shallow subaqueous environment. Progressive shoaling indicated by coarsening upward cycles (lobes) as tephra builds up to sea level. Rapid sedimentation by downslope mass flow-pyroclastic flow, lahars, debris flow, slumps, turbidity current. Minor deposition of mafic tuff with sediments of intermediate provenance.

Stage 3. Continued tephra buildup characterized by Plinian to Surtseyan eruptions. Progradation of pyroclastics with peripheral mass flow sedimentation. Pyroclasts become intercalated with deep basinal sediments.

Stage 4. Partial cessation of pyroclastic eruptions. Intermittent eruptions of partly vesiculated juvenile pumiceous debris. Possible volcanic collapse associated

TABLE 7 continued:

with moat filling (facies D) stage. Reworking of mafic and felsic tephra. Development of heterolithic lahars. Heterolithic ash flow tuff also present. Reworking of lahars and ash flow tuff, also mafic tuff and quartzofeldspathic arenite in shallow subaqueous environment.

Stage 5. Development of dome and breccia complex. Lateral collapse and slumping - mass flow of hyalotuff and monolithic debris units. Occasional pyroclastic flow deposition. Strongly vesiculated pumice present. May interfinger with medial to distal Stage 3 and 4 facies C deposits. Reworking of pyroclasts and lava flows by turbulent currents.

Stage 6. Continued degradation of dome complex. Quiescent basinal sedimentation of chert, feldspathic chert, sulphide iron formation, and black pelagic argillite. Local brecciation of chemogenic sediments by slumping. Mass flows of monolithic debris contain rip up clasts. Intercalation with interchannel or distal turbidite deposits. Mafic flows, hyaloclastite overlie and intercalate with turbidite deposits of intermediate to felsic, occasionally mafic provenance.

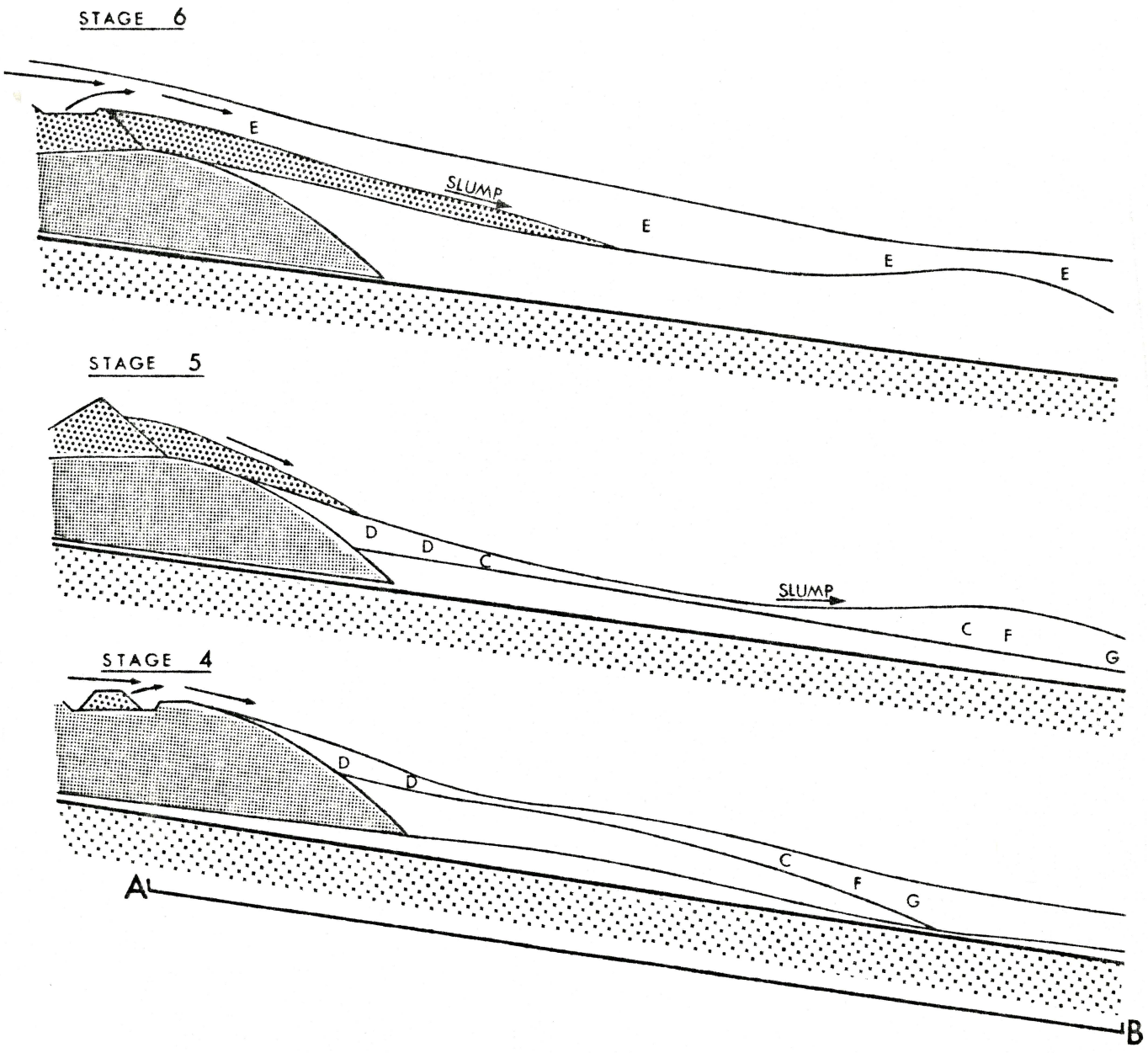

Figure 42. STAGES 4 - 6 IN THE DEVELOPMENT OF BERRY CREEK COMPLEX. SEE FIGURES 41, 44, TABLES 6, 7.

brecciated lava flows, which occur within the Berry Creek Complex, imply a subaerial provenance. Figure 46 (cf. Ayres 1982) and 45 (cf. Dimroth et al. 1982) illustrates the cross section and oblique profile, respectively, of an Archean volcanic island. The two diagrams clearly illustrate the volumetric relationship between the emergent

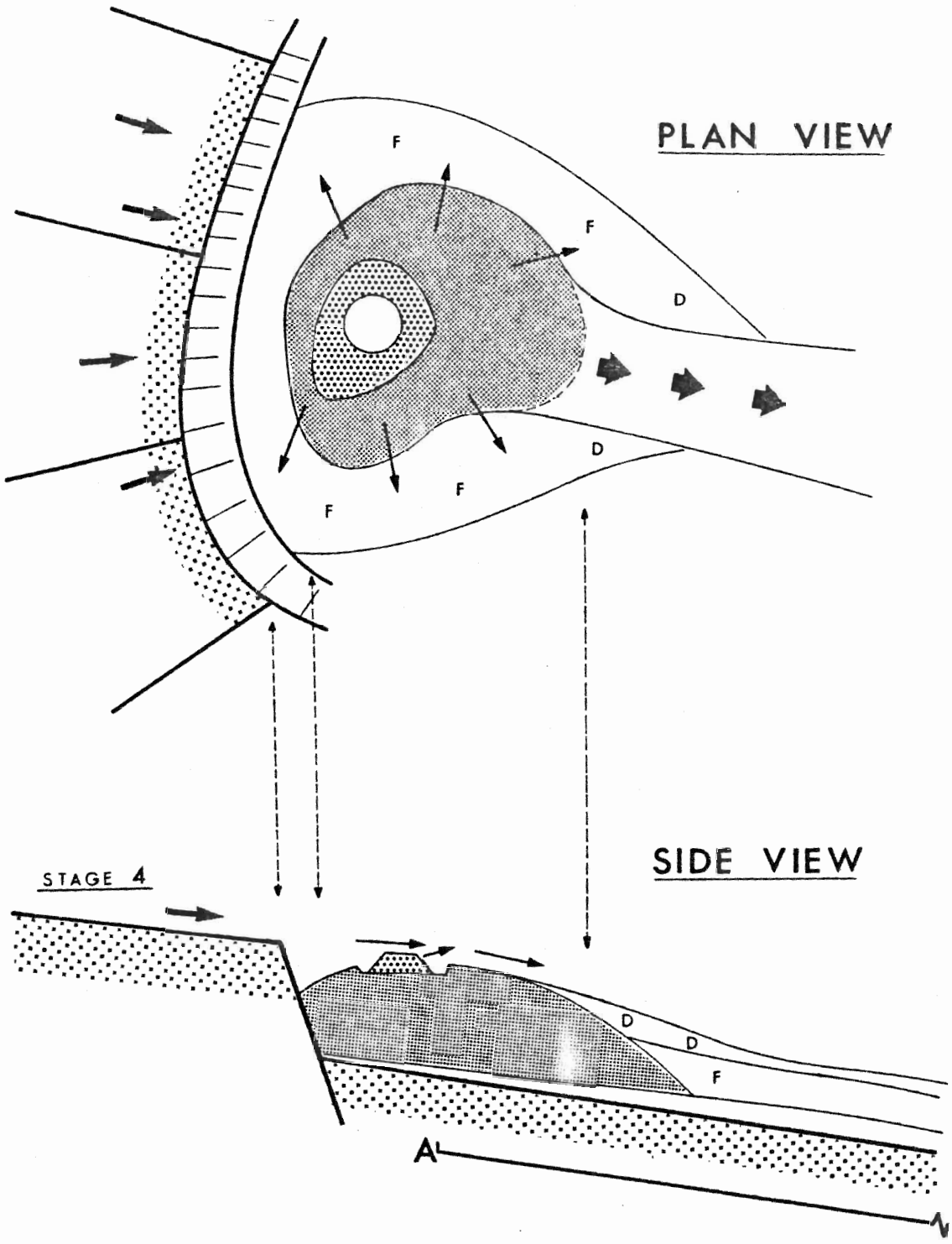

Figure 43. PLAN VIEW AND CROSS SECTION OF ALTERNATE FOR STAGE 4 DEVELOPMENT INCLUDING VOLCANIC COLLAPSE FEATURES. ADDITION OF MAFIC DEBRIS FROM TOPOGRAPHIC HIGH SUPPLEMENTS PRIMARY AND SECONDARY TEPHRA.

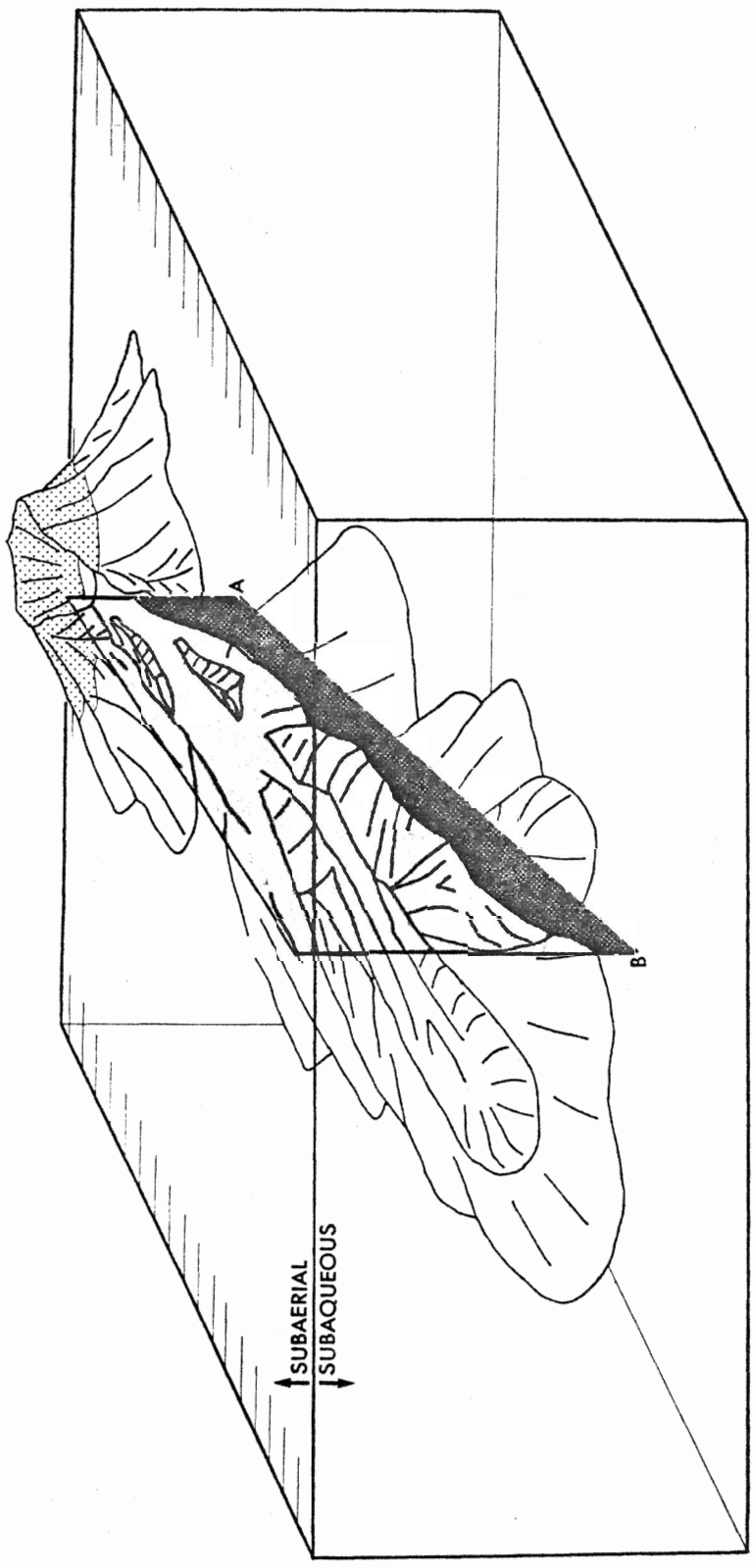

Figure 44. BLOCK DIAGRAM OF SCHEMATIC VOLCANO AND DEPOCENTRE. LIGHT STIPPLE REPRESENTS SUBAERIAL EXPOSURE DURING STAGES 4-6. CROSS SECTION SHOWS LOCATION OF FIGURES 41-43. MAFIC VOLCANO NOT SHOWN.

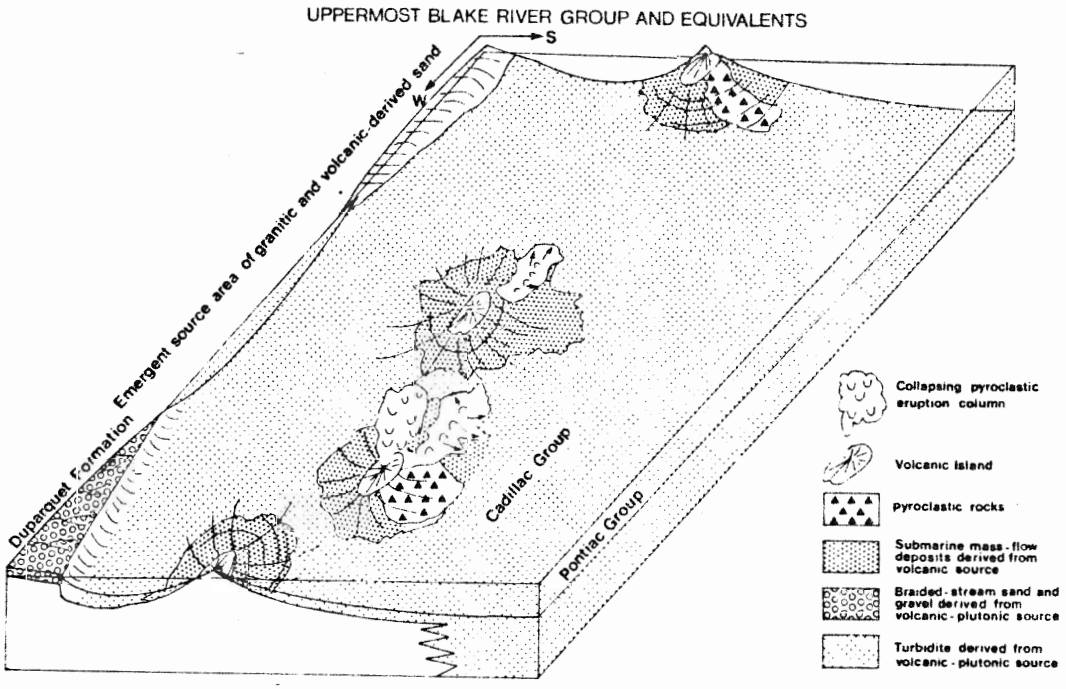

Figure 45. SCHEMATIC PHYSIOGRAPHIC DIAGRAM DURING EMERGENT PHASE OF BLAKE RIVER VOLCANOES. SMALL VOLCANIC ISLANDS WITH SUBAERIAL PLINIAN ERUPTION COLUMNS. APRONS OF MASS FLOWS AND TURBIDITY DEPOSITS (Dimroth et al. 1982)

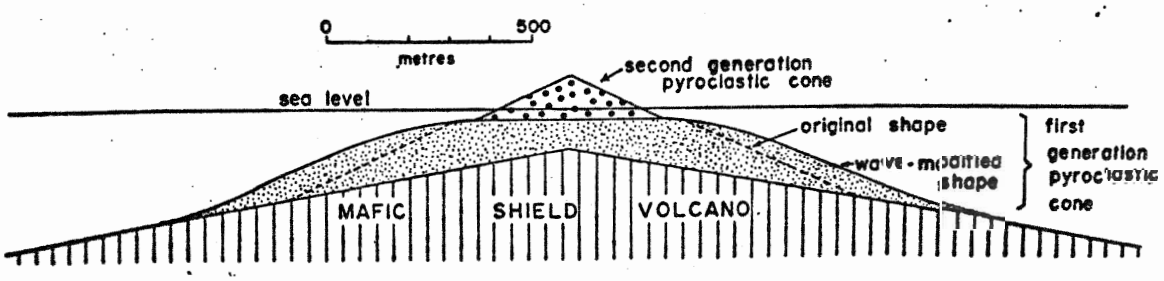

Figure 46. VOLCANIC ISLAND MODEL OF AYRES (1982). TWO GENERATIONS OF TEPHRA CONES. WAVE MODIFIED CONE SUPPORTS SUBAERIAL SECONDARY CONE. NOTE VOLUME RELATIONSHIP BETWEEN SUBAERIAL AND SUBAQUEOUS COMPONENTS.

vent complex and the predominantly subaqueous flanks.

Although the tephra are commonly derived from a

subaerial source, deposition is predominantly by subaqueous mass flow mechanisms (Ayres 1982; Dimroth and Demarcke 1978; Buck 1978; Tasse et al. 1978, 1982; Dimroth and Rocheleau 1979; Afifi 1981; Car and Ayres 1979). Sigurdsson et al. (1980), Carey and Sigurdsson (1980) and Ayres (1982) reported that modern volcanic islands, e.g., Dominica, Martinique, are characterized by relatively small subaerial exposures surrounded by gently sloping to steeply sloping subaqueous flanks.

Primary deposition of the Plinian to Vulcanian and/or Surtseyan derived pyroclastic flow units (Car 1976; Ayres 1977, 1982, 1983; Hallberg et al. 1976; Dimroth et al. 1983; Tasse et al.1978) within the subaqueous envinronment has been documented by Sigurdsson et al. (1980), Carey and Sigurdsson (1980), Embley (1976) and Sigurdsson and Carey (1981). Early accounts, as far back as the 1902 Mt. Pelee and Soufriere eruptions, have also reported pyroclastic underflows (basal segregation zone) penetrating the seawater interface and travelling for many kilometres (see Sigurdsson 1982). As previously discussed, the effects of different physical flow parameters significantly control the depositional pattern. The comparatively restricted distribution of the Berry Creek pyroclastic deposits (see Embley 1976; Sigurdsson and Carey 1981) suggests that deposition was confined to a small basin, volcanotectonic depression or caldera. Figures 47, 48 and 49 (cf. Sigurdsson and Carey 1981; Sparks et al. 1980) compare the

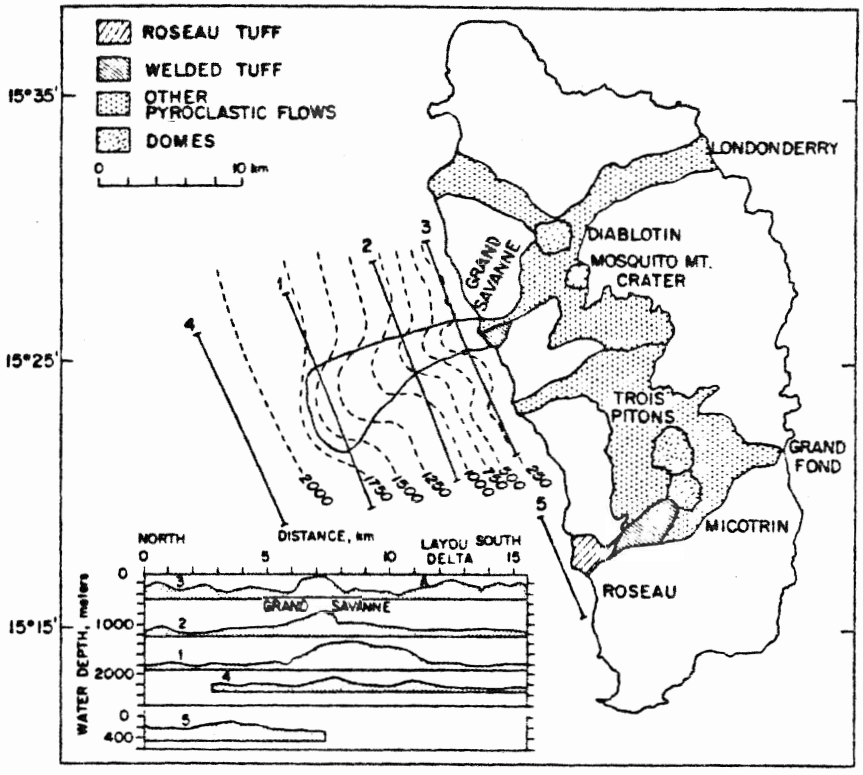

Figure 47. PYROCLASTIC DEPOSITS FROM DOMINICA SHOWING SUBAERIAL TO SUBAQUEOUS TRANSPORT. PROFILES GIVEN FOR THE GRAND SAVANNE AND PROXIMAL ROSEAU ASH FLOWS (Sigurdsson and Carey 1981).

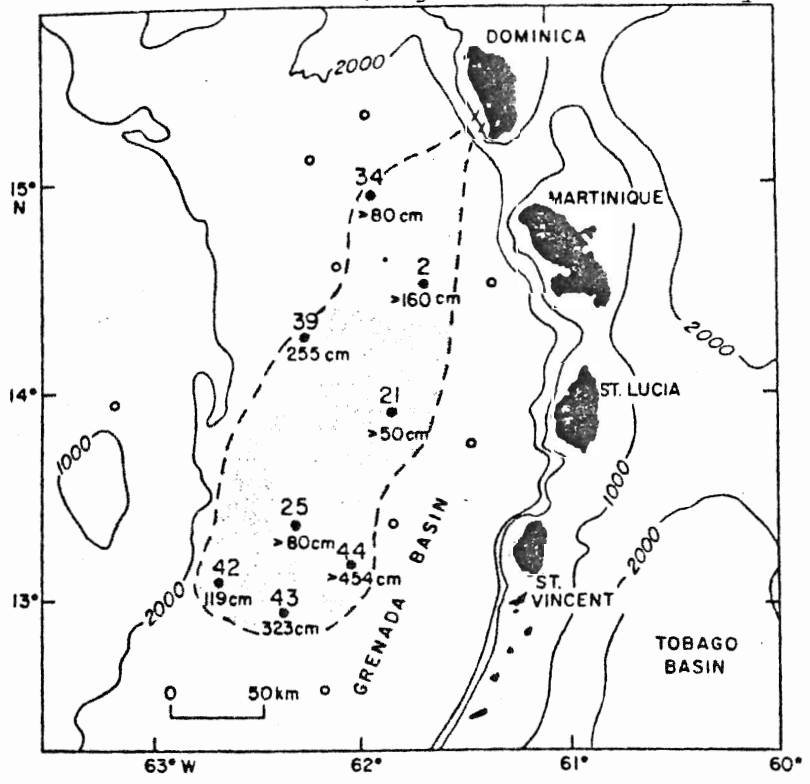

Figure 48. EXTENT OF SUBAQUEOUS ROSEAU PYROCLASTIC FLOW IN THE GRENADA BASIN (Carey and Sigurdsson 1980).

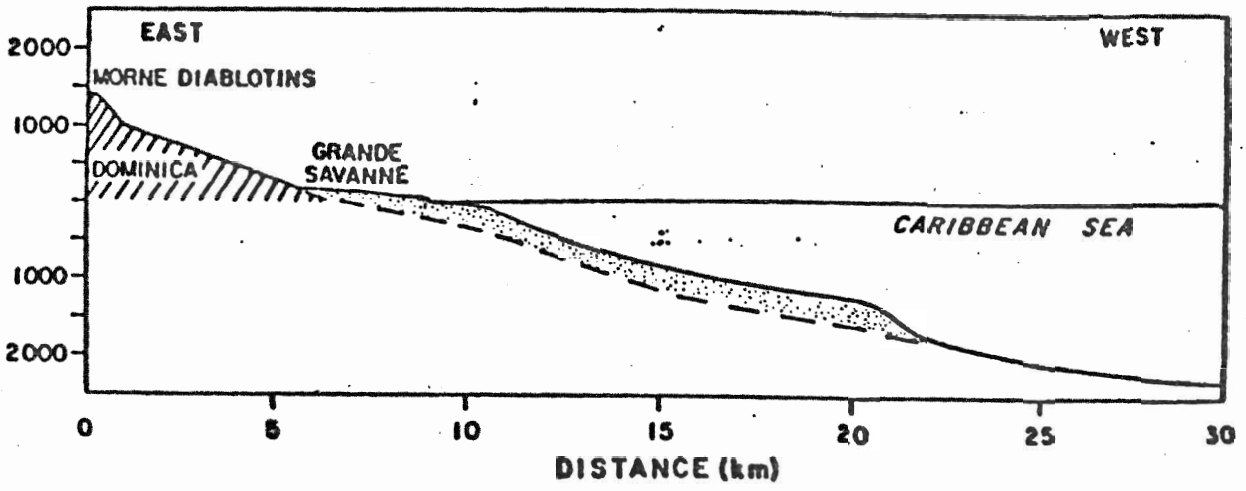

Figure 49. CROSS SECTION OF LITTORAL TO DEEP WATER DEPOSITION OF LOW MOBILITY GRAND SAVANNE ASH FLOW TUFF. HIGH ABLATION RATE AND HIGH DENSITY CONTRIBUTE TO RAPID DECELERATION AT SEAWATER INTERFACE (Sigurdsson and Carey 1981).

profile and distribution of the Grand Savanne and Roseau ash flow tuff deposits. The Berry Creek flows probably reflect a similar depositional profile to the Grand Savanne apron (see Figure 49). The Berry Creek model has been interpreted to contain a small subaerially exposed vent zone (see stippled area in central tephra cone, Figure 44). The association of the surf zone ash flow deposits and the brecciated lava flow in the Maybrun Road area also suggest an early littoral phase of deposition of the Berry Creek ash flows such as that displayed by the cross sectional profile of the Grand Savanne ash flow tuff units (see Figure49). Both flow types contain substantial coarse fragments of relatively nonvesicular dacite which apparently hinder the mobility of the flows in a subaqueous environment (Sigurdsson 1982; Sigurdsson and Carey 1981). The magnitude of the Plinian eruptive columns from the

Berry Creek vent zone can limit the lateral flow distribution.

In many Archean sequences, the presence of subaerial volcanism and sedimentation is indirectly recognized by heterolithic deposits (Attoh 1981; Ayres 1977, 1982, 1983; Buck 1978). Bailes (1980) and Ayres (1977, 1983) reported that the necessary mixing of volcanic components to produce heterolithic deposits was indicative of subaerial reworking. The effects of fluvial transport and secondary sedimentation have been discussed by Buck (1978), Gordanier (1976) and Ayres (1983). The rounded mafic to felsic clasts found in Facies D secondary laharic deposits probably represents an erosional phase of the subaerial volcano following cessation of the majority of the pyroclastic eruptions. The subrounded mafic clasts confirm the subaerial exposure of the lower mafic shield volcano. These clasts suggest that rapid erosion of the mafic volcano, flaring of the intermediate to felsic tephra cone, synvolcanic faulting surrounding volcanic collapse zones or a combination of these parameters produced the mixed assemblage. Figure 43 (Stage 4) diagrams the postulated source of the mafic clasts within the intermediate to felsic debris flows.

Goldie (1983) suggested that heterolithic lahars can be produced by eruptive expansion of the old volcanic roof zone. Recent eruptions at Mount St. Helens have shown that large debris avalanches are commonly heterolithic and are triggered by the forementioned mechanism (Hoblitt et al.

1981). Several authors, e.g., Fiske and Matsuda (1964), have suggested that heterolithic deposits are generated in the vent fallback zone. Subsequent eruptions may produce pumiceous deposits containing both accidental pumice and lithic clasts. Several heterolithic Facies C pyroclastic flow units formed by this mechanism (see Plate 11). The presence of pumice precludes any process involving secondary reworking and redeposition.

Subaerial and shallow subaqueous, intermediate to felsic, volcanic deposits are commonly characterized by a high pyroclastic to lava ratio (Fisher 1983). Deep subaqueous deposits, occurring below the pumice compensation level (Fisher 1983), rarely contain hydroclastic deposits except on steep slopes where mass downslope movement follows the eruptive phases. Kokelaar (1983) noted that the violence of eruptions decreases as the volume of water entering the vent area increases. The availability of water to the subaqueous vent inhibits explosive eruptions partly due to: 1) effects of hydrostatic pressure, and 2) limitations of thermal energy transfer by the magma (Kokelaar 1983). Although explosive eruptions are generated at depths to 500 metres, the rapid production of tephra creates a shallowing trend. A chain effect for pyroclastic eruptions at low hydrostatic pressures significantly increases the production of tephra (Schminke 1979). The early stages of the Berry Creek Complex probably follows a similar trend from shallow,

dominantly hydroclastic, Surtseyan type eruptions to a later subaerial Plinian to Vulcanian eruptive columns. The presence of ash flow tuff deposits implies Plinian rollover type of column collapse type eruptions (Ayres 1983; Sparks 1976; Fisher and Heiken 1982, Thurston 1980).

The vesicularity of the pumiceous or juvenile clasts is governed by water depth, primary volatile content of the magma, availability of phreatic or oceanic waters to the vent area, viscosity and temperature of the magma. Poorly vesiculated pumiceous fragments, common in the lower Berry Creek flow units, can be attributed to subaqueous hydromagmatic eruptions (Heiken 1972; Dimroth and Demarcke 1978) or near solidus magma chambers (domes). Hoblitt et al. (1981) reported microvesicular to subpumiceous dacitic clasts produced by phreatic assisted explosions in the cryptodome structure of Mount St. Helens. Density variations, which may occur within a single flow unit, and commonly recognized by phenoclast content and/or vesicle abundance in the Facies C pyroclasts, can be correlated with distance from the walls of the magma chamber-dome complex (Moore and Sisson 1981; Hoblitt et al. 1981).

The early eruptive products of the Berry Creek Complex probably originated from the shallow subaqueous Surtseyan type eruptions sustained by continuous to restricted access by oceanic waters. Figure 50 (modified after Kokelaar 1983) probably closely approximates the mechanism and environment during early Berry Creek volcanism. The presence of conglomerates (Sammons Bay-Snake Bay) and

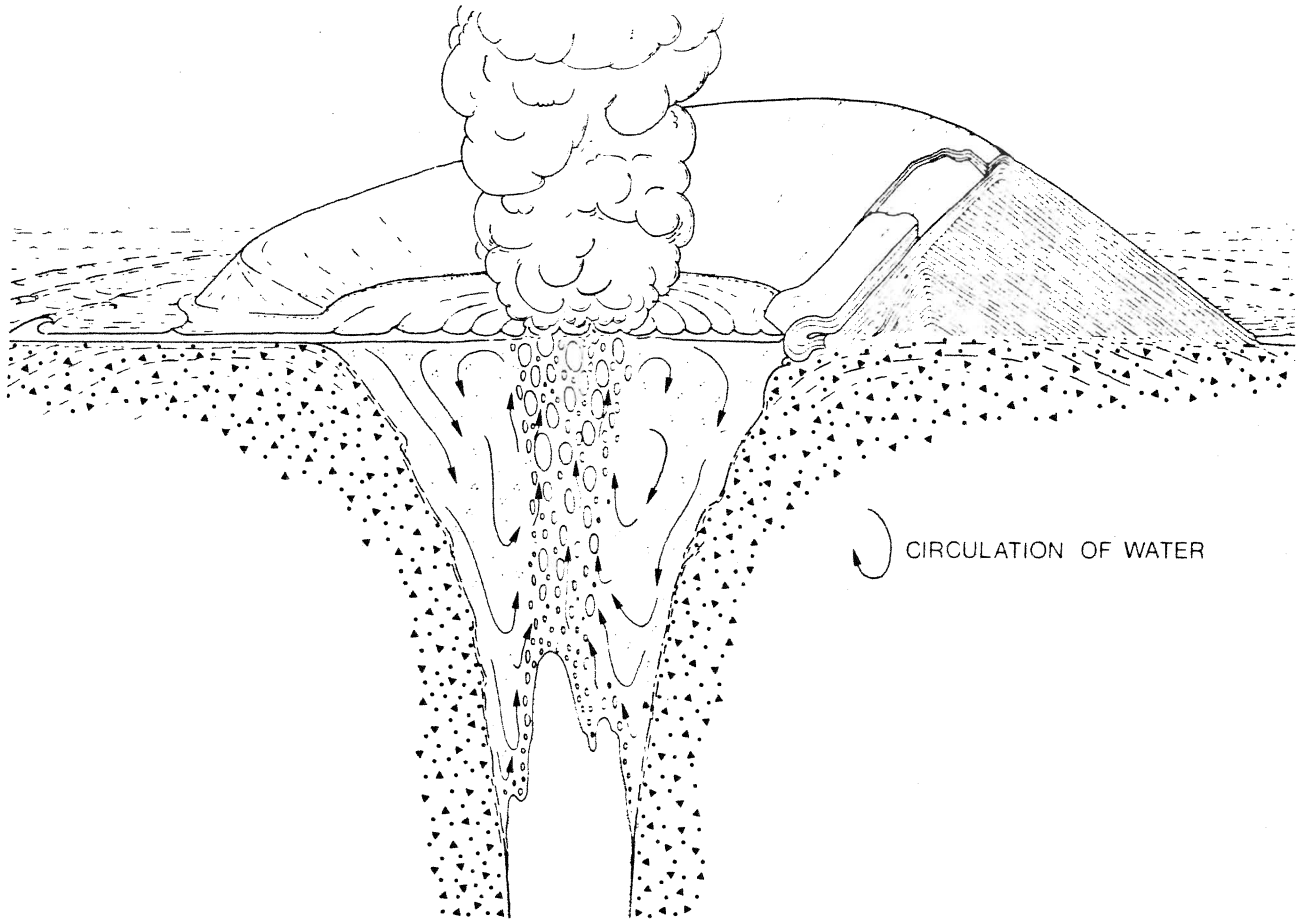

Figure 50. SURTSEYAN VOLCANO DURING TRANSIENT QUIESCENCE. BREACH IN WALL OF TEPHRA CONE ALLOWS INPUT OF OCEANIC WATERS. THERMAL ENERGY INSUFFICIENT TO PRODUCE CONTINUOUS EXPLOSIONS DURING BREACH STAGE (Kokelaar 1983).

lahars (Mayburn Road) derived from the mafic volcanic platform suggests that initial water depths were relatively shallow.

High and low density pumiceous fragments observed in the lower and upper Facies C deposits, respectively, contain abundant phenocrysts (phenoclasts) of quartz and feldspar. The high level magma chamber of the porphyritic dome complex developed initially hydroclastic eruptions characterized by feldspar phyric juvenile clasts, followed by moderately vesiculated pumice containing sparse phenocrysts. The latter are generated by the subaerial Plinian columns (Thurston 1980; Sparks et al. 1973) and are observed in upper Facies C and upper Facies B ash flow tuff deposits in Long Bay and Lobstick Bay, respectively. These shards and fragments exhibiting angular bubble wall boundaries and abundant void spaces are indicative of primary magmatic eruptions (Heiken 1972; Sparks 1978; Dimroth and Demarcke 1978). The lower Facies B debris flow deposits, in comparison, contain sparsely vesicular to nonvesicular dacite produced by Vulcanian eruptions, possibly with phreatic assistance. Fisher and Heiken (1982) noted that late vesiculation of these porphyritic dome complexes (core of Facies B) commonly produce strongly porphyritic, poorly vesicular juvenile clasts. This interpretation may characterize the middle to upper Facies B dome expansion and collapse deposits. Short-lived pyroclastic eruptions interrupted the passive dome growth

stage (Stage 4-6, Figure 42) and these deposits are commonly intercalated with the brecciated lava flows of Facies B. Fumarolic pipes are indicated by numerous alteration zones north of Lobstick Bay, fragmented relicts of sulphide iron formation in Lobstick Bay debris flows and cherty beds intercalated with turbidites, also in Lobstick Bay. After degassing of the porphyry complex, degradation of the metastable volcanic island occurred by wave action and possibly late collapse. Locally, a late stage of shallow subaqueous mafic volcanism accompanied the erosive phase.

GEOCHEMISTRY

INTRODUCTION

Forty seven rock samples from the Berry Creek - Sioux Narrows greenstone belt were analysed for major and trace elements compositions (see Figure 51). The regional reconnaissance study of the Archean supracrustal succession has emphasized sampling of the pyroclastic, epiclastic and autoclastic deposits of the Berry Creek metavolcanics and the lava flows and tuff of the subjacent mafic metavolcanics (Snake Bay, Adams River Bay, Black River, Kenu Lake). Samples from the overlying Lobstick Bay mafic metavolcanics were also analyzed. In addition, a number of random samples were analyzed from the gabbro, peridotite (pyroxenite) and serpentinized dunite of the Berry Lake Layered Sequence; the Mooseview Lake granodiorite lobe, and the Kishquabik Lake syenodiorite.

The samples were selected for analytical treatment according to the following restrictions (Jolly 1977, 1980; Tabatabai 1979): 1) samples with vesicular, amygdaloidal or hyaloclastic zones were avoided; 2) samples with extensive fracture fillings or small mafic veinlets were eliminated; 3) samples containing monomineralic or bimineralic domains (epidotization, carbonatization, sericitization) were generally rejected (see below); 4) heterolithic tuff breccias or similar volcanogenic deposits, often containing felsic to intermediate fragments/clasts in a more mafic matrix, were avoided.

Blocky dacite clasts were large enough to be removed

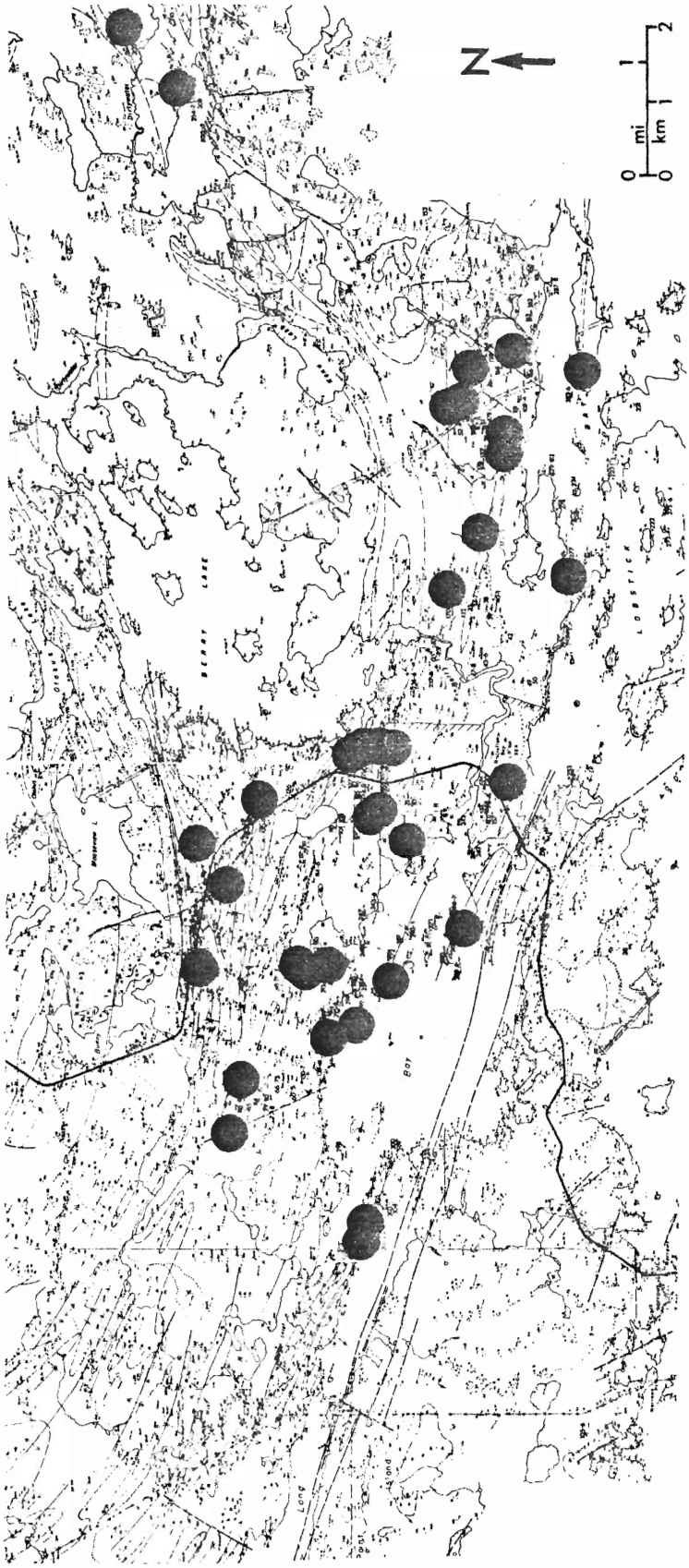

Figure 51. LOCATION MAP OF GEOCHEMICAL ANALYSES FROM THE BERRY CREEK AND ASSORTED ROCKS OF THE SIOUX NARROWS GREENSTONE BELT.

from the sample using the diamond saw (see notation CL in Appendix 2). Porphyritic (blastoporphyritic) or crystal rich metatuff and intrusions/flows, which are commonly avoided (Jolly 1980) were sampled for comparative data with the aphyric to sparsely phyric samples. Mafic to ultramafic cumulates were also sampled to examine the effects of mineral fractionation. As noted above, many samples showed effects of modification by development of metadomains. Several metadomains were analyzed and the data are compared to the least altered metavolcanics.

Sericitization is common in the felsic to intermediate metavolcanics (Barley 1981). Strong sericitization is developed in the Lobstick Bay and Long Bay areas near the regional fault system and is generally restricted to fine tuff and crystal tuff. Mylonitized sections of the dome breccia complex are characterized by sericitization with minor Fe metasomatism. Epidotization is locally developed in the proximity of the Keweenawan diabase dykes. Carbonatization occurs within tuffaceous sediments and lamprophyric dykes in Lobstick Bay.

Samples were analyzed by x-ray fluorescence spectrometry using USGS standards (see Appendix 1). Glass fusion discs and powder pellets were completed for each sample. Numerous duplicates and replicates were analyzed to determine the ranges of precision and accuracy.

GEOCHEMICAL SETTING

Geochemical characterization of the western Wabigoon Subprovince into domains or groups was attempted by Wilson et al. (1976), and subsequently modified by Wilson and Morrice (1977). From two stratigraphic sections, the greenstones were subdivided upward into the following four groups: Lower Mafic, Middle Mafic, Middle Felsic, Upper Diverse. Using a continuous and cyclic fractionation model, they compared volcanic stratigraphy across the western Wabigoon subprovince.

Figure 52 (cf. Wilson and Morrice 1977) displays the subdivisions within the Sioux Narrows-Kakagi Lake-Lake of the Woods greenstone belts. The Berry Creek metavolcanics fall into the Middle Felsic group (Wilson and Morrice 1977), revised from the Upper Diverse Group (Wilson et al. 1976). The former also includes the subjacent Adams River Bay and Black River mafic metavolcanics within the Middle Felsic Group. Table 8 shows a schematic chemostratigraphic section across the northern domain of the Sioux Narrows greenstone belt.

Detailed geochemistry and stratigraphy suggests that the mafic metavolcanics are probably part of the Middle Mafic Group. The Black River and Adams River Bay metavolcanics may be stratigraphic equivalents to the upper Snake Bay mafic metavolcanics (Middle Mafic Group). The latter comprise the Middle to Lower Mafic groups south of the Pipestone - Cameron Fault (Wilson and Morrice 1977,

TABLE 8. CHEMOSTRATIGRAPHY OF THE NORTHERN DOMAIN OF THE SIOUX NARROWS GREENSTONE BELT

Youngest		
Mafic to felsic metavolcanics	Lobstick Bay	Fe tholeiites, (basalt and basaltic andesite), Calc-alkaline (rhyolite and dacite)
Intermediate to felsic meta-volcanics	Berry Creek	Calc-alkaline (rhyolite and dacite)
Mafic to ultramafic metavolcanics	Berry Lake	Fe-Mg tholeiites, (basalt to komatiite)
	Kenu Lake Black River Adams River Bay	Fe tholeiites, (basalts to basaltic andesite)
Oldest		

Trowell et al. 1980). Revisions of the boundary subdivisions by Trowell et al. (1980) are shown in Figure 53, which also display the geochemical character of the metavolcanics. The Berry Creek metavolcanics and the subjacent mafic metavolcanic remnants (Kenu Lake, Black River) are located in Figure 53 (adapted from Trowell et al. 1980).

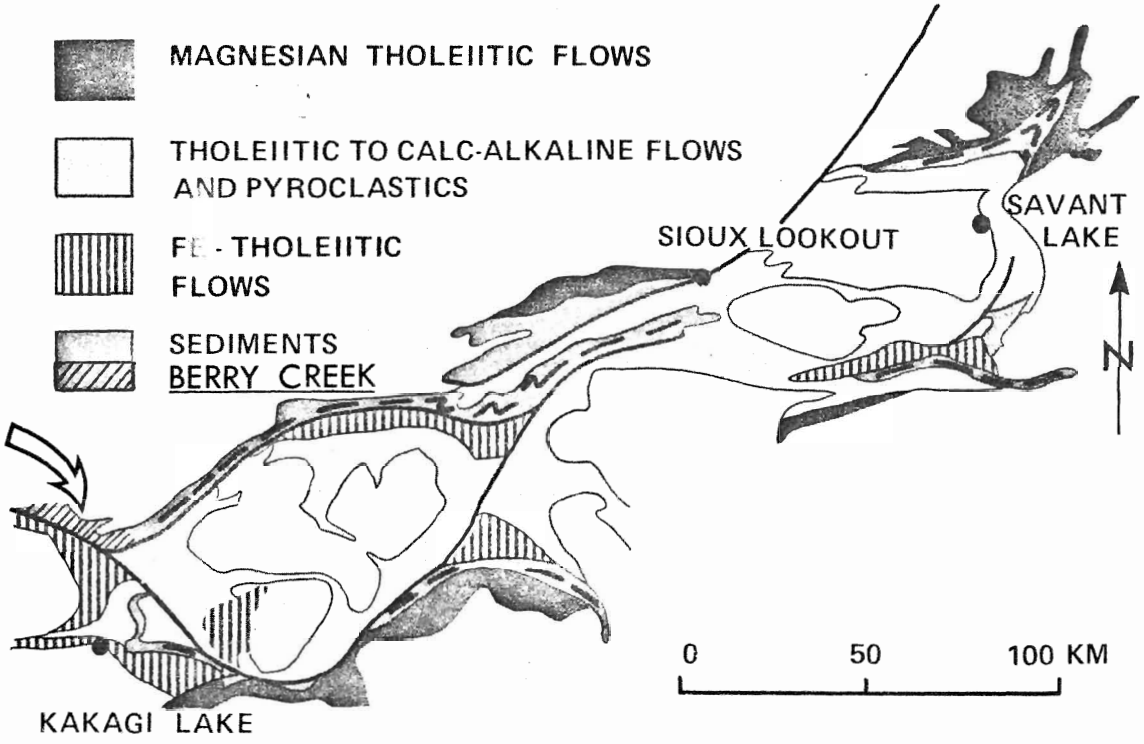

Figure 53. GEOCHEMICAL SUBDIVISIONS IN THE WABIGOON SUBPROVINCE (Trowell et al. 1980). ARROW INDICATES LOCATION OF BERRY CREEK COMPLEX

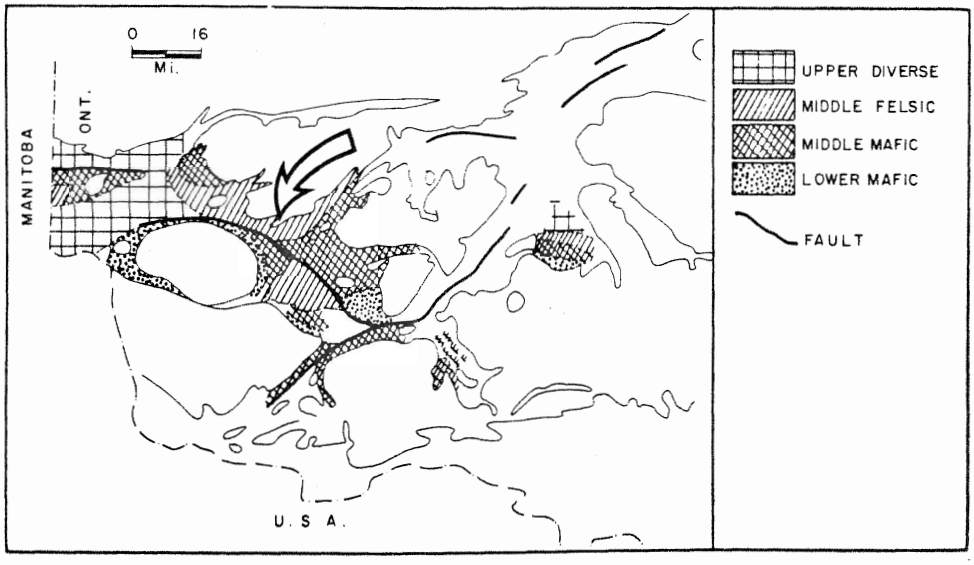

Figure 52. GEOCHEMICAL SUBDIVISIONS OF THE LAKE OF THE WOODS GREENSTONE BELT (Wilson and Morrice 1977) ARROW LOCATES BERRY CREEK COMPLEX.

GEOCHEMICAL DIAGRAMS

Introduction

With rocks of relatively high metamorphic grade, it is necessary to evaluate critically the composition of the rock types in light of elemental mobility. Geochemical interpretations should apply to those elements which reflect the primary compositions. After early success using incompatibles as **tectonic** indicators (Pearce and Cann 1973; Nesbitt and Sun 1976), use of trace elements and major elements (those which generally display monomineralic depletion, e.g., Mg, Ni) have dominated recent geochemical data reduction. Numerous studies have been based upon small segments of the available major and trace element analyses, in particular those elements preferentially partitioned into the melt relative to solid phases (e.g., Pearce and Cann 1971, 1973; Nesbitt and Sun 1976; MacLean et al. 1982; Pearce and Norry 1979).

Alkali and related alkali-earth elements (K, Rb, Sr, Na, Ba) are commonly mobile (see Tabatabai 1979), while other major elements, specifically SiO2, Al2O3 and many trace elements, are considered relatively immobile (Pearce and Cann 1971, 1973; Barley 1981; MacLean et al. 1982; Smith 1980; Nesbitt and Sun 1976; Pearce and Norry 1979; Jolly 1980). MacLean et al. (1982) conclude that Ti, Y, Zr, Nb, Sr and REE generally maintain primary compositional ranges in spite of high grade of metamorphism i.e., amphibolite

grade. Mortensen (1982) and Floyd and Winchester (1978) note that SiO2 and Al2O3 may be slightly mobile under metamorphic conditions. Considerable success with the application of the incompatible trace elements was reported by Floyd and Winchester (1975), MacLean et al. (1982) and Pearce and Cann (1973), for rocks ranging from low to high metamorphic grades. Further evidence of the degree of mobility of these elements is discussed by Barley (1981), Thurston (1980) and MacLean et al. (1982). Of special importance are the mobility of Y, TiO2, P2O5 and Al2O3 during sericitization of rocks of felsic to intermediate compositions (Barley 1981). Although limited mobility was observed by MacLean et al. (1982), the presence of low loss on ignition, small degrees of data scatter, and proportion changes of the entire REE spectrum, the data was considered undisturbed to slightly modified relative to the primary composition.

Mortensen (1982), among others, cautioned that data may be modified by synvolcanic processes including sea water alterations. Geothermal remobilization near volcanic domes (Mortensen 1982; MacLean et al. 1982; Thurston and Fryer 1983) may strongly alter the original chemical trends. Diagrams involving alkalis e.g., AMF diagrams, must be viewed with caution. Similarly depositional modifications by ash surge or cloud separation and/or subsequent reworking can alter the compositions of tuff from the primary magma composition (Cas 1983; Sparks and Walker 1977). Chemical similarities between tuff units,

clasts and flows suggest that these changes have not affected the average compositions of the Berry Creek metavolcanics except for local synvolcanic fumarolic alteration halos.

Type and Criteria

Major and trace element abundances from the analyzed samples are presented in Tables 9,10 and 11. The data are displayed on variation diagrams for comparison with data from previous studies of Archean supracrustals. Absence of complete trends can result from sampling bias and/or low sample density within a restricted area of the Sioux Narrows greenstone belt. Barley (1981) and Hallberg (1978) pointed out the problems of sampling small or isolated sections of metavolcanic belts. Full facies variations may not be exibited within the study areas. Unconformities (physical and geochemical) were recognized due to lenticularity and restricted lateral extent of calc-alkaline volcanic complexes. The impress on of cyclicity due to lateral intercalation of tholeiitic basalts and calc-alkaline volcanoclastics may account for rapidly variable trends (Barley 1981). Synvolcanic faulting, or caldera collapse can also disrupt geochemical stratigraphy (Beavon 1980). Misinterpretation of bimodal suites is common within detailed studies (Barley 1980, 1981) due to the local stratigraphic breaks.

Reduction of the data into komatiitic, tholeiitic

and/or calc-alkaline affinities was attempted as follows. 1) The AMF diagram is used to discriminate between calc-alkalic and tholeiitic suites (Irvine and Baragar 1971). However, due to an overlap of the calc-alkalic basalts within the tholeiitic field (Irvine and Baragar 1971), the MgO / Al2O3 - Alkalis / FeO (total) + TiO2 can be used to discriminate the tholeiitic and calc-alkalic mafic suites (Green 1975).

2) Similarly some overlap of the magnesian tholeiite, komatiite and iron tholeiite suites shown by the AMF diagram can be effectively separated using the Al2O3 - FeO (total) / FeO (total) + MgO and the Jensen cation plot (Al2O3 - MgO - FeO (total) + TiO2) (Jensen 1976; Naldrett and Arndt 1975). Arndt et al. (1977) and Green and Schulz (1977) discuss the compositional overlap between the komatiitic and tholeiitic suites using the discriminant analysis of the Naldrett and Arndt (1975) diagram. A combination of factors including the TiO2 and SiO2 values must also be considered (Arndt et al. 1977).

3) Chemical trends between suites are also compared using FeO (total) - MgO (see Jolly 1977, 1980); FeO (total) / FeO (total) + MgO - SiO2 (Carmichael 1964); FeO (total) - SiO2 (Giles 1981); Al2O3 - SiO2 (Goodwin 1977; Green 1975); and FeO (total) / MgO - TiO2 and FeO (total) / MgO - FeO (total) (Miyashiro 1975; Tabatabai 1979).

4) A discussion of alkali mobility within the samples is described by a alkali ratio diagram (K2O + Na2O - 100x

K2O / K2O + Na2O) (Buck 1978; Stauffer et al. 1975; Hughes 1972).

5) Major and trace elements have been combined in a series of binary and ternary discriminant plots (TiO2 - Zr; Zr - SiO2; Y - Sr; Y - Zr; Y - TiO2; Zr - Ni - TiO2). Interpretations of trace element ratios, e.g., Zr/Y, are related to a series of binary diagrams (Pearce and Norry 1979; Mortensen 1982; Nesbitt and Sun 1976).

RESULTS AND COMPARISONS

Major Elements

The alkali igneous spectrum diagram compares the field of igneous rocks with those rocks displaying either strongly potassic to spilitic modifications by metasomatism and/or metamorphism (Figure 54). Igneous spectrum boundaries conform to the discussions of Hughes (1972) and Stauffer et al. (1975). Detailed discussions of the effects of variations within this diagram (Buck 1978) indicate that some mobility of alkalis has affected both the mafic and intermediate to felsic suites of the Sioux Narrows greenstone belt. Albitization is extremely common in the greenschist to amphibolite grade metavolcanics. Migration of sodium was probably accompanied by potassic metasomatism as the latter may be accounted for by moderate to strong sericitization (commonly coarse grained muscovite) within the felsic metavolcanics. Potassic metasomatism around the Kishquabik Lake syenitoid may be displayed by the ubiquity of fine grained brown biotite. Jolly (1978) noted a

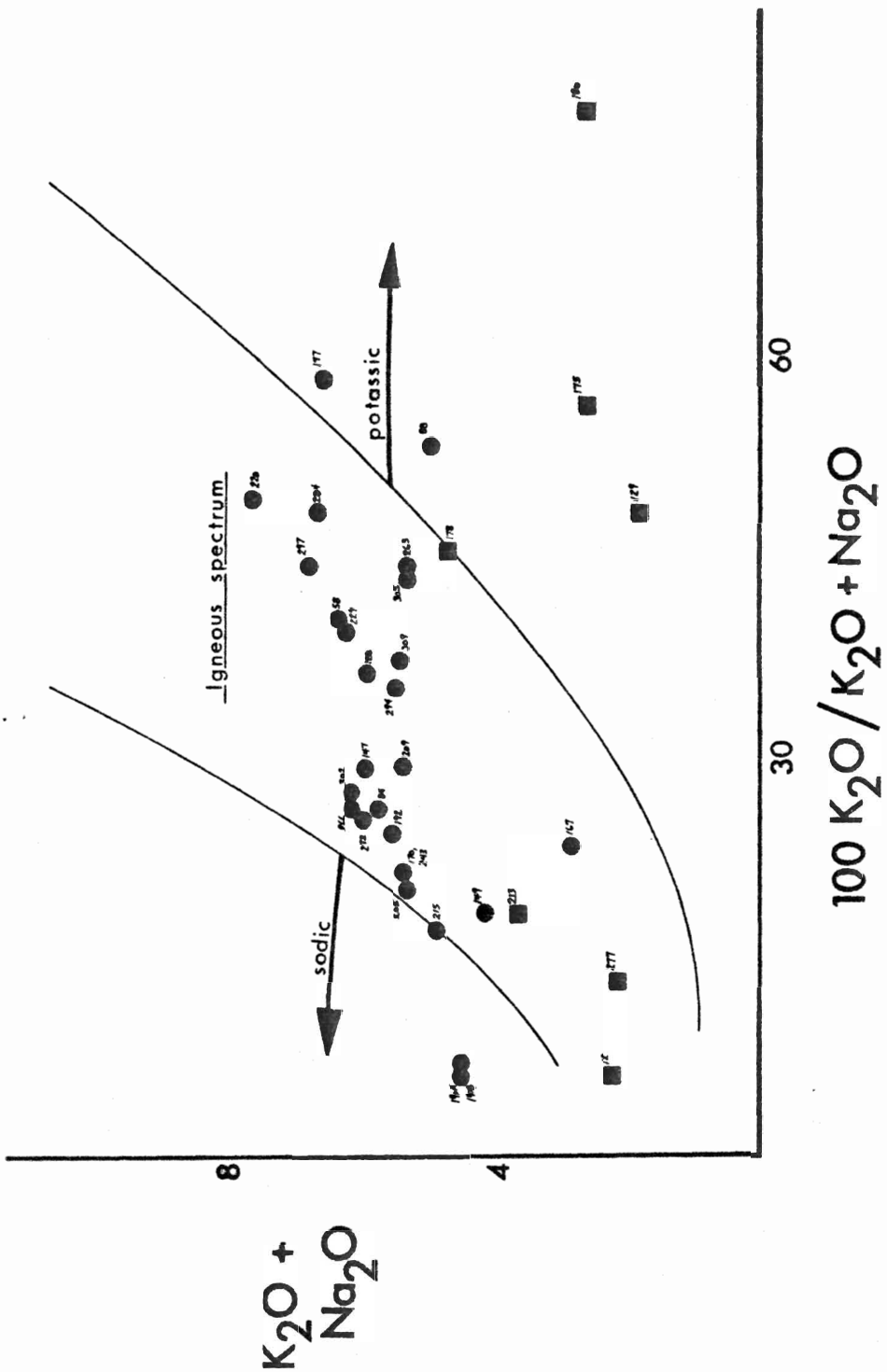

Figure 54. IGNEOUS SPECTRUM DIAGRAM.

TABLE 9. GEOCHEMICAL ANALYSES FROM MAFIC METAVOLCANICS OF THE SIOUX NARROWS GREENSTONE BELT.

Sample Number	12	129	175	178	180	213	277
SiO2	46.51	53.62	56.06	39.87	51.07	52.49	51.16
Al2O3	15.72	14.84	14.48	13.86	13.24	13.40	14.66
FeO*	10.71	15.99	15.55	27.41	9.47	15.35	12.13
MgO	7.15	2.03	3.48	4.66	6.61	5.38	5.48
CaO	12.64	8.00	4.67	6.08	14.54	7.33	10.54
Na2O	2.04	0.91	1.13	2.58	0.57	2.98	1.84
K2O	0.13	0.85	1.41	2.07	1.97	0.66	0.28
TiO2	0.55	0.31	1.11	1.31	0.76	1.06	1.20
MnO	0.17	0.50	0.47	0.57	0.17	0.27	0.18
P2O5	0.03	0.08	0.09	0.17	0.16	0.07	0.09
Total	98.05	97.13	98.46	98.57	98.56	98.99	97.56
Zr	36	61	75	71	65	55	57
Sr	63	136	97	202	244	157	246
Y	10.7	10.1	14.7	11.9	13.6	15.3	13.3
Ni	265	0.5	89.2	234	497	7.3	376

TABLE 10. GEOCHEMICAL ANALYSES FROM BERRY CREEK METAVOLCANICS.

	58	84	88	147	149	167	170
SiO2	68.19	66.03	63.76	68.38	69.72	61.19	71.52
Al2O3	16.37	16.32	16.53	15.74	16.60	19.45	15.73
FeO*	3.49	3.94	8.56	2.35	1.34	9.46	1.95
MgO	0.90	0.85	2.65	0.61	1.22	0.86	0.71
CaO	2.25	4.21	1.56	4.10	2.67	3.59	3.55
Na2O	3.79	4.22	2.35	4.24	3.40	2.16	4.20
K2O	2.51	1.51	2.60	1.70	0.75	0.64	1.11
TiO2	0.35	0.39	0.74	0.32	0.35	0.38	0.45
MnO	0.04	0.05	0.08	0.07	0.03	0.30	0.04
P2O5	0.06	0.05	0.07	0.03	0.03	0.05	0.11
Total	97.96	97.57	98.91	97.54	96.11	98.08	99.37
Zr	141	123	133	117	136	99	178
Sr	681	471	214	406	649	282	1466
Y	18	15.2	18.1	16.2	18.3	15.6	18.5
Ni	4.2	0.4	67	0	0	0	4.8

FeO* denotes FeO (total)

TABLE 10. GEOCHEMICAL ANALYSES FROM THE BERRY CREEK METAVOLCANICS.

Sample Number	177	188	190a	190b	192	205	209
SiO2	70.20	66.86	70.57	67.90	68.52	69.07	71.05
Al2O3	17.34	17.32	14.99	14.48	16.53	16.21	14.82
FeO*	2.02	3.12	2.48	1.77	3.54	2.42	1.63
MgO	0.49	1.03	0.22	0.29	0.56	0.85	2.14
CaO	1.37	4.22	4.77	7.16	4.81	4.48	2.63
Na2O	2.76	3.78	4.19	4.24	4.18	4.24	3.81
K2O	3.75	2.12	0.35	0.26	1.31	1.05	1.57
TiO2	0.33	0.32	0.32	0.28	0.38	0.45	0.33
MnO	0.03	0.04	0.05	0.07	0.06	0.06	0.06
P2O5	0.06	0.03	0.03	0.03	0.04	0.05	0.04
Total	98.35	98.84	97.96	96.46	98.92	98.89	98.08
Zr	159	111	132	NA	113	153	157
Sr	1130	495	1134	NA	530	633	238
Y	19.3	17.4	15.6	NA	16.1	17.2	18.5
Ni	1.8	0	0	NA	1.2	3.3	0

	215	220	229	243	263	266	272
SiO2	70.08	66.39	67.98	72.66	68.13	62.49	71.86
Al2O3	15.52	15.77	16.60	15.78	16.75	15.14	14.72
FeO*	3.00	2.82	3.20	0.72	0.85	4.68	1.80
MgO	0.43	0.44	0.60	0.38	0.38	1.73	0.50
CaO	4.66	3.31	3.25	3.38	2.87	5.43	3.42
Na2O	4.05	3.83	3.85	4.16	2.95	4.50	4.41
K2O	0.84	3.74	2.42	1.12	2.30	1.58	1.50
TiO2	0.31	0.34	0.42	0.29	0.36	0.63	0.28
MnO	0.05	0.05	0.05	0.03	0.02	0.08	0.04
P2O5	0.03	0.06	0.07	0.04	0.03	0.14	0.03
Total	98.97	96.74	98.44	98.56	94.65	96.40	98.58
Zr	NA	130.8	153.5	120.4	135.2	159.6	120.2
Sr	NA	431	836	555	462	1446	447
Y	NA	19.2	18.1	17.4	17.1	18.1	17.4
Ni	NA	0	0	0	0	13.2	0

FeO* denotes FeO(total)

TABLE 10. GEOCHEMICAL ANALYSES FROM BERRY CREEK METAVOLCANICS.

Sample Number	284	294	297	302	305	309
SiO2	67.00	68.49	64.49	72.36	73.02	71.16
Al2O3	16.07	16.37	15.53	14.81	13.29	16.45
FeO*	2.40	3.32	4.40	1.62	2.33	2.04
MgO	0.51	1.00	1.27	0.22	0.72	0.44
CaO	3.41	3.70	3.86	2.74	3.16	2.36
Na2O	3.46	3.53	3.76	4.40	2.97	3.42
K2O	3.15	1.91	2.98	1.63	2.24	1.99
TiO2	0.36	0.34	0.43	0.32	0.29	0.30
MnO	0.05	0.04	0.05	0.04	0.05	0.04
P2O5	0.07	0.04	0.09	0.05	0.05	0.03
Total	96.48	98.74	96.86	98.18	98.12	98.24
Zr	154	112	NA	NA	162	149
Sr	811	322	NA	NA	530	663
Y	19	15.8	NA	NA	19	18
Ni	0	6.0	NA	NA	0	1.0

TABLE 11. GEOCHEMICAL ANALYSES FROM BERRY LAKE LAYERED SEQUENCE.

Sample Number	95	125	97
SiO2	49.50	50.89	39.24
Al2O3	17.53	14.69	4.48
FeO*	7.66	12.42	15.56
MgO	9.18	8.87	28.26
CaO	12.89	9.65	2.16
Na2O	2.00	0.64	0.00
K2O	0.22	0.21	0.02
TiO2	0.28	0.68	0.22
MnO	0.15	0.19	0.32
P2O5	0.03	0.05	0.02
Total	99.49	98.29	90.28
Zr	29.8	44.5	10.1
Sr	74.6	160.1	2.4
Y	10.6	12.2	0.0
Ni	65.5	122.8	NA

FeO* denotes FeO(total)

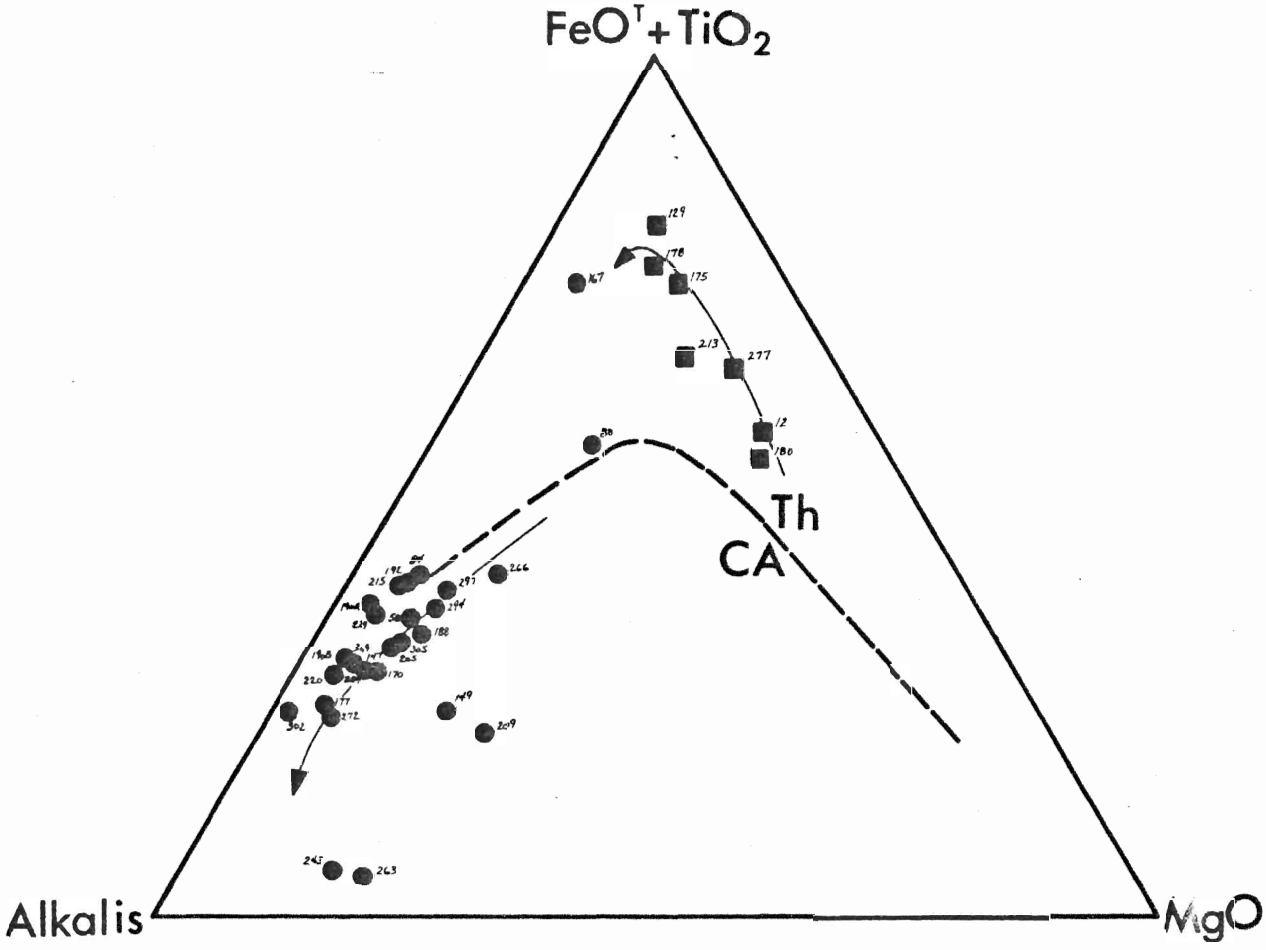

Figure 55. ALKALI - FEO(TOTAL) - MGO DIAGRAM.

similar degree of potassic metasomatism peripheral to an alkaline stock in the Abitibi belt.

Mobility of the alkalis should be considered in the criteria for discussion of the Alkali - MgO - FeO (total) + TiO2 diagrams. Figure 55 shows an adaptation of the AMF diagram of Irvine and Baragar (1971) and Jolly (1980). Due to very low TiO2 content (0.29 - 1.31 wt.%), the shift of data points toward the F apex is minimal. The mafic metavolcanics fall in the tholeiite field and exhibit moderate to strong Fe enrichment comparable to the tholeiitic suite and magnesian tholeiite suite of the

Abitibi belt (Jolly 1977) and the Thingmuli mafic volcanic suite (Carmichael 1964). Green (1975) plots similar trends of iron tholeiites from the Birch-Uchi, Abitibi, Yellowknife and Noranda regions. A comparable tholeiitic trend has been reported from the western Lake of the Woods, Wabigoon Subprovince (Car 1980).

Sample 178, a magnetite rich mafic clast from a Berry Creek tuff breccia (debris flow) contains the highest FeO (total) content (27.41 wt. %) and probably occurred at or near the inflection point of the tholeiitic trend along the magnetite saturation surface. The iron-rich tholeiites follow trends similar to other Archean mafic metavolcanic suites (Amukun 1979; Green and Schulz 1977; Ewart et al. 1969; Hallberg 1972; Blackburn 1981; Irvine and Baragar 1971).

Most rock data from the Berry Creek metavolcanic suite falls within the calc-alkaline field of the AMF diagram (Figure 55). The trend of increasing SiO2 is given by the arrow towards the alkali apex.

Sample number 167 shows a marked divergence from the remainder of the metavolcanic suite. The high FeO (total) content combined with low alkalis may reflect synvolcanic metasomatism. Sample 88, with high MgO and FeO (total) contents plus low alkali content, is a mixed metasediment, containing felsic to mafic detritus. The calc-alkaline suite is characterized by lower MgO than the trends of Jolly (1977, 1980) but are comparable to the transitional

calc-alkaline to tholeiitic suites of Blackburn (1981), Amukun (1979), Green (1975) and Irvine and Baragar (1971).

The Jensen cation plot (Al2O3 - MgO - FeO (total) + TiO2) (see Figure 56) was used to discriminate between Mg or Fe tholeiites, komatiites, and evolved tholeiitic to calc-alkaline suites (Jensen 1976). The main advantage of

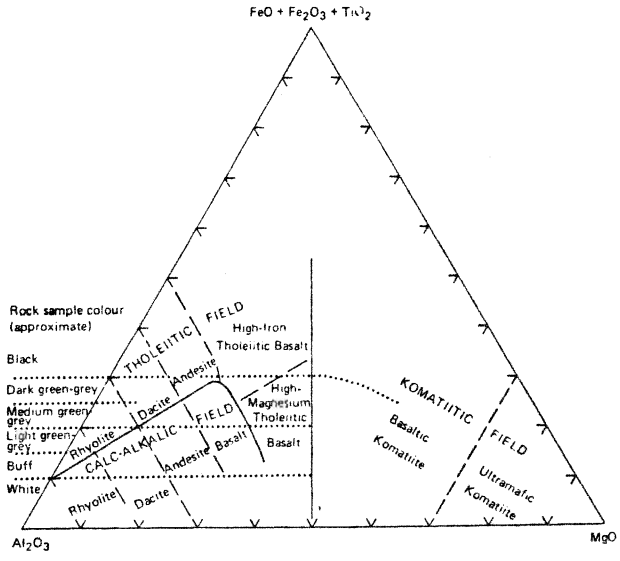

Figure 56. JENSEN DIAGRAM (AL2O3 - MGO - FFO(TOTAL)).

the Jensen diagram is the use of Al2O3 rather than alkalis, due to the high degree of mobility of the latter. In Figure 57, the mafic metavolcanics are iron-rich tholeiites while the subvolcanic sills (not shown) fall into the magnesian to low iron tholeiite fields; accumulate horizons fall in the komatiitic field (not shown, see Table 11).

Comparisons with Archean mafic metavolcanics reveal similarities between this study and Fe to Mg tholeiites of several mafic metavolcanic groups (Middle Mafic Groups) within the Wabigoon subprovince (see Figure 58). The

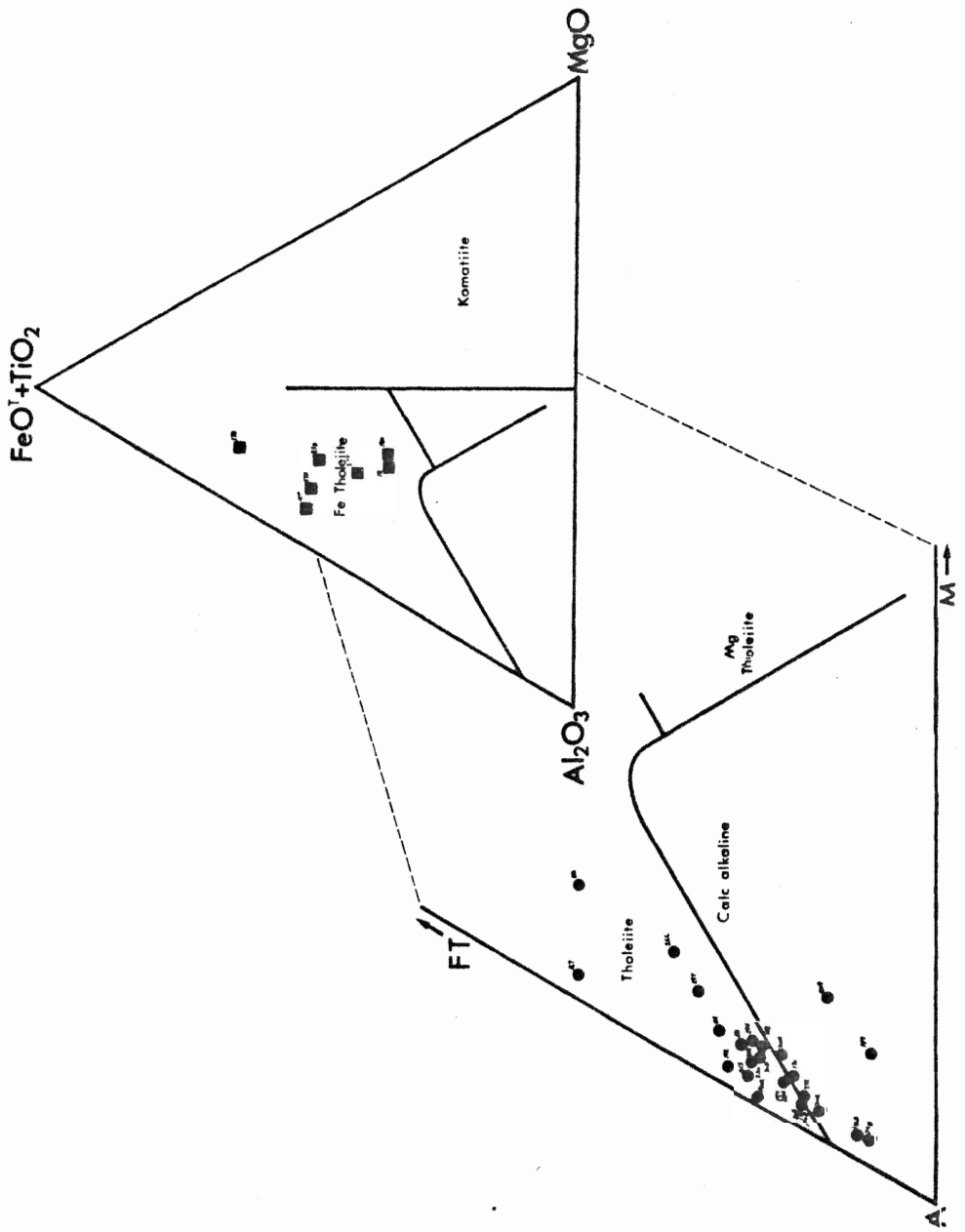

Figure 57. JENSEN DIAGRAM OF BERRY CREEK DATA.

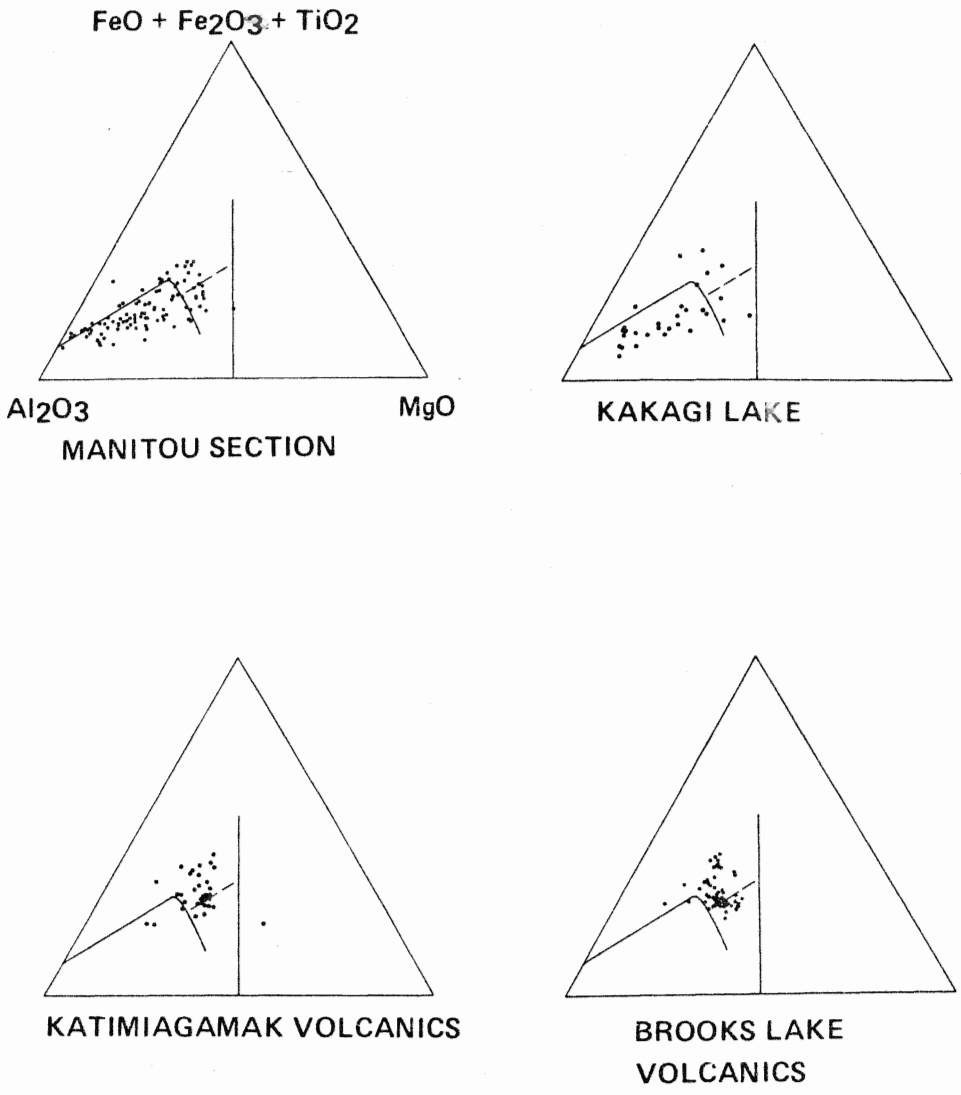

Figure 58. JENSEN DIAGRAMS FROM WESTERN WABIGOON SUBPROVINCE (Trowell et al. 1980)

Katamiagamak mafic metavolcanics fall in the Fe to Mg transition, and these volcanics are probable stratigraphic equivalents of the Snake Bay metavolcanics (sample 12). The dominant Fe-tholeiites become magnesian down section into the Lower Mafic Group (Wilson and Morrice 1977; Trowell et al. 1980; Goodwin 1977).

The felsic to intermediate volcanics fall into the transitional calc-alkaline to tholeiitic compositions, mainly due to the high FeO (total) and low MgO in many

samples. The low ferromagnesian contents result in very erratic Fe/Mg ratios. The majority of the calc-alkaline compositions display a poor trend from low SiO2 tholeiites to high SiO2 calc-alkaline or tholeiitic compositions due to late Fe depletion trend. Sample 266 (lowest SiO2 content) is strongly tholeiitic, and the trends towards the calc-alkaline transition probably reflects rapid crystallization and fractionation of Fe - Ti oxides within the subvolcanic chamber. Sample 209 displays high Mg/Fe ratios and subsequently falls into the calc-alkaline field. The high SiO2, high Mg/Fe contents are not consistent with the remainder of the suite. As noted in the AMF diagram, samples 88 and 167 display marked variations from the trends. Sample 167 is characterized by an increase in FeO (total) due to synvolcanic alteration. Although aluminum has also been increased, the large FeO (total) variation (4 times background) depletes the other components.

The calc-alkaline to tholeiitic suite shows marked differences compared to the Kakagi Lake section (Figure 58) especially defined by the low Fe/Mg ratio and the continuous trend from mafic to felsic compositions. The Manitou Lake section (Figure 58) follows a transitional trend from Fe and Mg tholeiites through a calc-alkaline suite. The high Fe enrichment of the early tholeiites becomes rapidly depleted toward the calc-alkaline trend.

Jolly (1975) noted that strong FeO (total) enrichment occurred within the intermediate members (basaltic andesite to low SiO2 dacites) of the Abitibi belt. Magnetite was

not reported within mafic tholeiitic basalts (Jolly 1977). Maximum FeO (total) enrichment within the Kakagi Lake Group occurs at low SiO2 values (basaltic andesites) with progressive Fe depletion into calc-alkaline andesite (Wilson and Morrice 1977, their Figure 12). The strongest iron enrichment occurs within the basaltic andesites of the Lake of the Woods mafic metavolcanics. Silica content is estimated at 55 wt.% near magnetite saturation.

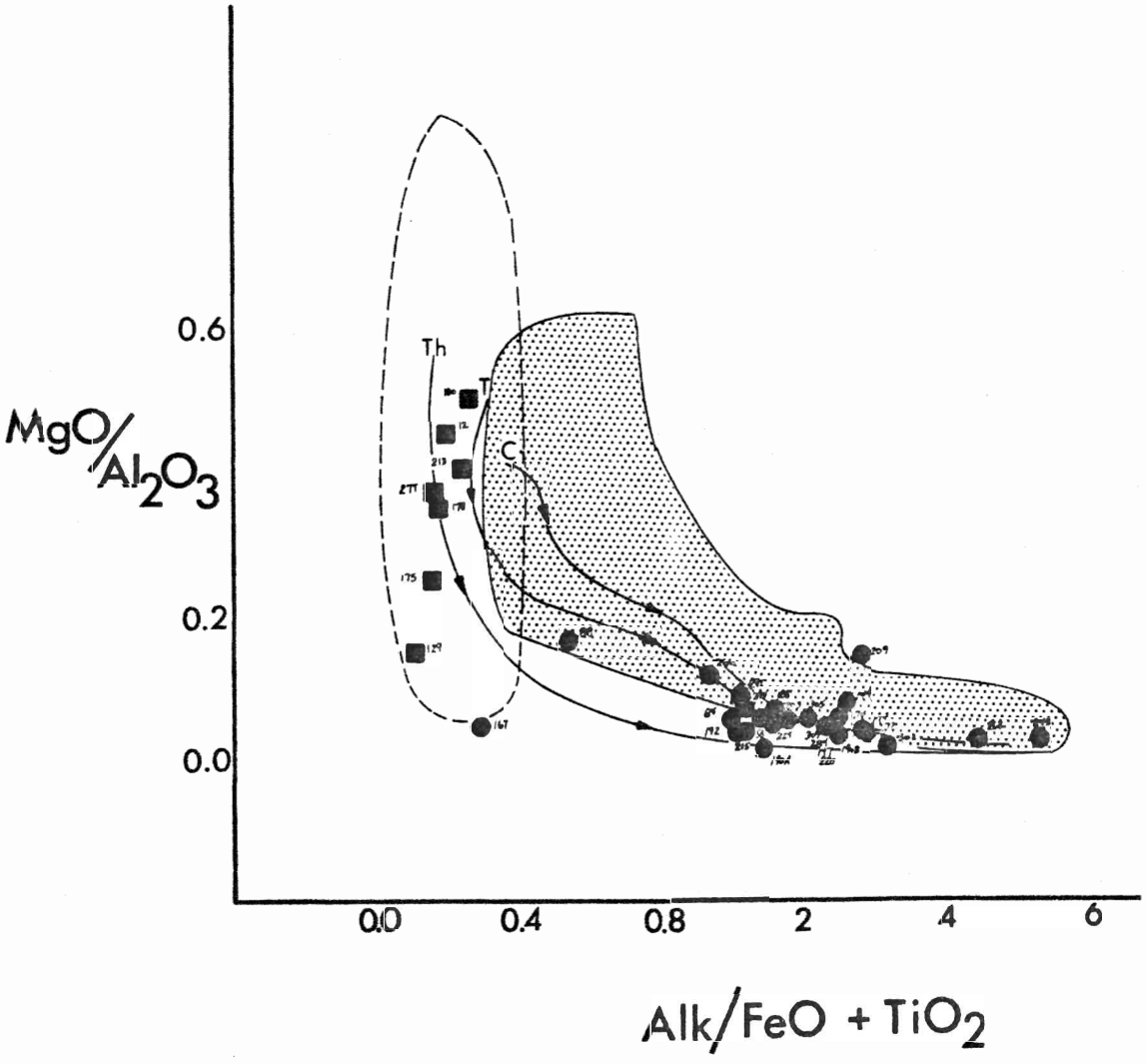

Figure 59. GREEN DIAGRAM (MGO/AL2O3 - ALK/FEO(TOTAL) + TIØ2)

The moderate to high Fe/Mg ratios reported in this study characterizes both the mafic and intermediate/felsic metavolcanics. The two suites are separated by a large andesitic compositional gap between 54 - 64 % SiO2 (calculated volatile free, see Tables 9 and 10).

Separation of the calc-alkaline and tholeiitic mafic metavolcanics using the AMF or Jensen diagrams may be less effective than the MgO/Al2O3 - Alkalis/FeO (total) + TiO2 diagrams (Green 1975; his Figure 3). Figure 59 shows the mafic metavolcanics to fall wholly within the tholeiitic field, and the data closely resembles the trend of Thingmuli (Carmichael 1964) with some tendencies toward the Talasea island arc tholeiites (Green 1975; Lowder and Carmichael 1970) and the metavolcanics from the western Lake of the Woods (Car 1980). The location of the calc-alkaline and tholeiitic fields is based on 1800 analyses of modern volcanics (Green 1975).

The stippled field of the calc-alkaline mafic volcanics (see trend of Cascades, Figure 59) clearly separates the two suites using the relationship of alkali and iron-titanium enrichments. The low MgO / Al2O3 ratio is characteristic of tholeiitic basalts compared to the komatiitic or basaltic komatiite suites (Green 1975). The high MgO (Al2O3 ratios are shown by the subvolcanic sill complex (see Table 11, samples 95, 97, 129). The intermediate to felsic end members are not effectively separated by this diagram, due to the similar trends of alkali enrichment and MgO, FeO (total) and Al2O3 depletion

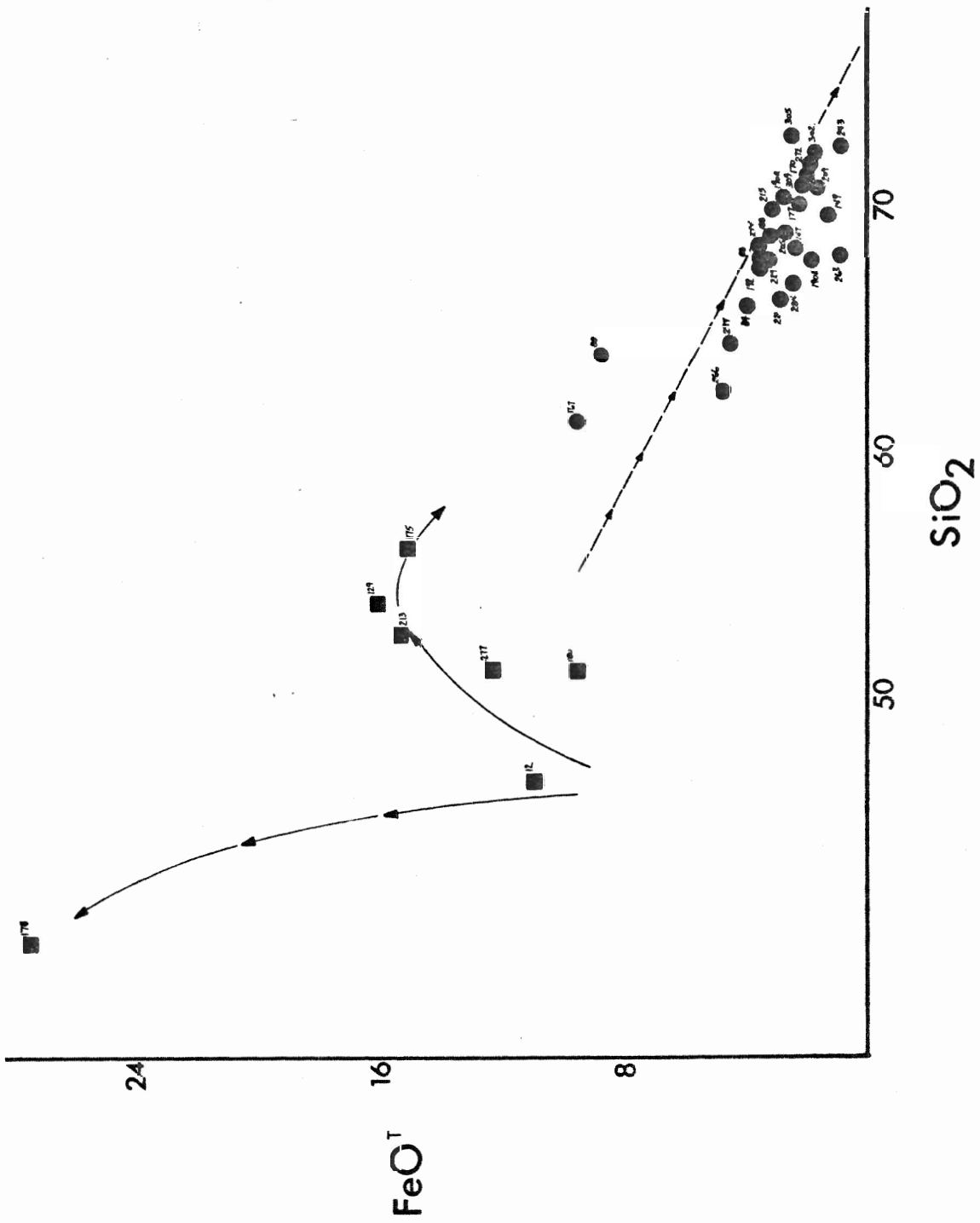

Figure 60. FEO (TOTAL) - SIO2 DIAGRAM.

for SiO2 contents in the rhyodacitic field. The low SiO2 dacite (sample 266) falls into the calc-alkaline field. Conflicting results between the Jensen and Green diagrams

is evident. As previously noted, sample 167 displays MnO, Al2O3 and FeO (total) enrichment, SiO2, MgO and alkali depletion.

The FeO (total) - SiO2 diagram (Figure 60) displays an iron enrichment trend by the mafic metavolcanics and a calc-alkaline inverse FeO (total) - SiO2 correlation. The calc-alkaline trend of Giles (1981) closely parallels the Berry Creek data, although the latter are relatively depleted with respect to FeO (total). The tholeiitic

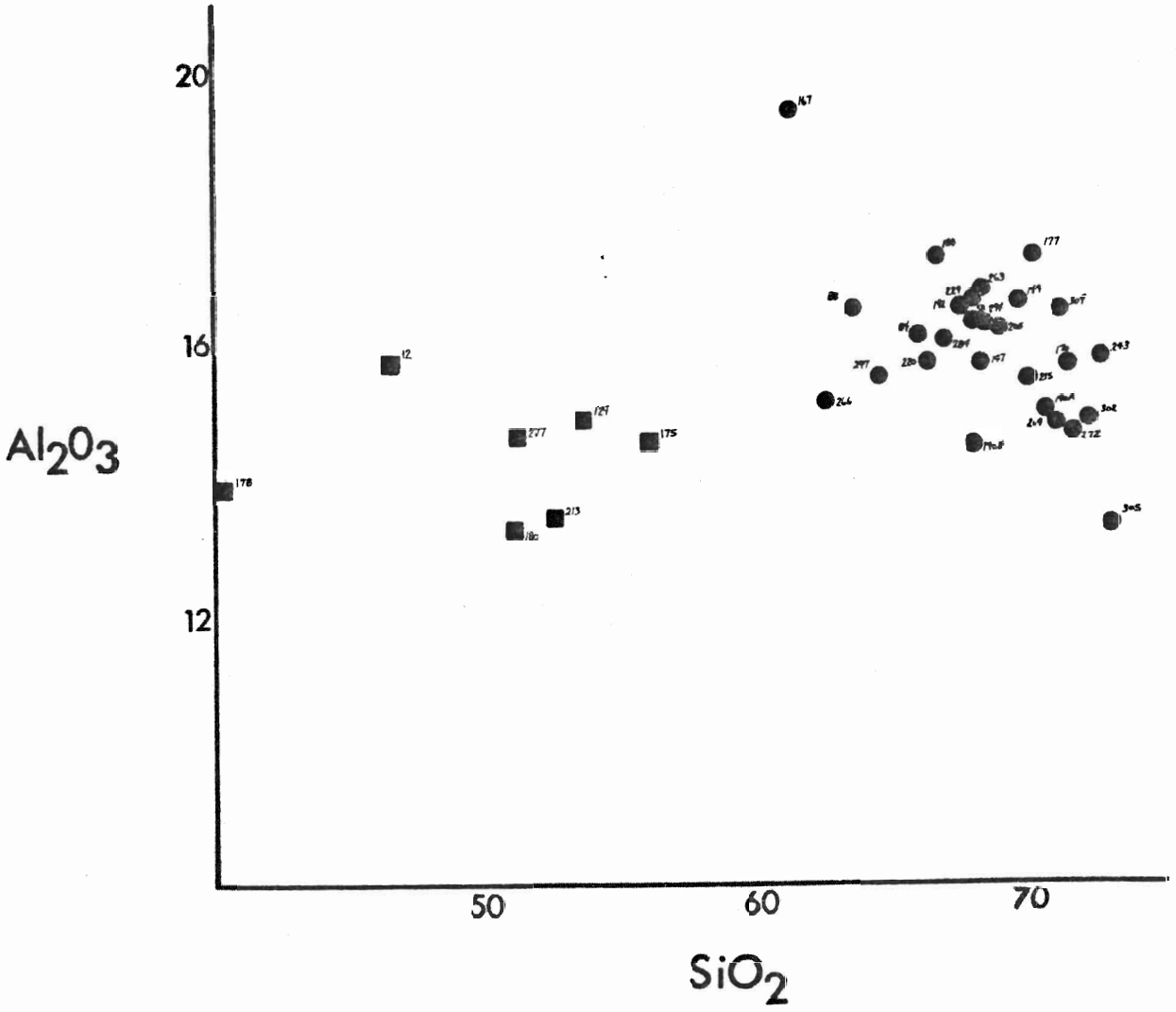

Figure 61. AL2O3 - SIO2 DIAGRAM.

samples indicate a low SiO2 magnetite saturation. The tholeiitic data is otherwise comparable to the data of Giles (1981).

Al2O3 - SiO2 diagrams are characterized by low alumina tholeiitic basalts and basaltic andesites (Green 1975; Goodwin 1968) and slightly higher Al2O3 dacites and rhylolites. The Al2O3 content of the Berry Creek mafic metavolcanics ranges from 13.2 - 15.7% (Figure 61). Baragar (1968), Glikson (1971) and Jolly (1975) discussed low alumina basalts containing average Al2O3 compositions near those of the Lake of the Woods basalts (average 14.1 wt. % Al2O3).

The slightly higher Al2O3 content of sample 12 (see Figure 61) is attributed to plagioclase accumulation. Green (1975) discussed aphyric and plagioclase phyric basalts with similar Al2O3 contents. The high Al2O3 content may be attributable to plagioclase resorption during rapid ascent and/or decompression (Green 1975).

The low Al2O3 tholeiites commonly show trends toward high Al2O3 basalts (Green 1975; Goodwin 1968) where the latter are associated with intermediate to felsic volcanics and the former characterize the lower volcanic sequences. The Al2O3 increase prior to intermediate to felsic volcanism was reported by Goodwin (1968) from the Swayze Metavolcanic Belt.

The plagioclase phyric basalt occurs within the lower section of the Middle Mafic Group of Wilson and Morrice

(1977; their figure 10) at or near the transition to the Lower Mafic Group. The presence of coarsely plagioclase phyric basalts within the Lower Mafic Group (Blackburn 1980) and the relatively high MgO content (7.15% MgO) in the porphyritic sample of the Snake Bay metavolcanics support this conclusion. The strongly plagioclase phyric basalts commonly occur at stratigraphic levels 300-500 metres below the point of onset of intermediate volcanism (Green 1975). Due to the presence of multiple glomeroporphyritic horizons, the relationship between the overlying metatuff and the porphyritic basalts is uncertain.

The dacites and rhyolites range from 13.3 - 17.3 wt.% Al2O3. Jakes and Gill (1970) noted that calc-alkaline rhyodacites from island arc suites contained 16-17.5 wt.% Al2O3 while similar compositions are reported from the Cascades (Hyndman 1972). The low Al2O3 content (13.3 wt%) was reported from rhyolitic tuff (sample 305). The remainder of the analyses cluster between 14.8 and 17.0 wt.%. Sample 167 displays an anomalous Al2O3 content of 19.45 wt. % and may represent fumarolic alteration. Petrographic descriptions show a variety of aluminous phases including chlorite, garnet and muscovite. The presence of chloritoid suggest FeO (total) and Al2O3 metasomatism.

Similar calc-alkaline and tholeiitic trends were displayed by the FeO (total)/MgO - TiO2 and FeO (total)/MgO - FeO (total) diagrams (Figure 62). The calc-alkaline

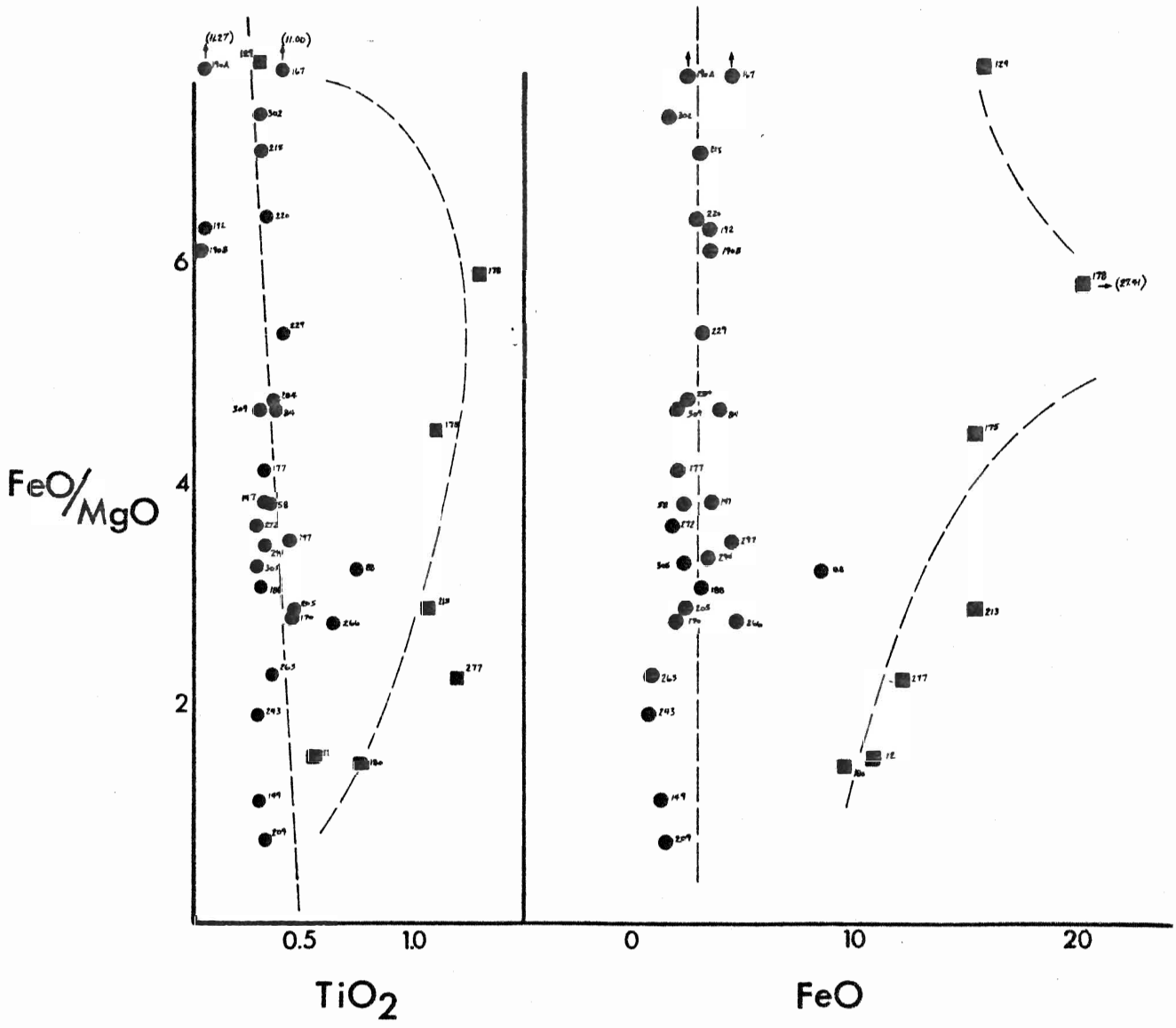

Figure 62. FEO(TOTAL)/MGO - TIO2 DIAGRAM.
FEO(TOTAL)/MGO - FEO DIAGRAM.

trends (linear FeO(total), TiO2 trends) (see Tabatabai 1979; Miyashiro 1975) correspond to other data from Archean metavolcanics. The strong variation in the FeO/MgO ratio in the calc-alkaline suite is caused by the low ferromagnesian content, presence of minor disseminated

sulphides, and possible mixing of tephra from several sources during deposition.

The mafic metavolcanics display characteristic tholeiitic trends (Miyashiro 1975; Tabatabai 1979), although the degree of TiO2 content and enrichment are lower than typical Archean tholeiites (Tabatabai 1979). The linear calc-alkaline trends display variable slopes but are generally subparallel to the FeO (total)/MgO axis. Depletion of FeO (total) and TiO2 with increasing FeO (total)/MgO is characteristic of calc-alkaline trends. The low TiO2 trend shown by Figure 62 is consistent with interpretation of a suite of low TiO2 tholeiites of komatiitic affinities. Although the TiO2 content is low, the enrichment trend has been developed (subvolcanics, 0.22 - 0.28; flows and tuff units, 0.31 - 1.31). The Berry Creek intermediate to felsic metavolcanics average about 0.33 wt. % TiO2. Comparable TiO2 compositions were reported in rhyodacites by Jakes and White (1972). Delaney (1978), in his calc-alkaline suite, reported values ranging from 0.78-0.81 wt.% TiO2. Archean tholeiites commonly contain 40-50% less TiO2 than mid ocean ridge basalts (MORB) at similar MgO content (Nesbitt and Sun 1976) suggesting a direct relationship with the degree of partial melting such that TiO2 depletion occurs at high degrees of partial melts.

FeO (total) - MgO diagrams are used to define the degree and location (composition) of probable maximum iron enrichment, and trends of the two metavolcanic suites.

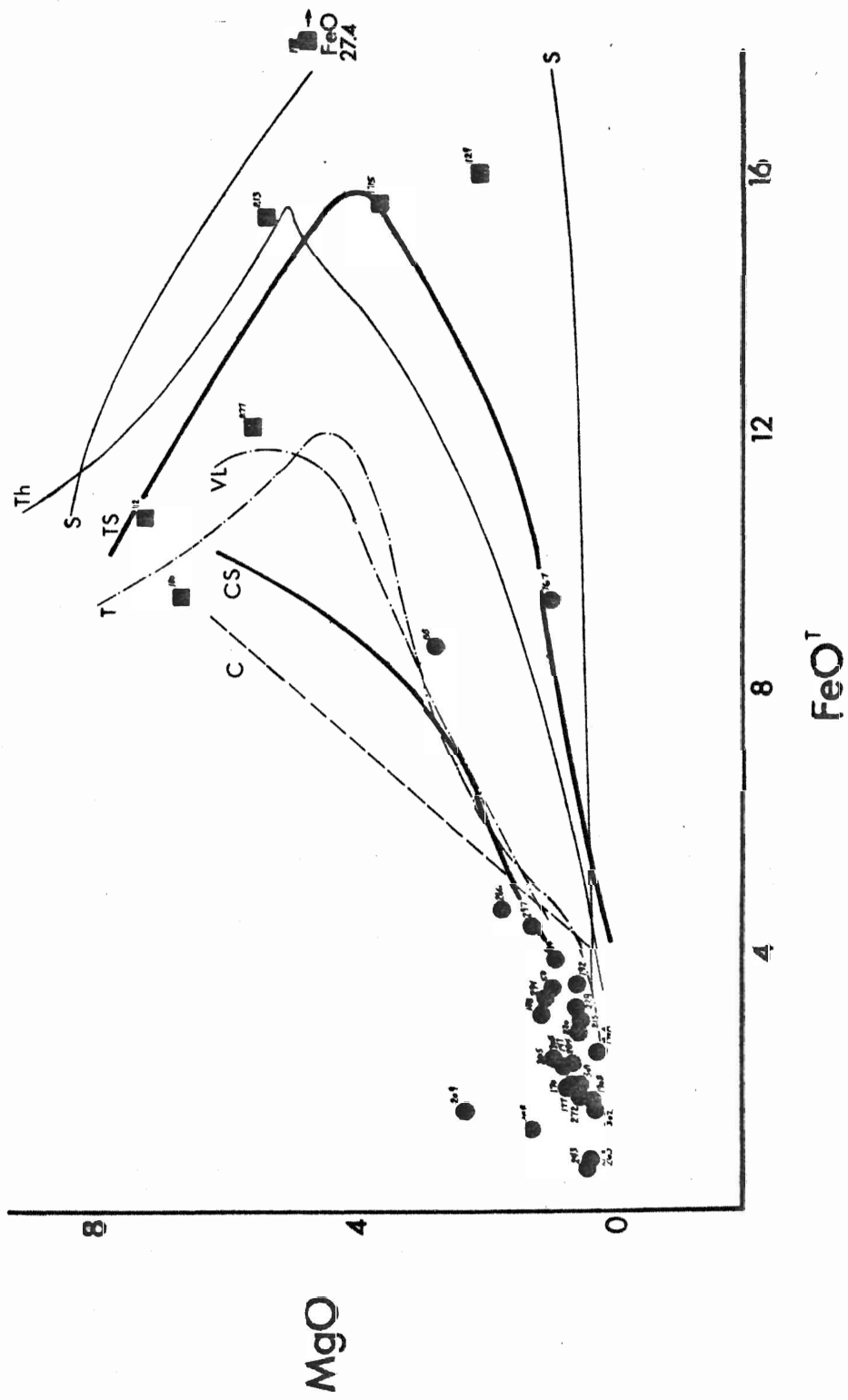

Figure 63. FEO(TOTAL) - MGO DIAGRAM.

Sample 178 displays the maximum FeO (total) enrichment (27.41%) at 4% MgO (Figure 63). The MgO content compares well with the data of Jolly (1975, 1977) but occurs at slightly lower MgO than the more magnesian suites. The tholeiitic suite of Jolly (1977, 1980) compares favourably with the Lake of the Woods mafic metavolcanics (Figure 63). The peak of iron enrichment is also comparable to the Thingmuli trend (Carmichael 1964), Talasea and Viti Levu (Lowder and Carmichael 1970: Jakes and Gill 1970). Sample 129, which occurs at the low end of the trend (2.03%, Figure 63) probably represents a late stage basaltic andesite. The latter occurred as a large clast within a Berry Creek tuff breccia unit.

The Berry Creek metavolcanics occur at the junction of the tholeiite and calc-alkaline trends (Figure 63). The compositional gap between the high SiO2 basaltic andesite (53%) and low SiO2 dacite (64%) effectively separates the two suites. The low SiO2 dacites are comparable to the calc-alkaline suite of Jolly (1980). As noted, samples 88 and 167 are divergent due to syndepositional and synvolcanic modifications, respectively.

Similar bimodal trends are revealed on SiO2 - FeO (total)/FeO (total) + MgO diagrams (Figure 64). Strong iron enrichment is shown by the mafic metavolcanics. The trends are comparable with Talasea (Lowder and Carmichael 1970) in the high MgO samples (12, 180, 213, 277) but characterizes similar trends to the Thingmuli

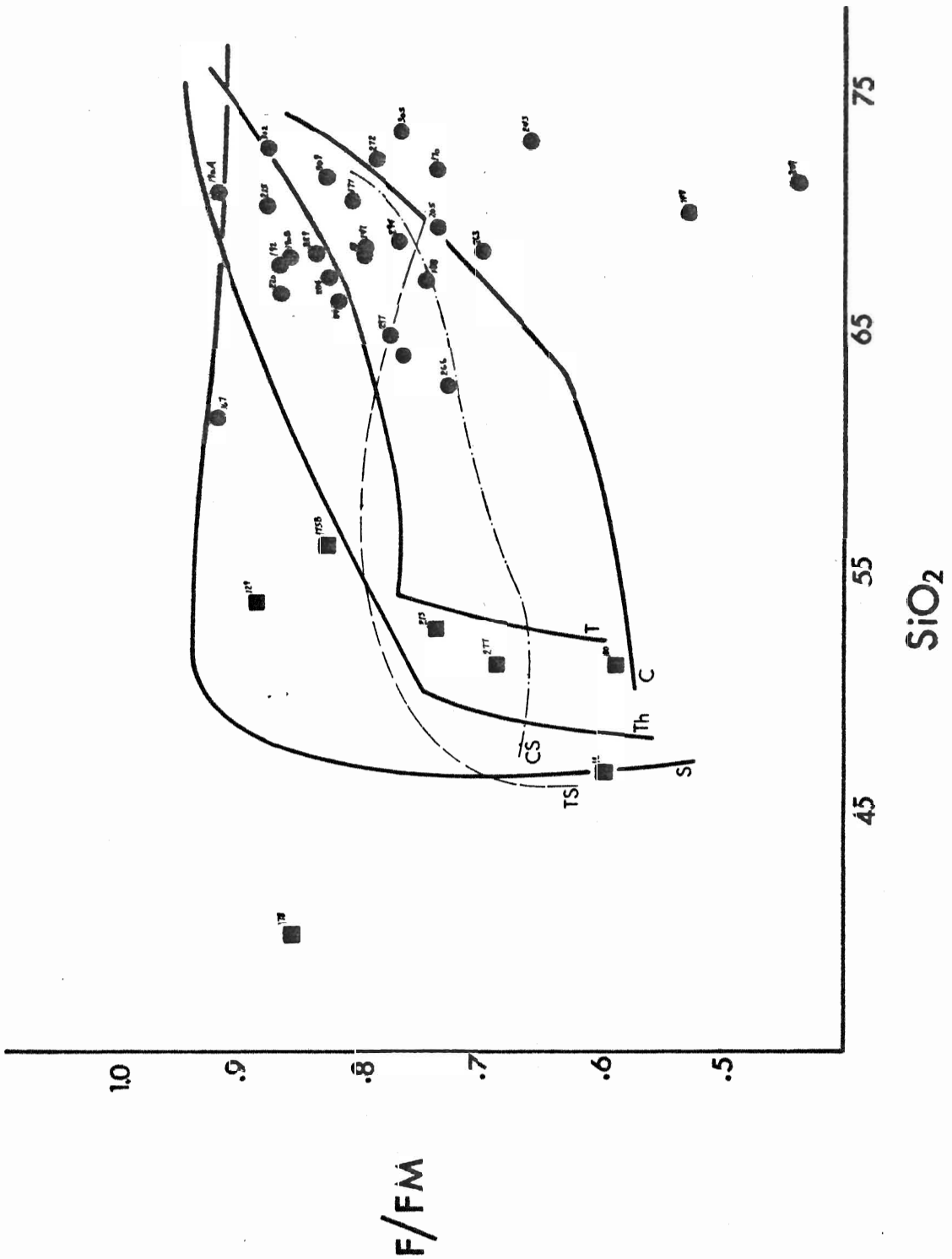

Figure 64. FEO(TOTAL)/FEO(TOTAL) + MGO - SIO2 DIAGRAM. 1964) or Skaergaard suites (Carmichael 1964). The accumulative, sample 178, peaks near the magnetite saturation level of the Skaergaard intrusion. The data

shows only a poor correlation with the tholeiitic suite of Jolly (1980).

The intermediate to felsic Berry Creek samples are scattered in the calc-alkaline trends of Talasea, Cascades and the Abitibi calc-alkaline suite (Lowder and Carmichael 1970; Jakes and Gill 1970; Jakes and White 1972; Jolly 1980). The trend of the Lake of the Woods mafic metavolcanics resembles the low fO2, shallow magma chambers of the Abitibi belt and Skaergaard intrusion. The low fO2 can be maintained by leakage from the magma chamber, again similar to the Skaergaard. The low FeO (total) from sample 180, a mafic pyroclastic unit, may have resulted from magnetite separation (high pH2O) in a shallow subaqueous vent zone. The anomalously low FeO (total)/ FeO (total) + MgO ratios are due to low ferromagnesian contents in pumiceous clasts (samples 170, 149, 243, 263). Sample 209, from a rhyolitic unit overlying mafic sediments, contains layers of ferromagnesians adjacent to the quartzofeldspathic layers. The proportion of layers are variable and are reflected in the anomalous chemistry.

The Al2O3 - FeO (total)/FeO (total) + MgO diagram was used by Naldrett and Arndt (1975) to classify komatiites and tholeiites. The field overlap between komatiites, basaltic komatiites and iron tholeiites was recognized by Arndt et al. (1977) and Green and Schulz (1977, their Figure 7). The overlapping data of the Sioux Narrows-Lake of the Woods mafic metavolcanics (Figure 65) are clearly

indifferent to the strongly tholeiitic trends of the Jensen diagram (Figure 57). Green and Schulz (1977) display the field of Fe-tholeiites from the Abitibi belt. The compositions are similar although the slightly lower Al2O3 values of the Munro Fe-tholeiites are evident. Arndt et al. (1977; their Figure 28) exhibits assorted basalts, komatiites, tholeiites and transitional compositions in an Al2O3 - FeO/FeO + MgO diagram.

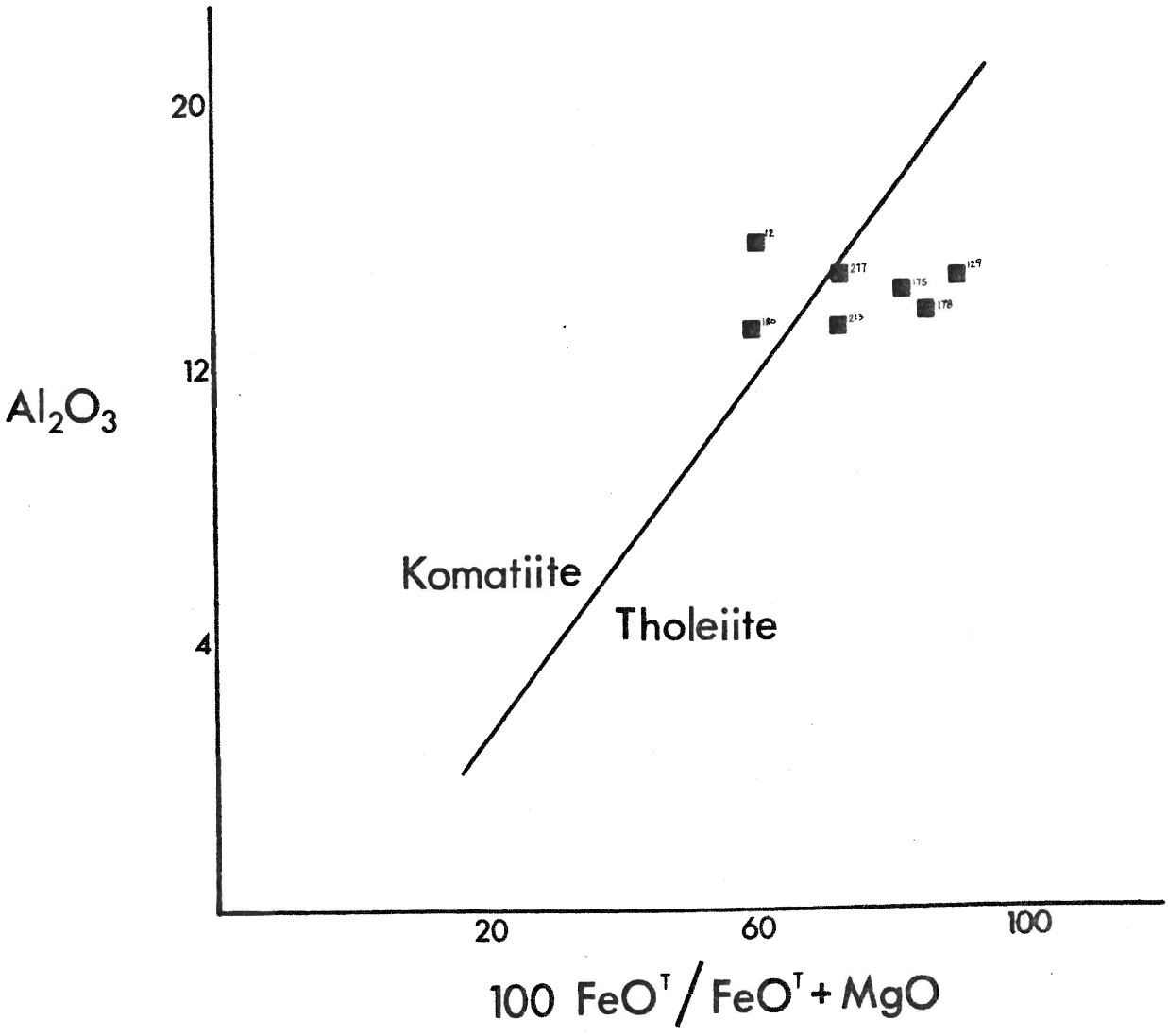

Figure 65. AL2O3 - FEO(TOTAL)/FEO(TOTAL) + MGO DIAGRAM.

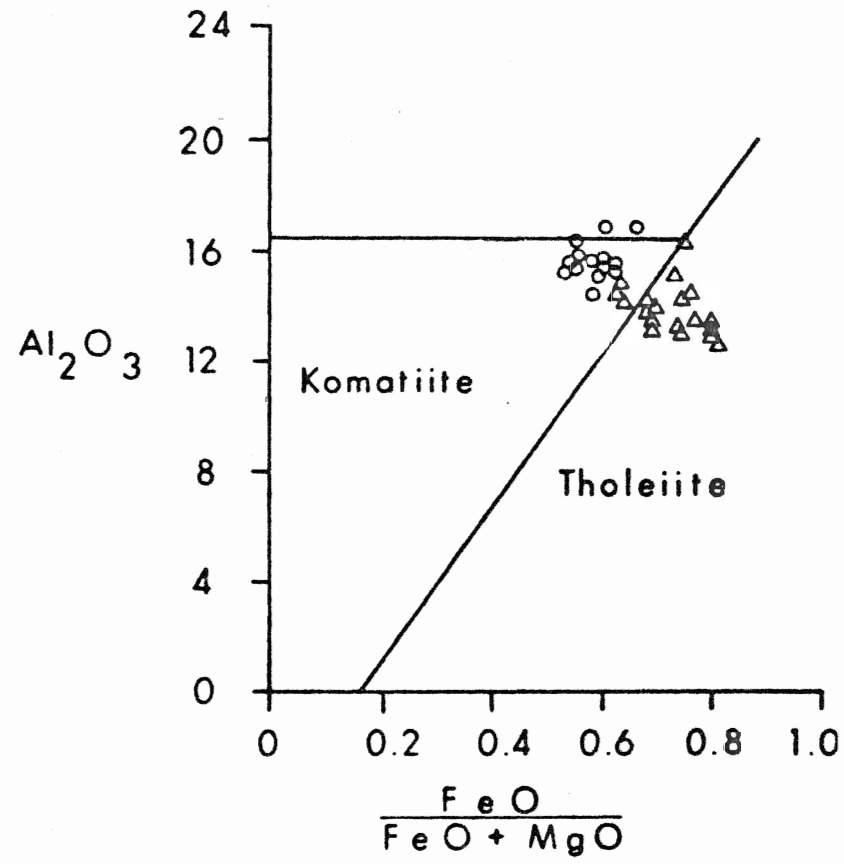

Figure 66. AL203 - FEO(TOTAL)/FEO(TOTAL) + MGO DIAGRAM. (adapted from Wilson and Morrice 1977)

The Lower and Middle Mafic Groups from the Kakagi Lake -Katamiagamak area are compared in Figure 66 (modified from Wilson and Morrice 1977). The similarities with the Sioux Narrows-Lake of the Woods samples are evident. The Lower Mafic Group is komatiitic while the Middle Mafic Group samples are tholeiitic with minor field overlap. The strong FeO (total) enrichment and lower Al203 contributes to the komatiitic field overlap by the Lake of the Woods mafic metavolcanics. It is possible that sample 180 was clinopyroxene phyric. The presence of clinopyroxene can shift compositon towards the komatiitic field (Barley 1981; Green and Schulz 1977).

The low TiO2 content of the Lake of the Woods - Sioux Narrows mafic metavolcanics is consistent with komatiitic affinities compared to the data on the TiO2 - SiO2 diagrams of Arndt et al. (1977, their Figure 25). TiO2 contents from this study transect the compositional gap displayed by Arndt et al. (1977). Tholeiitic TiO2 values should exceed that of a komatiite at a given SiO2, MgO. However, the low CaO/Al2O3 are not consistent with the high ratios of komatiites (generally greater than 0.6). Intrusive phases from the Berry Creek area (gabbros, amphibolites) have Cao/Al2O3 ratios ranging from 0.66 - 0.74.

The moderately high MgO/FeO (total) + MgO with relatively high Al2O3 contents are also comparable to magnesian tholeiites or basaltic komatiites. Using the criteria of Brooks and Hart (1974), Hallberg and Williams (1972), and Green and Schulz (1977), the intrusive rocks fall into the field of high Mg tholeiites and basaltic komatiites (see Table 11).

The high Al2O3 content of the subvolcanic gabbro suggests accumulation of plagioclase feldspar in the gabbroic zones with fractionation of olivine in serpentinized dunite zones.

Trace Elements

The immobile element diagrams are characterized by two distinct groupings due to the absence of andesitic rocks (SiO2, 56-62 %). The Zr-SiO2 diagram (Figure 67) shows the positive relationship between these variables. Zirconium

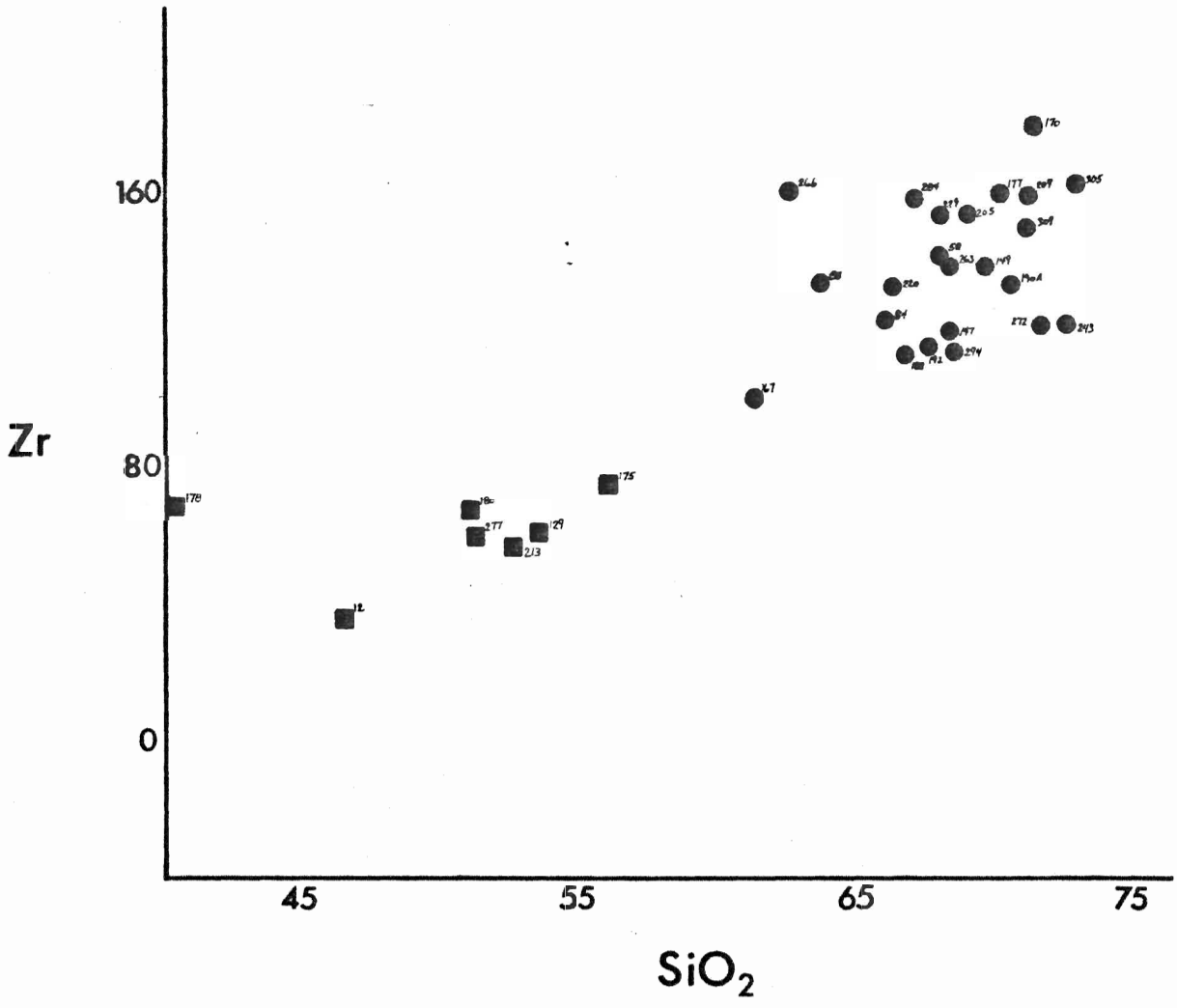

Figure 67. ZR - SIO2 DIAGRAM.

generally defines a fractionation index and behaves as an incompatible element from ultramafic to dacitic compositions. Diagrams using Zr, particularly Zr-SiO2, TiO2-Zr, Y-Zr, outline this pattern.

The mafic metavolcanics are low in zirconium (36-75 ppm) compared to the volcanics of similar major element compositions (Clarke 1970; Barley 1980, 1981; Trowell et al. 1980; MacLean et al. 1982) although lower Zr contents have been reported (Pearce and Norry 1979; Figure 6a, 6b). Sample 12, a plagioclase phyric basalt, from the Lower

Mafic - Middle Mafic transition zone, contains the lowest Zr content (36 ppm).

The intermediate to felsic compositions range from 99-178 ppm zirconium which are comparable to trace element data of Pearce and Norry (1979), Thurston (1982), and Trowell et al. (1980, Table 5.1). The high Zr meta-volcanics display abundant data scatter. Sample 167 is Zr depleted, consistent with SiO2 depletion and FeO (total) plus Al2O3 enrichment by metasomatism. Zr/TiO2 - SiO2 diagrams (Figure 68, modified from Mortensen 1982) display

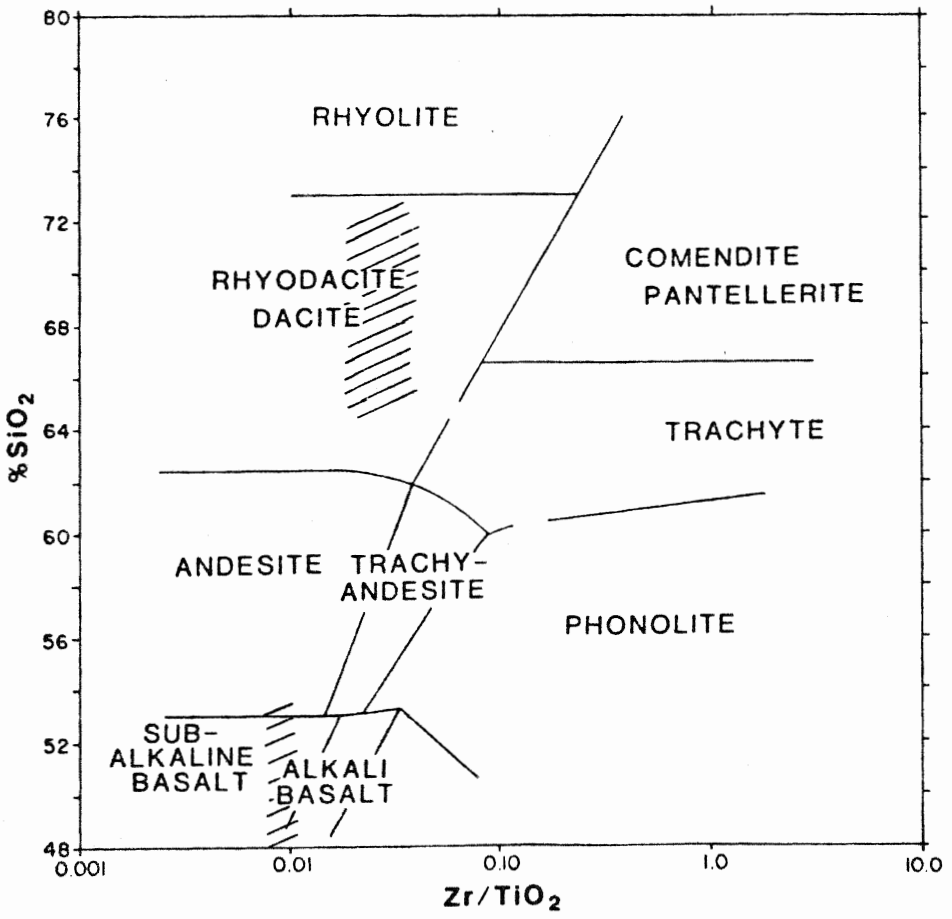

Figure 68. SIO2 - ZR/TIO2 DIAGRAM
(adapted from Mortensen 1982).

the fields of volcanic compositions. The Berry Creek metavolcanics, with Zr/TiO2 ratios of 0.03 - 0.05, fall into the rhyolite and rhyodacitic fields.

An yttrium - silica diagram of the Lake of the Woods metavolcanics displays tholeiitic trends for the mafic metavolcanics and a calc-alkaline depletion trend of the intermediate to felsic metavolcanics (compare Table 10 with Giles 1981, his Figure 2). Trends shown by Giles (1981) and Lambert et al. (1974) are comparable to the Berry Creek data. The low yttrium Mt. Ararat trend of Lambert et al. (1974) is slightly depleted but parallels the probable trend of this project. The yttrium values are comparable to those of quartz plagioclase porphyries and rhyodacites of the Kelly Greenstone Belt. Barley (1980) reported yttrium values ranging from 16-22 ppm yttrium. Zirconium contents are slightly lower than the Kelly rhyodacites (Barley 1980).

Trends of Y-Zr diagrams (Figure 69) commonly show positive slopes from basic to intermediate, less commonly to felsic members (Pearce and Norry 1979; Nesbitt and Sun 1976). The vector diagrams (Figure 70) of Pearce and Norry (1979) display the incompatible behaviour of yttrium and zirconium during the early stages of fractionation from ultramafic compositions.

Figure 69 displays two groups enriched in zirconium, or depleted in yttrium, relative to the chondrite curve (Nesbitt and Sun 1976). The composition of the mafic

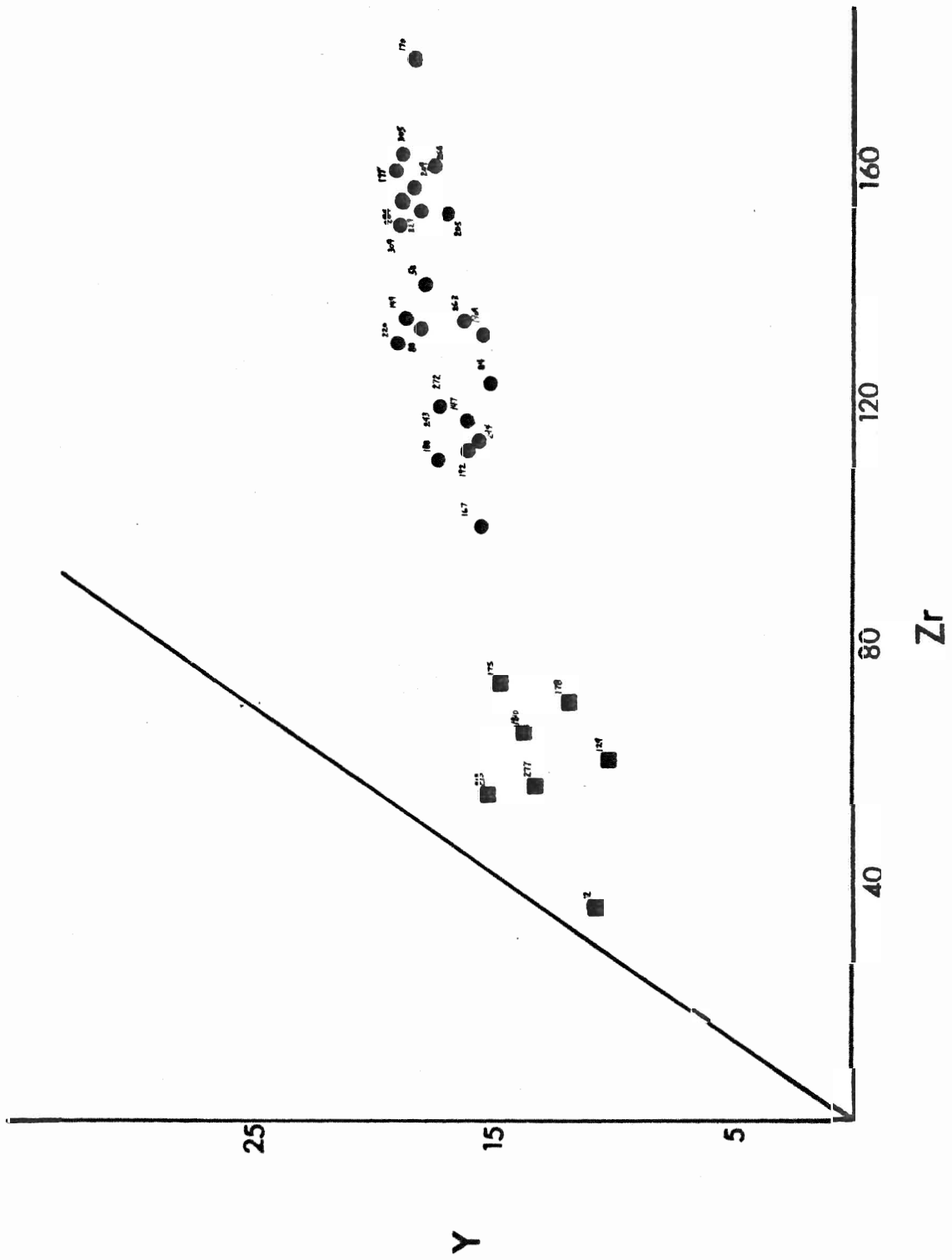

Figure 69. YTTRIUM - ZIRCONIUM DIAGRAM.

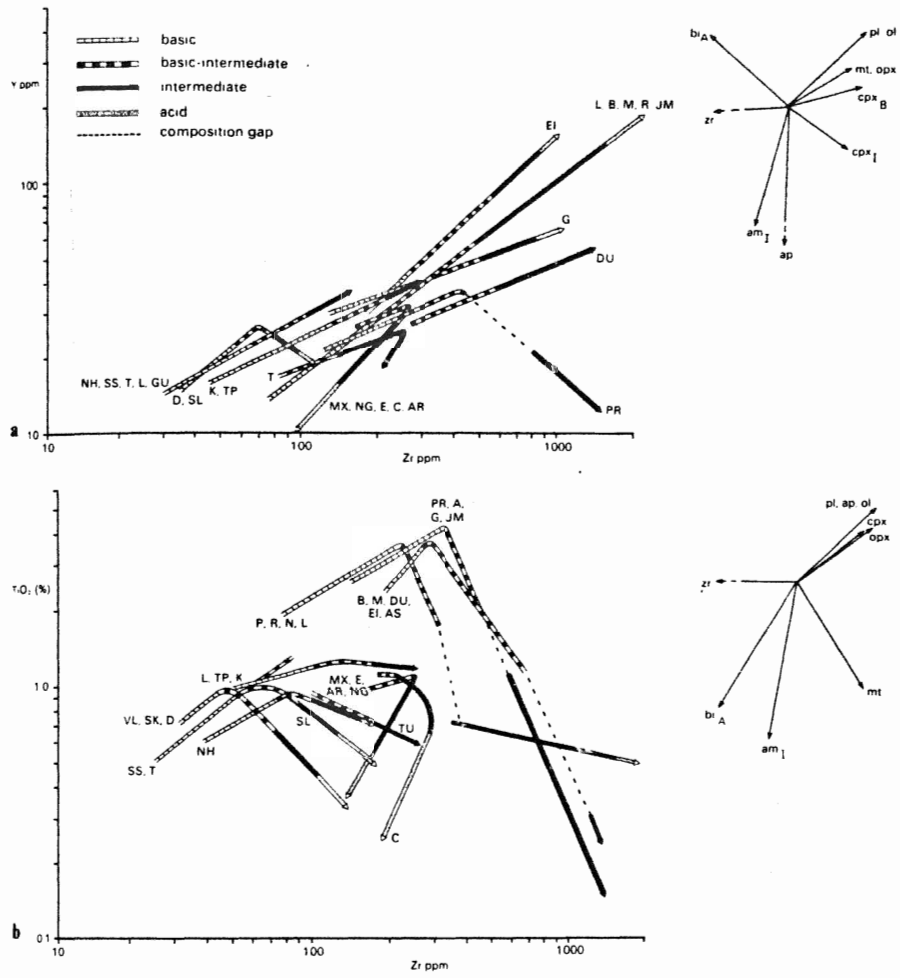

Figure 7Ø. PARTITION VECTOR DIAGRAMS (Pearce and Norry 1979).

metavolcanics is possibly explained by minor residual phase accumulation; with continuous zirconium enrichment. The tholeiitic chemistry of other data (Nesbitt and Sun 1976; Pearce and Norry 1979) is commonly characterized by lower Zr/Y ratios in the low MgO tholeiites. Giles' (1981) review of tholeiitic basalts (see Giles 1981; his Figure 2) also reports chondritic compositions with similar Zr contents.

Komatiitic to iron tholeiitic basalts of Barley (1981) display Y-Zr data similar to the mafic metavolcanics from

Lake of the Woods. The Lake of the Woods samples are usually lower in yttrium and zirconium at a given MgO content. MacLean et al. (1982) reported values of 14-32 ppm yttrium and 32-82 ppm zirconium for a suite of amphibolites and basalts. Low Y-Zr correlations with the Lake of the Woods mafic metavolcanics are probable. Yttrium and zirconium data from MacArthur Township (Tabatabai 1979) range from 11.0 ppm yttrium and 60.8 ppm zirconium and are comparable to Lake of the Woods tholeiites although lower than most other reported tholeiite data. Iron-rich basalts from the Uchi-Confederation belt (Thurston and Fryer 1983) have Y-Zr compositions similar to the Lake of the Woods mafic metavolcanics (14-17 ppm yttrium, 28-50 ppm zirconium). The former are high alumina basalts (17-18 wt % Al2O3) compared to the low alumina Lake of the Woods tholeiites. Nesbitt and Sun (1976) compared komatiitic and tholeiitic compositions and concluded that yttrium and zirconium behave as incompatibles. Yttrium depletion in residual phases is generally restricted to low MgO tholeiites (Fe-tholeiites).

The Pearce and Norry (1979) vector diagrams (Figure 70) display the late fractionation of yttrium and zirconium by amphibole, apatite, zircon and biotite in intermediate liquids. Nesbitt and Sun (1976) also noted the yttrium partitioning into augite. The yttrium trends vary slightly with pH2O due to the increased fractionation by amphibole and possibly pyroxene under high pH2O conditions (Giles

1981) at lower load pressures. Large degrees of plagioclase fractionation, common at low pH2O suggest that clinopyroxene and/or amphibole fractionation were limited (Cawthorn and O'Hara 1976). Therefore, the low yttrium (10-15 ppm) of the Lake of the Woods mafic volcanics may be attributed to a low yttrium-zirconium source.

The calc-alkaline suite of this study is comparable to the Tongan evolved suite (Pearce and Norry 1979; see Figure 7C) and the Archean Warrawoona Group (Barley 1981; his Figure 4).

The Berry Creek calc-alkaline metavolcanics fall in a field which includes fractionation trends with dacitic and rhyolitic compositions from several suites including Tonga, New Mexico, Ecuador, Ararat and Chile (Figure 7D) (Pearce and Norry 1979).

The data of Barley (1981) displays consistent yttrium values (20-25 ppm) comparable to the 16-21 ppm range of the Berry Creek samples. Zr content of the latter does not define a trend based on yttrium or silica contents. Condie (1981) noted that yttrium behaves similarly to the HREE. Rare earth element patterns can be correlated with Zr/Y ratios to discuss petrogenetic trends. The Lake of the Woods - Berry Creek rhyodacites were compared with Cycle 2 rhyodacites from Thurston (1982) and Thurston and Fryer (1983). The latter ranged from 10-18 ppm yttrium, 112-139 ppm Zr and 140-170 ppm Sr. Major and trace element correlations were related to REE patterns. The latter are

usually moderately to strongly fractionated with high Ce/Yb ratios. The REE data of Thurston and Fryer (1983) are comparable to the undepleted HREE of the Marda Complex (Taylor and Hallberg 1977) and Yellowknife (Condie and Baragar 1974).

Zr/Y ratios of the Berry Creek metavolcanics (6.4-9.6) compare favourably with the low Zr/Y ratios (8-10) of the undepleted HREE patterns. The Berry Creek metavolcanics are less enriched in Zr relative to the strongly depleted HREE patterns (Zr/Y, 13-15) of Arth and Hanson (1975), Condie and Harrison (1976) and Thurston and Fryer (1983). It could be noted that both types of patterns have been observed in a single volcanic belt (Glikson 1976; Fryer and Jenner 1978; Thurston 1980; Thurston and Fryer 1983).

The Lake of the Woods mafic metavolcanics have Zr/Y ratios ranging from 3.3 to 6.0 (increases with fractionation). These ratios are slightly enriched relative to C3 chondrite (Pearce and Norry 1979) and are comparable to the Hawaiian Zr/Y ratios. The Lake of the Woods data are significantly lower in both Y and Zr relative to the Hawaiian compositions. Intrusive phases of the Lake of the Woods metavolcanics have Zr/Y ratios from 2.8-3.6 which are very slightly enriched relative to C3 chondrite (Zr/Y, 2.5). MORBs have ratios near 2.9 and the Lawless low MgO tholeiites have low ratios of 2.8 (Nesbitt and Sun 1976).

The Y-TiO2 diagram (Figure 71) displays two distinctly different groups relative to the chondrite curve. The

mafic metavolcanics are characterized by FeO (total) and TiO2 enrichment (arrows designate general trends), and a low yttrium source relative to chondrite. Yttrium displays a slight increase during fractionation (Figure 71) relative to the source region. Slight decreases of yttrium in samples 277 and 178 may result from minor amphibole fractionation near the magnetite saturation surface. The trend is strongly divergent to reports by Giles (1981). Nesbitt and Sun (1976) reported similar, though to a lesser

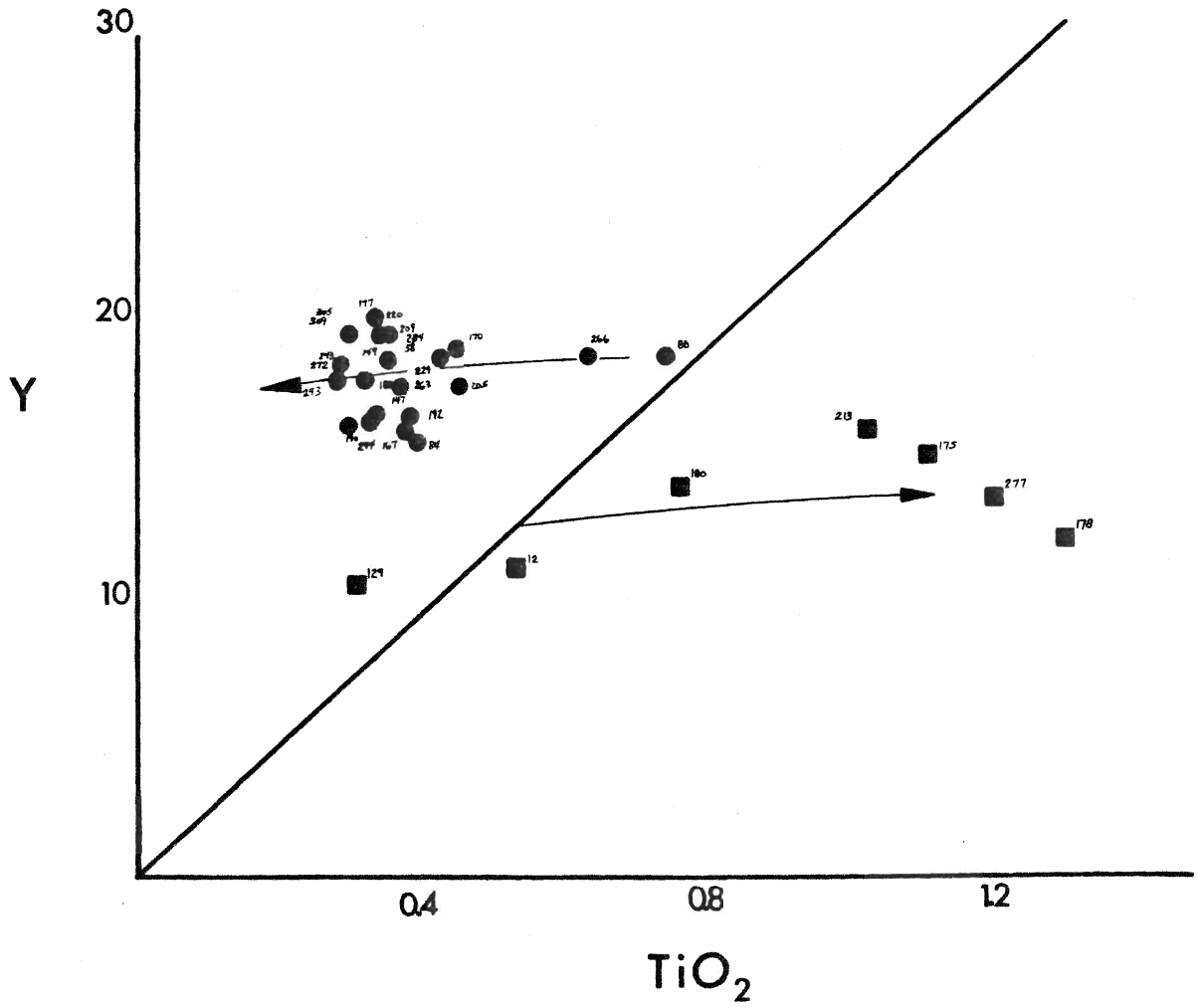

Figure 71. YTTRIUM - TIO2 DIAGRAM.

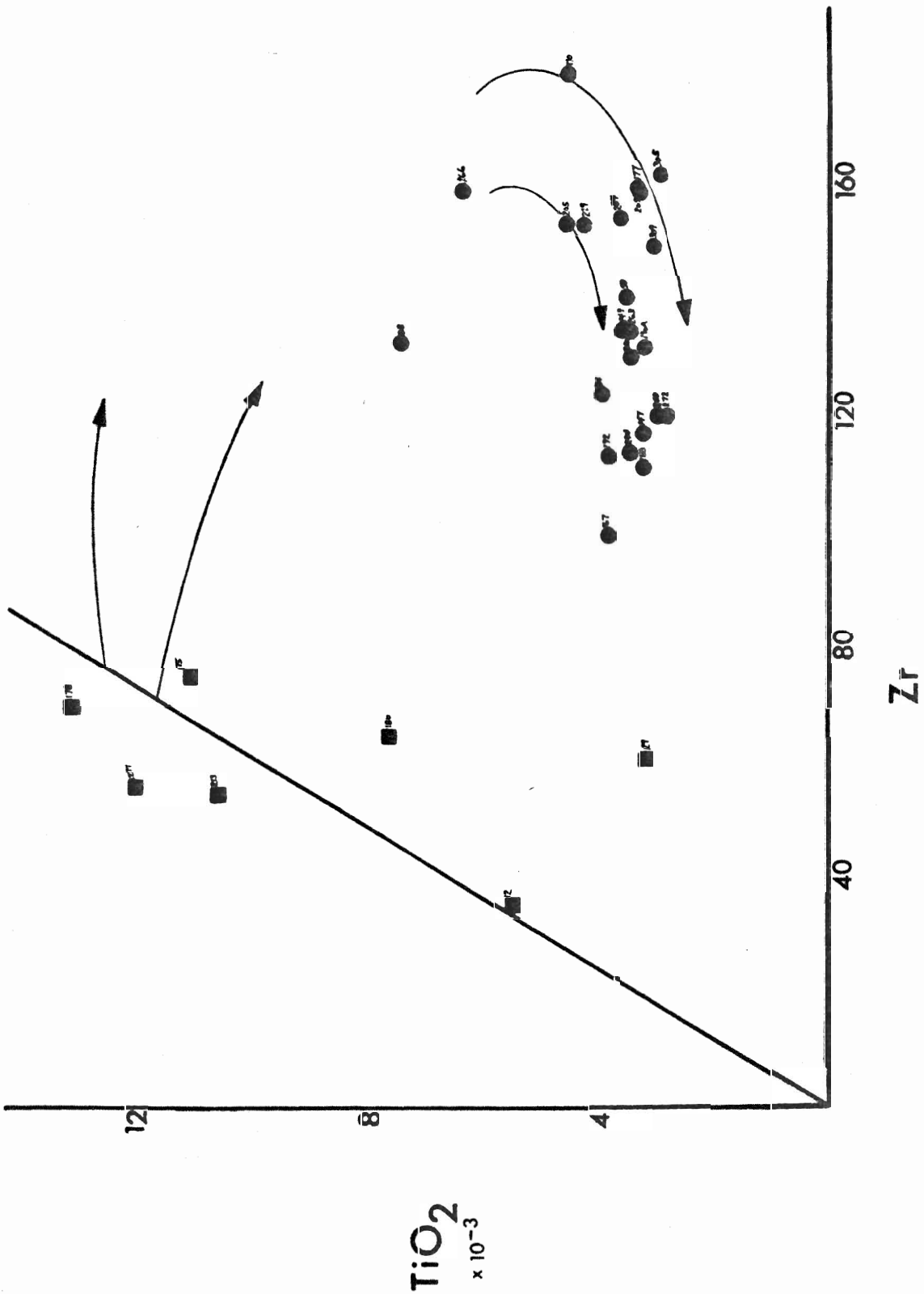

Figure 72. TIO2 - ZIRCONIUM DIAGRAM.

degree, yttrium depleted low MgO tholeiites from the Lawlers-Mt. White series. The depleted low MgO tholeiites of Nesbitt and Sun (1976) contain substantially higher Y, Ti and Zr relative to the Lake of the Woods mafic metavolcanics. As previously noted, divergence from the chondritic trend is common within low MgO tholeiites.

The Sioux Narrows-Lake of the Woods mafic metavolcanics are lower in TiO2 and yttrium and plot in the field of yttrium depleted high MgO tholeiites (compare Figure 71 with Nesbitt and Sun 1976; their Figure 3b). The calc-alkaline suites of the Berry Creek metavolcanics and the Warrawoona Group (Barley 1981) display non-chondritic fractionation trends following a TiO2 depletion with relatively consistent yttrium content. The lack of low SiO2 intermediate members (andesite compositional gap) is evident in the calc-alkalic suite. Behaviour of the Y-TiO2 trends during a complete fractionation series should compare favourably with Ti-Zr fractionation paths of Pearce and Norry (1979).

The TiO2-Zr diagram (Figure 72) displays near chondritic TiO2/Zr ratios for the mafic metavolcanics, while strongly fractionated Ti-poor data are reported of the Berry Creek metavolcanics. Scatter of the mafic metavolcanic analyses probably reflects the precision of the Zr analyses (see Appendix 1). The enrichment rates of TiO2 and Zr during tholeiitic evolution parallel the chondritic TiO2/Zr ratio. The data compares favourably

with basalts and basaltic andesites reported by Nesbitt and Sun (1976) and Pearce and Norry (1979; see Figure 70; their Figure 6b). Ewart and Taylor (1969) noted that the low TiO2 and low Zr compositions (40-50 ppm) were probably produced by a primitive source.

The calc-alkaline Berry Creek metavolcanics plot at or near the zircon inflection point of the calc-alkaline fractionation trend (Pearce and Norry 1979; Wood 1978). Sample 266, the low SiO2 dacite, and sample 177, are relatively high in zirconium and may reflect maximum Zr enrichment as shown by the trends of arrows in Figure 72. The lower Zr content of high SiO2 dacites and rhyolites are consistent with this fractionation trend. Examples of Ti-Zr trends from rhyodacites of Mexico, Ararat, and Ecuador are comparable to data from the Berry Creek Metavolcanics (Pearce and Norry 1979).

The large compositional gap precludes a fractionation series between the two suites. Although compositional gaps are common, the complete absence of high SiO2 basaltic andesites and andesites is inconsistent with fractionation (Hallberg 1980; Ayres 1969).

The small range of Sr data shown by the mafic metavolcanics in the Y-Sr diagram (Figure 73) suggests that the Sr mobility was relatively low. The data are comparable, although slightly lower, to data discussed by MacLean et al. (1982) and Giles (1981). The intermediate to felsic metavolcanics show wide Sr variation, which may reflect Sr mobility in the tuffaceous deposits. Two

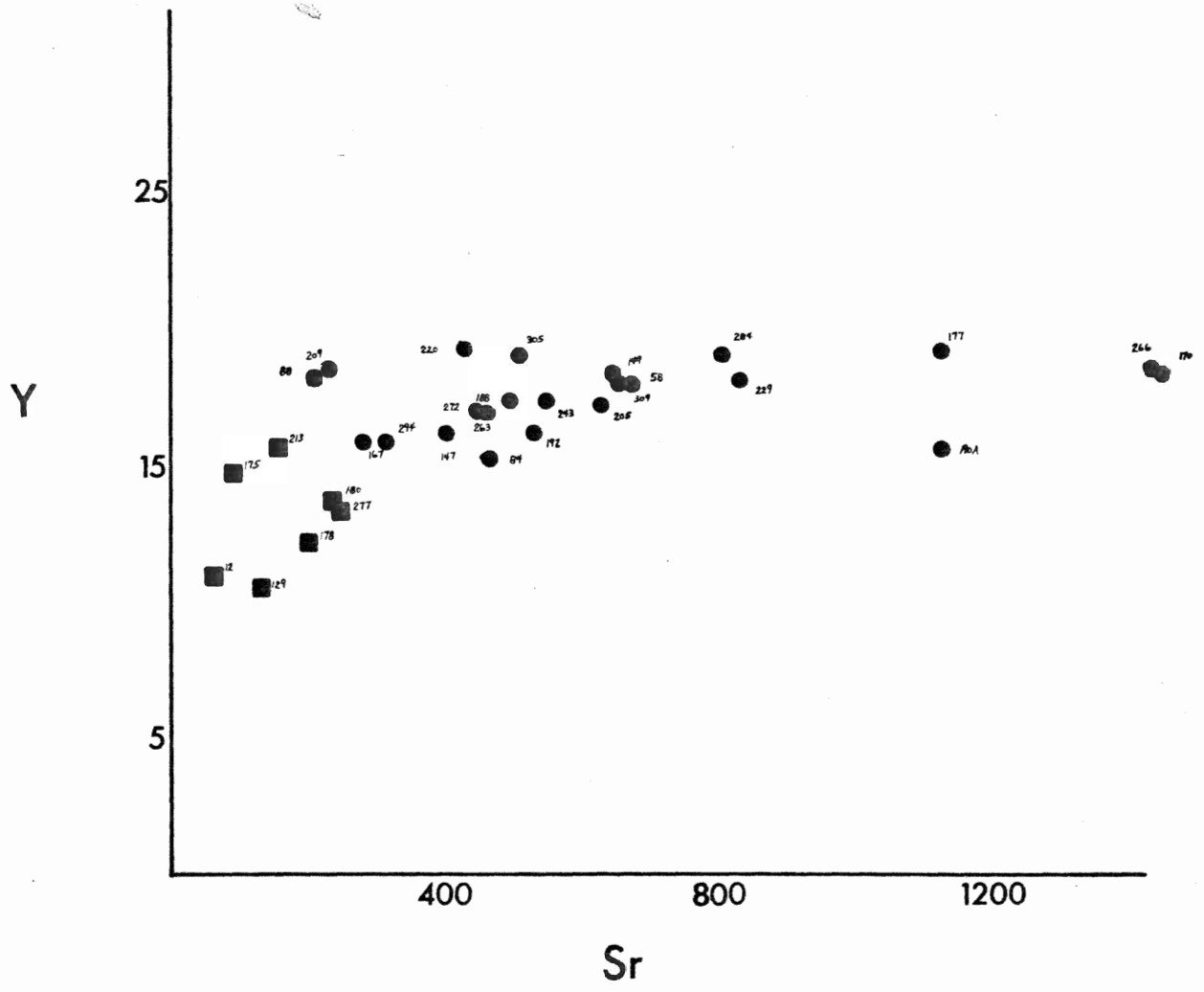

Figure 73. YTTRIUM - STRONTIUM DIAGRAM.

compositional groupings, one with high Sr, high Y, another with low Sr, low Y both display the bimodal trends shown in previous diagrams.

On the Zr - TiO2 - Ni diagram (Figure 74), the mafic metavolcanics fall into the field of komatiites, low Ti tholeiites, and tholeiites. The trends of komatiites and tholeiites (see Tabatabai 1979) define zones of olivine fractionation and Fe-Ti enrichment, respectively. The data suggest that the low TiO2 enrichment factor characterizes a transitional komatiite-tholeiite suite in the less evolved metavolcanics. The mafic metavolcanics along the 2a, 2b

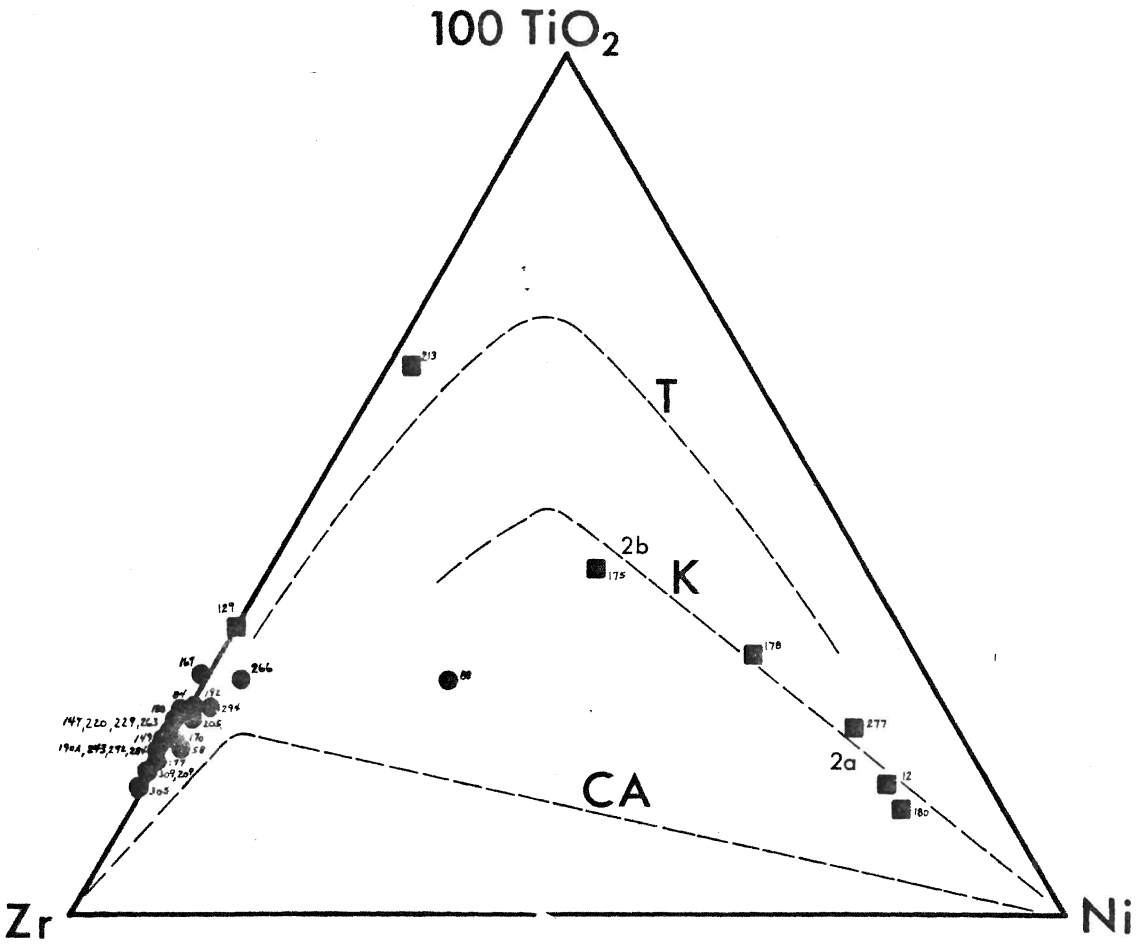

Figure 74. ZR - TIO2 - NI DIAGRAM.

trends compare with low TiO2 tholeiites discussed by Nesbitt and Sun (1976) and Hallberg, Carter and West (1976). High Ni tholeiitic basalts of Hallberg, Carter and West (1976) and basaltic komatiites of Nesbitt and Sun (1976) are similar to the transitional basalts of this study (samples 12, 180). Primitive komatiitic basalts of Clarke (1970) and oceanic tholeiites (high Ni) from Engel (1965) fall in the komatiitic high Ni trends. The data suggests that an overlapping field exists between komatiites, and the high Ni extension of the tholeiite field.

The intermediate to felsic metavolcanics occur near the junction of the tholeiitic and calc-alkaline trends (Figure 74). The low Ni-TiO2 data characterizes the evolved suites of Hallberg, Johnston and Bye (1976) although the latter are less evolved than the Berry Creek metavolcanics.

SYNTHESIS

Examination of major oxide and trace element diagrams confirm the field evidence that two distinct metavolcanic groups occur in the study area. A komatiitic to tholeiitic (low TiO2 tholeiites) affinity characterizes the ultramafic to mafic metavolcanics, whereas the evolved intermediate (high SiO2 dacites) and felsic metavolcanics display calc-alkaline to transitional tholeiitic patterns.

The data interpretations are clearly consistent with previous geochemical studies within the Sioux Narrows-Kakagi Lake greenstone belt. The Kakagi Lake calc-alkaline to tholeiitic metavolcanics form a fractionation series developed upon the subjacent Snake Bay and Katimiagamak mafic metavolcanics (Davis and Edwards 1982; Blackburn et al. 1982). The mafic suite displays a progression from magnesian to iron tholeiites with associated synvolcanic sills ranging from gabbro to peridotite.

Zircon U-Pb ages (Davis and Edwards 1982) have confirmed the contemporaneity of the Kakagi mafic sills and the intermediate to felsic Kakagi metavolcanics. The Stephen Lake metavolcanics and subvolcanic porphyries of

the Cedartree Lake Formation overlie the Kakagi Lake Group. Zircon U-Pb ages suggest contemporaneous development of the Stephen Lake metavolcanics and the Berry Creek Complex.

Giles (1981) and Barley (1980, 1981) have noted the importance of recognition between cyclicity and contemporaneity. Jolly (1975) noted that numerous vents and magma chambers may occur simultaneously. Tholeiitic and calc-alkaline assemblages can occur as laterally overlapping, contemporaneous suites, rather than a cyclic magma evolution pattern. Hallberg (1978) noted that apparent unconformities may be due to restricted, lateral extent of the calc-alkaline volcanic centres.

The northern domain, north of the Pipestone - Cameron Fault, exhibits a distinct geochemical discontinuity between the Berry Creek metavolcanics subjacent mafic metavolcanics (Kenu Lake, Adams River Bay, Black River). The absence of an andesitic to rhyolitic fractionation series equivalent to the Kakagi Lake Group characterizes the differences between the northern and southern domains of the greenstone belt. The lack of continuity (temporal and geochemical) between these two suites cannot be reconciled with a common origin as a fractionation series.

Silica histograms of the Berry Creek metavolcanics and the associated mafic metavolcanics reveal a gap between 55 and 64% SiO2. The andesite gap has been attributed to numerous physical and chemical mechanisms (Anhaeusser 1971; Thurston and Fryer 1983; Barker and Peterman 1974; Arth and Hanson 1975; Weaver 1977; Hawkesworth and O'Nions 1977;

Giles 1981; Hallberg 1972, 1980). Bimodal dacite-tholeiitic basalt suites commonly display an andesite gap (Barker and Peterman 1974; Wood 1978; Arth and Hanson 1975). The significance of the gap or discontinuity is directly related to the span of the compositional differences between the two suites (Smith 1980). Compositional gaps between mafic and intermediate to felsic (rhyodacitic) metavolcanics are common within the African and Australian Archean provinces (Condie and Harrison 1976; Hawkesworth and O'Nions 1977; Hallberg 1972, 1976, 1980; Arth and Hanson 1975; Taylor and Hallberg 1972; Anhaeusser 1971). Discontinuities between tholeiitic to calc-alkaline suites have been documented in the Abitibi belt of the Superior Province (Smith 1980; Goodwin and Smith 1980). Hallberg (1978) reported a continuum based on SiO2 histograms but Taylor and Hallberg (1977) suggested a crustal origin of the calc-alkaline suite based on REE data.

The absence of andesite may provide a field indicator of mantle versus crustal derivation, e.g., Norseman-Wiluna belt (Hallberg 1980). Thurston and Fryer (1983) suggest that magma mixing of tholeiitic basalts and crustal derived or mantle fractionated rhyolite may produce andesites, thereby producing an apparent continuum of compositions. Anhaeusser (1971) and Thurston and Fryer (1983) have suggested that the compositional gaps may occur due to temporary sealing of the volcanic vent during

continuous fractional evolution of the magma chamber. Similar mechanisms (Weaver 1977; Wood 1978; and others) suggest that the appearance of andesites is limited to a short crystallization interval that may be passed, without eruption, during quiescent fractionation of the magma chamber. However, zircon U-Pb ages of the Berry Creek metavolcanics (and Stephen Lake metavolcanics), are 13.7 +- 3.5 Ma younger than the Kakagi Sills and the Kakagi Lake Group. The significant age difference between the two suites suggests that the Berry Creek and Stephen Lake metavolcanics are not derived from quiescent fractionation of the mafic magma which produced the subjacent mafic metavolcanics.

The komatiitic (low Ti tholeiite) to tholeiitic association is characterized by strong iron enrichment, minor TiO2 enrichment, moderate to high Ni, low SiO2, Y, Zr, Sr and alkalis (Arndt et al. 1977). MgO depletion of the iron tholeiitic lava flows and tuff is exhibited by extensive cumulate olivine, now altered to serpentine, talc and forsterite, within subvolcanic sill complexes (Arndt et al. 1977). The low alumina, aphyric to strongly plagioclase phyric mafic flows are here attributed to a shallow, subvolcanic, low to increasing fO2 fractionation trend. A phenocryst assemblage probably consisted of magnesian olivine, plagioclase, possibly clinopyroxene (augite) and minor amphibole (Barley 1981; Pearce and Norry 1979; Jolly 1975). Magnetite and amphibole are late stage fractionation phases. The trends shown by relatively

continuous fractional evolution of the magma chamber. Similar mechanisms (Weaver 1977; Wood 1978; and others) suggest that the appearance of andesites is limited to a short crystallization interval that may be passed, without eruption, during quiescent fractionation of the magma chamber. However, zircon U-Pb ages of the Berry Creek metavolcanics (and Stephen Lake metavolcanics), are 13.7 +- 3.5 Ma younger than the Kakagi Sills and the Kakagi Lake Group. The significant age difference between the two suites suggests that the Berry Creek and Stephen Lake metavolcanics are not derived from quiescent fractionation of the mafic magma which produced the subjacent mafic metavolcanics.

The komatiitic (low Ti tholeiite) to tholeiitic association is characterized by strong iron enrichment, minor TiO2 enrichment, moderate to high Ni, low SiO2, Y, Zr, Sr and alkalis (Arndt et al. 1977). MgO depletion of the iron tholeiitic lava flows and tuff is exhibited by extensive cumulate olivine, now altered to serpentine, talc and forsterite, within subvolcanic sill complexes (Arndt et al. 1977). The low alumina, aphyric to strongly plagioclase phyric mafic flows are here attributed to a shallow, subvolcanic, low to increasing fO2 fractionation trend. A phenocryst assemblage probably consisted of magnesian olivine, plagioclase, possibly clinopyroxene (augite) and minor amphibole (Barley 1981; Pearce and Norry 1979; Jolly 1975). Magnetite and amphibole are late stage fractionation phases. The trends shown by relatively

immobile trace elements suggest an association with primitive magnesian tholeiites and komatiites (Nesbitt and Sun 1976; Pearce and Norry 1979; Giles 1981). Low yttrium, zirconium, strontium and titanium are characteristic of a depleted mantle source involving high degrees of partial melting (Clarke 1970; Floyd and Winchester 1975; Pearce and Norry 1979; Condie 1976; MacLean et al. 1982; Nesbitt and Sun 1976). Early fractionation of olivine, amphibole and/or clinopyroxene may explain the trends of the trace element compositions (Pearce and Norry 1979; Nesbitt and Sun 1976). The observed trace element data, e.g., Zr/Y ratios, indicate a composition slightly enriched relative to chondrites (Pearce and Norry 1979).

The trends of the mafic to ultramafic metavolcanics and subvolcanic sills of the Sioux Narrows greenstone belt, are comparable to komatiite-tholeiite associations described by Barley (1981); MacLean et al. (1982); Nesbitt and Sun (1976); Hallberg, Carter, and West (1976); Naldrett and Turner (1977); Jolly (1975, 1977); Viljoen and Viljoen (1969); Goodwin (1968); Hallberg (1972); Gelinas and Brooks (1974); Pearce and Birkett (1974); Green and Schulz (1977); Clarke (1970); and Hallberg and Williams (1972).

The calc-alkaline Berry Creek metavolcanics are characterized by moderate to high Al2O3, SiO2, Sr and alkalies, low Zr, Y, Ni, FeO (total), MgO and TiO2. The absence of andesite and low SiO2 dacite, coupled with the trace element patterns, suggest that the intermediate to

felsic suite was derived from a source independent of the underlying mafic metavolcanics. The implications of bimodal volcanism has been discussed by many authors, e.g., Ayres 1969, 1983; Barker and Peterman 1974; Thurston and Fryer 1983; Hallberg 1980.

Trace element compositions are comparable to depleted silicic metavolcanics (Condie 1976, 1981) which are characterized by low Y, Zr, Zr/Y, and TiO2. Fractionation models for yttrium and zirconium indicate that enrichment factors of 5-7 times are commonly generated in low liquid proportions of dacitic to rhyolitic composition (Wood 1978). In the Berry Creek metavolcanics, zirconium maintains an enrichment factor of 2-4 and yttrium also increases, the degrees of enrichment are generally not applicable to the fractionation model. Yttrium fractionation by amphiboles may be a factor producing the low yttrium contents (Brooks et al. 1982).

Davis and Edwards (1982) suggest that the relatively young Stephen Lake and Berry Creek metavolcanics were extruded during crustal remobilization involving granitoid diapirism and gneiss domes. Wilson and Morrice (1977) suggested that the Upper Diverse Metavolcanic Group was contemporaneous with granitic diapirism. The generation of calc-alkaline metavolcanic suites by crustal anatexis has also been suggested by Hallberg (1976, 1978, 1980) and Taylor and Hallberg (1977) for the Australian Marda Complex; Edwards (1982) for the Phinney-Dash Lakes complex;

Barker and Peterman (1974); Gelinas et al. 1977; and Smith (1980).

Low Zr/Y ratios and undepleted HREE, comparable to the Berry Creek metavolcanics are found in the Marda Complex (Taylor and Hallberg 1977), Yellowknife (Condie and Baragar 1974) and the Uchi-Confederation belt (Thurston 1980; Thurston and Fryer 1983). The low yttrium content of the calc-alkaline suite may reflect residual amphibole and/or clinopyroxene in the source region (Pearce and Norry 1979; Barley 1981; Arth and Hanson 1975; Wood 1978). Barker and Peterman (1974) have suggested the generation of dacitic liquids with a residuum of amphibole and other Si-poor phases. The liquidus phases quartz, alkali feldspar and plagioclase separate from the mafic residual assemblage. Low pressure fractionation of quartz, alkali feldspar, albitic plagioclase and minor biotite or amphibole produces a fractionation trend from low SiO2 to high SiO2 rhyodacites (Thurston and Fryer 1983 ; Barley 1981; Barker and Peterman 1974).

Various sources, based on partial melting models, have been discussed for the depleted siliceous metavolcanics. The calc-alkaline melts may have been derived by incremental partial melting (Sigvaldason 1974; Barker and Peterman 1974) of tonalite-trondhjemite, garnet amphibolite, amphibolite, gabbro or hydrous basalt (Barker and Peterman 1974; Wood 1978; Glikson 1976; Thurston and Fryer 1983; Smith 1980; Hawkesworth and O'Nions 1977; Hallberg 1978, 1980; and Taylor and Hallberg 1977). A

subduction or sagduction model (Smith 1980; Goodwin and Smith 1980; Barker and Peterman 1974; Condie and Harrison 1976) involving a more hydrous Archean crust (Barker and Peterman 1974) produces stable dacitic liquids. Andesitic liquids (liquidus phases plagioclase, clinopyroxene and amphibole) are unstable in the presence of moderate to high pH2O. Initial melts are dacitic liquids which eventually become tholeiitic liquids with deeper, more complete melting (Barker and Peterman 1974; Sigvaldason 1974) under different P,T conditions. A mechanism involving separation of felsic melts from rising granitoid diapirs (reactivation of sialic basement) has been suggested by Davis and Edwards (1982). Similar models of calc-alkaline felsic melts have been produced by Zeck (1970), Giles (1981), and Hallberg (1980). More detailed trace element and REE data are needed to further interpret the petrogenetic evolution of the calc-alkaline Berry Creek metavolcanics.

CONCLUSIONS

1) The Berry Creek Complex, an Archean metavolcanic and metasedimentary assemblage, forms much of the northern supracrustal domain of the Sioux Narrows greenstone belt.

2) The Berry Creek pyroclastic, epiclastic and autoclastic deposits represent an erosional cross section of a restricted intermediate to felsic volcanic centre built upon a lower mafic shield volcano.

3) Despite low to intermediate pressure amphibolite grade metamorphism, polyphase isoclinal folding and several stages of faulting, with local recrystallization, the focus of the project on detailed stratigraphic and textural studies has provided a framework for research on facies analysis. Several lithofacies have been recognized and are subdivided into proximal to distal members.

4) Paroxysmal Surtseyan, Plinian and Vulcanian eruptive columns produced substantial volumes of pyroclastic debris. The tuffaceous deposits consisted of lithic, intratelluric crystal, and vitriclastic components produced by hydroclastic, magmatic and/or phreatomagmatic eruptions.

5) Although the majority of the deposits are produced by subaerial eruptions, sedimentation is predominantly in a subaqueous environment forming a shallow littoral to deep water subaqueous fan accumulation.

6) Primary ash flow tuffs are transported from subaerial vents across a rapid vertical transition to the subaqueous fans. Preservation of vitriclasts precludes subaerial and/or subaqueous reworking. Extensive mobility in the subaqueous environment is aided by steep slopes, low ablation rates, moderate flow density, high velocity, absence of littoral facies, and mixing with the fluid medium.

7) The primary pyroclastic and secondary autoclastic debris flows are deposited by a combination of laminar and turbulent mass flow mechanisms on the subaqueous flanks. Grading, sorting, bedding, and other sedimentary structures suggest partly to totally turbulent flows. Flow mechanisms rapidly change from proximal high density laminar to medial and distal low density turbulent currents. Deposition occurred by traction, traction carpet and suspension sedimentation.

8) Pumice morphologies parallel the evolution of the Berry Creek volcanic centre. Vesiculation, sparse during early Surtseyan activity, becomes strong during late Facies C and Facies B Plinian columns. Sparse vesiculation occurs during late Vulcanian gas pocket and/or phreatomagmatic activity in the dome growth stage.

9) Volcanism and sedimentation follows the pattern of a metastable volcanic island, foundering after cessation of continuous explosive and effusive volcanism.

1Ø) The sediments of the Berry Creek Complex belong to the Modified Resedimented Association. Deposition occurred by westward progradation of modified suprafan lobes. Proximal facies belong to the inverse to normally graded, normally graded, and graded stratified associations. Proximal to medial turbidite sediments exhibit AA and AE Bouma sequences.

11) The Berry Creek Complex comprises an intermediate to felsic calc-alkaline suite overlying the Fe-tholeiitic mafic metavolcanics. The latter are characterized by the komatiite-tholeiite association.

12) Chemical similarities between the tuff units, rhyodacitic clasts, lava flows, and subvolcanic porphyry intrusions suggest that the various depositional parameters have not significantly affected the average compositions of the Berry Creek metavolcanics except for the local synvolcanic fumarolic alteration zones.

13) Major and trace element diagrams suggest that the compositional gap between the two suites is related to two distinct magmatic sources.

14) Low Y, Zr, TiO2 and Sr contents in the mafic metavolcanics suggest an origin involving a depleted komatiitic or magnesian tholeiitic source involving high degrees of partial melting. Fractionation in high level magma chambers produced strong Fe enrichment trends from basaltic and basaltic andesite compositions.

15) Low Y, Zr, TiO2, FeO, MgO in the Berry Creek Metavolcanics (pyroclastics, flows, subvolcanic porphyries) are characteristic to depleted siliceous volcanics. Magma was generated by partial melting of crustal sources, e.g., tonalite-trondhjemite, hydrous basalt or amphibolite, and may have involved residual accumulation of amphibole and/or pyroxene in the source area.

16) Conclusions 12 to 15 correlate with the 10-15 Ma difference in zircon U-Pb radiometric ages between the two suites. The Berry Creek metavolcanics are associated with crustal remobilization during Wabigoon diapirism. The massive granodiorite lobes intruding the Berry Creek metavolcanics may represent the shallow calc-alkaline magma chambers.

REFERENCES

AFIFI, A.M. 1981. Stratigraphy, petrology and structure of Precambrian metavolcanic rocks in the Iris district, Gunnison and Saguache Counties, Colorado. New Mexico Geological Society Guidebook, 32nd Field Conference, Western Slope, Colorado, p. 287-292.

ALLEN, J.R.L. 1970. Physical Processes of Sedimentation, Allen and Unwin, London, 248 pp.

AMUKUN, S.E. 1979. Geology of the Willet Lake area, District of Thunder Bay. Ontario Geol. Survey Report 183.

ANHAEUSSER, C.R. 1971. Cyclic volcanicity and sedimentation in the evolutionary development of Archean greenstone belts of shield areas. Spec. Publ. Geol. Soc. Australia 3, p. 57-70.

ARMSTRONG, N.V., HUNTER, D.R., and WILSON, A.H. 1982. Stratigraphy and petrology of the Archean Nsuze Group, northern Natal and southern Transvaal, South Africa. Precambrian Res. 19, p. 75-107.

ARNDT, N.T. 1977. Thick layered peridotite-gabbro lava flows in Munro Township. Canadian Journal of Earth Sciences 14, p. 2620-2637.

ARNDT, N.T., NALDRETT, A.J., and PYKE, D.R. 1977. Komatiitic and iron-rich tholeiitic lavas of Munro Township, northeast Ontario. Journal of Petrology 18, p. 319-369.

ARTH, J.A. and BARKER, F. 1976. Rare-earth partitioning vetween hornblende and dacitic liquid and implications for the genesis of trondhjemitic-tonalitic magmas. Geology 4, p. 534-536.

ATTOH, K. 1981. Pre- and post-Dore sequences in the Wawa volcanic belt, Ontario. GSC Paper 81-1B, p. 49-54.

AUGUSTITHIS, S.S. 1979. Atlas of the textural patterns of basic and ultrabasic rocks and their genetic significance. de Gruyter. New York.

AYRES, L.D. 1969. Early Precambrian stratigraphy of part of Lake Superior Park, Ontario, Canada, and its implications for the origin of the Superior Province. Ph.D. thesis, Princeton University, Princeton, N.J..

AYRES, L.D. 1977. Importance of stratigraphy in Early Precambrian volcanic terraines: Cyclic volcanism at Setting Net Lake, northwestern Ontario. In Volcanic Regimes in Canada edited by Baragar, Coleman and Hall, GAC Sp. Pap. number 16, p. 243-264.

AYRES, L.D. 1978. A transition from subaqueous to subaerial eruptive environments in the Middle Precambrian Amisk Lake Group at Amisk Lake, Saskatchewan- a progress report. Centre for Precambrian Studies, University of Manitoba Annual Report, p. 36-51.

AYRES, L.D. 1980. Preliminary stratigraphic investigation of the upper felsic-intermediate component of the Early Proterozoic Amisk Group, Amisk Lake, Saskatchewan. Centre for Precambrian Studies, University of Manitoba, 1980 Annual Report, p. 36-46.

AYRES, L.D. 1981. A subaqueous to subaerial transition zone in the Early Proterozoic metavolcanic sequence, Amisk Lake, Saskatchewan. Centre for Precambrian Studies, Univeristy of Manitoba, 1981 Annual Report, p. 49-61.

AYRES, L.D. 1982. Pyroclastic rocks in the geologic record. In Pyroclastic volcanism and deposits of Cenozoic intermediate to felsic volcanic islands with implications for Precambrian greenstone belt volcanoes. edited by L.D.Ayres, GAC Short Course Notes No. 2, p. 1-17.

AYRES, L.D. 1982. Pyroclastic rocks in Precambrian Greenstone Belt volcanoes. In Pyroclastic volcanism and deposits of Cenozoic intermediate to felsic volcanic islands with implications for Precambrian Greenstone Belt volcanoes. Edited by L.D. Ayres. GAC Short Course Notes Volume 2, University of Manitoba, p. 343-365.

AYRES, L.D. 1983. Bimodal volcanism in Archean greenstone belts exemplified by greywacke composition, Lake Superior Park, Ontario. Canadian Journal of Earth Sciences 20, p. 1168-1194.

BAILES, A.H. 1979. Sedimentology of a Proterozoic volcanoclastic turbidite suite which crosses the boundary between the Flin Flon and Kisseynew Belts at File Lake, Manitoba. GAC/MAC Abs. Programs, Quebec, p. 38.

BAILES, A.H. 1980. Origin of Early Proterozoic volcanoclastic turbidites, south margin of the Kisseynew Sedimentary Gneiss Belt, File Lake, Manitoba. Precambrian Res. 12, p. 197-225.

BARAGAR, W.R.A. 1966. Geochemistry of the Yellowknife volcanic rocks. Canadian Journal of Earth Sciences 3, p. 9-30.

BARLEY, M.E. 1980. The evolution of Archean calc-alkaline volcanics: a study of the Kelly greenstone belt and McPhee dome, eastern Pilbara block, Western Australia. Unpublished Ph.D. thesis, University of Western Australia.

BARLEY, M.E. 1981. Relations between volcanic rocks in the Warrawoona Group: continuous or cyclic evolution? Spec. Publ. Geol. Soc. Australia 7, p. 263-273.

BARKER, F. and PETERMAN, Z.E. 1974. Bimodal tholeiite-dacite magmatism and the early Precambrian crust. Precambrian Res. 1, p. 1-12.

BEAVON, R.V. 1980. A resurgent cauldron in the Early Paleozoic of Wales, U. K.. Jour. Volc. Geotherm. Res. 7, p. 157-174.

BELT, E.S., and BUSSIERES, L. 1981. Upper Middle Ordovician submarine fans and associates facies, northeast of Quebec City. Canadian Journal of Earth Sciences 18, p. 981-995.

BLACKBURN, C.E. and MACKASEY, W.O. 1977. Nature of the Quetico-Wabigoon boundary in the deCourcey-Smiley Lakes area, northwestern Ontario: discussion. Canadian Journal of Earth Sciences 14, p. 1959-1961.

BLACKBURN, C.E. 1981. Geology of the Boyer Lake-Meggisi Lake area, District of Kenora. Ont. Geol. Survey Report 202.

BLACKBURN, C.E., BREAKS, F.W., EDWARDS, G.R., POULSEN. K.H., TROWELL, N.F., and WOOD, J. 1982. Stratigraphy and structure of the western Wabigoon Subprovince and its margins, northwestern Ontario. GAC-MAC Field Trip Guidebook Trip 3, 105pp.

BREAKS, F.W., BOND, W.D., and STONE, D. 1978. Preliminary geological synthesis of the English River Subprovince, northwestern Ontario and its bearing upon mineral exploration. OCS MP 72, 55 pp.

BROOKS, C. and HART. S. 1972. An extursive basaltic komatiite from a Canadian Archean metavolcanic belt. Canadian Journal of Earth Sciences 9, p. 1250-1253.

BROOKS, C. and HART, S. 1974. On the significance of komatiite. Geology 2, p. 107-110.

BROOKS, C., LUDDEN, J., PIGEON, Y., and HUBREGTSE, J.J.M.W. 1982. Volcanism of shoshonite to high-K andesite affinity in an Archean arc environment, Oxford Lake, Manitoba. Canadian Journal of Earth Sciences 19, p. 55-67.

BROWN, B.A. 1976. Structural studies, eastern Lake of the Woods. Centre for Precambrian Studies, University of Manitoba Annual Report, p. 3-6.

BROWN, B.A. 1977. Structural geology of the central and eastern Lake of the Woods region: progress report. Centre for Precambrian Studies, University of Manitoba Annual Report, p. 85-88.

BUCK, P.S. 1978. A caldera sequence in the early Precambrian Favourable Lake volcanic complex, northwestern Ontario. Unpubl. MSc. Thesis, University of Manitoba, Winnipeg, Man., 140 pp.

BURWASH, E.M. 1934. Geology of the Kakagi Lake area. Ontario Dept. of Mines Annual Report 42, 4, p. 41-92.

CAR, D.P. 1976. Directions of transport in a volcanoclastic sequence, Western Peninsula Region, Lake of the Woods, northwestern Ontario. Centre for Precambrian Studies, University of Manitoba, Annual Report, p. 89-96.

CAR, D.P. 1980. A volcanoclastic sequence on the flank of an Early Precambrian stratovolcano, Lake of the Woods, northwestern Ontario. Unpublished MSc Thesis, University of Manitoba.

CAR, D.P. and AYRES, L.D. 1979. Facies relationships of an Archean dacitic fragmental sequence, Western Peninsula, Lake of the Woods, northwestern Ontario. GAC/MAC Abs. Programs, Quebec, p. 42.

CAREY, S.N. and SIGURDSSON, H. 1980. The Roseau ash: deep sea tephra deposits from a major eruptive on Dominica, Lesser Antilles Arc. Jour. Volc. Geotherm. Res. 7, p. 67-86.

CARLISLE, D. 1963. Pillow breccias and their aquagene tuffs, Quadra Island, British Columbia. Jour. Geology 71, p. 48-71.

CARMICHAEL, I.S.E. 1964. The petrology of Thingmuli, a Tertiary volcano in eastern Iceland. Journal of Petrology 5, p.435.

CAS, R.A.F. 1978. Silicic lavas in Paleozoic flyschlike deposits in New South Wales, Australia: behaviour of deep subaqueous silicic flows. Geol. Soc. Am. Bull. 89, p. 1708-1714.

CAS, R. 1979. Mass-flow arenites from a Paleozoic interarc basin, New South Wales: mode and environment of emplacement. Journal of Sedimentary Petrology 49, p. 29-44.

CAS, R.A.F. 1983. Submarine "crystal tuffs": their origin using a Lower Devonian example from southeastern Australia. Geol. Mag. 120, p. 471-486.

CAWTHORN, R.G. and O'HARA, M.J. 1976. Amphibole fractionation in calc-alkaline magma genesis. Am. Jour. Science 176, p. 309-329.

CHAN, M.A. and DOTT, R.H.Jr. 1983. Shelf and deep sea sedimentation in Eocene fore arc basin, western Oregon-fan or non fan? Amer. Assoc. Petrol. Geol. Bull. 67, p. 2100-2116.

CLARKE, D.B. 1970. Tertiary basalts of Baffin Bay: possible primary magma from the mantle. Contrib. Min. Pet. 25, p. 203-224.

CONDIE, K.C. 1981. Archean greenstone belts. Developments in Precambrian Geology 3. Elsevier, New York, 434 pp..

CONDIE, K.C. and BARACAR, W.R.A. 1974. Rare earth element distributions in volcanic rocks from Archean greenstone belts. Contrib. Min. Pet. 45, p. 237.

CONDIE, K.C. and HARRISON, N.M. 1976. Geochemistry of the Archean Bulawayan Group, Midlands Greenstone Belt, Rhodesia. Precambrian Res. 3, p. 253-271.

DAVIES, J.C. and MORIN, J.A. 1976. Geology of the Cedartree Lake area. District of Kenora, Ontario. Ontario Geoscience Report 134, 52 pp.

DAVIES, J.C. and PRYSLAK, A.P. 1967. Kenora-Fort Frances Sheet, Kenora and Rainy River Districts. Ontario Dept. of Mines Compilation Series Map 2115.

DAVIES, J.C. and WATOWICH, S.N. 1956. Deology of the Populus Lake area. Ont. Dept. of Mines 65, p. 1-24.

DAVIES, D.W., BLACKBURN, D.E., and KROGH, T.E. 1982. Zircon U-Pb ages from the Wabigoon-Manitou Lakes region, Wabigoon Subprovince, northwest Ontario. Canadian Journal of Earth Sciences 19, p. 254-266.

DAVIS, D.W. and EDWARDS, G.R. 1982. Zircon U-Pb ages from the Kakagi Lake area, Wabigoon Subprovince, northwest Ontario. Canadian Journal of Earth Sciences 19, p. 1235-1245.

DAVIS, D.W. and TROWELL, N.F. 1982. U-Pb zircon ages from the eastern Savant Lake-Crow Lake metavolcanic-metasedimentary belt, northwest Ontario. Canadian Journal of Earth Sciences 19, p. 868-877.

DAVISON, J.G. 1983. Prograding subaqueous pyroclastic flows in the Berry Creek Complex, Lake of the Woods, Ontario. Abs. GAC Meetings, Victoria, p. A16.

DELANEY, G. 1976. A reconnaissance study of the metamorphic petrology and volcanic geochemistry of a portion of the Island Lake greenstone belt, Manitoba. Unpublished MSc.thesis, Brock University, Ontario, Canada, 106 pp.

DeROSEN-SPENCE, A.F., PROVOST, G. and DIMROTH, E. 1979. Archean subaqueous rhyolite flows at Noranda, Quebec. GAC/MAC Abs. Programs, Quebec, p. 46.

DeROSEN-SPENCE, A.F., PROVOST, G., DIMROTH, E., GOCHNAUER, K. and OWEN, V. 1980. Archean subaqueous felsic flows, Rouyn-Noranda, Quebec, Canada, and their Quaternary equivalents. Precambrian Res. 12, p. 43-77.

DEWIT, M.J. and STERN, C. 1978. Pillow talk. Jour. Volc. Geotherm. Res. 4, p. 55-80.

DIMROTH, E. and DEMARCKE, J. 1978. Petrography and mechanism of eruption of the Archean Dalembert Tuff, Rouyn-Noranda, Quebec, Canada. Canadian Journal of Earth Sciences 15, p.1712-1723.

DIMROTH, E. 1977. Archean subaqueous autoclastic volcanic rocks, Rouyn-Noranda area, Quebec: classification, diagnosis and interpretation. GSC Paper 77-1A, p. 513-522.

DIMROTH, E. and LICHTBLAU, A.P. 1979. Metamorphic evolution of Archean hyaloclastites, Noranda area, Quebec, Canada, Part 1: Comparison of Archean and Cenozoic sea floor metasomatism. Canadian Journal of Earth Sciences 16, p. 1315-1340.

DIMROTH, E. and ROCHELEAU, M. 1979. Volcanology and sedimentology of the Rouyn-Noranda area, Quebec. Geol. Assoc. Can., Quebec 1979 Guidebook Field Trip A-1, 193 pp.

DIMROTH, E., COUSINEAU, P., LEDUC, M., SANSCHAGRIN, Y., and HOCQ, M. 1979. A facies model of subaqueous basalt flows. GAC/MAC Abs. Programs, Quebec, p. 46.

DIMROTH, E., IMREH, L., ROCHELEAU, M., and GOULET, N. 1982. Evolution of the south central part of the Archean Abitibi Belt, Quebec. Part 1: Stratigraphy and paleogeographic model. Canadian Journal of Earth Sciences 19, p. 1729-1758.

DONALDSON, J.A. and JACKSON, G.D. 1965. Archean sedimentary rocks of north Spirit Lake area, northwestern Ontario. Canadian Journal of Earth Sciences 2, p. 622-647.

DONALDSON, A.C. and SHUMACHER, R.C. 1981. Late Paleozoic molasse of central Appalachians. In: Sedimentation and Tectonics in alluvial basins. Edited by A.D. Miall. GAC Special Paper 23, p. 99-124.

DRUITT, T.H., and SPARKS, R.S.J. 1982. A proximal ignimbrite breccia facies on Santorini, Greece. Jour. Volc. Geotherm. Res. 13, p. 147-171.

DUFFIELD,M W.A., BACON, C.R., and ROGUEMORE, G.R. 1979. Origin of reverse-graded bedding in air-fall pumice, Coso Range, California. Jour. Volc. Geotherm. Res. 5, p. 35-48.

DUNLOP, J.S.R. and BUICK, R. 1981. Archean epiclastic metasediments derived from mafic volcanics, North Pole, Pilbara Block, Western Australia. Spec. Publ. Geol. Soc. Australia 7, p. 225-233.

EDWARDS, G.R. 1979. Geology of the Kakagi-Rowan-Pipestone Lakes area, northwestern Ontario. Ontario Geological Survey unpublished report.

EDWARDS, G.R. 1982 (in progress). Petrogenesis and Evolution of the Archean Phinney-Dash Lakes Complex and related rocks. PhD Thesis, Unversity of Western Ontario. London, Ontario.

EICHELBERGER, J.C. 1980. Vesiculation of mafic magma during replenishment of silicic magma reservoirs. Nature 288, p. 446-450.

EMBLEY, R.W. 1976. New evidence for occurrence of debris flow deposits in the deep sea. Geology 4, p. 371-374.

ERIKSSON, K.A. 1979. Marginal marine depositional processed from the Archean Moodies Group, Barberton Mountain Land, South Africa: evidence and significance. Precambrian Res. 8, p. 153-182.

ERIKSSON, K.A. 1979. Archean paleoenvironments in the Moodies and Fig Tree Groups of the Barberton Mountain Land, South Africa, with particular reference to land-sea transitions. GAC/MAC Abs. Programs, Quebec, p. 49.

ERIKSSON, K. A. 1981. Archean platform to trough sedimentation, east Pilbara Block, Australia. Spec. Publ. Geol. Soc. Australia 7, p. 235-244.

ERIKSSON, K.A. 1981. Geometry and internal characteristics of Archean submarine channel deposits, Pilbara Block, Western Australia. Jour. Sed. Petrol. 52, p. 383-393.

EWART, A. and TAYLOR, S.R. 1969. Trace element geochemistry of the rhyolitic volcanic rocks, central North Island, New Zealand. Phenocryst Data. Contrib. Min. Pet. 22, p. 127-146.

EWART, A., BRYAN, W.B. and GILL, J.B. 1973. Mineralogy and geochemistry of the younger volcanic islands of Tonga, SW Pacific. Journal of Petrology 14, p. 429.

FERREIRA, W.S. 1981. An example of a volcanic subaerial and surf environment in the Middle Precambrian Amisk Group at Amisk lake, Sakatchewan--a progress report. Centre for Precambrian Studies, University of Manitoba, 1980 Ann. Rept., p. 47-59.

FISHER, R.V. 1960. Classification of volcanic breccias. Geol. Soc. Am. Bull. 66, p. 973-982.

FISHER, R.V. 1961. Proposed classification of volcanoclastic sediments and rocks. Geol. Soc. Am. Bull. 72., p. 1409-1414.

FISHER, R.V. 1966. Rocks composed of volcanic fragments and their classification. Earth Sci. Reviews 1, p. 287-298.

FISHER, R.V. 1971. Features of coarse grained, high concentration fluids and their deposits. Jour. Sed. Petrol. 41, p. 916-927.

FISHER, R.V. 1977. Erosion by volcanic base surge density currents: U-shaped channels. Geol. Soc. Am. Bull. 88, p. 1287-1297.

FISHER, R.V. 1979. Models for pyroclastic surges and pyroclastic flows. Journal Volc. Geotherm. Res. 6, p. 305-318.

FISHER, R.V. 1982. Pyroclastic flows. In Pyroclastic volcanism and deposits of Cenozoic intermediate to felsic volcanic islands with implications for Precambrian greenstone belt volcanoes. edited by L. D. Ayres, GAC Short Course No. 2.

FISHER, R.V. 1983. A review of submarine volcanism, transport processes, and deposits. Jour. Geol. Soc. London 140, p. 965.

FISHER, R.V. and HEIKEN, G. 1982. Mt. Pelee, Martinique: May 8 and 20, 1902, pyroclastic flows and surges. Jour. Volcanol. Geothern. Res. 13, p. 339-371.

FISHER, R.V. and MATTISON, J.M. 1968. Wheeler Gorge turbidite conglomerate series, California; inverse grading. Jour. Sed. Petrol. 38, p. 1013-1023.

FISKE, R.S. 1963. Subaqueous pyroclastic flows in the Ohanapecosh Formation, Washington. Geol. Soc. Am. Bull. 74, p. 391-406.

FISKE, R.S. and MATSUDA, T. 1964. Submarine equivalents of ash flows in the Tokiwa Formation, Japan. Am. J. Sci. 262, p. 76-106.

FLINN, D. 1965. On the symmetry principle and the deformation ellipsoid. Geol. Mag. 102, p. 36.

FLOYD, P.A. and WINCHESTER, J.A. 1975. Magma type and tectonic setting discrimination using immobile elements. Earth and Planetary Sci. Letters 27, p. 211-218.

FORNARI, D.J., MOOSE, J.G. and CALK, L. 1979. A large submarine sand-rubble flow on Kilauea Volcano, Hawaii. Jour. Volc. Geotherm. Res. 5, p. 239-256.

FRANCIS, H. and HOWELLS, M.F. 1973. Transgressive welded ash flow tuffs among Ordovician sediments of NE Snowdonia, N. Wales. Jour. Geol. Soc. London 129, p. 629-641.

FRASER, N.H.C. 1943. Geology of the Whitefish Bay area, Lake of the Woods. Ontario Dept. of Mines, Annual Report 52, 4, p. 1-19.

GALLOWAY, W.E. 1976. Sediments and stratigraphic framework of the Copper River Fan Delta, Alaska. Jour. Sed. Petrol. 46, p. 726-737.

GELINAS, L. and BROOKS, C. 1974. Archean quench textured tholeiites. Can. Jour. Earth Sci. 11, p. 324-340.

GELINAS, L., BROOKS, C., PERRAULT, G., CARIGNAN, J., TRUDE., P., and GRASSO, F. 1977. Chemo-stratigraphic divisions within the Abitibi volcanic belt, Rouyn-Noranda District, Quebec. In Volcanic Regimes in Canada. Edited by Baragar, Coleman and Hall, p.265-295.

GELINAS, L., LAJOIE, J., BOUCHARD, M., SIMARD, A., VERPAELST, P. and CHALOT-PRAT, F. 1979. Origin of the Don, Clericy and Glenwood rhyolites, Noranda Regiona, Quebec. GAC/MAC Abs. Programs, Quebec, p. 52.

GHIBAUDO, G. 1980. Deep sea fan depoists in the Macigno Formation (Middle-Upper Oligocene) of the Gordana Valley, Northern Appenines, Italy. Jour. Sed. Petrol. 50, p. 723-742.

GILES, C.W. 1981. Archean calc-alkaline volcanism in the eastern Goldfields Province, Western Australia. Spec. Publs. Geol. Soc. Australia 7, p. 275-286.

GLIKSON, A.Y. 1971. Primitive Archean element distribution patterns: chemical evidence and geotectonic significance. Earth and Planetary Science Letters 12, p. 309.

GLIKSON, A.Y. 1976. Stratigraphy and evolution of primary and secondary greenstones: significance of data from shields of the southern hemisphere. In The Early History of the Earth. Edited by B.F. Windley. Wiley, London, England.

GOLDIE, R. 1983. Seminar on ancient and modern volcanoes. Geoscience Canada 10, p,. 195-203.

GOODWIN, A.M. 1968. Archean protocontinental growth and early crustal history of the Canadian Shield. 23rd Int. Geol. Congr. 70-40, p. 1-30.

GOODWIN, A.M. 1972. Superior Province. In Variations in Tectonic Styles in Canada. Edited by Price and Douglas. GAC Spec. Pap. Number 11, p. 527-624.

GOODWIN, A.M. 1977. Archean volcanism in Superior Province, Canadian Shield. In Volcanic Regimes in Canada. Edited by Baragar, Coleman and Hall. GAC Spec. Pap. Number 16, p. 205-241.

GOODWIN, A.M. and SMITH, I.E.M. 1980. Chemical discontinuities in Archean volcanic terrains and the development of Archean crust. Precambrian Res. 10, p. 301-311.

GORDANIER, W.D. 1976. The depositional environment of formation K, Favourable Lake Volcanic Complex, northwestern Ontario. Centre for Precambrian Studies. University of Manitoba, 1976 Annual Report, p. 73-84.

GREEN, J.C. and SCHULZ, K.J. 1977. Iron rich basaltic komatiites in the Early Precambrian Vermilion district, Minnesota. Canadian Journal of Earth Sciences 14, p. 2181-2192.

GREEN, N.L. 1975. Archean glomeroporphyritic basalts. Canadian Journal of Earth Sciences 12, p. 1770-1784.

HALLBERG, J.A. 1972. Geochemistry of Archean volcanic belts in the Eastern Goldfields region of western Australia. Jour. Petrol. 13, p. 45-56.

HALLBERG, J.A. 1978. Acid/intermediate volcanism in the Yilgarn Block, western Australia. In Proceedings of the 1978 Archean Geochemistry Conference, edited by Smith, I.E.M. and Williams, J.G. University of Toronto, p. 349-352.

HALLBERG, J.A. 1980. Archean gology of the Leonora-Laverton area. International Archean Symposium. Perth 1980. Northeastern Yilgarn Block Excursion Guide.

HALLBERG, J.A. and WILLLIAMS, D.A.C. 1972. Archean mafic and ultramafic rock associateions in the Eastern Goldfields Region, western Australia. Earth and Planetary Science Letters 15, p. 191-200.

HALLBERG, J.A., CARTER, D.N. and WEST, K.N. 1976. Archean volcanism and sedimentation near Meckatharra, Western Australia. Precambrian Res. 3, p. 577-595.

HALLBERG, J.A., JOHNSTON, C. and BYE, S.M. 1976. The Archean Marda Igneous Complex, Western Australia. Precambrian Res. 3, p. 111-136.

HARGREAVES, R. and AYRES, L.D. 1979. Morphology of Archean metabasalt flows, Utik Lake, Manitoba. Canadian Journal of Earth Sciences 16, p. 1452-1466.

HAWKESWORTH, C.J. and O'NIONS, R.K. 1977. The petrogenesis of some Archean volcanic rocks from Southern Africa. Journal of Petrology 18, p. 487-520.

HEIKEN, G.H. 1972. Morphology and petrography of volcanic ashes. Geol. Soc. Am. Bull. 83, p. 1961-1988.

HEIN, F.J. 1982. Depositional mechanisms of deep sea coarse clastic sediments, Cap Lnrage Formation, Quebec. Canadian Journal of Earth Sciences 19, p. 267-287.

HENDERSON, J.B. 1972. Sedimentology of Archean turbidites at Yellowknife, Northwest Territories. Canadian Journal of Earth Sciences 9, p. 882-902.

HENDERSON, J.B. 1975. Sedimentology of the Archean Yellowknife Supergroup at Yellowknife, District of Mackenzie. GSC Bulletin 246, 62 p.

HENDRY, H. 1978. Cap des Rosiers Formation at Grosses Roches, Quebec- deposits of the mid fan region on an Ordovician submarine fan. Canadian Journal of Earth Sciences 15, p. 1472-1488.

HERD, R.K. and ERMANOVICS, I.F. 1976. Geology of the Island Lake Map Area, Manitoba and Ontario. GSC Paper 76-1A, p. 393-398.

HISCOTT, R. and MIDDLETON, G. 1979. Depositional mechanics of thick bedded sandstones at the base of a submarine slope, Tourelle Formation (Lower Ordovician), Quebec, Canada. In Geology of Continental Slopes, edited by L.J. Doyle and O.H. Pilkey. SEPM Spec. Publ. 27, p. 307-326.

HOBLITT, R.P., MILLER, C.D. and VALLANCE, J.W. 1981. Origin and stratigraphy of the deposit produced by the May 18 directed blast. USGS Professional Paper 1250, p. 401-420.

HOLDAWAY, M.J. 1971. Stability of andalusite and the aluminum silicate phase diagram. Am. J. Sci. 271, p. 97-131.

HYDE, R.S. 1980. Sedimentary facies in the Archean Timiskaming Group and their tectonic implications, Abitibi greenstone belt, northeastern Ontario, Canada. Precambrian Res. 12, p. 161-195.

HYDE, R.S. and WALKER, R.G. 1977. Sedimentary environments and the evolution of the Archean Greenstone Belt in the Kirkland Lake Area, Ontario. GSC Paper 77-1A, p. 185-190.

HYNDMAN, D.W. 1972. Petrology of Igneous and metamorphic rocks. McGraw-Hill Book Co., New York, 533 p.

IRVINE T.N. and BARAGAR, W.R.A. 1971. A guide to the chemical classification of the common volcanic rocks. Can. Jour. Earth Sci. 8, p. 523-547.

JAKES, P. and GILL, J. 1970. Rare earth elements and the island arc series. Earth and Planetary Science Letters 9, p. 17-28.

JAKES, P. and WHITE, A.J.R. 1972. Major and trace element abundances in volcanic rocks in orogenic areas. Geol. Soc. Am. Bull. 83, p. 29-40.

JANDA R.J., SCOTT, K.M., NOLAN, K.M., and MARTINSON, H.A. 1981. Lahar movement, effects and deposits. USGS Professional Paper 1250, p. 461-478.

JENSEN, L.S. 1976. A new cation plot for classifying subalkalic volcanic rocks. Ontario Division of Mines, MP66, 22p.

JOHNS, G.W. 1982. MacQuarrie-McGeorge Townships Area. District of Kenora. In Summary of Field Work, 1981, Ontario Geological Suvery, Miscellaneous Paper, p. 22-25.

JOHNS, G.W. and DAVISON, J.G. 1982. Precambrian geology of the Long Bay-Lobstick Bay area, Kenora District; Ontario Geological Survey Map P. 2594 Geological Series - Preliminary Map, scale 1:15840.

JOHNS, G.W. and RICHEY, S. 1982. Precambrian Geology of the MacQuarrie Township area, Kenora District; Ontario Geological Survey Map P.2498 Geological Series - Preliminary Map, scale 1:15840.

JOLLY, W.T. 1975. Subdivision of the Archean lavas of the Abitibi area, Canada from Fe-Mg-Ni-Cr relations. Earth Plan. Sci. Letters 27, p. 200-210.

JOLLY, W.T. 1977. Relations between Archean lavas and intrusive bodies of the Abitibi Greenstone Belt, Ontario-Quebec in Volcanic Regimes in Canada. Edited by Baragar, Coleman and Hall, GAC Spec. Pap. Number 16, p. 312-330.

JOLLY, W.T. 1980. Development and degradation of Archean lavas, Abitibi area, Canada, in light of major element geochemistry. Journal of Petrology 21, p. 323-363.

JOLLY, W.T. 1982. Progressive metamorphism of komatiite and related Archean lavas of the Abitibi area, Canada. In Komatiites, edited by N.T. Arndt and E.G. Nisbet, Allen and Unwin, London, p. 247-266.

KESSLER, L.G. 1979. Sedimentary structure sequence and channel geometry in ancient submarine fan systems-examples of striking similarities to braided fluvial deposits. GAC/MAC Abs. Programs, Quebec, p. 61.

KOKELAAR, B.P. 1983. The mechanism of Surtseyan volcanism. Jour. Geol. Soc. London 140, p.939-944.

KUNTZ, M.A., ROWLEY, P.D., MACLEOD, N.S., REYNOLDS, R.L., MCBROOME, L.A., KAPLAN, A.M., and LIDKE, D.J. 1981. Petrography and particle size distribution of pyroclastic flow, ash-cloud and surge deposits. USGS Professional Paper 1250, p. 525-540.

LAJOIE, J. 1980. Volcanoclastic rocks. In Facies Models, edited by R.G.Walker. Geoscience Canada Reprint Series, p. 191-200.

LAMBERT, M.B. 1976. The Back River volcanic complex, District of Mackenzie. GSC Paper 76-1A, p. 363-367.

LAMBERT, M.B. 1977. The southwestern margin of the Back River volcanic complex, District of Mackenzie. GSC Paper 77-1A, p. 179-181.

LAMBERT, M.B. 1977. Anatomy of a greenstone belt. In Volcanic Regimes in Canada edited by Baragar, Coleman and Hall, GAC Spec. Pap. Number 16, p. 331-340.

LAMBERT, R.S.J., HOLLAND, J.G., and OWEN, P.F. 1974. Chemical petrology of a suite of calc-alkaline lavas from Mt. Ararat, Turkey. Journal of Geology 82, p. 419-438.

LONG, D.G.F. 1977. Resedimented conglomerates of Huronian (lower Aphebian) age, from the north shore of Lake Huron, Ontario, Canada. Canadian Journal of Earth Sciences 14, p. 2495-2509.

LONG, D.G.F. 1981. Dextral strike slip faults in the Canadian cordillera and depositional environments of related fresh-water intermontaine coal basins. In Sedimentation and Tectonics in Alluvial Basins, edited by A.D. Miall. GAC Spec. Pap. 23, p. 153-186.

LOWDER, G.C. 1970. The volcanoes and caldera of Talasea, New Britain: mineralogy. Contrib. Min. Pet. 26, p. 324-340.

LOWDER, G.C. and CARMICHAEL, I.S.E. 1970. The volcanoes and caldera of Talasea, New Britain: geology and petrology. Geol. Soc. Am. Bull. 81, p. 17-38.

LOWMAN, R.D.W. and BLOXAM, T.W. 1981. The petrology of the lower Paleozoic Fishguard volcanic group and associated rocks E of Fishguard, N Pembrokeshire, South Wales. Jour. Geol. Soc. London 138, p. 47-68.

MACLEAN, W.H., ST. SEYMOUR, K. and PRABHU, K.M. 1982. Sr. Y. Zr, Nb, Ti and REE in Grenville amphibolites at Montauban-les-Mines, Quebec. Canadian Journal of Earth Sciences 19, p. 633-644.

MANSFIELD, C.F. 1979. Upper Mesozoic subsea fan depoists in the southern Diablo range, California: record of the Sierra Nevada magmatic arc. Geol. Soc. Am. Bull. 90, p. 1025-1046.

MEYN, H.D. and PALONEN, P.A. 1980. Stratigraphy of an Archean submarine fan. Precambrian Res. 12, p. 257-285.

MIALL, A.D. 1981. Late Cretaceous and Paleogene sedimentation and tectonics in the Canadian Arctic Islands. In Sedimentation and Tectonics in Alluvial Basins, edited by A.D. Miall. GAC Spec. Pap. 23, p. 222-272.

MIDDLETON, G.V. and HAMPTON, M.A. 1976. Subaqueous sediment transport and deposition by subaqueous gravity flows. In Sediment transport and environmental management, edited by D.J. Stanley and D.J.P. Swift, John Wiley and Sons, New York, p. 197-220.

MIYASHIRO, A. 1973, 1975. Metamorphism and metamorphic belts. Allen and Unwin, London, 492 pp.

MOORE J.G. and SISSON, T.W. 1981. Deposits and effects of the May 18 pyroclastic surge. USGS Professional Paper 1250, p. 421-438.

MOORE, J.G., PHILLIPS, R.L., GRIGG, R.W., PETERSON, D.W., and SWANSON, D.A. 1973. Flows of lava into the sea, 1969-1971. Kilauea volcano, Hawaii. Geol. Soc. Am. Bull. 84, p. 537-546.

MORTENSEN, J.K. 1982. Geological setting and tectonic significance of Mississippian felsic metavolcanic rocks in the Pelly Mountains, southern Yukon Territory. Canadian Journal of Earth Sciences 19, p. 8-22.

MORTON, R.L. and NEBEL, M. 1983. Physical character of Archean felsic volcanism in the vicinity of the Helen iron mine, Wawa, Ontario, Canada. Precambrian Res. 20, p.39-62.

MORTON, R.L. and OSTERBERG, M. 1982. Archean felsic volcanism in the vicinity of the Helen Iron Mine, Wawa, Ontario. GAC/MAC Prog. Abs. 7, p. 68.

MUTTI, E. and RICCI-LUCCHI, F. 1975. The significance of certain sequential units in turbidite series. Soc. Geol. Fr. Bull. 16, p. 577-582.

NALDRETT, A.J. and ARNDT, N.T. 1975. Volcanogenic nickel deposits with some guides for exploration. American Institute of Mining, Metallurgical and Petroleum Engineers Transactions 260, p. 13-15.

NALDRETT, A.J. and TURNER, A.R. 1977. The geology and petrogenesis of a greenstone belt and related nickel sulfide mineralization at Yakabindie, western Australia. Precambrian Res. 5, p. 43-103.

NAYLOR, M.A. 1980. The origin of inverse grading in muddy debris flow deposits - a review. Jour. Sed. Petrol. 50, p. 1111-1116.

NEMEC, W., POREBSKI, S.J. and STEEL, R.J. 1980. Texture and structure of resedimented conglomerates: examples from Ksiaz Formation (Famennian-Tournaisian), southwestern Poland. Sedimentology 27, p. 519-538.

NESBITT, R.W. and SUN, S.S. 1976. Geochemistry of Archean spinifex textured peridotites and magnesian and low magnesian tholeiites. Earth and Planetary Science Letters 31, p. 433-453.

NILSEN, T.H. 1981. Upper Devonian and Lower Mississippian redbeds, Brooks Range, Alaska. In Sedimentation and Tectonics in Alluvial Basins, edited by A.D. Miall. GAC Special Paper 23, p. 187-219.

NISBETT, E.G., BICKLE, M.J. and MARTIN, A. 1977. The mafic and ultramafic lavas of the Belingue Greenstone Belt, Rhodesia. Jour. Petrol. 18, p. 521-566.

NORMARK, W.R. 1978. Fan valleys, channels, and depositional lobes on modern submarine fans: characters for recognition of sandy turbidite environments. Amer. Assoc. Petrol. Geol. Bull. 62, p. 912-931.

OKADO, H. 1980. Sedimentary environments on and around island arcs: an example of the Japan trench area. Precambrian Res. 12, p. 115-139.

PADGHAM, W.A. 1979. An Archean ignimbrite at Yellowknife, NWT. GAC/MAC Abs. Programs, Quebec, p. 71.

PAGE, R.O. and CLIFFORD, P.M. 1977. Physical volcanology of an Archean vent complex, Minnitaki Lake area, northwestern Ontario. GSC Report of Activities, Paper 77-1A, p. 441-443.

PARSONS, W.H. 1969. Criteria for the recognition of volcanic breccias-review in igneous and metamorphic petrology. Geol. Soc. Am. Mem. 115, p. 263-304.

PEARCE, J.A. and BIRKETT, T.C. 1974. Archean metavolcanic rocks from Thackeray Township, Ontario. Canadian Mineralogist 12, p. 509-519.

PEARCE, J.A. and CANN, J.R. 1971. Ophiolite origin investigated by discriminant anlysis using Ti, Zr, and y. Earth and Planetary Science Letters 12, p. 339-349.

PEARCE, J.A. and CANN, J.R. 1973. Tectonic setting of basic volcanic rocks determined using trace element analyses. Earth and Planetary Science Letters 19, p. 290-300.

PEARCE, J.A. and NORRY, M.J. 1979. Petrogenetic implication of Ti, Y, Zr and Nb variations in volcanic rocks. Contrib. Min. Pet. 69, p. 33-47.

PELOQUIN, A.S., AYRES, L.D. and NIKOLS, C. 1982. Morphology of an early Proterozoic rhyolite flow and associated fragmental unit near Flin Flon, Manitoba. Centre for Precambrian Studies, University of Manitoba, Ann. Rept., p. 62-71.

PHILLIPS, W.R., FUGE, R. and PHILLIPS, N. 1981. Convection and crystallization in the Griffel-Dalbeattie pluton. Jour. Geol. Soc. London 138, p. 351-366.

PICKERING, K.T. 1981. Two types of outer fan lobe sequence from the Late Precambrian Kongsfjord Formation submarine fan, Finnmark, north Norway. Jour. Sed. Petrol. 51, p. 1277-1286.

PICKERING, K.T. 1982. A Precambrian upper basin slope and prodelta in northeast Finnmark, north Norwary-a possible ancient upper continental slope. Jour. Sed. Petrol. 52, p. 171-186.

PRIOR, D.B., BORNHOLD, B.D., COLEMAN, J.M., and BRYANT, W.R. 1982. Morphology of a submarine slide, Kitimat Arm, British Columbia. Geology 10, p. 588-592.

RAMSAY, C.R. and KAMINENI, D.C. 1977. Petrology and evolution of an Archean metamorphic aureole in the Slave Craton, Canada. Journal of Petrology 18, p. 460-486.

RAMSAY, J.G. 1967. Folding and fracturing of rocks. McGraw-Hill, New York.

REID, F. 1983. Origin of the rhyolitic rocks of the Taupo volcanic zone, New Zealand. J. Volcanol. Geotherm. Res. 15, p. 315-338.

REYMER, A.P.S. 1983. Metamorphism and tectonics of a Pan-African terrain in southeatern Sinai. Precambrian Res. 19, p. 225-238.

RICHARDSON, S.W., GILBERT, M.C. and BELL, P.M. 1969. Experimental determination of kyanite-andalusite and andalusite-sillimanite equilibria: The aluminum silicate triple point. Am. J. Sci. 267, p. 259-272.

RICKETTS, B.D., WARE, M.J. and DONALDSON, J.A. 1982. Volcanoclastic rocks and volcanoclastic facies in the Middle Precambrian (Aphibian) Belcher Group, Northwest Territories, Canada. Canadian Journal of Earth Sciences 19, p. 1275-1294.

ROCHELEAU, M. 1979. Archean sedimentary environments in Rouyn-Noranda area. GAC/MAC Abs. Programs, Quebec, p. 74.

RODOLFO, K.S. and WARNER, R.J. 1980. Tectonic, volcanic and sedimentologic significance of volcanic glasses from Site 450 in the eastern Pairece Vela Basin, Deep Sea Drilling Project Leg 59: Initial Reports of the DSDP 59, p. 603-608.

ROOBOL, M.J. and SMITH, A.L. 1976. A pattern of alternating eruptive styles at Mount Pelee, Martinique. Geology 4, p. 521-524.

ROSE, W.I. 1978. The October 1974 basaltic tephra from Fuego Volcano: description and history of the magma body. Jour. Volcanol. Geotherm. Res. 4, p. 3-53.

ROSS, C.S. and SMITH, R.L. 1961. Ash flow tuffs: their origin, geologic relations, and identification. USGS Professional Paper 366, 81 pp.

ROWLEY, P.D., KUNTZ, M.A., and MACLEOD, N.S. 1981. Pyroclastic flow deposits. USGS Professional Paper 1250, p. 489-512.

RUPKE, N.A. 1977. Growth of an ancient deep-sea fan. Jour. Geology 85, p. 725-744.

SALLENGER, A.H. 1979. Inverse grading and hydraulic quivalence in grain flow deposits. Jour. Sed. Petrol. 49, p. 553-562.

SANGSTER, D.F. 1972. Precambrian volcanogenic massive sulphide deposits in Canada: a review. GSC Paper 72-77, 44p.

SCHMINKE, H.U. 1979. Submarine pyroclastic rocks and processes. GAC/MAC Abs. Programs, Quebec, p. 77.

SELF, S. 1982. Lava flows and domes. In Pyroclastic Volcanism and Deposits of Cenozoic Intermediate to Felsic Volcanic Islands with Implications for Precambrian Greenstone Belt Volcanoes. Edited by L.D. Ayres. GAC Short Course Notes Volume 2, University of Manitoba, p. 53-58.

SHERIDAN, M.F. 1979. Emplacement of pyroclastic flows: a review. In Ash flow tuffs, edited by C.E. Chapin and W.E. Elston. Geol. Soc. Amer. Sp. Paper 180, p. 125-134.

SIGURDSSON, H. 1982. Volcanogenic sediments in island arcs. In pyroclastic volcanism and deposits of Cenozoic intermediate to felsic volcanic islands with implications for Precambrian greenstone belt volcanoes, edited by L. D. Ayres. GAC Short Course Notes Volume 2, University of Manitoba, p. 221-293.

SIGURDSSON, H. and CAREY, S.N. 1981. Marine tephrochronology and quaternary explosive volcanism in the Lesser Antilles Arc. In Tephra studies, edited by S. Self and R.S.J. Sparks, D. Reidel Publ. Co., p. 255-280.

SIGURDSSON, H., SPARKS, R.S.J., CAREY, S.N., and HUANG, T.C. 1980. Volcanogenic sedimentation in the Lesser Antilles Arc. Journal of Geology 88, p. 523-540.

SIGVALDASON, G.E. 1974. Basalts from the centre of the assumed Icelandic mantle plume. Jour. Petrology 15, p. 497-524.

SIMPSON, J.E. 1972. Effects of the lower boundary on the head of a gravity current. J. Fluid Mechanics 53, p. 759-768.

SMITH, I.E.M. 1980. Geochemical evolution in the Blake River Group, Abitibi Greenstone Belt, Superior Province. Canadian Journal of Earth Sciences 17, p. 1292-1299.

SPARKS, R.S.J. 1976. Grain size variations in ignimbrites and implications for transport of pyroclastic flows.

Sedimentology 23, p. 147-188.

SPARKS, R.S.J. 1978. The dynamics of bubble formation and growth in magmas: a review and analysis. J. Volcanol. Geotherm. Res. 3, p. 1-37.

SPARKS, R.S.J. and WALKER, G.P.L. 1977. The significance of vitric enriched air-fall ashes associated with crystal enriched ignimbrites. Journal of Volcanol. Geotherm. Res. 2, p. 329-341.

SPARKS, R.S.J. and WILSON, L. 1976. A model for the formation of ignimbrite by gravitational column collapse. Jour. Geol. Soc. London 132, p. 441-451.

SPARKS, R.S.J., SIGURDSSON, H. and CAREY, S.N. 1980. The entrance of pyroclastic flows into the sea II. Theoretical considerations on subaqueous emplacement and welding. Jour. Volc. Geotherm. Res. 7, p. 97-105.

SPARKS, R.S.J., SIGURDSSON, H. and WILSON, L. 1977. Magma mixing: a mechanism for triggering acid explosive eruptions. Nature 267, p. 315-318.

SPRY, A. 1969. Metamorphic Textures. Pergamon Press. New York. 350p.

STAUFFER, M.R.M., MUKHERJEE, A.C. and KOO, J. 1975. The Amisk Group: an Aphebian (?) island arc deposit. Canadian Journal of Earth Sciences 12, p. 2021-2035.

STOCKWELL, C.H. 1964. Fourth report on structural provinces, orogenies and time classification of rocks of the Canadian Precambrian Shield. In Age determinations and geological studies, Part II Geological Studes. GSC Paper 64-17, 29p.

STOESER, D.B. 1975. Igneous rocks from Leg 30 of the Deep Sea Drilling Project: Initial reports of the Deep Sea Drilling Project 30, p. 401-414.

STUDEMEISTER, P.A. 1983. The greenschist facies of an Archean assemblage near Wawa, Ontario. Canadian Journal of Earth Sciences 20, p. 1409-1420.

TABATABAI, M. 1979. Petrography and geochemistry of the MacArthur Township area, Ontario. Unpubl. MSc. thesis, Brock University, St. Catharines, Ontario.

TASSE, N. GAUTHIEE, N., LAJOIE, J. et GELINAS, L. 1982. Les volcanoclastites des complexe rhyolitique de Cap d'Ours, Rouyn-Noranda Quebec: exemples des mecanismes de fragmentation et de mise enplace dans le volcanisme felsique. Canadian Journal of Earth Sciences 19, p. 1337-1349.

TASSE, M., LAJOIE, J. and DIMROTH, E. 1978. The anatomy and interpretation of an Archean volcanoclastic sequence. Noranda region, Quebec. Canadian Journal of Earth Sciences 15, p. 874-888.

TAYLOR, S.R. and HALLBERG, J.A. 1977. Rare-earth elements in the Marda calc-alkaline suite: an Archean geochemical analogue of Andean-type volcanism. Geoch. Cosmochim. Acta. 41, p. 1125-1129.

TEAL, P.R. and WALKER, R.G. 1977. Stratigraphy and sedimentology of the Archean Manitou Group, northwestern Ontario. In Report of Activities, Part A., GSC Paper 77-1A, p. 181-184.

THURSTON, P.C. 1980. Subaerial volcanism in the Archean Uchi-Confederation volcanic belt. Precambrian Res. 12, p. 79-98.

THURSTON, P.C. 1982. Economic evaluation of Archean felsic volcanic rocks using REE geochemistry. In Archean geology, edited by Glover, J.E. and Groves, D.I. Geol. Soc. Australia Spec. Publ. 7, p. 439-452.

THURSTON, P.C. and FRYER, B.J. 1983. The geochemistry of repetitive cyclical volcanism from basalt through rhyolite in the Uchi-Confederation Greenstone Belt, Canada. Contrib. Min. Pet., in press.

TROWELL, N.F., BLACKBURN, C.F. and EDWARDS, G.R. 1980. Preliminary geological synthesis of the Savant Lake-Crow Lake metavolcanic-metasedimentary belt, northwestern Ontario, and its bearing upon mineral exploration. OGS MP 89, 30p.

TURNER, C. and WALKER, R.G. 1973. Sedimentology, stratigraphy and curstal evolution of the Archean Greenstone Belt near Sioux Lookout, Ontario. Canadian Journal of Earth Sciences 10, p. 817-845.

VAN DER LINGEN, G.J. 1973. The Lord Howe Rise rhyolites. Deep Sea Drilling Project, Leg 21, p. 523-539.

VAN WAGONER, N. and VAN WAGONER, S. 1982. Shallow water volcanism and sedimentation in a portion of the Flin Flon-Snow Lake greenstone belt: a preliminary report. Centre for Precambrian Studies, University of Manitoba, 1982 Ann. Rept.

VILJOEN, M.J. and VILJOEN, R.P. 1969. Upper mantle project. Spec. Publ. Geol. Society of South Africa 2.

VON BRUNN, V. and HOBDAY, D.K. 1976. Early Precambrian tidal sedimentation in the Pongola Supergroup of South Afric. Jour. Sed. Petrol. 46, p. 670-679.

WALKER, G.P.L. 1972. Crystal concentration in ignimbrites. Contrib. Min. Pet. 36, p. 135-146.

WALKER, G.P.L. 1979. A volcanic ash generated by explosions where ignimbrite entered the sea. Nature 281, p. 642-646.

WALKER, G.P.L. 1980. The Taupo pumice: product of the most powerful known (ultraplinian) eruption? Jour. Volcanol. Geotherm. Res. 8, p. 69-94.

WALKER, G.P.L., WILSON, C.J.N., and FROGGATT, P.C. 1980. Fines depleted ignimbrites in New Zealand-the product of a turbulent pyroclastic flow. Geology 8, p. 245-249.

WALKER, R.G. 1975. Generalized facies models for resedimented conglomerates of the turbidite association. Geol. Soc. Amer. Bull. 86, p. 737-748.

WALKER, R.G. 1976. Contribution of sedimentology to Archean geology - a review. GAC/MAC Prog. Abstracts (Edmonton, 1976), p. 62.

WALKER, R.G. 1976. Facies Models 2. Turbidites and associated coarse clastic deposits. Geoscience Canada 3, p. 25-36.

WALKER, R.G. 1978. A critical appraisal of Archean basin-craton complexes. Canadian Journal of Earth Sciences 15, p. 1213-1218.

WALKER, R.G. 1978. Deep water sandstone facies and ancient submarine fans: models for exploration for stratigraphic traps. Amer. Assoc. Petrol. Geol. Bull. 62, p. 932-966.

WALKER, R.G. 1979. Archean sediments: Their role in interpretation of basin evolution. GAC/MAC Abs. Programs, Quebec, p. 84.

WALKER, R.G. and PETTIJOHN F.J. 1971. Archean sedimentation: Analysis of the Minnitaki Basin, northwestern Ontario, Canada. Geological Soc. Am. Bull. 82, p. 2099-2130.

WALTON, A.W. 1979. Volcanic sediment apron in the Tascotal Formation (Oligocene), Trans-Pecos, Texas. Jour. Sed. Petrol. 49, p. 303-314.

WEAVER, S.D. 1977. The Quaternary Caldera volcano Emuruangogolak, Kenya Rift, and the petrology of a bimodal ferrobasalt-pantellentic trachyte assocation. Bull. Volcanol. 40, p. 220-230.

WILKINSON, J.F.G. and DUGGAN, N.T. 1972. Some tholeiites from the Inverall area, New South Wales and their bearing on low pressure tholeiite fractionation. Jour. Petrol. 14, p. 339-348.

WILSON, C.J.N. 1980. The role of fluidization in the emplacement of pyroclastic flows: an experimental approach. Jour. Volc. Geotherm. Res. 8, p. 231-249.

WILSON, G.J.N. and WALKER, C.P.L. 1982. Ignimbrite depositional facies: the anatomy of a pyroclastic flow. Jour. Geol. Soc. London 139, p. 581-592.

WILSON, H.D.B. and MORRICE, M.G. 1977. The volcanic sequence in Archean shields. In Volcanic Regimes in Canada, edited by Baragar, Coleman and Hall, GAC Spec. Pap. number 16, p. 355-374.

WILSON, L., and HEAD, J.W. 1981. Morphology and rheology of pyroclastic flows and their deposits, and guidelines for future observations. USGS Professional Paper 1250, p. 513-524.

WINK, M.H. and NILSEN, T.H. 1980. The Rocks Sandstone, an Eocene sand rich deep sea fan deposit, northern Santa Lucia Range, California. Jour. Sed. Petrol. 50, p. 583-602.

WINKLER, H. 1979. Petrogenesis of metamorphic rocks. 8th Edition. Springer-Verlag. New York, 348 p.

WOOD, D.A. 1978. Major and trace element variations in the Tertiary lavas of eastern Iceland and their significance with respect to the Iceland geochemical anomaly. Journal of Petrology 19, p. 393-436.

WOOD, D.S. 1973. Patterns and magnitudes of natural strain in rocks. Phil. Trans. R. Soc London 274, p. 373-382.

WOOD, J. 1980. Epiclastic sedimentation and stratigraphy in the North Spirit Lake and Rainy Lake areas: a comparison. Precambrian Research 12, p. 227-255.

WRIGHT, J.V. and WALKER, G.P.L. 1977. The ignimbrite source problem: significance of a co-ignimbrite lag-fall deposit. Geology 5, p. 729-732.

WRIGHT, J.V., SMITH, A.L. and SELF, S. 1980. A working terminology of pyroclastic deposits. Jour. Volc. Geotherm. Res. 8, p. 315-366.

YAMAZAKI, T., KATO, T., MUROI, I., and ABE, M. 1973. Textural analyses and flow mechanisms of the Donsurubo subaqueous pyroclastic flow deposits. Bull. Volcanol. 37, p.231-244.

ZECK, H.P. 1970. An erupted migmatite from Cerro del Hoyaza, southeastern Spain. Contrib. Min. Pet. 26, p. 225-246.

APPENDIX 1

ANALYTICAL TECHNIQUES

Loss on Ignition Determination

Each of the samples was crushed to 180 mesh in a tungsten carbide swing mill and was dried in a 100 degrees C oven overnight. Porcelain crucibles were similarly dried and weighed to 4 decimal places. Approximately 1.0 grams of dried sample was placed into crucible and the total weight recorded. Crucibles and samples were heated, from an initially cold muffle furnace to 1100 degrees C for approximately 30 minutes. After cooling for 30 minutes inside the oven, the samples were returned to dessicators for a cooling period, before weighing to 4 decimal places. Weight loss for each crucible was calculated and normalized to loss on ignition per one gram of sample. The difference in weight is due to losses of water and other volatile phases, i.e., CO2, S2, etc.. Gains on ignition due to oxidation of ferrous to ferric iron (Fe+2 -- Fe+3) were not observed. The LOI results ranged from less than 1% to a maximum of 9.7%, the latter within strongly carbonatized biotite lamprophyre dykes.

Glass Fusion Discs

One gram of sample was added to ten grams of flux (90% lithium tetraborate, 10% lithium carbonate). An amount of flux equivalent to the LOI per gram was also added. After carefully and thoroughly mixing the powders, the mixture was fused in nonwetting platinum-gold crucibles in an 1100

degrees C muffle furnace. During the 30 minute furnace stage, the crucibles were swirled for several seconds to ensure complete melting and homogeneity of the mixture. The molten glass was then poured into a heated (sitting on top of Bunsen burner) platinum mold. After dissipation of convection cells within the melt, the burner was shut off and the disc allowed to cool. Contraction during cooling allows the disc to pop out of the mold ready for analysis. All discs were labelled on the shiny upper side. The discs are stored in a dessicator prior to and after completion of analyses.

Powder Pellets

Powdered samples were pressed into pellets for trace element analyses with a mechanical press. Two x-ray mix tablets were ground and added to the powdered rock to act as a binding agent.

Standard Samples

The following USGS standard powders were used for major and trace element analysis:

Major Elements

AGV	RGM	NIL
BCR	G-2	PPB
GSP	MRG	JB1

Trace Elements

GSP	AGV	G-2

A minimum of 3 and maximum of 9 standard values were used for data comparison. Input data was recorded on magnetic tape and reduced by computer program with major elements reported in weight percent (oxides) and trace elements in ppm.

The precision limits of major oxides and trace elements are presented below:

	wt%		ppm
SiO2	+- 1.Ø	Ba	+- 129.73
Al2O3	+- 1.Ø	Cu	+- 8.66
FeO	+- Ø.2	Ni	+- 1Ø.79
MgO	+- Ø.Ø5	Rb	+- 18.4Ø
CaO	+- Ø.2	Sr	+- 5Ø.12
Na2O	+- Ø.3	Y	+- 9.33
K2O	+- Ø.Ø5	Zn	+- 14.39
TiO2	+- Ø.1	Zr	+- 47.76
MnO	+- Ø.Ø5		
P2O5	+- Ø.Ø5		

The following table compares the USGS standard values with the accuracy of those results calculated in the present study. The reproducibility of the standards is included where multiple runs were completed (note number in brackets):

Sample Number	USGS	Brock AGV (3)	+-	USGS	Brock BCR (5)	+-
SiO2	59.72	59.98	0.22	54.85	54.44	0.49
Al2O3	17.22	17.25	0.15	13.68	13.50	0.23
FeO	6.84	6.78	0.14	13.52	13.35	0.08
MgO	1.55	1.44	0.30	3.49	3.51	0.45
CaO	5.00	4.97	0.07	6.98	6.94	0.07
Na2O	4.31	3.65	0.11	3.29	3.33	0.09
K2O	2.93	2.92	0.03	1.68	1.70	0.03
TiO2	1.05	1.06	0.01	2.22	2.21	0.03
MnO	0.10	0.10	0.01	0.19	0.19	0.01
P2O5	0.50	0.51	0.02	0.33	0.35	0.05
Sr	660	628.2				
Y	26	17.8				
Zr	220	202.7				
Ni	17	15.2				
		GSP (2)	+-		PPB (2)	+-
SiO2	67.31	66.82	0.37	48.18	46.71	0.03
Al2O3	15.9	15.08	0.04	7.26	7.05	----
FeO	4.33	4.36	----	11.03	11.15	0.05
MgO	0.96	1.03	0.08	24.42	24.04	0.11
CaO	2.02	2.04	0.02	3.75	3.81	0.03
Na2O	2.80	3.45	0.38	1.68	1.98	0.16
K2O	5.53	5.51	0.02	0.85	0.85	----
TiO2	0.66	0.66	----	1.12	1.15	0.01
MnO	0.25	0.22	0.0	0.19	0.17	----
Sr	230	209				
Y	32	28.1				
Zr	500	493.6				
Ni	9	11.6				

	RGM		G-2	
SiO2	73.44	73.23	69.19	69.56
Al2O3	13.80	14.17	15.35	15.66
FeO	1.87	1.86	2.67	2.54
MgO	0.28	0.24	0.77	0.71
CaO	1.12	1.26	1.98	1.96
Na2O	4.08	4.00	4.06	3.90
K2O	4.56	4.35	4.52	4.49
TiO2	0.27	0.28	0.50	0.49
MnO	0.04	0.04	0.04	0.04
P2O5	0.05	0.03	0.14	0.09
Sr			480	526
Y			12	23
Zr			300	320
Ni			5	4.1

	MRG (2)		+-	JB1 (2)		+-
SiO2	39.23	40.27	0.22	52.62	53.61	0.24
Fe2O3	8.56	8.81	0.03	14.62	14.73	0.05
FeO	17.80	17.87	0.02	9.01	9.02	----
MgO	13.51	13.82	0.12	7.76	7.56	0.09
CaO	14.72	14.71	0.01	9.35	9.41	----
Na2O	0.71	2.37	0.81	2.79	3.00	0.01
K2O	0.18	0.22	----	1.42	1.46	0.01
TiO2	3.75	3.75	0.01	1.34	1.32	----
MnO	0.17	0.16	----	0.15	0.16	----
P2O5	0.07	0.07	----	0.26	0.23	----

	NIL (2)		+-(2)
SiO2	52.43	53.97	0.16
Al2O3	13.59	13.91	0.07
FeO	9.96	10.41	----
MgO	0.28	0.62	0.12
CaO	3.24	3.24	0.02
Na2O	8.30	10.10	1.75
K2O	5.46	5.48	----
TiO2	0.49	0.51	----
MnO	0.76	0.76	----
P2O5	0.06	0.08	----

APPENDIX 2.

Geochemical Sample Descriptions

0012	WR	Plagioclase phyric basalt, Snake Bay metavolcanics, leopard rock
0058	WR	Tuff, Berry Creek metavolcanics, glassy epidotized
0084	WR	Crystal tuff, Berry Creek metavolcanics, quartz and feldspar crystals
0088	WR	Epiclastic metasediment, Berry Creek, quartz feldspar wacke, 15-25 % biotite
0095	WR	Gabbro, Berry Lake Sill, medium grained, pyroxene cumulate
0097	WR	Serpentinite, Berry Lake Sill, medium grained, olivine and pyroxene cumulate
0125	WR	Amphibolite, Berry Lake Sill, fine to medium grained
0129	CL	Tuff breccia, Berry Creek metavolcanics, garnet and hornblende rich mafic clasts
0147	CL	Tuff breccia, Berry Creek metavolcanics, pumice and lithic fragments, blue quartz
0149	CL	Tuff breccia, Berry Creek metavolcanics, pumice clasts
0167	WR	Tuff, Berry Creek metavolcanics, altered, garnet, hornblende, chloritoid
0170	CL	Tuff breccia, Berry Creek metavolcanics, hetero-lithic, pumice and lithic clasts
0175	WR	Mafic tuff, Berry Creek metavolcanics, hornblende, garnet
0177	CL	Tuff breccia, Berry Creek metavolcanics, mafic matrix with dacitic clasts, porphyritic
0178	CL	Tuff breccia, Berry Creek metavolcanics, heterolithic with mafic and felsic clasts, sample of mafic clast
0180	WR	Tuff breccia, Adams River Bay metavolcanics, lithic and crystal fragments and minor pumice
0188	WR	Crystal tuff, Berry Creek metavolcanics, quartz and feldspar crystals

Ø190A CL Tuff breccia, Berry Creek metavolcanics, abundant pumice and dacite porphyry clasts, sample of dacite porphyry

Ø190B CL Tuff breccia, Berry Creek metavolcanics, sample of pumice

Ø192 WR Lapilli tuff, Berry Creek metavolcanics, crystal fragments, minor pumice

Ø2Ø5 WR Lapilli tuff, Berry Creek metavolcanics

Ø2Ø9 WR Lava flow, Berry Creek metavolcanics

Ø213 WR Mafic tuff, Berry Creek metavolcanics, amphibolite

Ø215 CL Tuff breccia, Berry Creek metavolcanics, dacite porphyry clasts

Ø22Ø WR Crystal tuff, Berry Creek metavolcanics, quartz and feldspar crystals

Ø229 WR Crystal tuff, Berry Creek metavolcanics

Ø243 CL Tuff breccia, Berry Creek metavolcanics, dacite clasts

Ø26Ø WR Tuff, Berry Creek metavolcanics

Ø263 WR Crystal tuff, Berry Creek metavolcanics, feldspar and quartz crystals

Ø266 CL Tuff breccia, Berry Creek metavolcanics, abundant pumice shards and fragments, sample of pumice

Ø272 CL Tuff breccia, Berry Creek metavolcanics, lithic clasts of dacite porphyry

Ø277 WR Basalt, Lobstick Bay metavolcanics, non-porphyritic massive

Ø284 CL Pyroclastic breccia, Lobstick Bay metavolcanics, dacite porphyry clasts

Ø294 WR Tuff, Berry Creek metavolcanics

Ø297 WR Tuff, Berry Creek metavolcanics, pumice shards, abundant crystals of quartz and feldspar

Ø3Ø2 CL Tuff breccia, Berry Creek metavolcanics, heterolithic, lapilli-blocks, clasts of quartz phyric felsite

Ø3Ø5	WR	Tuff, Berry Creek metavolcanics, bedded to laminated, glassy
Ø3Ø9	CL	Tuff breccia, Berry Creek metavolcanics, monolithic, dacite porphyry clast